UNIVERSITY OF CALIFORNIA SAN DIEGO

The Molecular Basis of Protein Kinase C Regulatory Mechanisms in Cancer and Neurodegenerative Disease

A dissertation submitted in partial satisfaction of the
requirements for the degree
Doctor of Philosophy

in

Biomedical Sciences

by

Timothy R. Baffi

Committee in charge:

Professor Alexandra Newton, Chair
Professor Steven Dowdy
Professor J. Silvio Gutkind
Professor Tony Hunter
Professor Susan Taylor

2019

The dissertation of Timothy R. Baffi is approved, and it is acceptable in quality and form for publication on microfilm and electronically:

_____

_____

_____

_____

_____

Chair

University of California San Diego

2019

DEDICATION

To:

Pops, The Original Dr. Baffi

EPIGRAPH

It is the pervading law of all things organic and inorganic,

of all things physical and metaphysical,

of all things human, and all things super-human,

of all true manifestations of the head, of the heart, of the soul,

that the life is recognizable in its expression,

that form ever follows function. This is the law.

—Louis Sullivan

TABLE OF CONTENTS

LIST OF FIGURES

LIST OF TABLES

ACKNOWLEDGEMENTS

I would like to express my gratitude to the many mentors, family members, and friends that greatly enriched my graduate experience.

First and foremost, I would like to thank my advisor, Alexandra Newton, for her unwavering support, dedication, and enthusiasm for science and mentoring her students. I enjoyed designing experiments, analyzing data, and dissecting research questions on a daily basis, and learned how to think as a scientist from her mentorship. Alexandra always had her door open to me to pour over the latest results, and some of my fondest grad school memories were discussing our hypotheses together in her office to decide on the next critical experiment. Alexandra's investment in her students is unparalleled, and I feel extremely fortunate to have had the opportunity to work and learn in the Newton Lab. Additionally, I would like to thank all the other members of the Newton Lab for providing a fun, collegial, and supportive environment. I've learned so much from all of you and I have immense respect for each member as a scientist and friend.

In addition to my thesis advisor, I would particularly like to acknowledge my thesis committee members: Susan Taylor for the many times I was invited to present in your lab meeting, all the thought-provoking discussions on protein structure and biology, and the exciting collaboratoins that have arisen over the past year; Tony Hunter for providing insights into the important unanswered questions in the field and the latest techniques that could be used to answer them; Silvio Gutkind for reminding me of the importance to contextualize my work on PKC within a greater signaling pathway, cell process, or disease context; and Steve Dowdy for serving as my SPAC advisor, setting a direction for my thesis project during my advancement, and guiding me through the intellectual hurdles of graduate school. I view my annual committee

meetings as integral leaps in my thesis work that spurred the next year of productive experiments, and I greatly enjoyed discussing my work, learning from all of you, and being inspired by the takeaways of the meeting.

I would consider many other mentors instrumental in my development as a scientist over the years through various aspects of training, instruction, or guidance. At UCSD, I would like to acknowledge Maya Kunkel, C.C. King, Joan Heller-Brown, Jack Dixon, Jin Zhang, Arshad Desai, Gina Butcher, Leanne Nordeman, and Patrick Savaiano. At my undergrad institution of Claremont McKenna College and associated campuses, I would like to thank Julia Massimelli, Jennifer Armstrong, Newton Copp, Scot Gould, Matthew Croughan, and E.J. Crane. At Genentech, I would like to thank Mark Sliwkowski, Don Dowbenko, Bob Kiss, Brian Horvath, Donald Lee, and Michael Laird. At BioMarin Pharmaceutical, I would like to thank Gordon Vehar, Melita Dvorak-Ewell, and Michael Vellard. I would also like to acknowledge other influential members of my scientific journey Stu Builder, Chuck O'Neill, Charles Cooney, Robert Langer, and Eric Davis.

Additionally, my friends have provided unwavering support throughout the ups and downs of graduate school. For all the camaraderie and years of friendship, I would like to thank steven Edelstone, JD O'Keefe, Joey Blouse, Josh Gevertz, Colby Pines, Michael Brondello, Ross Geiger, Jared Wong, Nate Cox, Andy Lindquist, Alex Poyhonen, Brian Sutter, Russell Page, Bennett Naden, Rafer Dannenhauer, Kevin O'Neill, Quinn Chasan, Shawn Ali, James Yurkovich, Nick Kalogriopoulos, Nathan Jameson, Ian Montijo, Nikos Protopsalits, and Afsheen Banisadr.

My family has been a continuous encouragement and blessing in my life. I would like to particularly thank my father Robert for being a constant source of support and inspiration, my mother Rosemary for her investment in every facet of my life, my sister Jane for her positive and

optimistic spirit, and the rest of the Baffi clan.

Finally, I would like to thank Katie Lavieri, the love of my life, for her steadfast commitment to our relationship and my well-being through all of the late nights and constant work associated with graduate school. You are my rock, and I would not have found the will to persevere through the toughest times of my PhD without you.

Chapter 2 in part is a reprint of material to be submitted in:

Baffi TR, Kornev AP, King CC, Del Rio J, Bogomolovas J, Chen J, Taylor SS, Newton AC. "mTORC2 controls PKC and Akt via phosphorylation of a conserved TOR-interaction motif" *In Preparation.*

The dissertation author was the primary author of this work.

Chapter 3 in part is a reprint of material published in:

Baffi TR, Van AN, Zhao W, Mills GB, Newton AC. "Protein kinase C quality control by phosphatase PHLPP1 unveils loss-of-function mechanism in cancer." *Molecular Cell.* 2019 Apr 18;74(2):378-392. DOI: 10.1016/j.molcel.2019.02.018

The dissertation author was the primary author of this work.

This work was supported by NIH R35 GM122523 and NIH GM43154 to ACN. TRB was supported by the PhRMA Foundation Pre Doctoral Fellowship in Pharmacology/Toxicology (#20183844) and the UCSD Graduate Training Program in Cellular and Molecular Pharmacology (T32 GM007752).

VITA

2019	Doctor of Philosophy in Biomedical Sciences, University of California, San Diego
2013	Bachelor of Arts in Molecular Biology, Claremont McKenna College

PUBLICATIONS

Baffi TR, Van AN, Zhao W, Mills GB, Newton AC. "Protein kinase C quality control by phosphatase PHLPP1 unveils loss-of-function mechanism in cancer." *Molecular Cell.* 2019 Apr 18;74(2):378-392.

DOI: 10.1016/j.molcel.2019.02.018

Huang LC*, Ross KE*, **Baffi TR**, Drabkin H, Kochut KJ, Ruan Z, D'Eustachio P, McSkimming D, Arighi C, Chen C, Natale DA, Smith C, Gaudet P, Newton AC, Wu C, Kannan N. "Integrative annotation and knowledge discovery of kinase post-translational modifications and cancer-associated mutations through federated protein ontologies and resources." *Scientific Reports.* 2018 Apr 25;8(1):6518.

DOI: 10.1038/s41598-018-24457-1

McSkimming DI, Dastgheib S, **Baffi TR**, Byrne DP, Ferries S, Scott ST, Newton AC, Eyers CE, Kochut KJ, Eyers PA, Kannan N. "KinView: a visual comparative sequence analysis tool for integrated kinome research." *Molecular Biosystems*, 12(12):3651-3665.

DOI: 10.1039/c6mb00466k

* equal contribution

MANUSCRIPTS IN PROGRESS

Baffi TR, et al. "mTORC2 controls PKC and Akt via phosphorylation of a conserved TOR-interaction motif." *In Preparation.*

ABSTRACT OF THE DISSERTATION

The Molecular Basis of Protein Kinase C Regulatory Mechanisms in Cancer and Neurodegenerative Disease

by

Timothy R. Baffi

Doctor of Philosophy in Biomedical Sciences

University of California San Diego, 2019

Professor Alexandra Newton, Chair

Protein kinase C (PKC) isozymes transduce the myriad of signals downstream of phospholipid hydrolysis that potentiate an array of cellular processes including proliferation, differentiation, migration, and memory. PKC function is dysregulated in a variety of pathological states, including cancer and neurodegenerative disease. To maintain signaling fidelity, PKCs rely upon precise regulatory mechanisms that orchestrate the phosphorylations and conformational transitions that specify their signaling output. This thesis describes the molecular mechanisms by which PKC phosphorylation and autoinhibition depends upon the kinases PDK1 and

mTORC2, and is opposed by PHLPP phosphatases, to produce a primed enzyme that is appropriately tuned to respond to activating signals. Specifically, we uncover the molecular basis for the controversial role of mTORC2 in AGC kinase activation by identifying a novel and conserved mTOR phosphorylation site in the C-terminal tail. Phosphorylation of this, which we term the TOR-Interaction Motif (TIM), promotes PDK1 phosphorylation of the activation loop and intramolecular autophosphorylation of the hydrophobic motif to control activation of PKC and related AGC kianse Akt. Examination of the interrelated processes of phosphorylation and autoinhibition unveils a critical role for the pseudosubstrate in protecting PKC from dephosphorylation by phosphatase PHLPP1, which selectively promotes the dephosphorylation and degradation of aberrantly active PKCs to provide a PKC quality control mechanism. High-throughput protein-level analysis from patient samples reveals that PKC quality control is a critical signaling node that sets PKC expression levels and serves as a prominent loss-of-function mechanism to impair PKC tumor-suppressive function in cancer. Critically, diseases driven by PKC dysregulation rely upon impaired PKC quality control. LOF PKC mutations in chordoid glioma act in a dominant-negative fashion to globally suppress PKC output; whereas, GOF PKC mutations in spinocerebellar ataxia drive phosphoproteome-wide changes in the cerebellum. Taken together, this thesis expands upon biochemical mechanisms of PKC maturation to identify the structural and molecular determinants of PKC phosphorylation and implicates PHLPP1 as the master regulator of PKC signaling fidelity through PKC quality control. This work is not only relevant to the pathology of disease-associated mutations in cancer and neurodegenerative disease, but also to the development of therapeutics that attempt to modulate PKC activity by targeting these regulatory mechanisms.

Chapter 1

Tipping Point: The Balance of PKC Signaling is Dysregulated in Disease

1.1 PKC Structure & Function

Signal transduction by protein kinase constitutes the predominant mechanism of cellular communication to detect, integrate, and amplify signals in the extracellular environment to illicit coordinated cellular responses (Hunter, 1995). The protein kinase C (PKC) family of Ser/Thr kinases belongs to the AGC family of phosphotransferases that catalyze the transfer of the ATP γ-phosphate to hydroxyl groups of Ser and Thr side chains on protein substrates (Prince et al., 2011). PKC isozymes are the primary diacylglycerol (DAG) and Ca^{2+}-responsive enzymes that transduce signals from the plasma membrane to the intracellular environment to regulate diverse cellular processes (Newton, 1995).

All PKCs contain a C-terminal catalytic domain and an N-terminal regulatory domain (Parker et al., 1986) (Figure 1.1). The catalytic portion consists of the kinase domain and

a C-terminal extension, the C-tail, which is a characteristic feature of AGC kinases required for catalytic activity and regulation by various adaptors (Kannan et al., 2007). The catalytic domain is rendered catalytically competent by phosphorylation at three highly conserved sites at the kinase domain activation loop and two sites in the C-tail, the turn and hydrophobic motifs (Keranen et al., 1995). The nine PKC isozymes are stratified into three groups, classified by their regulatory domains. Conventional PKCs (cPKCs; α, β, γ) harbor a Ca^{2+}-binding C2 domain (Parker et al., 1986), tandem diacylglycerol-binding C1 domains (Burns and Bell, 1991), and an autoinhibitory pseudosubstrate segment (House and Kemp, 1987). Novel PKCs (nPKCs; δ, ε, θ, η), in contrast, possess a novel C2 domain that is incapable of binding Ca^{2+} (Sossin and Schwartz, 1993), and rely instead upon increased sensitivity to agonists, as their C1B domain binds DAG with 100-fold higher affinity than that of cPKCs due a Tyr to Trp substitution (Dries et al., 2007; Hurley et al., 2008). Additionally, the C2 domain of nPKCs precedes the pseudosubstrate and C1 domains, and displays inverse topology, presumably to accommodate the differential domain orientation (Pappa et al., 1998). Atypical PKCs (aPKCs; ζ, λ/ι) respond to neither Ca^{2+} nor DAG (Kazanietz et al., 1994; Pu et al., 2006), and are instead regulated by sphingosine 1-phosphate (Kajimoto et al., 2019) and protein:protein interactions via a PB1 domain (Lamark et al., 2003; Tobias and Newton, 2016). Notably, atypical PKCs are further distinguished by a glutamic acid at their hydrophobic motif, which functions as a phosphomimetic (Tobias et al., 2015).

Due to the multitude of family members, diversity of activating stimuli, and abundance of substrates, PKCs signal through numerous pathways to regulate diverse and often antagonistic cellular processes dependent upon the nature of the signal, cell type, and cellular environment (Coussens et al., 1986). PKCs have a well-established role in regulating cell proliferation by

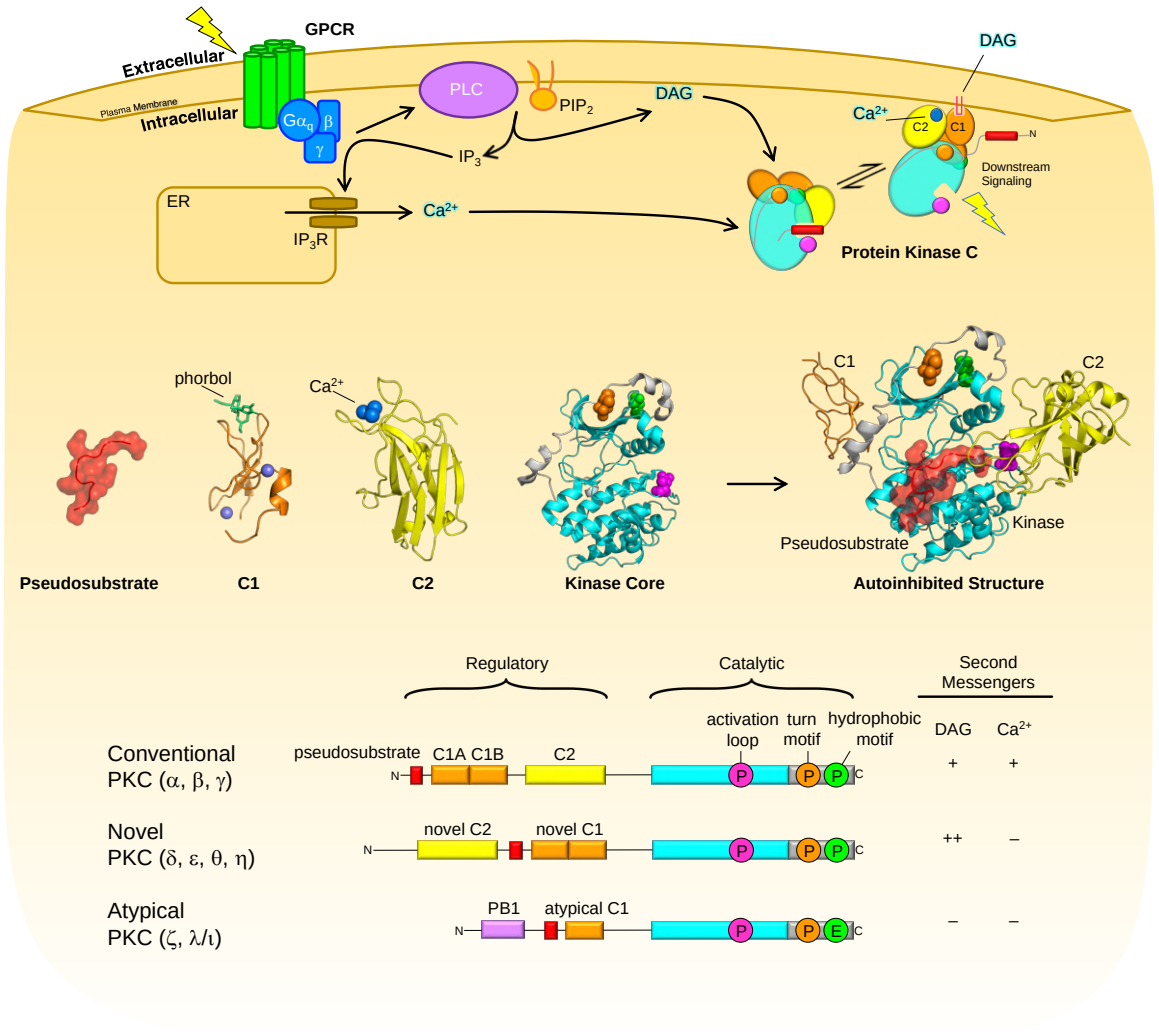

Figure 1.1: **PKC Structure & Function.** Conventional PKC is activated downstream of signals that result in lipid hydrolysis. Generation of Ca^{2+} and DAG recruits PKC to membranes to initiate downstream signaling. In addition to the AGC kinase core, PKC isozymes contain Ca^{2+}-binding C2 domains, DAG-binding C1 domains, and an autoinhibitory pseudosubstrate. PKCs are classified by their ability to respond to second-messengers and are phosphorylated in conserved motifs termed the activation loop, turn motif, and hydrophobic motif.

direct phosphorylation of cell-cycle components, as well as indirectly through the PI3K/Akt, Wnt-β-catenin, and MAPK pathways (Black and Black, 2013). PKC's pro-proliferative effects are perhaps best illustrated by the requirement of PKCθ for T-cell activation (Valge et al., 1988). Underscoring the complexity of PKC signaling, other PKCs have opposing effects on proliferation, however, as evidenced by the positive and negative regulation of D-type cyclin expression by PKCε and PKCα, respectively (Clark et al., 2004). These divergent outcomes in PKC regulation of cell proliferation may be explained, in part, by the ability of ERK to exert both proliferative and anti-proliferative effects due to differential signal duration downstream of PKC-mediated MAPK pathway activation (Mebratu and Tesfaigzi, 2009). Thus, PKCs are ubiquitous initiators of core intracellular signaling pathways that regulate cell proliferation, the consequence of which varies by isozyme and is signal and context dependent.

PKC function is also critical in the brain, where cPKCs are key regulators of postsynaptic transmission (Tanaka and Nishizuka, 1994). Originally purified from brain extracts in which its regulation by Ca^{2+} and phospholipids was first described (Kishimoto et al., 1983), cPKCs are responsible for key neuronal processes such as long-term depression (LTD), mediated by the internalization of AMPA and NMDA glutamate receptors upon PKC phosphorylation (Linden and Connor, 1991). Indeed, PKC is well-known to phosphorylate numerous transporters, ion channels, and GPCRs to generally promote receptor desensitization in many tissues, underscoring its central role in both signal propagation and signal termination (Gereau and Heinemann, 1998; Namkung and Sibley, 2004). Additionally, PKC regulates cytoskeleton dynamics through the phosphorylation of MARKS, GAP43, and Tau (Correas et al., 1992; He et al., 1997; Stumpo et al., 1989). PKC also indirectly regulates microtubule and neurofilament stabilization to influence cytoskeletal reorganization through the phosphorylation and inhibition of GSK3β (Goode et al.,

1992). Many of these PKC-mediated neuronal processes depend upon PDZ-domain containing scaffold proteins including PICK1, PSD95, and SAP97 (Lin et al., 2006; O'Neill et al., 2011; Staudinger et al., 1997). Thus, PKC function in the brain is tightly regulated by its subcellular localization and interaction with effectors proteins to fine-tune its output and direct distinct signaling programs.

1.2 PKC Unbalanced in Disease

Evidenced by its essential role in cell proliferation and neurotransmission, the integrity of PKC signaling must be maintained to avoid pathophysiologies that result from dysregulation of these cellular processes (Figure 1.2) This notion is substantiated by the abundance of PKC somatic and germline mutations, differential expression, and signaling pathway alterations in cancer and neurodegenerative disease. PKC is a recently-appreciated tumor suppressor, whose function is frequently lost by a variety of mechanisms in the context of cancer (Newton, 2018b; Newton and Brognard, 2017). Conversely, PKC's expanding functions in synaptic plasticity generally support a role in neurodegeneration associated with enhanced activity (Callender and Newton, 2017). Advances in genomic sequencing and proteomic technologies from patient samples have proven important tools for identifying and dissecting the specific PKC contributions to these disease states.

PKC isozymes have a storied history in cancer biology, beginning with the discovery that the C1 domain is the receptor for the tumor-promoting phorbol esters, which potently activate PKCs (Kikkawa et al., 1983; Ono et al., 1989). Indeed, repetitive treatment of mice with phorbol esters following administration of a subthreshold amount of carcinogen was sufficient to promote papilloma formation and spontaneous conversion to carcinoma (Griner and Kazanietz,

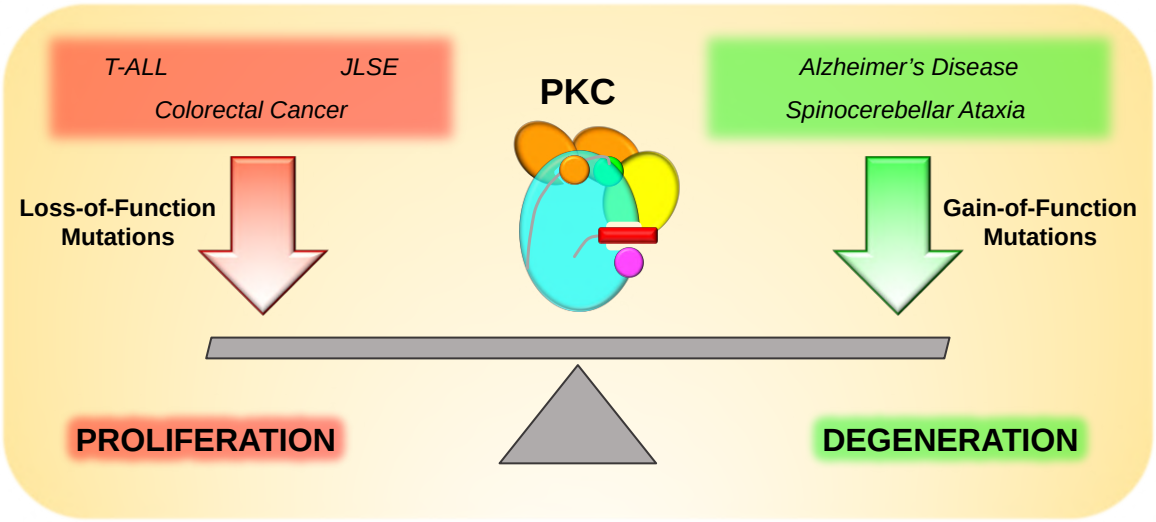

Figure 1.2: **PKC Unbalanced in Disease.** PKC is frequently mutated in disease. Loss-of-function mutations are generally associated with proliferative diseases including cancer and lupus. Gain-of-function mutations, conversely, are observed in neurodegenerative diseases such as Alzheimer's Disease and Spinocerebellar Ataxia.

2007). This finding lead to the hypothesis that PKCs, as with many other viral oncogenic kinases identified at the time (Hunter et al., 1984), should be inhibited in cancer. What was not considered, however, was that phorbol esters, in addition to activating PKC, also promote its down-regulation (Parker et al., 1995). Thus, it was unclear whether the tumor-promoting effects of phorbol esters were due to PKC activation, or to its down-regulation. Three decades of failed clinical trials with PKC inhibitors cast doubt on the role of PKC as an oncogenic target in cancer. A meta-analysis of non-small cell lung cancer clinical trials revealed that the use of PKC inhibitors in combination with chemotherapy was not only ineffective, but often detrimental to patient outcome compared to chemotherapy alone (Zhang et al., 2015). This finding is perhaps not surprising considering the ample evidence for some isozymes that PKC overexpression did not promote tumors but rather protected them from phorbol ester-induced oncogenesis (Reddig et al., 1999), with the unambiguous exceptions of PKCε and atypical PKCs (Oster and Leitges, 2006; Reddig et al., 2000; Regala et al., 2005; Wheeler et al., 2003). Furthermore, examination

of known PKC substrates suggests a tumor-suppressive, rather than oncogenic, role, as PKC dampens the activity of the prevalent oncogenic drivers EGFR, HER2, K-Ras and PI3K (Bivona et al., 2006; Lee et al., 2011; Ouyang et al., 1998). Furthermore, PKC's well known role in promoting receptor internalization, as has been shown for EGFR, HER2, and TGF-β receptors, may dampen pro-survival signaling at the source of these pathways (Baffi et al., 2004; Cochet et al., 1984; Gunaratne et al., 2012; Ouyang et al., 1998;). Additionally, PKC phosphorylates and stabilizes the tumor-suppressor p53 (Yoshida et al., 2006; Youmell et al., 1998), suggesting that PKC may influence both the attenuation of oncogenic signaling, as well as the maintenance of genome integrity. It was not until a recent biochemical analysis of cancer-associated PKC mutations revealed the majority of these mutations were in fact loss-of-function (LOF) that PKC's tumor-suppressive function was fully appreciated (Antal et al., 2015a). Consistent with the mutational profile of tumor-suppressors, these mutations were distributed across most domains of PKC genes, targeting regions involved in catalysis, ligand binding, and post-translational modification to inactivate PKC. Convincingly, CRISPR-mediated correction of a heterozygous LOF mutation in PKCβ suppressed the ability of a K-Ras-driven colon cancer cell line to form tumors in mice (Antal et al., 2015a). These findings initiated a flurry of reports supporting a tumor-suppressive role for many PKC isozymes in a variety of cancers. Substantiating PKC attenuation of oncogenic K-Ras, PKC was also found to disrupt the K-Ras interaction with calmodulin required for tumorigenicity in pancreatic cancer (Wang et al., 2015). PKC was also recently implicated in suppressing oncogenic Akt signaling in endometrial cancer through regulation of a PP2A phosphatase family member (Hsu et al., 2018). Indeed, the co-occurrence of GOF oncogene mutations with LOF PKC mutations in cancer highlights PKC antagonism of pro-survival signaling and suggests oncogenic driver mutations may be most advantageous when

PKC is inactivated (Antal et al., 2015a). This hypothesis is consistent with tumor suppressor loss functioning as the critical and rate-limiting step of oncogenesis (Weinberg, 1991), and may underlie the requirement for phorbol ester-mediated downregulation of PKC to potentiate the tumorigenic properties of low level carcinogen. PKC loss was also observed in cancer at the level of expression, where low PKC levels correlated with more severe disease in colorectal cancer, bladder cancer, and T-ALL (Dowling et al., 2016; Langzam et al., 2001; Milani et al., 2014). While the cause of this reduced expression is not known, PKC levels may be utilized as prognostic markers for some cancers.

Contrary to other tumor suppressors and the two-hit hypothesis that selects for homozygous mutation or deletion (Knudson, 1971), mutation of a single PKC allele is sufficient for tumorigenesis, suggesting that PKC is haploinsufficient for tumor suppression (Antal et al., 2015a). PKC LOF mutations also exert their effects, in part, by acting as dominant-negatives, which may obviate the need for biallelic mutation (Antal et al., 2015a). The precise mechanism by which this occurs has not be described, and whether there are post-translational means to impair PKC function in cancer remains to be explored. Taken together, PKC's tumor-suppressive function constitutes the brakes to oncogenic signaling, and numerous mechanisms abrogate this signaling safeguard to facilitate tumorigenesis.

While PKC activity is typically is lost in cancer, its enhanced activity is associated with neurodegeneration. It was recently shown that rare PKCα variants co-segregate with affected family members with Alzheimer's Disease (AD) (Alfonso et al., 2016). One of these mutations in the catalytic domain causes an 30% increase in the catalytic rate of the enzyme, which enhances PKC output without promoting its down-regulation (Callender et al., 2018). Additionally, PKC is heavily implicated in AD due to its direct and indirect regulation of Tau phosphorylation, as

well as its functions both upstream and downstream of amyloid beta (Callender and Newton, 2017).

PKC dysregulation in neurodegenerative disease is perhaps most strongly tied to spinocerebellar ataxia (SCA), where PKCγ mutations are the hallmark of SCA14 (Chen et al., 2003; Yabe et al., 2003). Expressed almost exclusively in the cerebellum, PKCγ orchestrates the maturation of Purkinje neurons by regulating the process of climbing fiber elimination and synapse pruning to fine-tune motor control (Chen et al., 1995). SCA14-associated PKCγ mutations have been reported to be hyperactive, and PKC activity alone is sufficient to cause an ataxic phenotype in mouse models (Adachi et al., 2008; Ji et al., 2014). The specific mechanisms governing PKC hyperactivation are not well described, however, with hypotheses attributing PKCγ mutation pathology to differential PKCγ localization or the formation of protein aggregates (Seki et al., 2005; Takahashi et al., 2015). Although PKCγ mutations comprise just a subset of SCA diagnoses, deregulation of Ca^{2+} homeostasis is a central theme of cerebellar ataxias that may converge on PKCγ signaling, as hallmarks of other forms of SCA include mutations in PKC effectors such as the upstream receptor mGluR1 (SCA44) (Watson et al., 2017), Ca^{2+} channel subunits (SCA6, SCA42) (Zhuchenko et al., 1997; Kimura et al., 2017), and mediators of intracellular Ca^{2+} release like the IP_3 receptor (SCA15, SCA16, SCA29) (van de Leemput et al., 2007; Novak et al., 2010; Zambonin et al., 2017) . PKCγ activity is unequivocally involved in Purkinje cell processes, as acute treatment of isolated Purkinje neurons with phorbol esters induces a dramatic loss of dendrites, while PKC inhibition promotes dendritic outgrowth, or arborization (Schrenk et al., 2002). Thus, how PKCγ mutations induce degeneration of these cells may open avenues for therapeutic intervention and even provide insights into the general pathology cerebellar ataxias and other neurodegenerative disorders.

1.3 The PKC Lifecycle: Maturation, Activation, and Down-regulation

The highly regulated process of PKC maturation primes the enzyme for specific spatiotemporal activation and underpins its regulation throughout the entirety its signaling lifetime (Antal and Newton, 2014)(Figure 1.3). Following synthesis, PKCs are matured by a series of ordered phosphorylations and conformational transitions that result in autoinhibition to achieve catalytic competence and stability (Newton, 2003). The activation loop is phosphorylated by the phosphoinositide-dependent protein kinase 1 (PDK1) in a PI3K-independent manner (Dutil et al., 1998; Le Good et al., 1998; Sonnenburg et al., 2001), and the two C-tail phosphorylations are mediated by the mammalian target of Rapamycin complex 2 (mTORC2) by an unknown mechanism (Sarbassov et al., 2004; Facchinetti et al., 2008; Guertin et al., 2006; Ikenoue et al., 2008). While the activation loop and hydrophobic motif phosphorylations are necessary for efficient catalysis (Edwards and Newton, 1997; Orr and Newton, 1994), the turn motif phosphorylation imparts protein stability (Bornancin and Parker, 1996). PKC phosphorylation at the hydrophobic motif also requires the protein chaperone Hsp90, dependent upon a PxxP motif in the PKC C-tail (Gould et al., 2009). Upon phosphorylation, the PKC pseudosubstrate occupies the active-site of the kinase domain. PKC phosphorylation and autoinhibition is accompanied by the conformational transition from the unprimed, open conformation to the primed, closed conformation, which is stable and protected from ubiquitination and proteolysis. In the primed state, PKC's regulatory domains are masked against the kinase domain, such that both C1 domains are inaccessible, and the C2 domain clamps over the pseudosubstrate to maintain autoinhibition (Antal et al., 2014, 2015b).

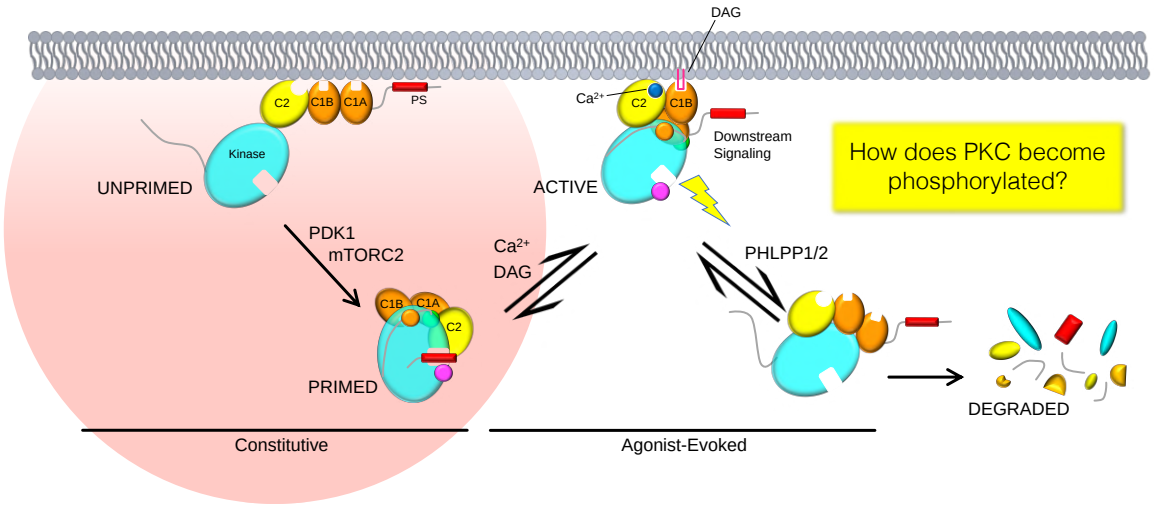

Figure 1.3: **The PKC Lifecycle: Maturation, Activation, and Down-regulation.** Newly-synthesized PKC exists in an unprimed state that is neither phosphorylated nor catalytically competetent and must become matured through the activities of PDK1 and mTORC2 in order to achieve the mature, primed state. It is only the fully phosphorylated, autoinhibited, and stable PKC that accumulates in the cell and can become activated by second messengers. In the active state, PKC is sensitive to dephosphorylation by PHLPP phosphatases and degradation. The major open question in the model of PKC processing is the mechanism by which PDK1 and mTORC2 lead to PKC phosphorylation, catalytic competence, and autoinhibition.

Primed cPKCs are cytosolically localized in the phosphorylated and catalytically competent but inactive state, poised to respond to fluctuations in the second-messengers DAG and Ca^{2+}. Upon the increase in concentration of extracellular signaling molecules such as a neurotransmitters that bind G-protein coupled receptors (GPCRs) and activate $G\alpha_q$-coupled signaling, phospholipase C (PLC) hydrolyzes the phospholipid phosphatidylinositol 4,5-bisphosphate (PIP_2) into its constituents DAG and inositol 1,4,5-trisphosphate (IP_3). IP_3-stimulated release of intracellular Ca^{2+} stores from the endoplasmic reticulum (ER) recruits PKC to the plasma membrane via the Ca^{2+}-bound C2 domain interaction with the anionic phospholipids PIP_2 and phosphatidyl serine (PS) (Newton et al., 2016). The reduction in dimensionality upon PKC association with the lipid membrane potentiates the C1 domain search for DAG (Newton and Koshland, 1989). Binding of predominantly the C1B domain to DAG retains PKC on the mem-

brane and expels the pseudosubstrate to activate the kinase and initiate substrate phosphorylation (Orr et al., 1992). The duration of PKC activation correlates with the metabolism of DAG.

In the activated state, PKCs display two orders of magnitude enhanced sensitivity to dephosphorylation. PKC down-regulation is initiated through dephosphorylation of the hydrophobic motif by PH domain leucine-rich repeat-containing protein phosphatases (PHLPP) and subsequent dephosphorylation of the activation loop and turn motif by PP2A-family phosphatases (Gao et al., 2008; Keranen et al., 1995). Complete PKC dephosphorylation, dependent upon Pin1 isomerization of the turn motif site (Abrahamsen et al., 2012) terminates its activity and dissociates PKC from the membrane, where it subject to ubiquitination and proteasome-dependent degradation (Chen et al., 2007). Dephosphorylated PKC may re-enter the pool of signaling-competent enzyme dependent via Hsp70-mediated re-phosphorylation through its interaction with the dephosphorylated turn motif (Gao and Newton, 2002). Thus, the interplay between the regulatory mechanisms controlling PKC phosphorylation, dephosphorylation, and autoinhibition specify PKC expression and spatiotemporal output, and become frequently dysregulated in disease.

This thesis investigates the molecular mechanisms of PKC regulation by phosphorylation and autoinhibition and how dysregulation of these processes manifests in disease (Figure 1.4). Using biochemical, structural, and live-cell FRET-based biosensors, we undertake two mechanistic studies to investigate the requirement of mTORC2 in maturation of PKC by phosphorylation and the determinants of autoinhibition that yield a catalytically competent and stable enzyme, respectively. These coordinated processes underlie all PKC functions as they determine PKC catalytic activity, cellular levels, and responsiveness to second-messengers. In cancer, the iden-

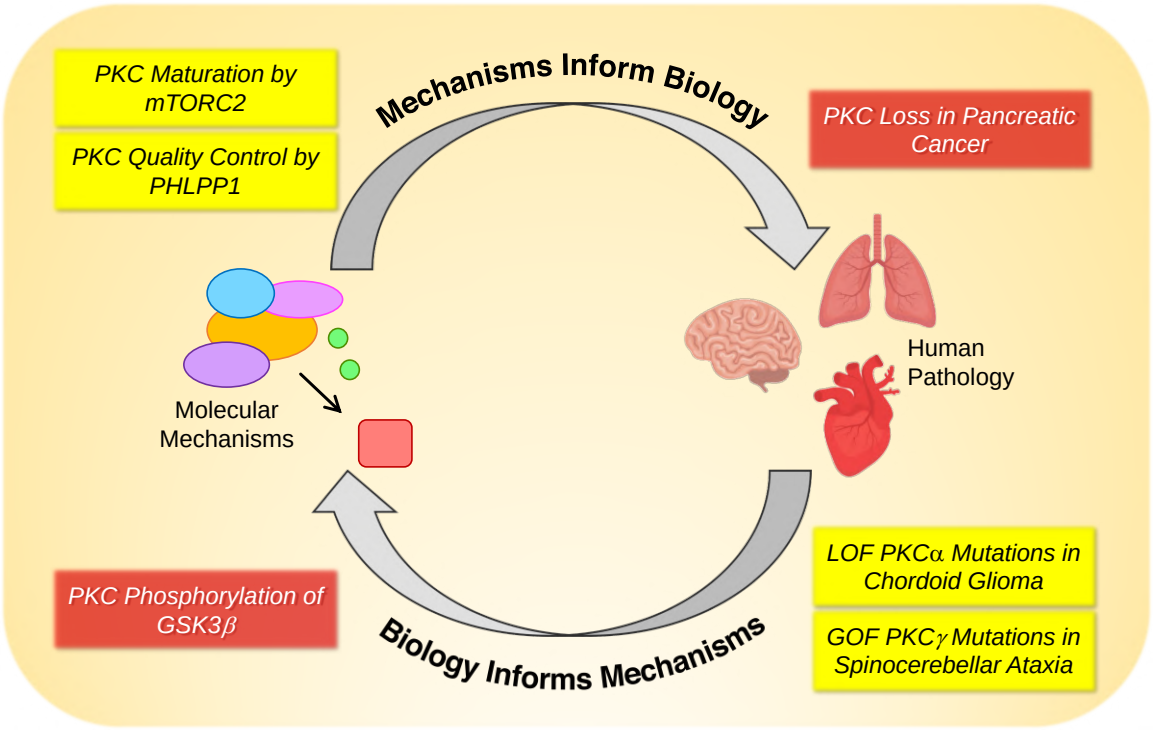

Figure 1.4: **Approach for Studying PKC Function in Disease.** This thesis investigates the molecular mechansisms underlying the pathology of dysregulated PKC signaling in disease. Studies to understand the molecular basis of PKC phosphorylation describe the molecular details of PKC maturation by mTORC2 and PKC quality control by PHLPP1, which reveal a conserved PKC loss-of-function mechanism in cancer, with particular relevance in pancreatic cancer. In a complementary fashion, a second approach begins with human diseases for which PKC mutations have been implicated as disease drivers. Understanding the mechanisms by which disease-associated mutations dysregulate PKC signaling informs the pathophysiology of the affected downstream pathways and cell processes. Specifically, gain-of-function mutations in spinocerebellar ataxia lead to the identification of a PKC-mediated phosphorylation on GSK3β involved in cytoskeletal defects in neurodegenerative disease.

tification of PHLPP1-mediated PKC quality control presents a pervasive PKC LOF mechanism that provides a novel post-translational means by which PKC function in suppressed, in addition to the described genetic and transcriptional mechanisms. Having established the molecular basis of PKC processing, we apply this knowledge to disease-associated mutations in chordoid glioma and spinocerebellar ataxia to ascertain how mutant PKC interacts with these processing checkpoints to induce proliferative or degenerative disorders. Understanding the critical determinants of proper PKC function, we uncover how causative disease-associated mutations subvert regulatory mechanisms to drive pathophysiology. What is more, we utilize these aberrant enzymes to discover pathological neomorphic functions and signaling pathways that contribute to our understanding of PKC biology. Specifically, biochemical characterization of a recurrent PKCα mutation in chordoid glioma revealed a potential mechanism for the dominant-negative effects of LOF PKC mutations in cancer to globally suppress PKC function. In a related fashion, phosphoproteomic analysis of mice harboring SCA14 PKCγ mutations identified the direct PKC phosphorylation site on GSK3β responsible for its PKC-mediated inhibition and implicated cytoskeleton dysfunction as a potential source degeneration in cerebellar ataxias. Moreover, our findings present avenues for developing therapies to target dysregulated PKC regulatory mechanisms and the associated downstream pathways. Taken together, the reciprocal application of PKC molecular mechanisms with human disease reveals novel functions not readily apparent in a non-pathological state and informs new approaches for targeted therapeutic intervention.

Chapter 2

mTORC2 Controls PKC and Akt via Phosphorylation of a Conserved TOR-Interaction Motif

2.1 Abstract

The widely-accepted model for activation of the kinases PKC and Akt involves mTORC2 phosphorylation of the hydrophobic motif. However, the biochemical mechanism of this phosphorylation event and identity of the cellular hydrophobic motif kinase remain controversial. Here we identify a distinct mTOR-mediated phosphorylation we term the TOR-Interaction Motif (TIM), which is conserved in all mTOR-dependent kinases. TIM mutations in PKCβII (T634) or Akt1 (T443) abolish cellular kinase activity by impairing activation loop and hydrophobic motif phosphorylation. We show that the activation loop kinase PDK1 and mTORC2 bind PKC via the

TIM and hydrophobic motif and cooperate to activate PKC and Akt. Reinterpretation of a previously reported PKCβII crystal structure reveals a PKC homodimer that is disrupted by TIM phosphorylation and mTOR activity. Our data support a model in which TIM phosphorylation by mTORC2 relieves PKC dimerization, recruiting PDK1 to phosphorylate the activation loop and triggering intramolecular hydrophobic motif autophosphorylation. These studies provide the framework for a general AGC kinase activation mechanism.

2.2 Introduction

The ability of cells to respond to changes in their environment relies upon effective signal transduction orchestrated by protein kinases. Precise phosphorylation mechanisms and autoinhibitory constrains that ensure the fidelity of these signaling pathways are critical to maintain cellular homeostasis and frequently become deregulated in disease (Blume-Jensen and Hunter, 2001). Among the effectors whose activity are precisely tuned to prevent aberrant signaling are the protein kinase C (PKC) family Ser/Thr kinases (Newton, 2018).

PKC isozymes transduce signals resulting from receptor-mediated phospholipid hydrolysis to influence a wide range of cellular processes including cell growth, receptor desensitization, and differentiation (Griner and Kazanietz, 2007; Nishizuka, 1984), with emerging functions in cancer and neurodegenerative disease (Newton, 2018). Supporting a general role as tumor-suppressors, cancer-associated PKC mutations are overwhelmingly loss-of-function and target evolutionarily conserved kinase features (Antal et al., 2015a; McSkimming et al., 2016; Newton and Brognard, 2017). Additionally, a prevalent loss-of-function mechanism in cancer involves the suppression of PKC protein levels by its negative regulator, the phosphatase PHLPP1 (Baffi et al., 2019; Gao et al., 2005, 2008). In pancreatic cancer, patient survival strongly correlates with high PKC protein

levels and markers of PKC stability (Baffi et al., 2019). Aberrant PKC activity, in contrast, is observed in neurodegenerative diseases such as Alzheimer's, where PKC variants that increase the catalytic rate of the kinase co-occur with disease (Alfonso et al., 2016; Callender and Newton, 2017; Callender et al., 2018). Increased PKC activity in neurodegeneration is not restricted to alterations in the kinase domain, however, as germline mutations that cause spinocerebellar ataxia primarily target its regulatory domains, enhancing PKC activity by largely unknown mechanisms (Adachi et al., 2008; Chen et al., 2003; Lui et al., 2016). Therefore, regulation of PKC output is critical for its cellular function.

In addition to an AGC kinase family catalytic domain, PKCs contain N-terminal regulatory modules consisting of ligand-binding domains tethered to the kinase core by an autoinhibitory pseudosubstrate segment, which serves to restrain catalytic activity in the absence of the appropriate signals (Newton, 2010). Release of the pseudosubstrate for conventional (cPKC; α, β, γ) and novel (nPKC; ε, δ, θ, η) PKCs occurs through binding the lipid second messenger diacylglycerol (DAG) (Orr et al., 1992). Additionally, cPKCs possess a C2 domain that binds Ca^{2+} to direct signaling to the plasma membrane (Scott et al., 2013). Thus, fluctuations in the second messengers that engage PKC on the membrane effectively direct spatial and temporal PKC output (Antal and Newton, 2013).

Shortly after synthesis, PKCs are matured by constitutive phosphorylations at three conserved sites (Keranen et al., 1995): the activation loop by the phosphoinositide-dependent kinase PDK1(Dutil et al., 1998; Le Good et al., 1998), and two sites on the C-terminal tail (C-tail) mediated by mTORC2, the turn motif and hydrophobic motif (Guertin et al., 2006). The activation loop and hydrophobic motif phosphorylations are required for PKC activity (Edwards and Newton, 1997; Orr and Newton, 1994); whereas, turn motif phosphorylation is not necessary

for catalysis, and instead promotes protein stability (Bornancin and Parker, 1996). The final event of PKC maturation, phosphorylation of the hydrophobic motif, triggers a conformational change that results in pseudosubstrate occupation of the active-site, effectively autoinhibiting the enzyme (Baffi et al., 2019). It is this catalytically competent, yet autoinhibited form of PKC that is stable and poised to respond to second messengers. Enzymes that do not become autoinhibited and are aberrantly active independent of agonist are targeted by PHLPP1-mediated PKC quality control, which dephosphorylates the hydrophobic motif, leading to PKC degradation (Baffi et al., 2019). Therefore, hydrophobic motif phosphorylation is the lynchpin that activates PKC and simultaneously promotes autoinhibition, stabilizing the enzyme.

The current dogma proposes that the atypical kinase complex mTORC2 is the long-sought-after hydrophobic motif kinase that directly activates several AGC kinases by phosphorylating the turn motif and hydrophobic motif sites (Oh et al., 2010; Sarbassov et al., 2005). In addition to regulating PKC, mTORC2 is necessary for the phosphorylation of the related AGC kinases Akt, SGK, and PKN; and this requirement is evolutionarily conserved (Garcia-Martinez and Alessi, 2008; Roelants et al., 2017; Sarbassov et al., 2005; Yang et al., 2017). Curiously, AGC kinase member S6K depends, instead, upon mTORC1 (Burnett et al., 1998), and three novel PKCs, δ, θ, and η, are mTOR-independent (Ikenoue et al., 2008).

The role of mTORC2 has been most extensively studied in Akt. The turn motif phosphorylation of Akt, like that of atypical PKCζ, occurs co-translationally on the ribosome via direct mTORC2 phosphorylation to promote protein stability by preventing ubiquitination during synthesis (Oh et al., 2010; Tobias et al., 2015). The Akt hydrophobic motif phosphorylation, distinct from that of PKC, enhances, but is not required for, catalysis (Yang et al., 2002); rather, activation loop phosphorylation is necessary and sufficient for Akt activity (Balasuriya et al.,

2018). Canonical activation of Akt involves the generation of PIP_3, which recruits Akt to the plasma-membrane via its PH domain, resulting in PDK1-dependent activation loop phosphorylation and mTORC2-mediated hydrophobic motif phosphorylation (Alessi et al., 1996; Bellacosa et al., 1998; Chan et al., 1999; Franke et al., 1995). In cells, catalytic competence of Akt is required for hydrophobic motif phosphorylation, however, suggesting that this site is governed by a kinase-intrinsic mechanism (Facchinetti et al., 2008; Toker and Newton, 2000). We have previously reported that Akt hydrophobic motif phosphorylation is induced in the absence of mTORC2 by any signal that disrupts the interface between Akt's PH domain and its kinase domain, as occurs upon binding to the plasma membrane (Warfel et al., 2011). Whether Akt membrane recruitment activates PKC principally through disengaging the PH domain autoinhibition or by promoting activation loop and hydrophobic motif phosphorylation through PDK1 and mTORC2, however, remains contested (Chu et al., 2018; Ebner et al., 2017). Further obfuscating the requirements for Akt activation, mTORC2 is only capable of phosphorylating the Akt turn motif *in vitro* (Ikenoue et al., 2008); the hydrophobic motif site of Akt and PKC, alternatively, are regulated via autophosphorylation triggered by PDK1 phosphorylation of the activation loop (Balendran et al., 1999; Behn-Krappa and Newton, 1999; Toker and Newton, 2000). That the turn motif and hydrophobic motif phosphorylations of PKC and Akt are regulated independently challenges the notion that mTORC2 directly phosphorylates both of these sites. Thus, in the absence of a mechanism for hydrophobic motif phosphorylation, the function of mTORC2 in regulating AGC kinases is unclear.

Here we provide evidence for a distinct mTORC2 phosphorylation site, which we term the TOR-Interaction Motif (TIM), that controls the activation of PKC and Akt. TIM phosphorylation is sensitive to mTOR inhibition and mTORC2-deficiency, and mutation of the TIM

site abolishes PKC and Akt cellular kinase activity by preventing activation loop and hydrophobic motif phosphorylation. Overexpression of PDK1 is sufficient to rescue activity and recover phosphorylation in the absence of mTORC2. For PKC, mTORC2 and PDK1 bind the TIM site and hydrophobic motif of the C-tail and cooperate to regulate the rate-determining step of PKC maturation. Comparative analysis of the TIM motif in PKC structures reveals an unappreciated PKC homodimer that is regulated by TIM phosphorylation and mTOR activity. Thus, identification of the TOR-Interaction Motif as the bona fide target of mTORC2 establishes that the hydrophobic motif is regulated by autophosphorylation. Moreover, this PKC activation mechanism implicates mTORC2-dependent conformational rearrangements that recruit PDK1 to the C-tail as the critical step in AGC kinase activation.

2.3 Results

Defect in PKC Maturation Upon Loss of mTORC2

cPKC priming phosphorylations (Figure 2.1A), enzymatic activity, and cellular stability are dependent upon mTORC2 (Facchinetti et al., 2008; Ikenoue et al., 2008). To assess the nature of the mTOR requirement, we characterized PKC function in Sin1 KO ($Sin1^{-/-}$) and Rictor KO ($Ric^{-/-}$) mouse-embryonic fibroblasts (MEFs), which lack critical components of the mTORC2 complex and abolish mTORC2 function (Guertin et al., 2006; Jacinto et al., 2006). Endogenous PKC phosphorylation at the activation loop, turn motif, and hydrophobic motif sites was ablated in both Sin1 KO and Rictor KO MEFs, which could not be rescued by agonist stimulation, targeting to the plasma membrane, or protecting PKC phosphorylations with active-site inhibitors (Gould et al., 2011) (Figure 2.1B; Figure 2.8B, 2.8C, 2.8E). Accordingly, basal and agonist-evoked cellular PKC activity was also dramatically reduced in Sin1 KO MEFs compared

to WT MEFs using the C Kinase Activity Reporter (CKAR) (Ross et al., 2018; Violin et al., 2003) (Figure 2.1C, Figure 2.8A). Consistent with dependence upon mTORC2, but not mTORC1 (Jacinto et al., 2004; Sarbassov et al., 2004), overexpressed PKCβII was sensitive to mTORC1/2 inhibitor Torin, but not mTORC1 inhibitor Rapamycin, and PKC phosphorylation deficiency in Sin1 KO MEFs was rescued by expression of Sin1 (Figure 2.1D).

To further characterize the PKC defect in the absence of mTORC2, we used a live-cell PKC conformation reporter, Kinameleon, which reads out intramolecular PKC rearrangements that alter FRET between flanking CFP and YFP molecules (Antal et al., 2014). Using this reporter, we have previously shown that PKC maturation by phosphorylation induces an increase in the FRET emission of the reporter, which is dependent upon hydrophobic motif phosphorylation, PKC catalytic activity, and the autoinhibitory pseudosubstrate (Baffi et al., 2019). Furthermore, only mature PKC which has become appropriately primed can undergo a further conformational transition to the high-FRET active state upon agonist stimulation (Baffi et al., 2019). Consistent with a role for mTORC2 in PKC priming, Sin1 KO MEFs expressing PKCβII-Kinameleon displayed reduced FRET compared to those reconstituted with Sin1, similar to cells expressing catalytically-dead PKCβII (K371R, KD) (Figure 2.1E). Neither did Sin1 KO MEFs expressing PKCβII-Kinameleon show a FRET change in response to PDBu stimulation, whereas Sin1 KO MEFs reconstituted with Sin1 displayed the characteristic FRET increase of that observed in WT MEFs (Figure 2.1F). As an additional measure of the PKC folding deficiency in the absence of mTORC2, we used a FRET-based translocation assay to assess PKC ligand sensitivity in live cells. We have previously shown that compared to properly primed enzyme, which is recruited to membranes relatively slowly due to efficient masking of its ligand-binding domains in the autoinhibited conformation, unprimed PKC exhibits a roughly 5-fold faster translocation rate

upon agonist stimulation, owing to the increased accessibility of the C1 domains (Antal et al., 2014). Accordingly, PKCβII translocated more rapidly in Sin1 KO MEFs ($WT^{-/-}$) than in +/+ MEFs ($WT^{+/+}$) or in Sin1 KO MEFs reconstituted with Sin1 ($WT^{-/-}$ +Sin1) (Figure 2.1G; $t_{1/2}$= 1.10 ± 0.08 min versus 8.2 ± 0.3 min and 6.1 ± 0.4 min, respectively). Compared to PKC in WT MEFs, PKC in Sin1 KO MEFs was observed to rapidly redistribute from the cytosol to the plasma membrane upon PDBu-stimulation, which was rescued by Sin1 expression in Sin1 KO MEFs (Figure 2.1H). To confirm that enhanced PKC translocation in mTORC2-deficient cells was due to impaired masking of the C1 domains, we introduced a mutation in the ligand-binding site of the PKCβII C1A domain that impairs the ability to bind phorbol esters (Antal et al., 2014; Dries et al., 2007). Rapid PKCβII translocation in Rictor KO MEFs ($WT^{Ric-/-}$) was identical to that of kinase-dead PKCβII mutant D466N in +/+ MEFs ($D466N^{+/+}$); however, mutation of the C1A domain to impair phorbol ester binding slowed the rate of translocation in Rictor KO MEFs ($W58Y^{Ric-/-}$) (Figure 2.8D). Mutating the C1A domain in +/+ MEFs ($W58A^{+/+}$), however, had no effect on PKC translocation due to effective masking of this domain in the primed conformation (Figure 2.8D). Since loss of hydrophobic motif phosphorylation rendered PKC incapable of adopting the primed conformation (Baffi et al., 2019) and PKC phosphorylation was reduced upon loss of mTORC2, we reasoned that phosphomimetic substitutions at the C-tail phosphorylation sites may permit proper folding and recover PKC translocation kinetics in mTORC2-deficient cells. Although Glu substitution at the turn and hydrophobic motif phospho-acceptor sites (T641E/S660E) exhibited normal translocation in +/+ MEFs ($EE^{+/+}$), the Glu substitution mutant displayed the same rapid translocation as WT PKCβII in the Sin1 KO MEFs ($EE^{-/-}$), suggesting that mTORC2 regulation of PKC conformation acts independently from phosphorylation of the C-tail sites (Figure 2.1G; $t_{1/2}$= 6.2 ± 0.3 min versus 2.3 ± 0.1 min

respectively).

We next addressed whether mTOR activity regulates the initial phosphorylation of newly-synthesized PKC or the steady-state phosphorylation of mature PKC. WT MEFs expressing PKCβII were subjected to a time-course of Torin treatment and analyzed for phosphorylation by electrophoretic mobility-shift analysis. The phosphorylation of mature PKC was surprisingly resistant to mTOR inhibition: 24 hrs of Torin treatment was not sufficient to achieve a comparable fraction of unphosphorylated PKC to that observed in Sin1 KO MEFs (Figure 2.1I). In contrast, the phosphorylation of mTORC1 substrate S6K1 was abolished within 1 hr of mTOR inhibition (Figure 2.8G). Reasoning that mTORC2 may exclusively regulate the phosphorylation of nascent PKC, we performed a time-course of mTOR inhibition in the presence of the protein synthesis inhibitor, cycloheximide (CHX). Upon addition of CHX, the Torin-dependent accumulation of unphosphorylated PKC was blocked at all timepoints (Figure 2.1J). Importantly, the hydrophobic motif phosphorylation of S6K1 was rapidly lost upon mTOR inhibition in the presence of CHX, suggesting a distinct regulatory mechanism for S6K1 and mTORC1 (Figure 2.1J). To investigate the role of mTORC2 in PKC phosphorylation during maturation, we performed pulse-chase analysis to monitor the pool of newly-synthesized PKC. Following synthesis, PKC undergoes an electrophoretic mobility shift corresponding to the tightly-coupled phosphorylation of the turn and hydrophobic motifs with a half-time of approximately 30 min (the activation loop phosphorylation does not cause a mobility shift) (Borner et al., 1989). mTOR inhibition during maturation retarded PKC progression to the phosphorylated species, similar to the effect of a kinase-deficient PKC mutant (Figure 2.1K). Since mTOR activity is critical for processing both the turn motif and hydrophobic motif sites, we next asked which phosphorylation site was rate-limiting with respect to mTOR activity. To assess whether phosphorylation of the turn mo-

tif or the hydrophobic motif is the rate-determining step of PKC maturation, phosphomimetic mutants of the turn (T641E) or hydrophobic (S660E) motifs were subjected to pulse-chase analysis. Interestingly, while both PKC phosphomimetic mutants progressed to the phosphorylated species in untreated conditions, neither mutant became phosphorylated upon mTOR inhibition (Figure 2.1L). Thus, negative charge at neither the turn nor hydrophobic motif was sufficient to bypass the requirement for mTOR activity, suggesting that phosphorylation of neither site is rate-limiting. Taken together, mTORC2 regulates PKC conformation, activity, and the rate-limiting step of PKC phosphorylation independently of phosphorylation at either the turn motif or hydrophobic motif sites.

Figure 2.1: **Defect in PKC Maturation Upon Loss of mTORC2.**
(A) Diagram of cPKC secondary structure showing kinase domain (cyan), C-terminal tail (C-tail, grey), C2 domain (yellow), C1 domains (orange), and pseudosubstrate (PS, red). Three constitutive phosphorylations at the activation loop (magenta), turn motif (orange), and hydrophobic motif (green) are shown as circles.
(B) Immunoblot (IB) of triton-solubilized lysates from WT (+/+), Rictor KO (*Ric*$^{-/-}$), or Sin1 KO (*Sin1*$^{-/-}$) MEFs probed with the indicated antibodies.
(C) PKC activity in WT (+/+) or Sin1 KO (*Sin1*$^{-/-}$) cells expressing CKAR2 and treated with PDBu (200nM). Data represent the normalized FRET ratio changes (mean ± SEM) from 3 independent experiments.
(D) IB of triton-solubilized lysates from WT (+/+), Rictor KO (*Ric*$^{-/-}$), or Sin1 KO (*Sin1*$^{-/-}$) MEFs, expressing YFP-PKCβII and HA-Sin1, treated with Rapamycin (10nM) or Torin (200nM), and probed with the indicated antibodies.
(E) Basal PKC conformation analyzed by the FRET ratio (mean ± SEM) of WT (+/+) or Sin1 KO (*Sin1*$^{-/-}$) MEFs expressing PKCβII Kinameleon C wild-type (WT) or kinase-dead K371R (KD), and HA-Sin1. Each data point represents the FRET ratio from individual cells relative to the average maximum signal.
(F) PKC conformation dynamics analyzed by FRET ratio changes (mean ± SEM) of WT (+/+) or Sin1 KO (-/-) MEFs expressing PKCβII Kinameleon C wild-type (WT) or kinase-dead K371R (KD), and HA-Sin1 and treated with PDBu (200nM).
(G) PKC translocation analysis of mYFP-PKCβII WT or T641E/S660E (EE) monitored by FRET ratio changes (mean ± SEM) in WT (+/+) or Sin1 KO (-/-) MEFs co-expressing myristoylated-palmitoylated mCFP and HA-Sin1, and treated with PDBu (100nM).
(H) PKC translocation analysis monitored by live-cell YFP-channel fluorescence images of WT (+/+) or Sin1 KO (*Sin1*$^{-/-}$) MEFs expressing PKCβII Kinameleon C and HA-Sin1, and treated with PDBu (200nM) for the indicated timepoints.
(I) IB mobility shift analysis of triton-solubilized lysates from WT (+/+) MEFs expressing PKCβII for 24hrs prior to Torin treatment (250nM).
(J) IB mobility shift analysis of triton-solubilized lysates from COS7 cells expressing PKCβII for 24hrs prior to treatment with Torin (250nM) and Cycloheximide (250μM) for the indicated times prior to lysis.
(K) Autoradiograph (^{35}S) and IB analysis of newly synthesized PKC pulse-chase HA immunoprecipitates from COS7 cells expressing HA-PKCβII WT or K371R (Kinase-Dead) and treated with Torin (250nM) during the chase.
(L) Autoradiograph (^{35}S) and IB analysis of newly synthesized PKC pulse-chase HA immunoprecipitates from WT MEFs expressing the indicated PKCβII constructs and treated with Torin (250nM) during the chase.
In immunoblots, the double asterisk (**) denotes the position of mature, fully phosphorylated PKC; the single asterisk (*) denotes the position of PKC phosphorylated at either the turn motif or hydrophobic motif; and the dash (-) indicates the position of unphosphorylated PKC. ****p < 0.0001 by Student's t-test.

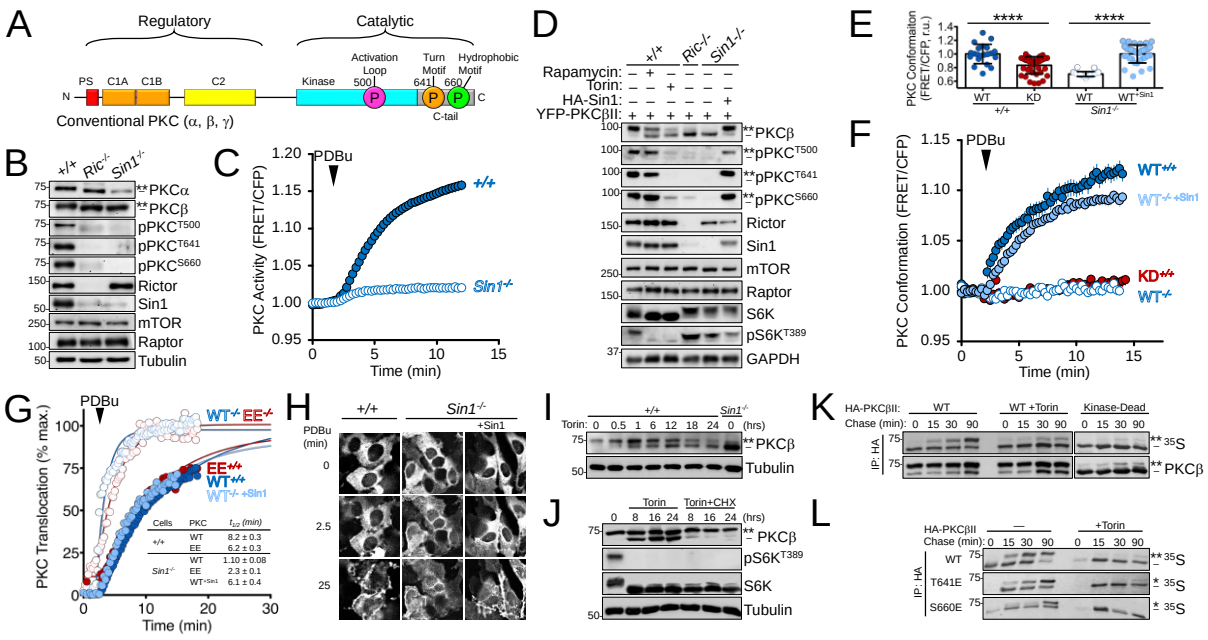
A
Regulatory
Catalytic
PS
C1A
C1B
C2
Kinase
Activation Loop
Turn Motif
Hydrophobic Motif
500
641
660
N
C
C-tail
Conventional PKC (α, β, γ)
B
+/+
Ric-/-
Sin1-/-
**PKCα
**PKCβ
pPKCT500
pPKCT641
pPKCS660
Rictor
Sin1
mTOR
Raptor
Tubulin
C
PDBu
+/+
Sin1-/-
PKC Activity (FRET/CFP)
Time (min)
D
Rapamycin:
Torin:
HA-Sin1:
YFP-PKCβII:
**PKCβ
**pPKCT500
**pPKCT641
**pPKCS660
Rictor
Sin1
mTOR
Raptor
S6K
pS6KT389
GAPDH
E
PKC Conformation (FRET/CFP, r.u.)
****
****
WT
KD
WT
WT+Sin1
+/+
Sin1-/-
F
PDBu
PKC Conformation (FRET/CFP)
Time (min)
WT+/+
WT-/- +Sin1
KD+/+
WT-/-
G
PDBu
PKC Translocation (% max.)
Time (min)
WT-/- EE-/-
EE+/+
WT+/+
WT-/- +Sin1
Cells
PKC
t1/2 (min)
+/+
WT
8.2 ± 0.3
EE
6.2 ± 0.3
Sin1-/-
WT
1.10 ± 0.08
EE
2.3 ± 0.1
WT+Sin1
6.1 ± 0.4
H
+/+
Sin1-/-
+Sin1
PDBu (min)
0
2.5
25
I
+/+
Sin1-/-
Torin:
0 0.5 1 6 12 18 24 0 (hrs)
**PKCβ
Tubulin
J
Torin
Torin+CHX
0 8 16 24 8 16 24 (hrs)
**PKCβ
pS6KT389
S6K
Tubulin
K
HA-PKCβII:
WT
WT +Torin
Kinase-Dead
Chase (min):
0 15 30 90 0 15 30 90 0 15 30 90
IP: HA
**35S
**PKCβ
L
HA-PKCβII
—
+Torin
Chase (min):
0 15 30 90 0 15 30 90
IP: HA
WT
T641E
S660E
**35S
*35S
*35S

PDK1 Overexpression Bypasses mTORC2 Dependence of PKC and Akt

Given that mTORC2-deficiency abrogates all three constitutive PKC phosphorylations, we hypothesized that the known activation loop kinase, PDK1, may be involved in mTORC2 regulation of PKC (Dutil et al., 1998; Le Good et al., 1998). To address whether PDK1 and mTORC2 cooperate to effect the rate-limiting step of PKC phosphorylation, we asked whether PDK1 overexpression rescues the processing defect upon mTOR inhibition. Whereas pulse-chase of PKC in the presence of Torin blocked the mobility shift to the phosphorylated species, overexpression of PDK1 in Torin-treated cells recovered PKC processing (Figure 2.2A). This effect was dependent upon PDK1 catalytic activity, as kinase-dead PDK1 mutant K110N (kdPDK1) did not restore the phosphorylation of newly-synthesized PKC (Figure 2.2A). The phosphorylated PKC species observed upon PDK1 rescue appeared as an intermediate mobility band between the unphosphorylated and fully phosphorylated PKC, suggestive of differential phosphorylation at the C-tail. Analysis of PKCβII phosphorylation state in +/+ MEFs treated with Torin or in Sin1 KO MEFs revealed that PDK1 expression rescued PKC phosphorylation at the activation loop and hydrophobic motif, but not the turn motif site (Figure 2.2B). Importantly, PKC catalytic activity was required for the rescue of hydrophobic motif phosphorylation, as kinase-dead mutant PKCβII K371R (kdPKC) did not become phosphorylated upon expression of PDK1 (Figure 2.2B). The PDK1-mediated rescue of PKC activation loop and hydrophobic motif phosphorylation in the absence of mTORC2 was also observed in Torin-treated COS7 cells and Rictor KO MEFs (Figure 2.11A, 2.11C). Supporting PDK1-mediated rescue of PKC function in the absence of mTORC2, PDK1 expression in Torin-treated WT MEFs or Sin1 KO MEFs restored PDBu-stimulated PKC activity; whereas, expression of kinase-dead PDK1 displayed no or worsened effect (Figure 2.2C). Thus, PDK1 supplementation bypasses the mTORC2-requirement for

PKC activation by promoting phosphorylation at the activation loop and hydrophobic motif in a manner dependent upon both PDK1 and PKC catalytic activity.

The AGC kinase family member, Akt, is also regulated by PDK1 and mTORC2 (Alessi et al., 1997; Sarbassov et al., 2005), so we next assessed whether PDK1 was capable of rescuing mTORC2-dependent Akt phosphorylation. The isolated catalytic domain of Akt1 is not appreciably phosphorylated in Sin1 KO cells; however, Sin1 reconstitution induces robust phosphorylation at the turn and hydrophobic motif sites (Figure 2.2D). As seen for PKC, PDK1 expression induced Akt1 phosphorylation exclusively at the activation loop and hydrophobic motif sites (Figure 2.2D). This effect also required the catalytic activity of both PDK1 and Akt: introduction of kinase-dead mutations in either PDK1 (K110N; kdPDK1) or Akt1 (K368M; kdAkt) abrogated the rescue of hydrophobic motif phosphorylation (Figure 2.2D). Activation loop phosphorylation of catalytically impaired Akt was only partially rescued, likely due to the fact that hydrophobic motif phosphorylation stabilizes phosphate on the activation loop (Chan et al., 2015). Thus, PDK1 cooperates with mTORC2 to regulate PKC and Akt activity and compensates for mTORC2-deficiency by promoting activation loop and hydrophobic motif phosphorylation, dependent upon both PDK1 catalytic activity and intrinsic PKC/Akt catalytic activity (Figure 2.2E).

Figure 2.2: **PDK1 Overexpression Bypasses mTORC2 Dependence of PKC and Akt.**
(A) Autoradiograph (^{35}S) and IB analysis of newly synthesized PKC pulse-chase HA immunoprecipitates from COS7 cells expressing FLAG-PKCβII and FLAG-PDK1, and treated with Torin (250nM) during the chase.
(B) IB analysis of triton-solubilized lysates or FLAG immunoprecipitates from WT (+/+) or Sin1 KO (*Sin1*$^{-/-}$) MEFs expressing FLAG-PKCβII WT or kinase-dead K371R (kd), FLAG-PDK1WT or kinase-dead K110N (kd), and HA-Sin1. Cells were treated with or without Torin (200nM) during transfection for 24hrs prior to lysis. (right) Quantification of PKC phosphorylation reflects the percentage of the faster mobility species phosphorylated at the hydrophobic motif (S660).
(C) PKC activity in WT (+/+) or Sin1 KO (*Sin1*$^{-/-}$) MEFs expressing CKAR2 and mCherry-PKCβII, and treated with PDBu (200nM). Data represent the normalized FRET ratio changes (mean ± SEM) from three independent experiments. (right) Quantification of PKC activity reflects the normalized area under the curve (AUC; mean ± SEM) 10min after PDBu treatment.
(D) IB analysis of triton-solubilized lysates or FLAG immunoprecipitates from Sin1 KO (*Sin1*$^{-/-}$) MEFs expressing FLAG-Akt1 catalytic domain (141-480) WT or kinase-dead K179M (kd), FLAG-PDK1 WT or kinase-dead K110N (kd), and HA-Sin1. (right) Quantification of Akt phosphorylation reflects the normalized phospho-signal relative to total Akt for the activation loop (pThr^{308}), turn motif (pThr^{450}), or hydrophobic motif (pSer^{660}).
(E) Schematic of mTORC2 and PDK1 function in the phosphorylation of PKC and Akt: (left) mTORC2-containing cells produce kinase that is phosphorylated at the activation loop (AL), Turn Motif (TM), and Hydrophobic Motif (HM); (middle) mTORC2-deficient cells produce kinase with impaired phosphorylation at all three sites; (right) PDK1 overexpression in mTORC2-deficient cells rescues phosphorylation at the AL and HM, but not the TM.
In immunoblots, the double asterisk (**) denotes the position of mature, phosphorylated PKC; the single asterisk (*) denotes the position of PKC phosphorylated at the hydrophobic motif, and the dash (-) indicates the position of unphosphorylated PKC. Immunoblots represent the average of at least three independent experiments. *$p < 0.05$, **$p < 0.01$, ***$p < 0.001$, ****$p < 0.0001$ by One-way ANOVA and Tukey HSD Test. IB quantifications represent the mean ± SEM from at least 3 independent experiments.

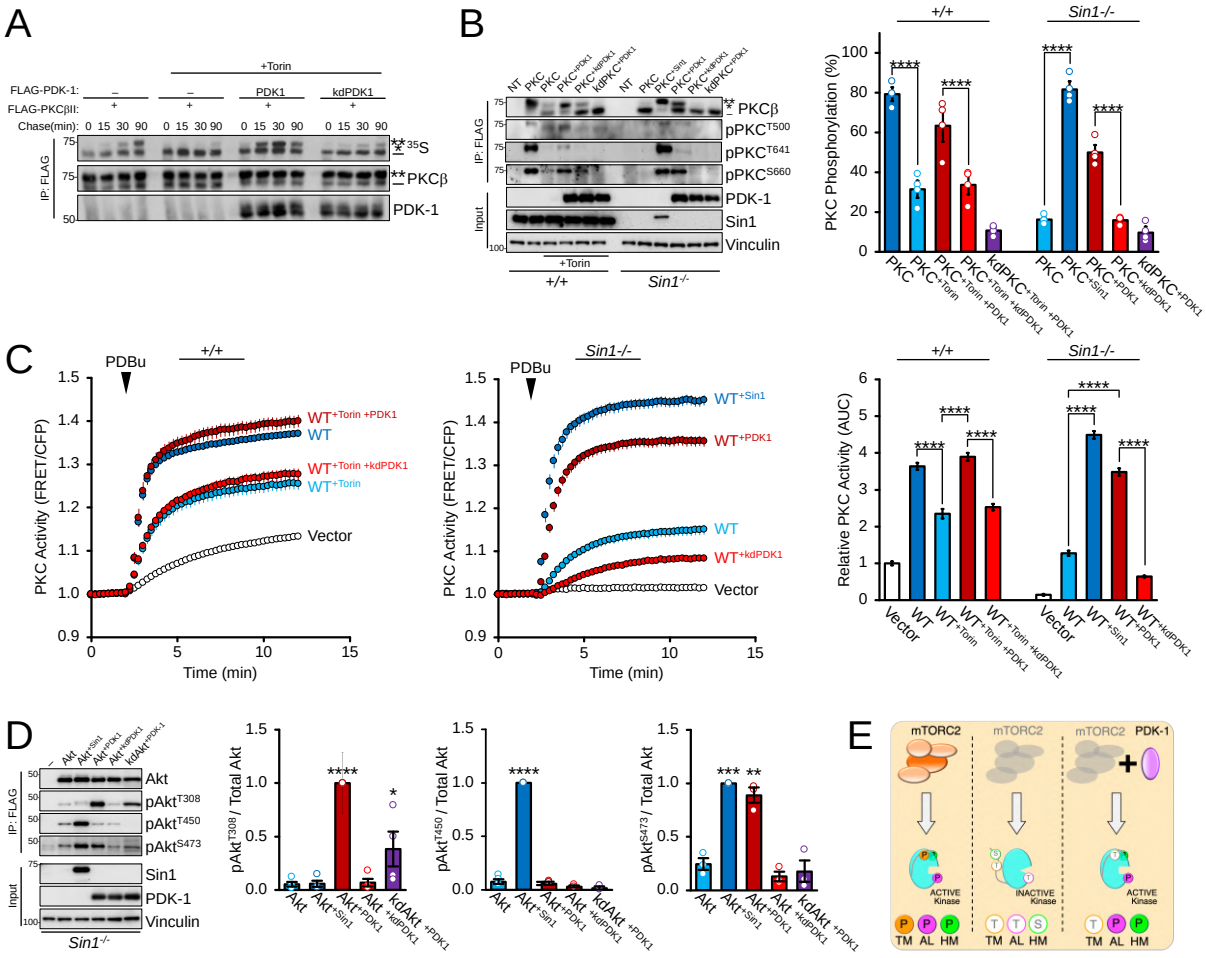
A
+Torin
FLAG-PDK-1:
FLAG-PKCβII:
Chase(min): 0 15 30 90 0 15 30 90 0 15 30 90 0 15 30 90
PDK1
kdPDK1
IP: FLAG
**35S
*PKCβ
PDK-1
B
NT PKC PKC PKC+PDK1 PKC+kdPDK1 kdPKC+PDK1
IP: FLAG
Input
*PKCβ
pPKCT500
pPKCT641
pPKCS660
PDK-1
Sin1
Vinculin
+Torin
+/+
Sin1-/-
PKC Phosphorylation (%)
C
PDBu
+/+
Sin1-/-
PKC Activity (FRET/CFP)
Time (min)
WT+Torin +PDK1
WT
WT+Torin +kdPDK1
WT+Torin
Vector
WT+Sin1
WT+PDK1
WT+kdPDK1
Relative PKC Activity (AUC)
D
IP: FLAG
Input
Akt
pAktT308
pAktT450
pAktS473
Sin1
PDK-1
Vinculin
Sin1-/-
pAktT308 / Total Akt
pAktT450 / Total Akt
pAktS473 / Total Akt
E
mTORC2
PDK-1
ACTIVE Kinase
INACTIVE Kinase
TM AL HM

Structural Divergence and mTORC2 Binding Site in the PKC C-tail Confer mTORC2 Dependence

That the PKC and Akt turn motif phosphorylations are mTORC2-dependent but cannot be rescued by PDK1 overexpression suggests that this site is a direct target of mTOR. This finding, however, does not explain how mTOR activates these kinases, as the turn motif phosphorylation is neither necessary nor sufficient to substitute for loss of mTORC2. In order to identify critical regions for mTOR-mediated PKC activation, we pursued a structural approach to map the mTORC2 binding site on PKC. Pulse-chase and co-immunoprecipitation analysis demonstrated that mTOR physically associates with PKCβII during processing and binds exclusively to the faster electrophoretic mobility, unphosphorylated species of PKC (Figure 2.3A, Figure 2.9A). Pulldown studies with the isolated PKCβII domains revealed that mTOR most robustly associates with the PKC catalytic domain (Figure 2.9B). Thus, in order identify mTORC2 binding sites, the PKCβII catalytic domain sequence (296-673) was walked on a peptide array and overlaid with cell lysate expressing mTORC2 component Sin1 or the mTOR kinase (Figure 2.9C). Both components bound strongly to the active-site tether and hydrophobic motif regions in the C-tail (Figure 2.3B, Figure 2.9C). Alanine scans of the identified sequences implicated several Phe residues comprising the respective motifs that were critical for binding (Figure 2.3B). Since the hydrophobic motif binding site contained the phospho-acceptor Ser, we asked if phosphorylation at this site affected mTOR binding. Compared to peptide array sequences with unmodified Ser at the hydrophobic motif, those containing phosphorylation of the PKCβII hydrophobic motif ($pSer^{660}$) abolished mTOR binding (Figure 2.3B). Thus, mTORC2 recognizes conserved motifs in the PKC C-tail to bind newly-synthesized, unphosphorylated PKC.

Next, we took advantage of the diversity of the greater PKC family to investigate how

mTORC2 regulates only a subset of kinases despite recognizing conserved motifs. While six PKC isozymes require mTORC2 for phosphorylation; three novel PKCs (δ, η, θ) are mTORC2-independent (Ikenoue et al., 2008). Yet, motif analysis of the C-tail active-site tether and hydrophobic motif revealed a high degree of conservation among these enzymes, including residues critical for mTORC2 binding that are conserved broadly across AGC kinases (Crooks et al., 2004; Kannan et al., 2007) (Figure 2.3C). Therefore, to determine the structural basis for mTORC2 dependence, PKCδ/β chimeras were engineered that contained sequence from mTORC2-dependent and -independent isozymes to assess the sequence requirements for mTORC2 dependence (Figure 2.3C). Whereas PKCβII turn motif and hydrophobic motif phosphorylation were exquisitely sensitive to either mTOR inhibition (+/+, Torin) or ablation (*Sin1*$^{-/-}$), PKCδ was insensitive (Figure 2.3D). Replacement of the C-terminal 25 amino acids of PKCδ with those of PKCβII, such that the chimera contained the hydrophobic motif of PKCβII (PKCδ/β HM), had no effect on mTORC2 dependence (Figure 2.3D). Substitution of the C-terminal 45 amino acids to include the PKCβII turn motif and hydrophobic motif phosphorylation sites (PKCδ/β TM), however, induced mTORC2 sensitivity of the turn motif, but not the hydrophobic motif (Figure 2.3D). Underscoring the dispensability of the turn motif for activity and processing, this enzyme retained cellular catalytic activity and phosphorylation kinetics upon mTOR inhibition, similar to that of PKCδ (Figure 2.9D, 9E, 9F). To confirm the differential regulation of the turn motif and hydrophobic motif phosphorylations by mTORC2, an identical chimera between mTORC2-independent PKCθ and PKCβII (PKCθ/β TM) produced the same result: the PKCβII turn motif, but not hydrophobic motif, phosphorylation became mTORC2-dependent when fused to an mTORC2-independent PKC at the active-site tether (Figure 2.9G). Extending the junction a further seven residues or more to include the entire PKCβII active-site tether

(PKCδ/β AST), however, resulted in a chimera that was dependent upon mTORC2 for turn motif and hydrophobic motif phosphorylation (Figure 2.3D, Figure 2.9G). The residues preceding the active-site tether of AGC kinase differ substantially despite a high degree of structural similarity (Taylor and Kornev, 2011); Asp^{629} in PKCδ and many mTORC2-independent kinases, for example, is not conserved in mTORC2-dependent enzymes (PKCβII Asn^{625}). This residue in PKA (Asp^{323}), is necessary for catalytic activity, despite the lack of a defined role in catalysis (Gibbs and Zoller, 1991). Accordingly, an Asp to Asn mutation in the turn motif PKC chimera (PKCδ/β TM D625N) converted the hydrophobic motif to an mTORC2-dependent phosphorylation site (Figure 2.3D), suggesting that the structural integrity of the active-site tether is critical for mTORC2-independent hydrophobic motif phosphorylation.

To ascertain the role of the active-site tether in mTORC2-dependence, we compared the structures of various AGC kinase C-tails (van Eis et al., 2011; Knighton et al., 1991; Leonard et al., 2011; Lin et al., 2012; Xu et al., 2004) (Figure 2.3E). Unexpectedly, the high degree of structural complementarity in the C-tail of AGC kinases diverges exclusively in PKCβII to form an α-helix in place of the highly conserved active-site tether (Leonard et al., 2011; Taylor et al., 2012) (Figure 2.3E). Whereas the conserved Asp that confers mTORC2-independent hydrophobic motif phosphorylation forms contacts to structure the apex of the active-site tether, the PKCβII novel helix is clamped down by the C1B domain at this position in the full-length structure (Figure 2.3F). Taken together, PKC chimeras and structural analysis reveal distinct regulation of the turn and hydrophobic motif sites by mTORC2, wherein mTORC2-dependence of the turn motif is regulated at the level of the phosphorylation site sequence, and the structural integrity of a canonical active-site tether confers mTORC2-independent phosphorylation of the hydrophobic motif.

Figure 2.3: **Structural Divergence and mTORC2 Binding Site in the PKC C-tail Confer mTORC2 Dependence.**
(A) Co-immunoprecipitation autoradiograph (^{35}S) and IB analysis of newly synthesized PKC pulse-chase HA or Myc immunoprecipitates from COS7 cells expressing HA-PKCβII and Myc-mTOR. The double asterisk (**) denotes the position of mature, fully phosphorylated PKC and the dash (-) indicates the position of unphosphorylated PKC.
(B) (top) IB analysis of 1-step, 15-mer peptide arrays of the PKCβII C-tail overlaid with triton-solubilized lysate from WT MEFs expressing HA-Sin1 or Myc-mTOR and probed with antibodies for Sin1 (HA) or mTOR (Myc). (right) Peptide arrays of the indicated hydrophobic motif sequences were generated with phospho-serine (pS) or unphosphorylated serine (S) and probed for mTOR as described. (bottom) Alanine-scans of the indicated C-tail peptides and probed for Sin1 and mTOR as described.
(C) (left) Schematic of mTORC2-dependent and independent PKC isozymes. (top) Schematic of PKCδ/PKCβII chimeras (PKCδ/β), indicating the location of the junction (PKCβII numbering) of the N-terminal PKCδ sequence (blue) and C-terminal PKCβII sequence (red). The position of the turn motif (orange) and hydrophobic motif (green) phosphorylations are indicated. (bottom) Motif analysis of the C-terminal tail for 3 mTORC2-dependent cPKCs (α,β,γ) and 3 mTORC2-independent nPKCs (δ,θ,η).
(D) IB of triton-solubilized lysates from WT (+/+) or Sin1 KO (-/-) MEFs expressing mCherry-tagged PKCδ, PKCβII, or indicated PKCδ/β chimera treated with Torin (250nM) and probed with antibodies against the PKCβ (pThr^{641}) or PKCδ (pSer^{645}) turn motif, hydrophobic motif (pSer^{660}), and total PKC (dsRED).
(E) Alignment of the kinase domain (space-filling, white) and C-tail (cartoon, color) from crystal structures of PKCβII (PDB ID: 3PFQ), PKCθ (PDB ID: 1XJD), PKCη (PDB ID: 3TXO), Akt1 (PDB ID: 4EKL), and PKA (PDB ID: 2CPK) with indicated structural features. **(F)** (top) Alignment of the C-tail from crystal structures of PKCβII (PDB ID: 3PFQ) and PKCθ (PDB ID: 5F9E) showing the positions of the PKCδ/β chimera junctions and (bottom) the position of the C1B domain in the full-length PKCβII structure

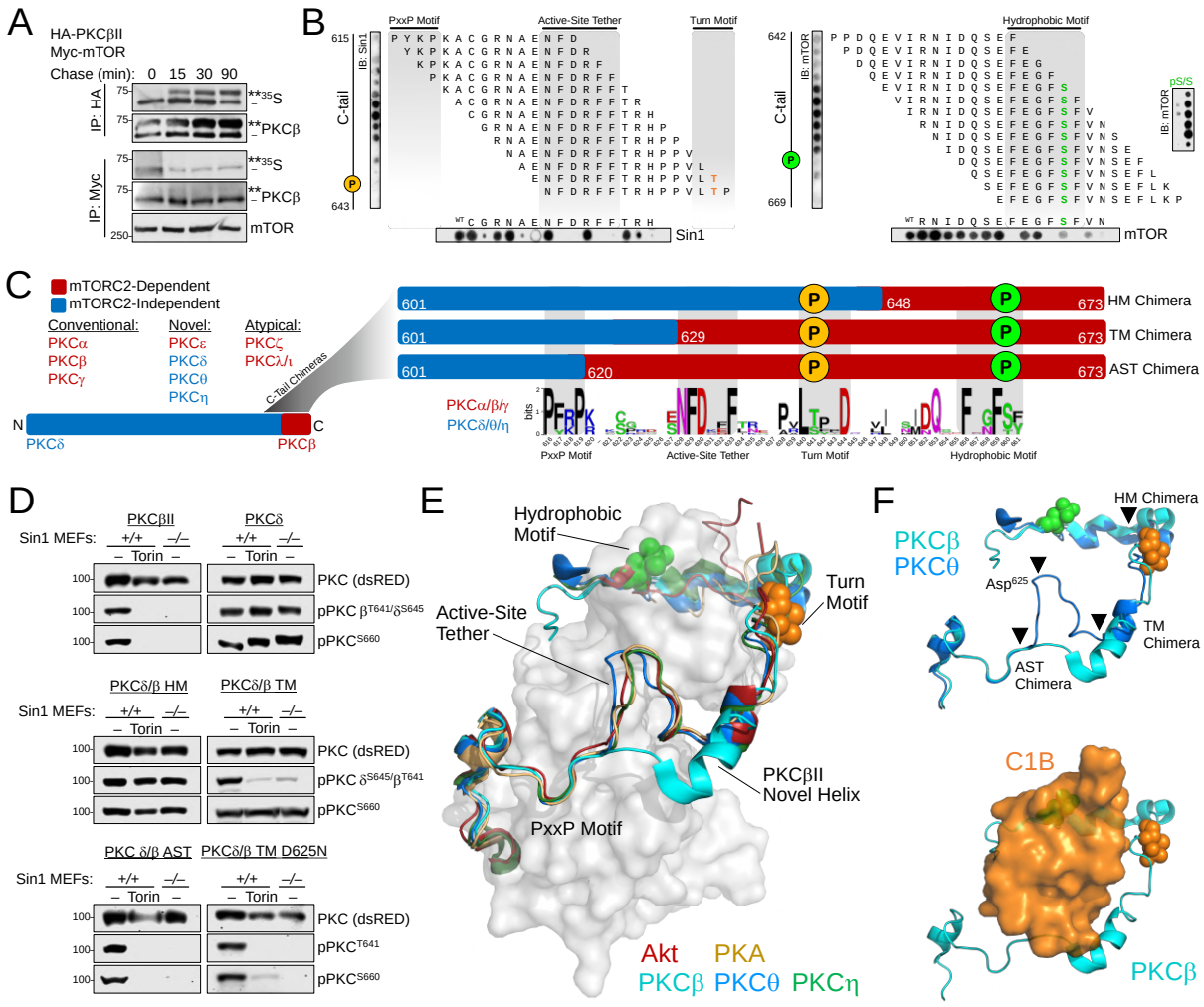
A
HA-PKCβII
Myc-mTOR
Chase (min): 0 15 30 90
IP: HA
IP: Myc
**35S
**PKCβ
mTOR
B
PxxP Motif
Active-Site Tether
Turn Motif
Hydrophobic Motif
C-tail
IB: Sin1
IB: mTOR
pS/S
Sin1
mTOR
C
mTORC2-Dependent
mTORC2-Independent
Conventional:
PKCα
PKCβ
PKCγ
Novel:
PKCε
PKCδ
PKCθ
PKCη
Atypical:
PKCζ
PKCλ/ι
C-Tail Chimeras
N
C
PKCδ
PKCβ
HM Chimera
TM Chimera
AST Chimera
PKCα/β/γ
PKCδ/θ/η
bits
D
PKCβII
PKCδ
Sin1 MEFs:
+/+
–/–
– Torin –
PKC (dsRED)
pPKC βT641/δS645
pPKCS660
PKCδ/β HM
PKCδ/β TM
pPKC δS645/βT641
PKCδ/β AST
PKCδ/β TM D625N
pPKCT641
E
Hydrophobic Motif
Turn Motif
Active-Site Tether
PKCβII Novel Helix
PxxP Motif
Akt
PKA
PKCβ
PKCθ
PKCη
F
HM Chimera
PKCβ
PKCθ
Asp625
TM Chimera
AST Chimera
C1B
PKCβ

TOR-Interaction Motif Phosphorylation is Critical for PKC and Akt Activity

Although mTORC2 independently regulates PKC turn motif and hydrophobic motif phosphorylation, neither site is rate-limiting for PKC maturation, suggesting that this process depends upon a distinct phosphorylation event. Consequently, we utilized protein sequence alignments to identify novel mTORC2-regulated phosphorylation sites in the active-site tether that confer kinase activity. Surprisingly, we identified a conserved Thr preceding the turn motif phosphorylation site in the mTORC2 binding region of the active-site tether, which was present exclusively in mTORC2-dependent AGC kinases. (Turn Motif -7; Figure 2.4A). This residue is located in an invariant F-D-X_2-F-pT motif we term the TOR-Interaction Motif (TIM; Figure 2.4A). Kinome analysis (Metz et al., 2018) of AGC kinases that contain this motif include those reported to be mTOR-regulated such as the six PKC family members, as well as the Akt, SGK, and PKN family kinases (Figure 2.4B). Intriguingly, the mTORC1-regulated p70S6K family and two kinases not known to be regulated by mTOR, the MSK and RSK family kinases, also conserve the TOR-Interaction Motif (Figure 2.4B). To assess whether TIM phosphorylation was necessary for kinase function, we generated TIM site Ala mutants in PKCβII (T634A) and Akt1 (T443A) and assessed the effect of TIM mutation on cellular kinase activity and phosphorylation state. Although mutation of the TIM or turn motif alone had minimal effect on PKC cellular activity, the double mutation (AA; T634A/T641A) abolished PKC response to agonist (Figure 2.4C). Akt1 TIM mutation alone, however, was sufficient to abrogate enzymatic activity of the isolated catalytic domain, while turn motif mutation (T540A) had no effect (Figures 4D). The residues comprising the TOR-interaction motif did not appear to be involved in catalysis, so we next asked how TIM phosphorylation conferred kinase activity. Phosphorylation state analysis revealed a dramatic reduction in activation loop and hydrophobic motif phosphorylation of the inactive

PKC and Akt TIM mutants (Figure 2.4E and 2.4F). Interestingly, the PKN family members PKN1 and PKN2, showed greater dependence upon the turn motif site, and the effect of TIM mutation had opposite effects on activation loop phosphorylation in PKN1 and PKN2 (Figure 2.10A). These results establish the importance of phosphorylation sites in the active-site tether of AGC kinases and suggest that the precise function of these phosphorylations may vary between kinases.

Having established that the TIM site is critical for PKC and Akt activity, we next assessed whether TIM phosphorylation is regulated by mTOR. Inhibition of mTOR in HEK-293t cells expressing PKCβII effectively blocked TIM phosphorylation (pPKC$^{\mathrm{T634}}$) (Figure 2.4G). mTORC2 integrity was also required for TIM phosphorylation, as Sin1 KO MEFs expressing PKCβII lacked detectable phosphorylation at Thr^{634}, which was restored upon Sin1 reconstitution (Figure 2.4H). These experiments suggest that mTORC2-dependent TIM phosphorylation promotes activation loop and hydrophobic motif phosphorylation to facilitate PKC and Akt activation. Moreover, this finding clarifies the roles of the upstream kinases involved in PKC and Akt activation, providing evidence that direct mTOR phosphorylations at the TIM and turn motif sites promote PDK1 phosphorylation of the activation loop and autophosphorylation of the hydrophobic motif. (Figure 2.4I).

Figure 2.4: **TOR-Interaction Motif Phosphorylation is Critical for PKC and Akt Activity.**
(A) Sequence alignment of the active-site tether region indicating TOR-interaction motif (red) and turn motif (blue) phosphorylation sites for mTOR-dependent and independent AGC kinases.
(B) AGC kinase branch of the Kinome tree indicating the conservation of the TOR-interaction motif Thr.
(C) PKC activity in COS7 cells expressing CKAR2 and the indicated mCherry-PKCβII and treated with UTP (100μM) and PDBu (200nM). Data represent the normalized FRET ratio changes (mean ± SEM) from three independent experiments. (right) Quantification of PKC activity represents the normalized area under the curve (AUC; mean ± SEM).
(D) Akt activity in COS7 cells expressing BKAR and the indicated mCherry-Akt1 and treated with GDC-0068 (20μM). Data represent the normalized FRET ratio changes (mean ± SEM) from 3 independent experiments. Quantification (right) of PKC activity represents the normalized area under the curve (AUC; mean ± SEM).
(E) IB of triton-solubilized FLAG immunoprecipitates from HEK-293t cells expressing FLAG-PKCβII WT, T634A, T641A, or T634A/T641A (AA) and probed with the indicated antibodies. (right) Quantification of PKC phosphorylation (mean ± SEM) represents the percent of the faster-mobility, phosphorylated species.
(F) IB of triton-solubilized FLAG immunoprecipitates from HEK-293t cells expressing the catalytic domain (141-480) FLAG-Akt1 WT, T443A, or T450A and probed with the indicated antibodies. (right) Quantification of Akt phosphorylation (mean ± SEM) reflects the normalized phospho-signal relative to total Akt for the activation loop (pThr^{308}) or hydrophobic motif (pSer^{660}).
(G) IB analysis of whole-cell lysates from HEK-293t cells expressing FLAG-PKCβII, treated with Torin (250nM) for 36hrs co-transfection, and probed with the indicated antibodies. (right) Quantification reflects the normalized phospho-signal relative to total PKC for the TOR-interaction motif (pThr^{634}).
(H) IB analysis of triton-solubilized lysates and FLAG immunoprecipitates from WT (+/+) or Sin1 KO (*Sin1*$^{-/-}$) MEFs expressing FLAG-PKCβII and HA-Sin1 and probed with the indicated antibodies.
(I) Model of mTOR-dependent AGC kinase phosphorylation sites and their upstream kinases: PDK1 is the activation loop kinase, the TOR-interaction motif and turn motif are phosphorylated by mTOR, and the hydrophobic motif proceeds by intramolecular auto-phosphorylation.
**p < 0.01; ****p < 0.0001; n.s., not significant by One-way ANOVA and Tukey HSD Test or Student's t-test. IB quantifications represent the mean ± SEM from at least 3 independent experiments.

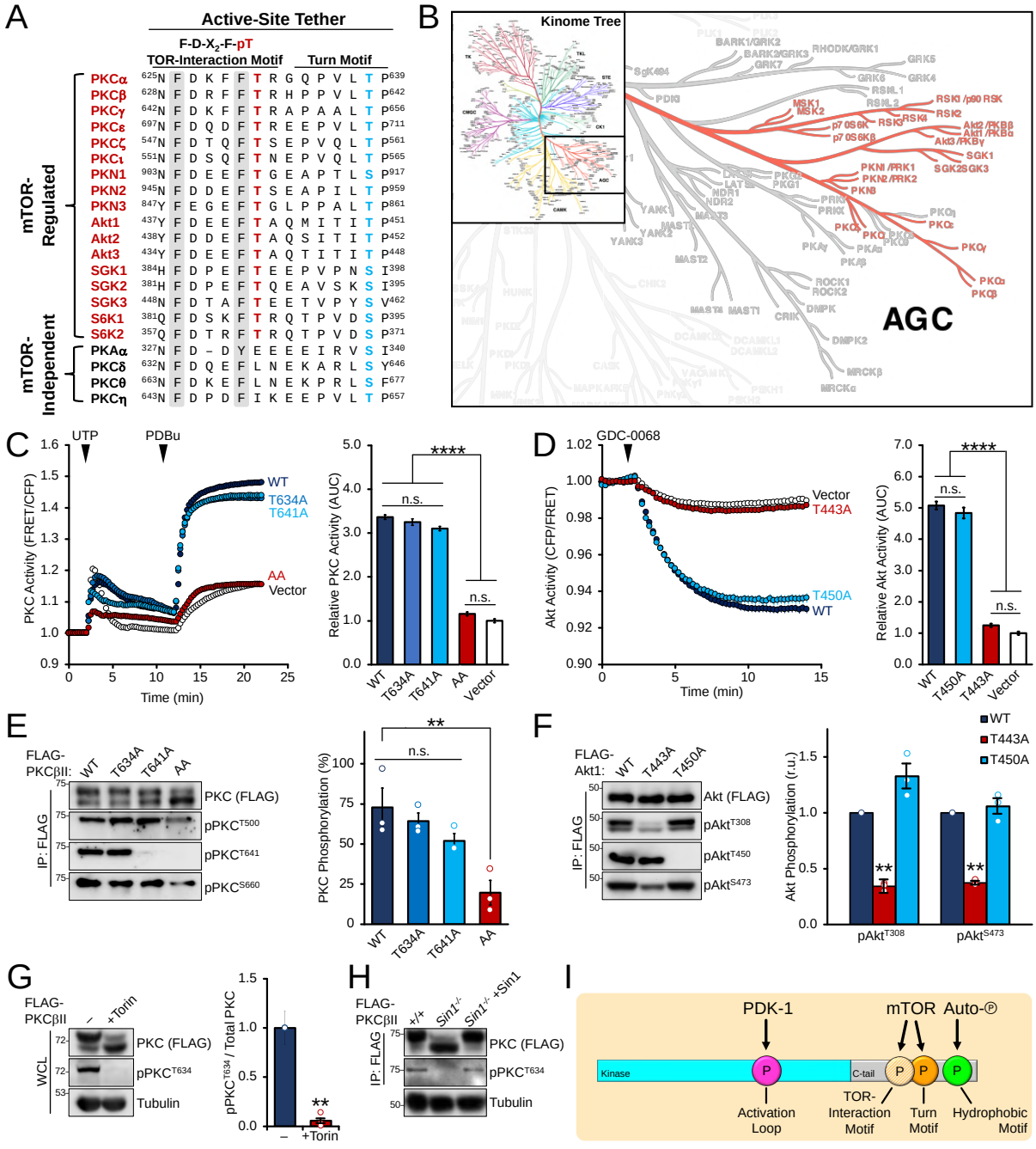
A
Active-Site Tether
F-D-X2-F-pT
TOR-Interaction Motif
Turn Motif
mTOR-Regulated
mTOR-Independent
PKCα 625N F D K F F T R G Q P V L T P639
PKCβ 628N F D R F F T R H P P V L T P642
PKCγ 642N F D K F F T R A P A A L T P656
PKCε 697N F D Q D F T R E E P V L T P711
PKCζ 547N F D T Q F T S E P V Q L T P561
PKCι 551N F D S Q F T N E P V Q L T P565
PKN1 903N F D E E F T G E A P T L S P917
PKN2 945N F D D E F T S E A P I L T P959
PKN3 847Y F E G E F T G L P P A L T P861
Akt1 437Y F D E E F T A Q M I T I T P451
Akt2 438Y F D D E F T A Q S I T I T P452
Akt3 434Y F D E E F T A Q T I T I T P448
SGK1 384H F D P E F T E E P V P N S I398
SGK2 381H F D P E F T Q E A V S K S I395
SGK3 448N F D T A F T E E T V P Y S V462
S6K1 381Q F D S K F T R Q T P V D S P395
S6K2 357Q F D T R F T R Q T P V D S P371
PKAα 327N F D – D Y E E E E I R V S I340
PKCδ 632N F D Q E F L N E K A R L S Y646
PKCθ 663N F D K E F L N E K P R L S F677
PKCη 643N F D P D F I K E E P V L T P657
B
Kinome Tree
AGC
C
UTP
PDBu
PKC Activity (FRET/CFP)
Time (min)
WT
T634A
T641A
AA
Vector
Relative PKC Activity (AUC)
****
n.s.
D
GDC-0068
Akt Activity (CFP/FRET)
Vector
T443A
T450A
WT
Relative Akt Activity (AUC)
E
FLAG-PKCβII:
IP: FLAG
PKC (FLAG)
pPKCT500
pPKCT641
pPKCS660
PKC Phosphorylation (%)
**
F
FLAG-Akt1:
Akt (FLAG)
pAktT308
pAktT450
pAktS473
Akt Phosphorylation (r.u.)
G
WCL
pPKCT634
Tubulin
pPKCT634 / Total PKC
–
+Torin
H
+/+
Sin1-/-
Sin1-/- +Sin1
I
PDK-1
mTOR
Auto-P
Kinase
C-tail
Activation Loop
TOR-Interaction Motif
Turn Motif
Hydrophobic Motif

mTORC2 Recruits PDK1 to the PKC C-tail

Given that mTORC2 and PDK1 cooperate to regulate the rate-limiting step of PKC phosphorylation, we hypothesized that mTOR activity may be facilitating PDK1 binding to PKC via TIM phosphorylation. For the AGC kinases S6K, RSK, and SGK, phosphorylation of the hydrophobic motif is a prerequisite for activation loop phosphorylation, which allows PDK1 to dock onto the C-tail via the PIF-pocket in the PDK1 N-lobe (Biondi et al., 2000, 2001). For PKC and Akt, however, PDK1 utilizes a hydrophobic groove in the PIF pocket, rather than the phosphate groove, to recognize the unphosphorylated hydrophobic motif (Collins et al., 2005). Supporting a role for mTORC2 in facilitating binding to unphosphorylated PKC, PDK1 preferentially bound the nascent, unphosphorylated PKC species two-fold better than the phosphorylated form; however, mTOR inhibition reduced PDK1's ability to associate with unphosphorylated PKC (Figure 2.12A). Thus, to determine how mTOR may be recruiting PDK1, we investigated the effect of TIM and turn motif phosphorylation on PDK1 binding. Peptide arrays of the PKC C-tail overlaid with Sin1 or PDK1 revealed that TIM and turn motif phosphorylation had little effect on the ability of either protein to bind the active site tether (Figure 2.5A). While both proteins displayed affinity for the active-site tether and the hydrophobic motif, Sin1 bound the active-site tether more strongly, whereas more robust hydrophobic motif association was observed for PDK1 (Figure 2.5A). In cellular immunoprecipitation assays, PDK1 associated with hydrophobic motif-phosphorylated PKCβII C-tail (601-673), which was abrogated by mutation of the hydrophobic motif but not of the TIM or turn motif (Figure 2.5B). Substitution of the TIM site with a negatively charged Glu did not confer PDK1 binding in the absence of hydrophobic motif phosphorylation, suggesting that mTOR regulation of PDK1 binding is mediated through the hydrophobic motif and is regulated at the level of C-tail accessibility, rather than

by altered binding affinity upon phosphorylation (Figure 2.5C). To assess whether mTORC2 promotes PDK1-mediated PKC processing via TIM phosphorylation, we tested the ability of PDK1 to rescue the function of the PKCβII TIM and turn motif mutant (T634A/T641A). The cellular activity of PKCβII T634A/T641 (AA) was enhanced by PDK1 expression, and further impaired by expression of kinase-dead mutant PDK1 K110N (kdPDK1) (Supplementary Figure 2.5D). Furthermore, while PKCβII T634A and T634E both impaired the ability of PDK-1 to rescue hydrophobic motif phosphorylation upon mTOR inhibition or loss of mTORC2, the defect in the T634A mutant was more severe (Figure 2.12B). As an additional measure that mTOR regulates PDK1 binding of PKC via accessibility of the PKC hydrophobic motif, PIF peptide, which binds the PDK1 hydrophobic docking site, the PIF pocket, with several orders of magnitude higher affinity than other AGC kinases, suppressed PKC phosphorylation in the presence or absence of mTOR inhibition (Figure 2.5D). That PIF peptide suppresses PKC phosphorylation upon mTOR inhibition, presumably by competing with PKC for access to PDK1, suggests that mTOR activity enhances the ability of PDK1 to bind the unphosphorylated hydrophobic motif. Accordingly, we have previously shown that although PDK1 displays higher affinity for the phosphorylated PKC hydrophobic motif peptide, PDK1 preferentially binds unphosphorylated full-length PKC, likely due to increased accessibility of the C-tail in this conformation (Gao et al., 2001). Thus, mTORC2 activity and TIM phosphorylation enhance PDK1 binding and function, respectively, suggesting that PDK1 is recruited to PKC via mTORC2-mediated TIM phosphorylation.

To gain structure insight into the binding events required for PKC maturation, we modeled the binding of Sin1 and PDK1 with PKC. We first docked the kinase domain of PKCβII with the structure of the yeast Sin1 CRIM domain, the known direct interaction partner that

recruits AGC kinases to TOR (Tatebe et al., 2017) (Figure 2.5E). Corroborating our peptide arrays, the majority of the poses produced by unbiased docking, positioned the CRIM domain in contact with the active-site tether (Figure 2.13A). It has been shown that the acidic loop of the CRIM domain targets mTORC2 to its substrates and is required for mTORC2-mediated phosphorylation of PKC and Akt (Cameron et al., 2011). In our model, several negatively-charged residues that comprise this loop interact with Arg^{635} of PKC at the TIM+1 position, anchored by a hydrophobic interaction between Phe^{361} of the CRIM domain and Phe^{633} of PKC at the TIM-1 position (Figure 2.5E; inset). We then utilized a model of a PDK1:RSK complex to dock PDK1 to the C-tail of PKCβII. A possible binding pose between PDK1 and PKC involves an extended conformation of the C-tail, such that PDK1 can simultaneously bind the PKC hydrophobic motif through its PIF pocket and accommodate the PKC activation loop in its active site (Figure 2.5F). Thus, experimental binding studies and structural analysis support a model in which mTORC2-mediated TIM phosphorylation recruits PDK1 by promoting accessibility of the PKC C-tail.

Figure 2.5: **mTORC2 Recruits PDK1 to the PKC C-tail.**
(A) IB analysis of 1-step, 15-mer peptide arrays of the PKCβII C-tail overlaid with triton-solubilized lysate from WT MEFs expressing HA-Sin1 or FLAG-PDK1 and probed with antibodies for Sin1 (HA) or PDK1 (FLAG). Peptides bound strongly by Sin1 (blue), PDK1 (red), or both (purple) are indicated.
(B) IB of triton-solubilized lysates or FLAG or IgG control immunoprecipitates from HEK-293t cells expressing FLAG-PDK1 and GST-PKCβII C-tail (601-673) constructs and probed with the indicated antibodies. PIF peptide was used as a positive control for PDK1 binding. (bottom) Quantification of relative C-tail co-immunoprecipitation with PDK1 (mean $\pm$ SEM) from 3 independent experiments.
(C) IB of triton-solubilized lysates or FLAG or IgG control immunoprecipitates from HEK-293t cells expressing FLAG-PDK1 and GST-PKCβII C-tail (601-673) constructs and probed with the indicated antibodies. PIF peptide was used as a positive control for PDK1 binding.
(D) IB of triton-solubilized lysates from +/+ MEFs, expressing FLAG-PKCβII and the indicated GST-C-tail constructs, treated with Torin (250nM) for 24hrs during transfection, and probed with the indicated antibodies. (bottom) Quantification of PKC phosphorylation (mean $\pm$ SEM) represents the percent of the faster-mobility, phosphorylated species from 3 independent experiments.
(E) Docking of the Sin1 CRIM domain NMR structure (PDB ID: 2RVK) to the catalytic domain of PKCβII (PDB ID: 2I0E). (inset) Interactions of the CRIM domain acidic loop with the PKCβII TOR-interaction motif helix.
(F) Homology model of PDK1 (PDB ID: 1H1W) binding to PKCβII.

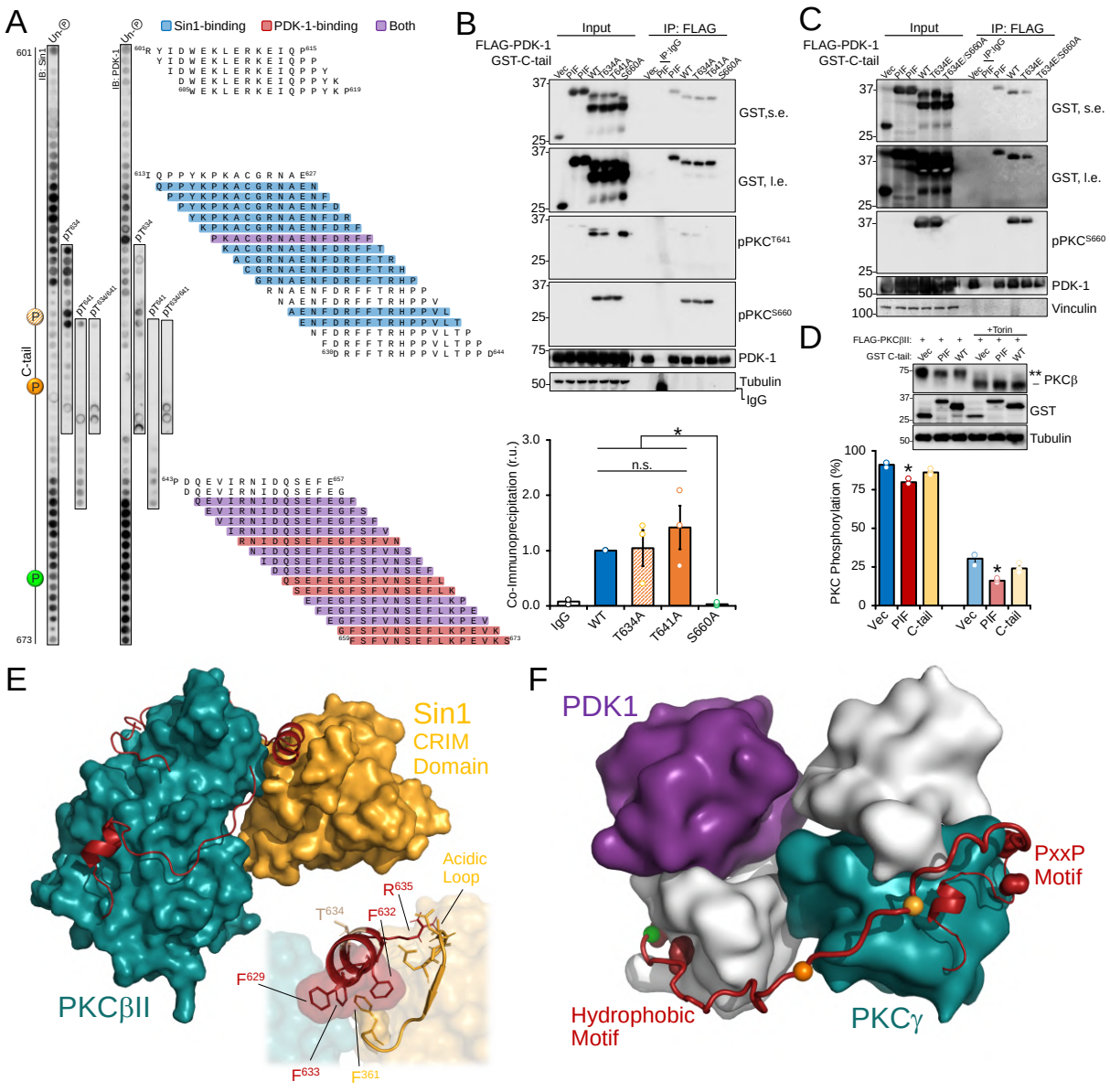
A
Sin1-binding
PDK-1-binding
Both
IB: Sin1
IB: PDK-1
C-tail
B
Input
IP: FLAG
FLAG-PDK-1
GST-C-tail
GST,s.e.
GST, l.e.
pPKCT641
pPKCS660
PDK-1
Tubulin
IgG
Co-Immunoprecipitation (r.u.)
n.s.
C
GST, s.e.
GST, l.e.
pPKCS660
PDK-1
Vinculin
D
FLAG-PKCβII:
GST C-tail:
+Torin
PKCβ
GST
Tubulin
PKC Phosphorylation (%)
Vec
PIF
C-tail
E
Sin1
CRIM
Domain
Acidic
Loop
PKCβII
F
PDK1
PxxP
Motif
Hydrophobic
Motif
PKCγ

TOR-Interaction Motif Coordinates the Dimerization of Immature PKC

To explore the role of conformational changes in the PKC C-tail, we compared the only two reported PKC structures in which the active-site tether is resolved. The kinase domains of the PKCβII catalytic domain (Grodsky et al., 2006) and full-length (Leonard et al., 2011) structures share nearly identical architecture; however, there was a large deflection in the trajectory of the C-tail in active-site tether region, that differed from the canonical AGC active-site tether (Figure 2.6A). The active-site tether in the full-length structure adopted an inward position (TIM In), in which the TIM helix was clamped down due to the binding of the C1B domain on the C-tail (Leonard et al., 2011) (Figure 2.6A). Conversely, the active-site tether of the isolated catalytic domain adopted an outward orientation (TIM Out), in which the Phe residues of the TIM were exposed (Figure 2.6A). Accordingly, we then asked whether there were any C-tail interactions in the catalytic domain structure that accounted for the unusual position of the active-site tether in the absence of the C1B domain. Examining the crystal packing of the catalytic domain structure revealed a symmetrical, head-to-head PKC homodimer, forming a dimerization interface through hydrophobic interactions in the TOR-Interaction Motif Helix (TIM Helix) (Figure 2.6B).

We have previously shown that mature PKC translocates to membranes as a monomer (Antal et al., 2015b). To ascertain whether immature PKC self-associates in a cellular context, we performed co-immunoprecipitation assays between differentially-tagged PKC proteins. Whereas very little association of WT PKCβII proteins was observed under resting conditions in which the majority of PKC is in the mature form, chronic Torin treatment resulted in a four-fold enhancement of PKC association, consistent with dimerization (Figure 2.6C). Furthermore, the co-immunoprecipitated PKC was devoid of phosphorylation at the hydrophobic motif, indicating that dimerization occurred only between immature PKC molecules (Figure 2.6C). To test whether

TIM phosphorylation regulates its dimerization, we tested the association of the PKCβII TIM and turn motif mutant PKCβII T634A/T641A (AA). Surprisingly, PKCβII AA displayed greatly enhanced basal association which could not be further increased by mTOR inhibition (Figure 2.6C). Thus, these data suggest that immature PKC dimerizes through the active-site tether TIM Helix, which is relieved upon mTORC2 phosphorylation at the TIM and turn motif sites. We have shown here that immature PKC, produced as a result of mTORC2 deficiency, adopts an open conformation with exposed C1 domains, and that the conformational changes upon maturation serve to mask the C1B domain against the active-site tether. Consequently, we examined whether the presence of the C1B domain in mature PKC blocks dimerization. To assess the role of the C1B domain in PKC dimerization, we tested the propensity of the isolated PKCβII catalytic domain (Cat) to associate with a full-length PKC. Compared to two isolated catalytic domains, the full-length protein exhibited reduced association with Cat, suggesting that the C1B domain impairs the dimerization of mature PKC (Figure 2.6D).

Structural analysis of potential steps of PKC processing implicates the TIM helix as a polyvalent scaffold during maturation. The TIM helix Out position of nascent PKC forms an interface for PKC homodimerization (Figure 2.6E; PKC:PKC). This conformation also presents the primary binding site of the PKC C-tail to Sin1, mediating the recruitment of mTORC2 (Figure 2.6E; PKC:Sin1). Following phosphorylation by mTORC2, PKC interaction with PDK1 necessitates an extended conformation of the C-tail that is incompatible with dimerization. (Figure 2.6E; PKC:PDK1). Finally, the full-length structure of mature PKC shows the clamping of the C1B domain over the C-tail, stabilizing the TIM In position, which masks the hydrophobic residues required for mTORC2 binding and precludes PKC dimerization (Figure 2.6E; PKC:C1B). Thus, the TIM site and mTOR activity mediate the dissociation of an immature PKC homodimer to

promote PKC processing.

Figure 2.6: **TOR-Interaction Motif Coordinates the Dimerization of Immature PKC.**
(A) Alignment of PKCβII catalytic domain (PDB ID: 2I0E) and full-length (PDB ID: 3PFQ) crystal structures showing the kinase domain (space-filling, white), C-tail (red, cyan), and position of the TIM phosphorylation site (Thr^{634}, tan).
(B) PKC dimer from PKCβII X-ray structure (PDB ID: 2I0E) showing the PKC kinase (teal) and C-tail (red) with dimer partner (PKC) kinase (tan) and C-tail (blue). The dimerization interface at the TOR-interaction helix (TIM Helix) is shown with interacting Phe residues.
(C) IB of triton-solubilized lysates and HA or IgG control immunoprecipitates from HEK-293t cells expressing HA- and mCherry-PKCβII WT or T634A/T641A (AA), and probed with the indicated antibodies. (right) Quantification of relative PKC co-immunoprecipitation (mean $\pm$ SEM) from 3 independent experiments.
(D) IB of triton-solubilized lysates or FLAG immunoprecipitates from HEK-293t cells expressing full-length (FL) or catalytic domain (Cat, 296-673) HA- and FLAG-PKCβII and probed with the indicated antibodies. (right) Quantification of relative PKC co-immunoprecipitation (mean $\pm$ SEM) from 3 independent experiments.
(E) Structural diagram of PKC dimeric and monomeric states governed by mTORC2. (PKC:PKC) PKCβII TOR-interaction motif (TIM) helix dimerization interface from 2 PKC molecules (red, blue) is shown with hydrophobic interactions and Thr phosphorylation in space-filling. (PKC:Sin1) TIM helix (red) is shown interfacing with the Sin1 CRIM domain (light orange). (PKC:PDK1) PKC kinase domain (teal) in complex with PDK1 (purple) bound to the hydrophobic motif. (PKC:C1B) Masked TIM helix is shown interfacing with the C1B domain (orange) in the autoinhibited, monomeric conformation.
(F) Model of PKC maturation by phosphorylation. Newly-synthesized PKC exists as a homodimer mediated by the TOR-interaction motif (TIM) helix, with membrane targeting domains exposed, and is neither phosphorylated nor catalytically active (UNPRIMED). TIM and turn motif phosphorylation by mTORC2 relieve the PKC dimer, exposing the C-terminal tail to recruit PDK1. Bound PDK1 phosphorylates PKC at the activation loop, triggering intramolecular auto-phosphorylation at the hydrophobic motif, autoinhibition, and masking of the TIM helix by the C1B domain (PRIMED). This species of PKC, which is stable and catalytically competent, is maintained in an inactive state by the pseudosubstrate, poised for activation by the second-messengers diacyglycerol and Ca^{2+}.
*$p < 0.05$; n.s., not significant by Student's t-test.

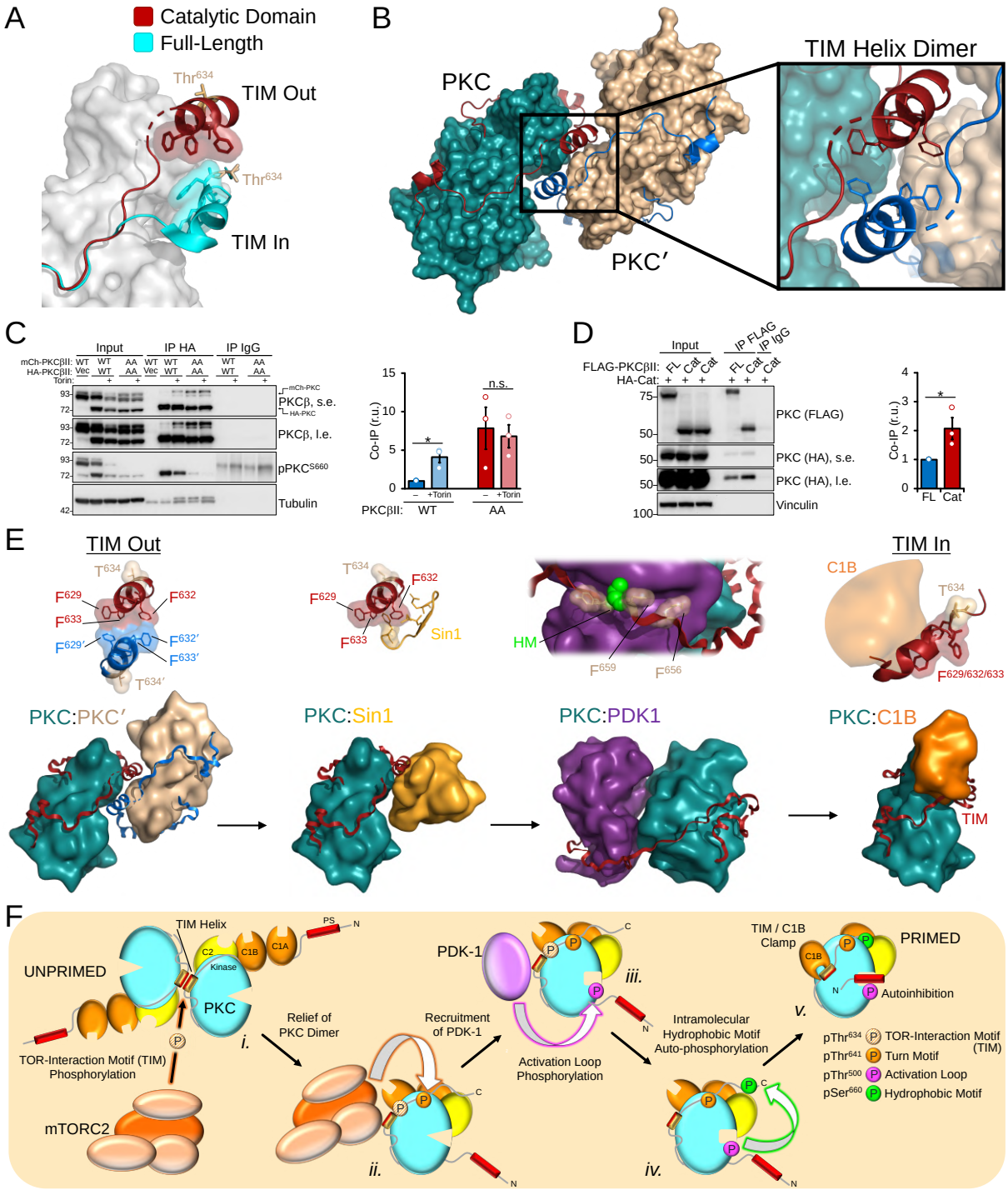
A
Catalytic Domain
Full-Length
Thr634
TIM Out
Thr634
TIM In
B
PKC
TIM Helix Dimer
PKC′
C
Input
IP HA
IP IgG
mCh-PKCβII:
HA-PKCβII:
Torin:
PKCβ, s.e.
PKCβ, l.e.
pPKCS660
Tubulin
Co-IP (r.u.)
n.s.
PKCβII:
WT
AA
D
Input
IP FLAG
IP IgG
FLAG-PKCβII:
HA-Cat:
PKC (FLAG)
PKC (HA), s.e.
PKC (HA), l.e.
Vinculin
Co-IP (r.u.)
E
TIM Out
TIM In
C1B
HM
PKC:PKC′
PKC:Sin1
PKC:PDK1
PKC:C1B
TIM
F
UNPRIMED
TIM Helix
PKC
TOR-Interaction Motif (TIM) Phosphorylation
mTORC2
Relief of PKC Dimer
Recruitment of PDK-1
PDK-1
Activation Loop Phosphorylation
Intramolecular Hydrophobic Motif Auto-phosphorylation
TIM / C1B Clamp
PRIMED
Autoinhibition
TOR-Interaction Motif (TIM)
Turn Motif
Activation Loop
Hydrophobic Motif

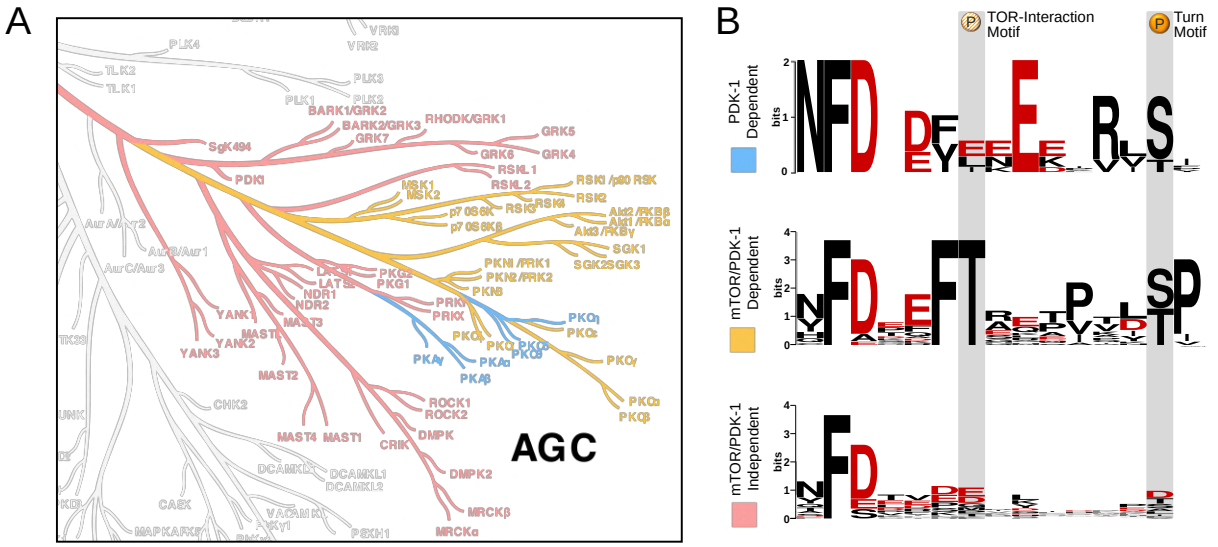

Figure 2.7: **Negative Charge in the Active-Site Tether Is a Conserved Feature of PDK1-Dependent AGC Kinases.**
(A) AGC branch of the Kinome tree displaying kinases dependence upon PDK1 (blue), mTOR and PDK1 (gold), or neither mTOR nor PDK1 (red). Included in the mTOR/PDK1-depenent category are the MSK and RSK family kinases, which have not been reported to be mTOR-dependent, but conserve the TOR-interaction motif **(B)** Motif analysis of the active-site tether in AGC kinases, stratified by dependence upon PDK1 (top), mTOR and PDK1 (middle), or neither mTOR nor PDK1 (bottom). The RSK and MSK kinase families were included in the mTOR/PDK1-dependent group due to conservation of the TOR-interaction motif, although their dependence upon mTOR is not known. The TOR-interaction motif and turn motif sites positions are highlighted and negatively-charged amino acids are shown in red.

Negative Charge in the Active-Site Tether Is a Conserved Feature of PDK1-Dependent AGC Kinases

Having established the role for TIM phosphorylation in activating PKC, we hypothesized that negative charge in the active-site tether may serve as a general AGC kinase activation mechanism by recruiting PDK1. To investigate this possibility, we categorized AGC kinases by their requirement for PDK1 (blue), mTOR and PDK1 (gold), or neither kinase (red), and evaluated negative charge in the active-site tether by motif analysis (Crooks et al., 2004) (Figure 2.7A). Following the highly conserved NFD motif present in nearly all AGC kinases, PDK1-dependent kinases display extensive negatively charge residues, whereas mTOR/PDK1-dependent kinases

instead conserve the TOR-interaction motif phosphorylation site Thr (Figure 2.7B). Specifically, the invariant Glutamic Acid at the TIM+2 position of PKA and mTOR-independent PKC enzymes may compensate for the lack of a phosphorylatable residue to recruit PDK1 (Figure 2.7B). In support of this, phosphorylation of the turn motif of PKA, a PDK1-dependent and mTOR-independent kinase, dramatically enhances PDK1 binding via the hydrophobic motif (Romano et al., 2009). Furthermore, kinases that require neither PDK1 nor mTORC2 exhibit a high degree of variability in the active-site tether, with fewer negatively charged residues and poor conservation of the turn motif phosphorylation site (Figure 2.7B). Thus, negative charge in the active site tether, conferred by negatively charged residues or phosphorylations at the TIM and turn motif, may be a conserved feature in AGC kinases to recruit PDK1.

2.4 Discussion

The prevailing findings of this study revise the activation mechanisms of PKC and Akt by providing evidence that mTORC2 is not the direct hydrophobic motif kinase. Rather, mTORC2 performs the first and rate-limiting step of PKC maturation by phosphorylating the newly identified TOR-Interaction Motif (TIM) and turn motif sites (Figure 2.6F; i). This is accomplished by mTORC2 component Sin1 and the mTOR kinase recognizing determinants in the C-tail active-site tether and hydrophobic motif that confer binding to the immature, unphosphorylated PKC species. Dissociation of the PKC dimer upon phosphorylation recruits PDK1 to the unphosphorylated hydrophobic motif to promote activation loop phosphorylation (Figure 2.6F; iii). For Akt, activation loop phosphorylation is sufficient to activate the kinase; whereas, for PKC, this site alone does not enable phosphorylation of downstream substrates, but may provide the low rate of catalytic activity required to autophosphorylate at the hydrophobic motif (Figure 2.6F;

iv). Predicated upon hydrophobic motif phosphorylation, the final step of PKC maturation is autoinhibition via the pseudosubstrate to yield the catalytically competent and stable PKC species (Figure 2.6F; v). The conformational changes driven by activation loop phosphorylation and hydrophobic motif autophosphorylation result in clamping of the C1B domain over the C-tail, locking the active-site tether in the TIM In position. This process serves the interdependent functions of stabilizing the catalytically competent and phosphorylated PKC, as well as preventing self-association of the mature form.

Characterization of TOR-interaction motif phosphorylation as a requirement for PKC processing may have been hindered by the potentially transient nature of phosphorylation at this site, as evidenced by the low rate of identification in proteomic studies (Hornbeck et al., 2015). First reported by mass spectrometry as a PKC autophosphorylation in insect cell expression (Flint et al., 1990), TIM phosphorylation may be more sensitive to phosphatases due to its outward orientation on a exposed segment of the C-tail. The critical role for TIM phosphorylation specifically during PKC processing and compensation by the turn motif phosphorylation suggests that this site may only be required in the recruitment of PDK1 and is dispensable thereafter. Whether this phosphorylation plays a more dynamic role in kinases such as Akt that are transiently activated by PDK1 merits further investigation. That negatively charged amino acids do not compensate for TIM phosphorylation may be explained by properties of the kinase domain that co-evolved with the C-tail to require phosphorylation (Kannan et al., 2007; Pearlman et al., 2011). PKA, for example contains a stretch of 4 Glu residues instead of the TIM phosphorylation site and autophosphorylates at the turn motif (Keshwani et al., 2012), which may obviate the need for mTORC2. The active-site tether region in is a conserved chimeric PDK1 binding element for PKA, Akt, and PKN (Romano et al., 2009), and requirement for phosphorylation

site at this position in PKC may reflect the need for a phosphorylation switch to toggle affinities between dimerization partners and regulators that also bind this region, such as PDK1 and chaperone Hsp90 (Gould et al., 2009; Taylor and Kornev, 2011). Interestingly, in addition to known mTORC2 substrates, the TOR-Interaction Motif was conserved in mTORC1 substrates S6K1 and S6K2, as well as the MSK and RSK family kinases, whose mTOR-dependence has not yet been assessed. A conserved TOR Signaling (TOS) Motif present in the S6K N-terminus was previously described for substrates recognized by mTORC1 (Schalm and Blenis, 2002), suggesting that other regions may distinguish between the TOR complexes. That the hydrophobic motif of S6K has also been characterized as an autophosphorylation site, despite its prevalent use as a marker for mTORC1 activity, suggests that TIM phosphorylation in S6K by mTORC1 may serve a similar function (Romanelli et al., 2002).

The turn motif phosphorylation, which is the constitutive and stable mTOR phosphorylation, may additionally serve the interdependent functions of preventing the re-dimerization of mature PKC and conferring the ability to autophosphorylate at the hydrophobic motif. In support of this, we have previously shown *in vitro* that mature PKC dephosphorylated at the activation loop and hydrophobic motif, but retaining the turn motif phosphorylation, was capable of re-autophosphorylating at the hydrophobic motif (Dutil et al., 1998). Dephosphorylation of the turn motif site, however, abolished the ability of PKC to re-autophosphorylate, but could be rescued by incubation with catalytically competent PDK1 (Dutil et al., 1998). Thus, the turn motif phosphorylation locks in place the conformational changes conferred by activation loop phosphorylation, allowing PDK1-independent re-autophosphorylation and extending the signaling lifetime of PKC. Indeed, the turn motif phosphorylation plays a critical role in stabilizing AGC kinases by anchoring the C-tail to the kinase domain (Hauge et al., 2007). In this manner,

turn motif phosphorylation may serve as a stamp that mTORC2 has adequately processed the nascent PKC dimer, protecting immature PKC from degradation through the subsequent processes of activation loop and hydrophobic motif phosphorylation until it is ultimately stabilized in the fully phosphorylated and autoinhibited, mature conformation.

Elucidating the hydrophobic motif as an mTORC2- and PDK1-dependent autophosphorylation highlights the regulation of kinase activation through non-catalytic regions, and the various roles of hydrophobic motif phosphorylation among AGC kinases (Pearce et al., 2010; Yang et al., 2009). PKC hydrophobic motif phosphorylation is essential for its catalytic activity likely through interactions formed with the C-helix upon phosphorylation. For Akt, hydrophobic motif phosphorylation confers maximal activity, and may fine-tune substrate specify and signaling duration, perhaps by stabilizing activation loop phosphorylation (Manning and Toker, 2017). For some AGC kinases, however, hydrophobic motif phosphorylation occurs first to create a docking site for PDK1 (Leroux et al., 2018). In all cases, activation loop phosphorylation is the critical event for activation, and this process appears to be regulated primarily by PDK1 binding, which is achieved by a multitude of mechanisms (Mora et al., 2004). Notably, the requirement of PIP_3 for PDK1-dependent activation loop phosphorylations differs among kinases, as PKCs are phosphorylated by PDK1 in a PI3K-indepenent manner (Dutil et al., 1998). It was shown that chimeric Akt, in which the Akt catalytic domain was fused to the PKC regulatory domain, was dependent upon PI3K activation for activation loop and hydrophobic motif phosphorylation, suggesting that localization of the interaction may influence the ability of PDK1 to phosphorylate the activation loop and dictate whether PIP_3 is required (Andjelkovi et al., 1999). That the PDK1 step of PKC activation is regulated at the level of binding is not surprising, as PDK1 exists at low nanomolar concentrations, while its substrates may outnumber that by as many as

two orders of magnitude in the cell (Hein et al., 2015). Given the lack of a canonical AGC kinase C-tail, it logically follows that PDK1 specificity, and therefore activity towards its substrates, would be regulated by binding this regulatory element. Thus, recruitment of PDK1 to the C-tail of PKC in a manner that permits phosphorylation of the activation loop is the rate-determining step of PKC maturation.

An unexpected finding from this study is the ability of immature PKC to homodimerize. Dimerization of mature PKC has previously been proposed *in vitro* in the presence of Ca^{2+} and phosphatidylserine or in cells upon activation; however, these studies do not take into account the reduction in dimensionality upon PKC engagement on a lipid membrane or vesicle, and may have limited physiological basis (Huang et al., 1999; Swanson et al., 2014). It is unlikely that mature, autoinhibited PKC dimerizes due to its ability to autophosphorylate in a concentration-independent manner, indicative of monomeric function (Newton and Koshland, 1987). Neither is the activated form likely to dimerize, as the C2-mediated translocation of PKCβII relies upon intramolecular, rather than intermolecular contacts with the kinase domain (Antal et al., 2015b). Additionally, analysis of cellular PKCα activation demonstrated that PKC translocation is a diffusion-driven process hampered by oligomerization and strongly suggesting that PKC translocation occurs as a monomer (Hui et al., 2017). Thus, our finding in this study that newly-syntheiszed PKC exists as an immature homodimer regulated by mTORC2-mediated TIM phosphorylation is likely to be the only physiologically relevant dimer that is consistent with PKC biochemistry. In an interesting parallel, it was shown that mTORC2 phosphorylates STE-family kinase MST1 to impair its homodimerization and activity (Sciarretta et al., 2015). Akt has been proposed to dimerize (Datta et al., 1995; Dudek et al., 1997); however, whether mTORC2-mediated TIM phosphorylation also regulates Akt dimerization or, alternatively, disrupts the

interface between the PH domain and the kinase domain to promote activation remains to be determined. A full-length Akt crystal structure may provide insight; although, full-length Akt structures have thus far been refractory to crystallization without substantial C-tail truncations that remove the TIM and hydrophobic motif sites (Wu et al., 2010).

The physiological importance of hydrophobic motif phosphorylation is perhaps best illustrated by its frequent dysregulation in cancer. The PKC hydrophobic motif Ser is among the most highly mutated phosphorylation sites among cancer-associated kinase alterations (Huang et al., 2018). Additionally, PHLPP1-dependent PKC quality control that mediates hydrophobic motif dephosphorylation and PKC degradation is exploited in cancer to suppress PKC protein levels (Baffi et al., 2019). Thus, maintaining the integrity of the PKC processing machinery that permits hydrophobic motif phosphorylation is critical to PKC's tumor-suppressive function. Akt hydrophobic motif phosphorylation, conversely, generally serves an oncogenic role, and constitutively active or amplified Akt is prevalent in the wide variety of cancers that frequently harbor PI3K pathway alterations (Yuan and Cantley, 2008). It was recently shown in triple-negative breast cancer that sustained activation loop and hydrophobic motif phosphorylation marked resistance to PI3K inhibition (Mundt et al., 2018). Patient-derived xenograft models from PI3K-resistant triple-negative breast tumors could be sensitized to PI3K pathway inhibitors by combination with mTOR inhibitors, suggesting that mTORC2 may play a role in Akt reactivation and therapeutic resistance upon inhibition of growth factor signaling (Mundt et al., 2018). Targeting mTOR in cancer, however, should be approached with caution. Although ATP-competitive mTORC1/2 inhibitors are being preferentially developed over mTORC1-specific Rapamycin analogs due to their efficacy in suppressing oncogenic Akt and other cell growth pathways (Benjamin et al., 2011), this approach would have the unwanted consequence of inhibiting PKC

processing, depleting the levels of an important tumor-suppressor. Therefore, exploring methods to promote mTOR-independent PKC processing, perhaps by targeting PKC dimerization or association with PDK1, may potentiate the efficacy of mTOR therapeutics.

Our work detailing the molecular basis of PKC and Akt regulation by mTORC2 provides new lines of investigation into the regulatory mechanisms of AGC kinases. Understanding the determinants for signal propagation through these kinases will facilitate the identification of new therapeutic strategies to modulate the cellular processes they regulate.

Figure 2.8: **Supplemental Data Related to Figure 2.1.**
(A) PKC basal activity in WT (+/+) or Sin1 KO (*Sin1*$^{-/-}$) MEFs expressing CKAR and RFP-tagged PKCβII WT, phosphomimetic T641E/S660E (EE), or CKAR alone and treated with PKC inhibitor Gö6976 (1μM). The reduction in FRET Ratio (mean ± SEM) represents the unstimulated PKC activity prior to inhibitor addition from 3 independent experiments.
(B) IB analysis of triton-solubilized lysates from COS7 cells expressing RFP-tagged PKCβII and treated with Torin (250nM) for 24hrs co-transfection followed by Gö6983 (1μM) for the indicated timepoints to trap PKC phosphorylation.
(C) IB analysis of triton-solubilized lysates from WT (+/+) or Rictor KO (*Ric*$^{-/-}$) MEFs expressing RFP-tagged PKCβII and treated with UTP (1μM) or PDBu (200nM) for 15min prior to lysis.
(D) PKC translocation analysis of mYFP-PKCβII WT, kinase-dead D466N, or C1 binding-deficient mutant W58Y monitored by FRET ratio changes (mean ± SEM) in WT (+/+) or Rictor KO (*Ric*$^{-/-}$) MEFs co-expressing myristoylated-palmitoylated mCFP and treated with PDBu (100nM).
(E) IB analysis of triton-solubilized lysates from WT (+/+) or Sin1 KO (*Sin1*$^{-/-}$) MEFs expressing PKCα WT, myristoylated PKCα (Myr-PKCα), PKCβII WT, or myristoylated-palmitoylated PKCβII (MP-PKCβII) and probed with antibodies against the turn motif (Thr$^{638/641}$), hydrophobic motif (Ser$^{657/660}$), and total PKCα or PKCβ. Myr-PKCα and MP-PKCβII contain the N-terminal Src myristoylation and Lyn myristoylation-palmitoylation sequences, respectively.
(F) PKC activity monitored by FRET ratio changes (mean ± SEM) in WT (+/+) or Sin1 KO (*Sin1*$^{-/-}$) MEFs expressing CKAR and RFP myristoylated-palmitoylated PKCβII treated with PDBu (200nM) and PKC inhibitor Gö6976 (1μM).
(G) IB analysis of triton-solubilized lysates from COS7 cells expressing treated with mTOR inhibitor PI-103 (1μM) for the indicated timepoints and probed with the indicated antibodies.
(H) Autoradiograph (^{35}S) and IB analysis of newly synthesized PKC pulse-chase PKCα immunoprecipitates from COS7 cells expressing PKCβII and treated with mTOR inhibitor PI-103 (1μM) during the chase. PI-103 is a poor mTOR inhibitor which retards, but does not block, the phosphorylation of PKC, enabling the quantification of T641E phosphorylation dynamics. (right) Quantification of PKCβII WT and T641E phosphorylation kinetics. Both proteins exhibit a similar reduction in the rate of phosphate incorporation upon mTOR inhibition, suggesting that turn motif phosphorylation is not the rate-determining step controlled by mTOR activity. The double asterisk (**) denotes the position of mature, fully phosphorylated PKC; the single asterisk (*) denotes the position of PKC phosphorylated at either the turn motif or hydrophobic motif; and the dash (-) indicates the position of unphosphorylated PKC.

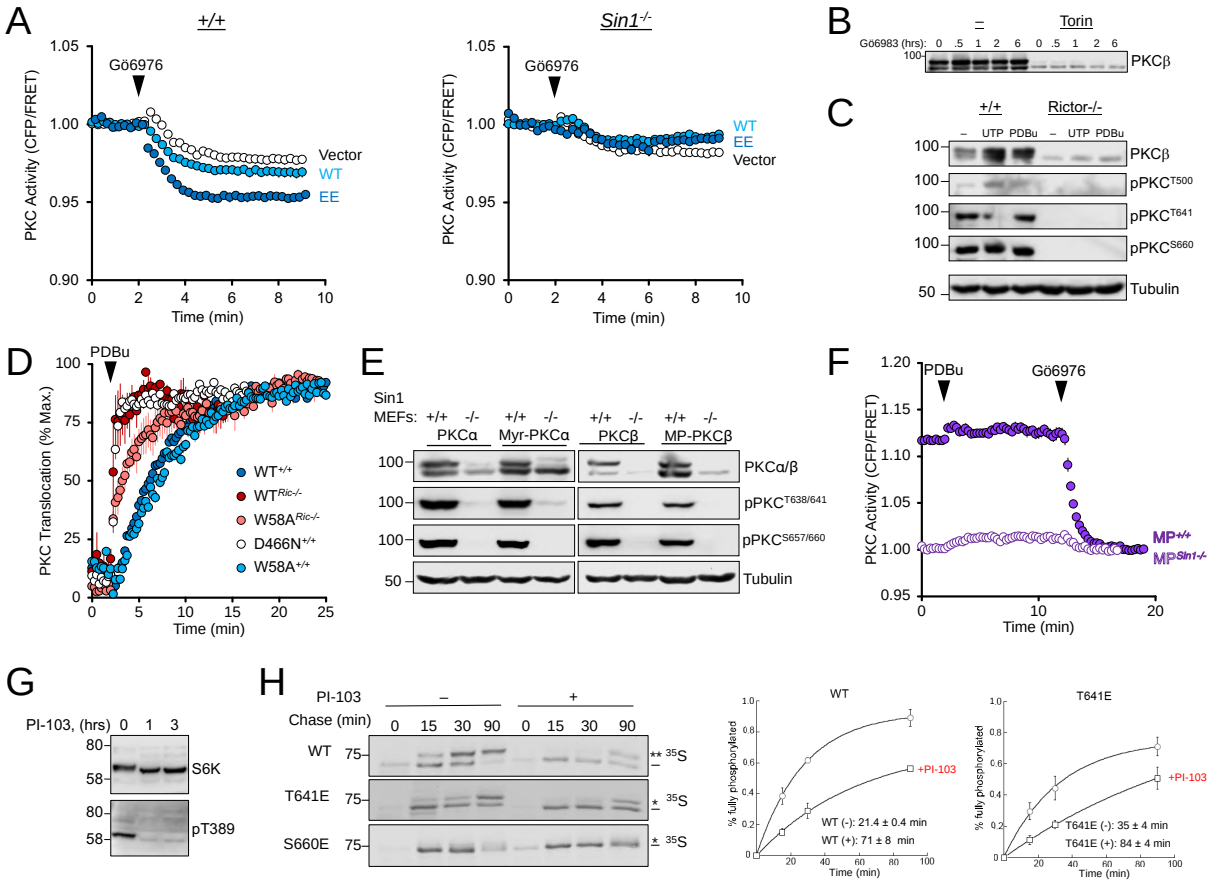
A
+/+
Sin1-/-
Gö6976
PKC Activity (CFP/FRET)
Time (min)
Vector
WT
EE
B
–
Torin
Gö6983 (hrs): 0 .5 1 2 6 0 .5 1 2 6
PKCβ
C
+/+
Rictor-/-
– UTP PDBu – UTP PDBu
PKCβ
pPKCT500
pPKCT641
pPKCS660
Tubulin
D
PDBu
PKC Translocation (% Max.)
WT+/+
WTRic-/-
W58ARic-/-
D466N+/+
W58A+/+
E
Sin1
MEFs: +/+ -/- +/+ -/- +/+ -/- +/+ -/-
PKCα
Myr-PKCα
PKCβ
MP-PKCβ
PKCα/β
pPKCT638/641
pPKCS657/660
Tubulin
F
PDBu
Gö6976
PKC Activity (CFP/FRET)
Time (min)
MP+/+
MPSin1-/-
G
PI-103, (hrs) 0 1 3
S6K
pT389
H
PI-103
Chase (min) 0 15 30 90 0 15 30 90
WT
T641E
S660E
35S
WT
T641E
% fully phosphorylated
+PI-103
WT (-): 21.4 ± 0.4 min
WT (+): 71 ± 8 min
T641E (-): 35 ± 4 min
T641E (+): 84 ± 4 min
Time (min)

Figure 2.9: **Supplemental Data Related to Figure 2.3.**
(A) Co-immunoprecipitation IB analysis of triton-solubilized lysates and HA or Myc immunoprecipitates from COS7 cells expressing HA-PKCβII and Myc-mTOR, Myc-Raptor, or HA-Sin1. The double asterisk (**) denotes the position of mature, fully phosphorylated PKC and the dash (-) indicates the position of unphosphorylated PKC.
(B) GST Pull-down IB analysis of triton-solubuilized lysates and GST pulldown from COS7 cells expressing GST-tagged PKCβII N-terminus+C1 domains (NC1;1-156), C2 domain (), catalytic domain (Cat;296-673), C-tail (CT;628-673), and Myc-mTOR and probed with the indicated antibodies. Hsp70 was used as a positive control for C-tail binding.
(C) IB analysis of a 3-step walk of 15-mer peptide arrays of the PKCβII N-term overlaid with triton-solubilized lysate from WT MEFs expressing mTORC1 Myc-Raptor, mTORC2 component HA-Sin1, or Myc-mTOR and probed with antibodies for Raptor (Myc), Sin1 (HA) or mTOR (Myc). The Raptor negative control array was also used for the mTOR blot.
(D) PKC activity monitored by FRET ratio changes (mean ± SEM) in COS7 cells expressing CKAR and mCherry-tagged PKCδ, PKCβII, or PKCδ/b TM chimera (PKC$\delta^{1\text{-}632}$/βII$^{629\text{-}673}$) and treated with PDBu (200nM).
(E) Autoradiograph (^{35}S) and IB analysis of newly synthesized PKC pulse-chase HA immunoprecipitates from COS7 cells expressing HA-tagged PKCδ/b TM chimera (PKC$\delta^{1\text{-}632}$/βII$^{629\text{-}673}$) and treated with Torin (250nM) during the chase. double asterisk (**) denotes the position of mature, fully phosphorylated PKC; the single asterisk (*) denotes the position of PKC phosphorylated at either the turn motif or hydrophobic motif; and the dash (-) indicates the position of unphosphorylated PKC.
(F) Autoradiograph (^{35}S) and IB analysis of newly synthesized PKC pulse-chase HA immunoprecipitates from COS7 cells expressing HA-tagged PKCδ or PKCβII and treated with Torin (250nM) during the chase. The double asterisk (**) denotes the position of mature, fully phosphorylated PKC and the dash (-) indicates the position of unphosphorylated PKC.
(G) IB of triton-solubilized lysates from WT (+/+) or Sin1 KO (-/-) MEFs expressing mCherry-tagged PKCη, PKCθ/β TM chimera (PKC$\theta^{1\text{-}663}$/PKCβII$^{629\text{-}673}$), or the indicated PKCδ/β chimera treated with Torin (250nM) and probed with antibodies against the PKC turn motif (TM), hydrophobic motif (HM), and total PKC (dsRED).

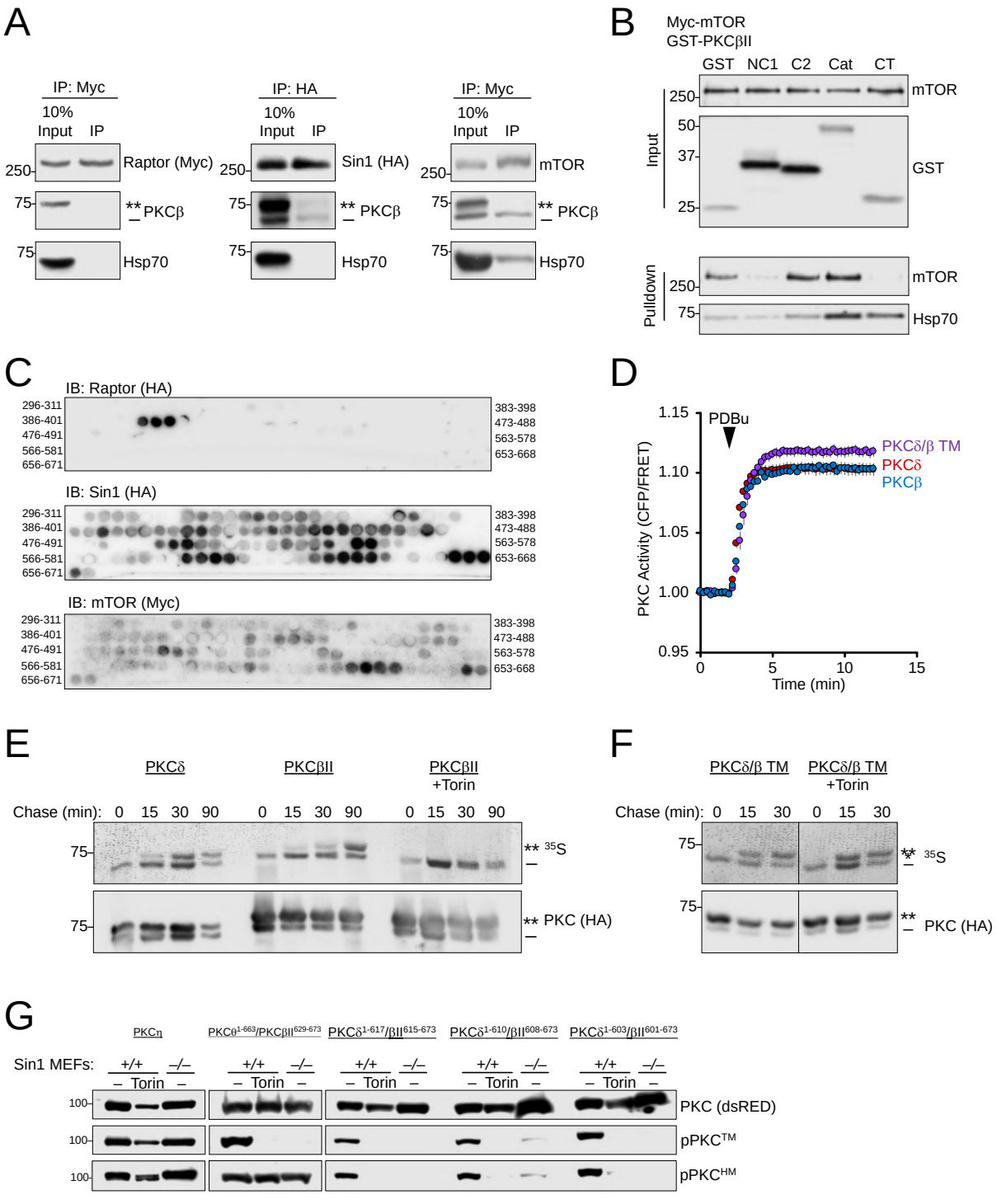
A
IP: Myc
10% Input
IP
250
Raptor (Myc)
75
** PKCβ
75
Hsp70
IP: HA
10% Input
IP
250
Sin1 (HA)
75
** PKCβ
75
Hsp70
IP: Myc
10% Input
IP
250
mTOR
75
** PKCβ
75
Hsp70
B
Myc-mTOR
GST-PKCβII
GST NC1 C2 Cat CT
Input
250
mTOR
50
37
GST
25
Pulldown
250
mTOR
75
Hsp70
C
IB: Raptor (HA)
296-311
386-401
476-491
566-581
656-671
383-398
473-488
563-578
653-668
IB: Sin1 (HA)
IB: mTOR (Myc)
D
PDBu
PKCδ/β TM
PKCδ
PKCβ
PKC Activity (CFP/FRET)
1.15
1.10
1.05
1.00
0.95
0
5
10
15
Time (min)
E
PKCδ
PKCβII
PKCβII +Torin
Chase (min): 0 15 30 90 0 15 30 90 0 15 30 90
75
** 35S
75
** PKC (HA)
F
PKCδ/β TM
PKCδ/β TM +Torin
Chase (min): 0 15 30 0 15 30
75
** 35S
75
** PKC (HA)
G
PKCη
PKCδ1-663/PKCβII629-673
PKCδ1-617/βII615-673
PKCδ1-610/βII608-673
PKCδ1-603/βII601-673
Sin1 MEFs: +/+ –/– +/+ –/– +/+ –/– +/+ –/– +/+ –/–
– Torin –
100
PKC (dsRED)
100
pPKCTM
100
pPKCHM

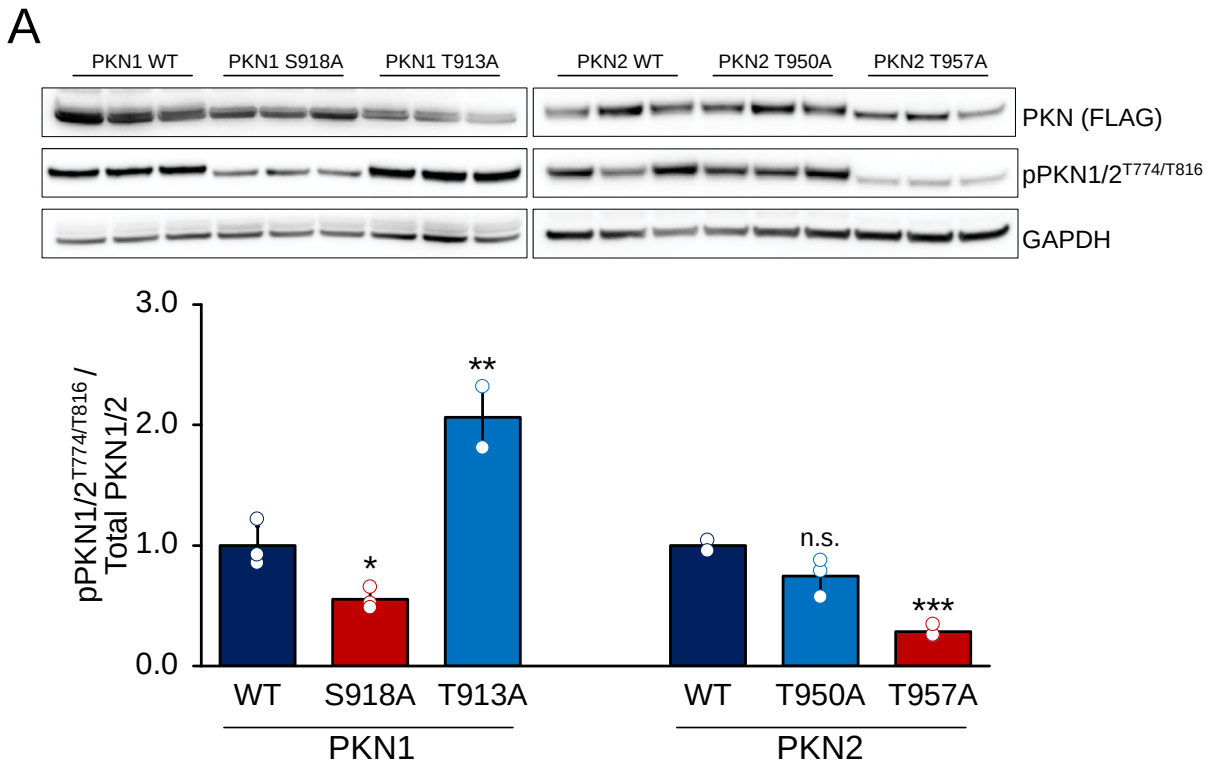

Figure 2.10: **Supplemental Data Related to Figure 2.4.**
(A) IB analysis of triton-solubilized lysates from HEK-293t cells expressing FLAG-tagged PKN1, PKN2, turn motif mutants PKN1 S918A and PKN2 T957A, or TOR-interaction motif mutants PKN1 T913A and PKN2 T950A and probed with antibodies against the PKN activation loop (PKN1/2$^{T774/T816}$), total PKN (FLAG), and GAPDH loading control. (bottom) Quantification of PKN phosphorylation (mean ± SEM) reflects the normalized activation loop phospho-signal (PKN1/2$^{T774/T816}$) relative to total PKN from 3 biological replicates.

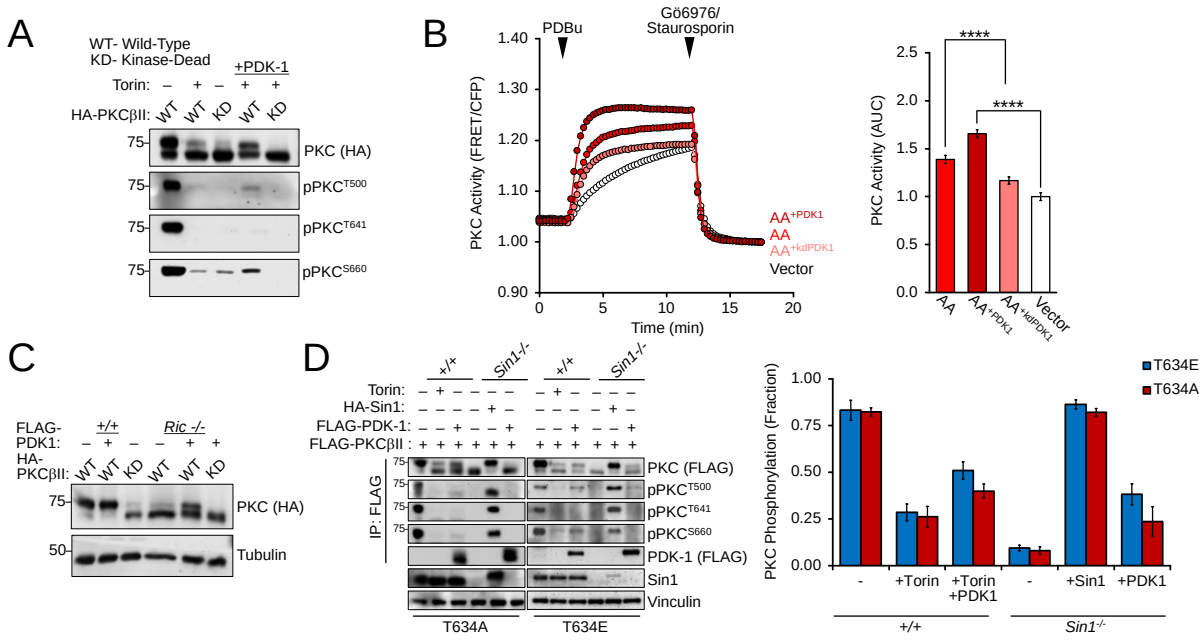

Figure 2.11: **Supplemental Data A Related to Figure 2.5.**
(A) IB analysis of triton-solubilized lysates from COS7 cells expressing HA-tagged PKCβII WT or Kinase-Dead (KD) and FLAG PDK1, treated with Torin for 24hrs co-transfection, and probed with the indicated antibodies.
(B) PKC activity monitored by FRET ratio changes (mean ± SEM) in COS7 cells expressing CKAR2, mCherry- PKCβII T634A/T641A (AA), and FLAG-tagged PDK1 WT or kinase-dead K110N (kdPDK1) and treated with PDBu (200nM) and inhibitors Gö6976 (1μM)/Staurosporin (1μM). (right) Quantification of PKC activity represents the area under the curve (AUC) from 3 independent experiments. Traces were normalized to the levels following inhibitor addition.
(C) IB analysis of triton-solubilized lysates from WT (+/+) or Rictor KO (*Ric*$^{-/-}$) MEFs expressing HA-tagged PKCβII WT or Kinase-Dead (KD) and FLAG PDK1 and probed with the indicated antibodies.
(D) IB analysis of triton-solubilized lysates from WT (+/+) or Sin1 KO (*Sin1*$^{-/-}$) MEFs expressing FLAG-PKCβII, FLAG PDK1, and HA-Sin1, treated with Torin for 24hrs co-transfection and probed with the indicated antibodies. Vinculin was used as a loading control. (right) Quantification of PKC phosphorylation (mean ± SEM) reflects the fraction of the slower mobility, fully phosphorylated PKC from three independent experiments.
****p < 0.0001 by One-way ANOVA and Tukey HSD Test or Student's t-test.

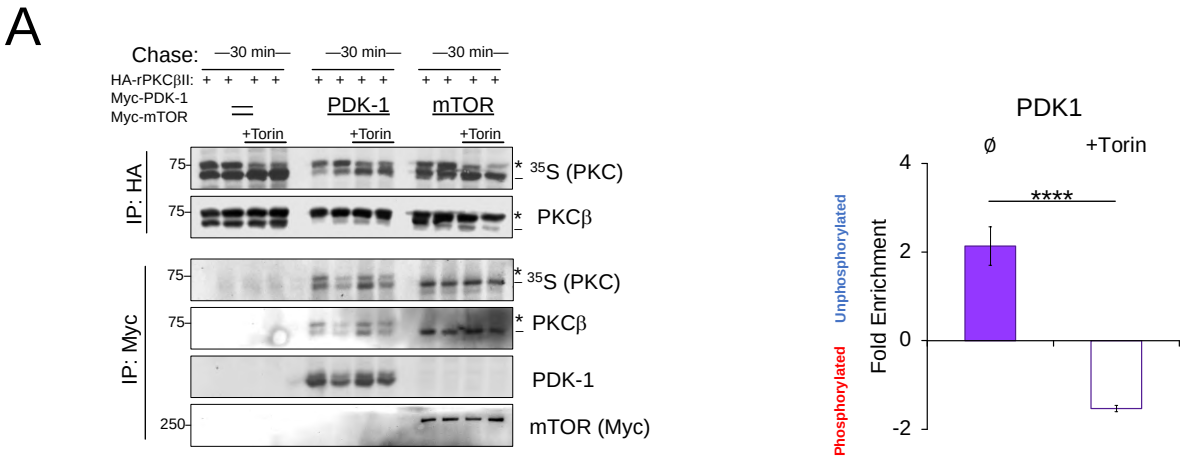

Figure 2.12: **Supplemental Data B Related to Figure 2.5.**
(A) Autoradiograph (^{35}S) and IB analysis of newly synthesized PKC by pulse-chase. Cos7 cells expressing Myc-PDK1 or Myc-mTOR and HA-PKCβII subjected to a 30min chase with Torin (250nM) treatment following ^{35}S pulse, lysed and immunoprecipitated with either HA or Myc antibodies. (**) denotes the position of mature, fully phosphorylated PKC; the single asterisk (*) denotes the position of PKC phosphorylated at either the turn motif or hydrophobic motif; and the dash (-) indicates the position of unphosphorylated PKC.

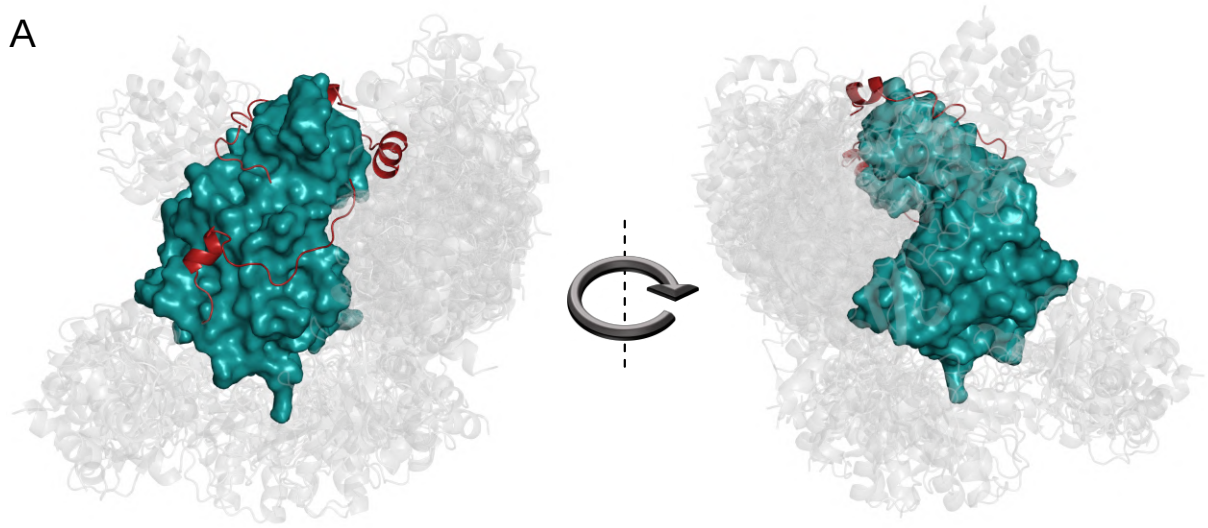

Figure 2.13: **Supplemental Data C Related to Figure 2.5.**
(A) Molecular docking of Sin1 CRIM domain (PDB ID: 2RVK) and PKCβII catalytic domain (PDB ID: 2I0E). All poses of the CRIM domain are shown in grey cartoon docked to the PKC kinase domain (teal, space filling) and PKC C-tail (red, cartoon). The highest density of predicted CRIM domain poses was observed in the active-site tether region of the PKC C-tail, consistent with the Sin1 binding site, as determined by peptide array (Figure 2.3B, Figure 2.5A).

EXPERIMENTAL MODEL AND SUBJECT DETAILS

Cell Culture and Transfection

COS7 cells, HEK-293t cells, +/+ MEFs, *Ric*$^{-/-}$ MEFs, and *Sin1*$^{-/-}$ MEFs were cultured in DMEM (Corning) containing 10% fetal bovine serum (Atlanta Biologicals) and 1% penicillin/streptomycin (Gibco) at 37°C in 5% CO_2. Generation of the Sin1 KO and Rictor KO MEFs was described previously (Jacinto et al., 2006; Guertin et al., 2006). Transient transfection was carried out using the Lipofectamine 3000 Transfection Reagent (Thermo Fisher Scientific).

METHOD DETAILS

Plasmids and Constructs

The C Kinase Activity Reporter (CKAR) and Kinameleon C reporter were previously described (Violin et al., 2003; Antal et al., 2014). All constructs were generated by QuikChange Mutagenesis (Agilent) or subcloning into pcDNA3 or pCMV vectors with N-terminal affinity tags. Rat PKC was used throughout with the exception of the chimera experiments pertaining to Figures 2.3 and 2.9. Mouse Akt1 was used.

FRET Imaging and Analysis

Cells were imaged as described previously (Gallegos et al., 2006). For activity experiments COS7 cells were co-transfected with the indicated mCherry-tagged PKC construct and CKAR. For Kinameleon experiments, the indicated Kinameleon construct containing mYFP and mCFP was transfected alone. For translocation experiments, MEFs were co-transfected with the indicated mYFP-tagged construct and plasma-membrane targeted mCFP at a ratio of 10:1. Baseline images were acquired every 15 s for 2 min prior to ligand addition. Förster resonance energy

transfer (FRET) ratios represent mean ± SEM from at least three independent experiments. All data were normalized to the baseline FRET ratio of each individual cell unless noted that absolute FRET ratio was plotted or traces were normalized to levels post-inhibitor addition. When comparing translocation kinetics, data were also normalized to the maximal amplitude of translocation for each, as previously described, in order to compare translocation rates (Antal et al., 2014). Every CKAR experiment contained an mCherry-transfected control to measure endogenous activity, and an mCherry-tagged WT control.

Immunoblotting and Antibodies

Cells were lysed in PPHB: 50 mM $NaPO_4$ (pH 7.5), 1% Triton X-100, 20 mM NaF, 1 mM $Na_4P_2O_7$, 100 mM NaCl, 2 mM EDTA, 2 mM EGTA, 1 mM Na_3VO_4, 1 mM PMSF, 40 mg/ml leupeptin, 1mM DTT, and 1 mM microcystin. Triton-soluble fractions were analyzed by SDS-PAGE on 7% big gels to observe phosphorylation shift, transfer to PVDF membrane (Biorad), and western blotting via chemiluminescence SuperSignal West reagent (Thermo Fisher) on a FluorChem Q imaging system (ProteinSimple). In Western blots, the double asterisk (**) denotes the position of mature, and the single asterisk (*) denotes the position of partially phosphorylated PKC at the turn or hydrophobic motif; whereas, the dash (-) indicates the position of unphosphorylated PKC. The turn motif and hydrophobic motif phosphorylations, but not the activation loop phosphorylation, induces an electrophoretic mobility shift that retards the migration of the phosphorylated species. The pan anti-phospho-PKC activation loop antibody (PKC pThr^{500}) was described previously (Dutil et al., 1998). The anti-phospho-PKCα/βII turn motif (pT$^{638/641}$; 9375S), anti-phospho-PKCδ/θ, pan anti-phospho-PKC hydrophobic motif (βII pS^{660}; 9371S), anti-mTOR, anti-Rictor, anti-Raptor, anti-Sin1, anti-Vinculin, anti-Myc tag, anti-S6K,

anti-phospho-S6K^{T389}, anti-phospho-Akt^{T308},anti-phospho-Akt^{T450}, anti-phospho-Akt^{S473} antibodies and Calyculin A were purchased from Cell Signaling. Anti-PKCβ (610128) and PKCα (610128) antibodies were purchased from BD Transduction Laboratories. The DsRed antibody was purchased from Clontech. The anti-HA antibody for immunoblot was purchased from Roche. The anti-HA (clone 16B12; 901515) and anti-FLAG (Clone L5; 637301) antibodies used for immunoprecipitation were purchased from BioLegend. The anti-α-tubulin (T6074) and anti-FLAG immunoblot antibodies were from Sigma. UTP, PDBu, Gö6983, Gö6976, and BisIV were purchased from Calbiochem.

Pulse-Chase Experiments

For pulse-chase experiments, COS7 cells were incubated with Met/Cys-deficient DMEM for 30 min at 37 °C. The cells were then pulse-labeled with 0.5 mCi/ml [^{35}S]Met/Cys in Met/Cys-deficient DMEM for 7 min at 37°C, media were removed, washed with dPBS (Corning), and chased with DMEM culture media (Corning) containing 200 mM unlabeled methionine and 200 mM unlabeled cysteine. At the indicated times, cells were lysed in PPHB and centrifuged at 13,000 x g for 3 min at 22 °C, supernatants were pre-cleared for 30 min at 4 °C with Protein A/G Beads (Santa Cruz), and protein complexes were immunoprecipitated from the supernatant with either an anti-HA, anti-Myc, or anti-FLAG monoclonal antibody overnight at 4 °C. The immune complexes were collected with Protein A/G Beads (Santa Cruz) for 2 hrs, washed 3x with PPHB, separated by SDS-PAGE, transferred to PVDF membrane (Biorad), and analyzed by autoradiography and western blot. Co-immunoprecipitation experiments were performed similarly, omitting the labeling and autoradiography steps.

Peptide Array

For peptide arrays, experiments were performed as described in (Romano et al., 2009).

Molecular Docking

Molecular docking experiments were performed using ZDOCK.

QUANTIFICATION AND STATISTICAL ANALYSIS

Statistical significance was determined via Repeated Measures One-Way ANOVA and Brown-Forsythe Test or Student's t-test performed in GraphPad Prism 6.0a (GraphPad Software). The half-time of translocation was calculated by fitting the data by non-linear regression using a one-phase exponential association equation with GraphPad Prism 6.0a (GraphPad Software). Western blots were quantified by densitometry using the AlphaView software (Protein Simple).

Acknowledgements

Chapter 2 in part is a reprint of material to be submitted in:

Baffi TR, Kornev AP, King CC, Del Rio J, Bogomolovas J, Chen J, Taylor SS, Newton AC. "mTORC2 controls PKC and Akt via phosphorylation of a conserved TOR-interaction motif" *In Preparation.*

The following individuals contributed to this work: Timothy R. Baffi designed and performed the experiments and wrote the manuscript supervised by Alexandra C. Newton, Charles C. King and Jason Del Rio assisted with the peptide arrays, Julius Bogomolovas performed the PKN experiments supervised by Ju Chen, and Alexandr P. Kornev performed the molecular docking and modeling experiments and provided structural analysis with Susan S. Taylor.

Chapter 2 in part is a reprint of material to be submitted in:

- **Baffi TR**, Kornev AP, King CC, Del Rio J, Bogomolovas J, Chen J, Taylor SS, Newton AC. "mTORC2 controls PKC and Akt via phosphorylation of a conserved TOR-interaction motif" *In Preparation.*

  The dissertation author was the primary author of this work.

Chapter 3

Protein Kinase C Quality Control by Phosphatase PHLPP1 Unveils Loss-of-Function Mechanism in Cancer

3.1 Abstract

Protein kinase C (PKC) isozymes function as tumor suppressors in increasing contexts. In contrast to oncogenic kinases, whose function is acutely regulated by transient phosphorylation, PKC is constitutively phosphorylated following biosynthesis to yield a stable, autoinhibited enzyme that is reversibly activated by second messengers. Here, we report that the phosphatase PHLPP1 opposes PKC phosphorylation during maturation, leading to the degradation of aber-

rantly active species that do not become autoinhibited. Cancer-associated hotspot mutations in the pseudosubstrate of PKCβ that impair autoinhibition result in dephosphorylated and unstable enzymes. Protein-level analysis reveals that PKCα is fully phosphorylated at the PHLPP site in over 5,000 patient tumors, with higher PKC levels correlating (1) inversely with PHLPP1 levels and (2) positively with improved survival in pancreatic adenocarcinoma. Thus, PHLPP1 provides a proofreading step that maintains the fidelity of PKC autoinhibition and reveals a prominent loss-of-function mechanism in cancer by suppressing the steady-state levels of PKC.

3.2 Introduction

Cellular homeostasis depends on exquisite regulation of protein kinase and phosphatase activity to allow precise responses to extracellular signals (Brognard and Hunter, 2011). Deregulation of phosphorylation mechanisms is a hallmark of disease, with aberrant kinase and phosphatase activity driving an abundance of pathologies. One kinase family whose activity must be precisely tuned to avoid pathophysiologies is protein kinase C (PKC). PKC family members transduce myriad signals downstream of phospholipid hydrolysis to regulate diverse cellular functions such as proliferation, apoptosis, migration, and differentiation (Griner and Kazanietz, 2007; Newton, 2018). Although assumed to be oncoproteins for decades, analysis of cancer-associated mutations and protein-expression levels supports a general tumor-suppressive role for PKC isozymes, accounting for the failure and, in some cases, worsened patient outcome of PKC inhibitors in cancer clinical trials (Antal et al., 2015b; Zhang et al., 2015). Conversely, enhanced activity is associated with degenerative diseases, such as Alzheimer's disease and spinocerebellar ataxia, and increased risk of cerebral infarction (Newton, 2018). Even small changes in PKC activity drive pathogenesis, as illustrated by a germline mutation in affected family members

with Alzheimer's disease that causes a modest 30% increase in the catalytic rate of the enzyme (Callender et al., 2018). Thus, tight regulation of PKC signaling output is essential.

PKC isozymes are multi-domain Ser/Thr kinases whose activity is governed by reversible release of an autoinhibitory pseudosubstrate segment (Newton, 2018). For conventional PKC (cPKC) isozymes (Figure 3.1A; α, β, and γ), this is controlled by binding of the lipid second messenger diacylglycerol (DAG) to the second of two tandem C1 domains. Ca^{2+} binding to a plasma membrane-directing C2 domain facilitates activation of these isozymes by localizing them on the membrane, thereby increasing the probability of binding DAG. Engaging both the C2 and C1B domains on membranes provides the energy to release the pseudosubstrate, allowing substrate phosphorylation and downstream signaling. This activation is short-lived, with the enzyme reverting to the autoinhibited conformation upon return of Ca^{2+} and DAG to unstimulated levels. Like many kinases, PKC is also regulated by phosphorylation. However, unlike many kinases, these phosphorylations occur shortly after biosynthesis and are constitutive (Borner et al., 1989; Keranen et al., 1995). Newly synthesized cPKC is matured by phosphorylation at three conserved positions: the activation loop by the phosphoinositide-dependent kinase PDK-1 (Dutil et al., 1998; Le Good et al., 1998) and two C-terminal sites, the turn and hydrophobic motifs (Keranen et al., 1995). The C-tail phosphorylations depend upon both the kinase complex mammalian target of rapamycin complex 2 (mTORC2) (Guertin et al., 2006) and the intrinsic catalytic activity of PKC, with *in vitro* studies showing that PKC autophosphorylates by an intramolecular reaction at the hydrophobic motif (Behn-Krappa and Newton, 1999).

Mechanisms that prevent the phosphorylation of PKC, such as loss of PDK-1, inhibition of mTORC2, or impairment of PKC's intrinsic catalytic activity, result in PKC degradation (Balendran et al., 2000; Guertin et al., 2006; Hansra et al., 1999). Indeed, it is this sensitivity of

the unphosphorylated species to degradation that accounts for the ability of phorbol esters, potent PKC agonists, to cause the downregulation of PKC (Jaken et al., 1981). The membrane-engaged active conformation of PKC is highly sensitive to dephosphorylation (Dutil et al., 1994), and dephosphorylation at the hydrophobic motif by the Pleckstrin homology (PH) domain leucine-rich repeat protein phosphatase (PHLPP) serves as the first step in the degradation of PKC, triggering subsequent PP2A-dependent dephosphorylation at the turn motif and activation loop (Gao et al., 2008; Hansra et al., 1999; Lu et al., 1998). Thus, PKC signaling output is regulated not only by second messengers but also by mechanisms that establish the level of PKC protein in the cell. Understanding how to modulate these levels has important therapeutic implications, as high PKC levels correlate with improved survival in diverse cancers (Newton, 2018).

Here, we report a quality control mechanism in which PHLPP1 ensures the fidelity of PKC maturation by proofreading the conformation of newly synthesized PKC. Specifically, phosphorylation of the hydrophobic motif is necessary to adopt an autoinhibited conformation, and it is this autoinhibited conformation that protects the hydrophobic motif from dephosphorylation by PHLPP1, protecting PKC from degradation. In cancer, hotspot mutations in the pseudosubstrate are loss of function (LOF) because of this proofreading mechanism. The ratio of hydrophobic motif phosphorylation to total PKCα in over 5,000 tumor samples reveals a near 1:1 ratio, validating mechanistic studies showing that if PKC is not phosphorylated at the hydrophobic motif, it is degraded. Finally, high levels of PKC hydrophobic motif phosphorylation (and hence total PKC) correlate inversely with PHLPP1 levels and co-segregate with improved patient survival in pancreatic adenocarcinoma, implicating PKC phosphorylation as both a prognostic marker and therapeutic target. Thus, PHLPP1-dependent quality control provides a general LOF mechanism for a tumor suppressor in cancer by targeting post-translational modifications.

3.3 Results

PKC Priming Phosphorylations Are Necessary for Maturation and Activity

PKC priming phosphorylations (Figures 1A and 1B) have been presumed to be necessary for catalytic competence based on biochemical studies (Bornancin and Parker, 1997; Cazaubon et al., 1994; Edwards and Newton, 1997; Orr and Newton, 1994). To assess whether phosphorylation at these sites is also necessary in a cellular context, we measured the agonist-evoked activity of wild-type (WT) PKCβII or mutants with non-phosphorylatable residues at each of the three priming sites in cells using the C kinase activity reporter (CKAR) (Violin et al., 2003). Phorbol 12,13-dibutyrate (PDBu) treatment caused a robust increase in CKAR phosphorylation in COS7 cells expressing WT PKC or turn motif mutant (T641A) that was reversed by addition of PKC inhibitor (Figure 3.1C). In contrast, cells expressing activation loop (T500V) or hydrophobic motif (S660A) mutants displayed no increase in CKAR phosphorylation above that of endogenous PKC. Thus, phosphorylatable residues at the activation loop and hydrophobic motif, but not turn motif, are necessary for cellular PKC activity. Western blot analysis with phospho-specific antibodies revealed that WT PKCβII protein was phosphorylated at the C-terminal sites (causing an electrophoretic mobility shift [asterisk]; Keranen et al., 1995) and at the activation loop (Figure 3.1D). The T641A protein was phosphorylated at the activation loop and hydrophobic motif, whereas the T500V and S660A proteins were unphosphorylated at all three sites, exhibited by their faster mobility (dash) and lack of reactivity with phospho-specific antibodies (Figure 3.1D). To assess whether negative charge at the hydrophobic motif is sufficient for cellular PKC activity, we examined the PDBu-stimulated activity of phosphomimetic PKC mutants with Glu substitutions at either or both of the C-tail phosphorylation sites (Figure 1E).

Replacement with Glu at the turn motif (T641E), hydrophobic motif (S660E), or both C-terminal sites (T641E/S660E) resulted in activation kinetics comparable to those observed with WT PKCβII (see Figure 3.1C). In contrast, PKCβII T641E/S660A was inactive, revealing a requirement for negative charge at the hydrophobic motif irrespective of turn motif phosphorylation. Thus, phosphorylation of the activation loop and hydrophobic motif, but not the turn motif, is necessary for PKC maturation and enzymatic activity in cells.

Figure 3.1: **PKC Priming Phosphorylations Are Necessary for Maturation and Activity.**
(A) cPKC domain structure showing pseudosubstrate (red), C1 domains (orange), C2 domain (yellow), kinase domain (cyan), C-terminal tail (gray), and three priming phosphorylations (circles).
(B) Crystal structure of PKCβII kinase domain (cyan; PDB: 3PFQ) highlighting priming phosphorylations (space filling) and pseudosubstrate residues 18-26 (red) modeled into the active site.
(C) COS7 cells expressing CKAR alone (endogenous) or co-expressing the indicated mCherry-PKCβII WT or Ala mutant constructs were treated with PDBu (200 nM) followed by Gö6983 (1 μM).
(D) Immunoblot (IB) analysis of COS7 cells transfected with the indicated PKCβII constructs and probed with indicated phospho-specific or total PKC antibodies.
(E) COS7 cells expressing CKAR alone (endogenous) or co-expressing the indicated mCherry-PKCβII phosphomimetic Glu substitution constructs were treated with PDBu (200 nM) followed by Gö6983 (1 μM).
CKAR data represent the normalized FRET ratio changes (mean $\pm$ SEM) from at least 3 independent experiments of >100 cells for each condition.

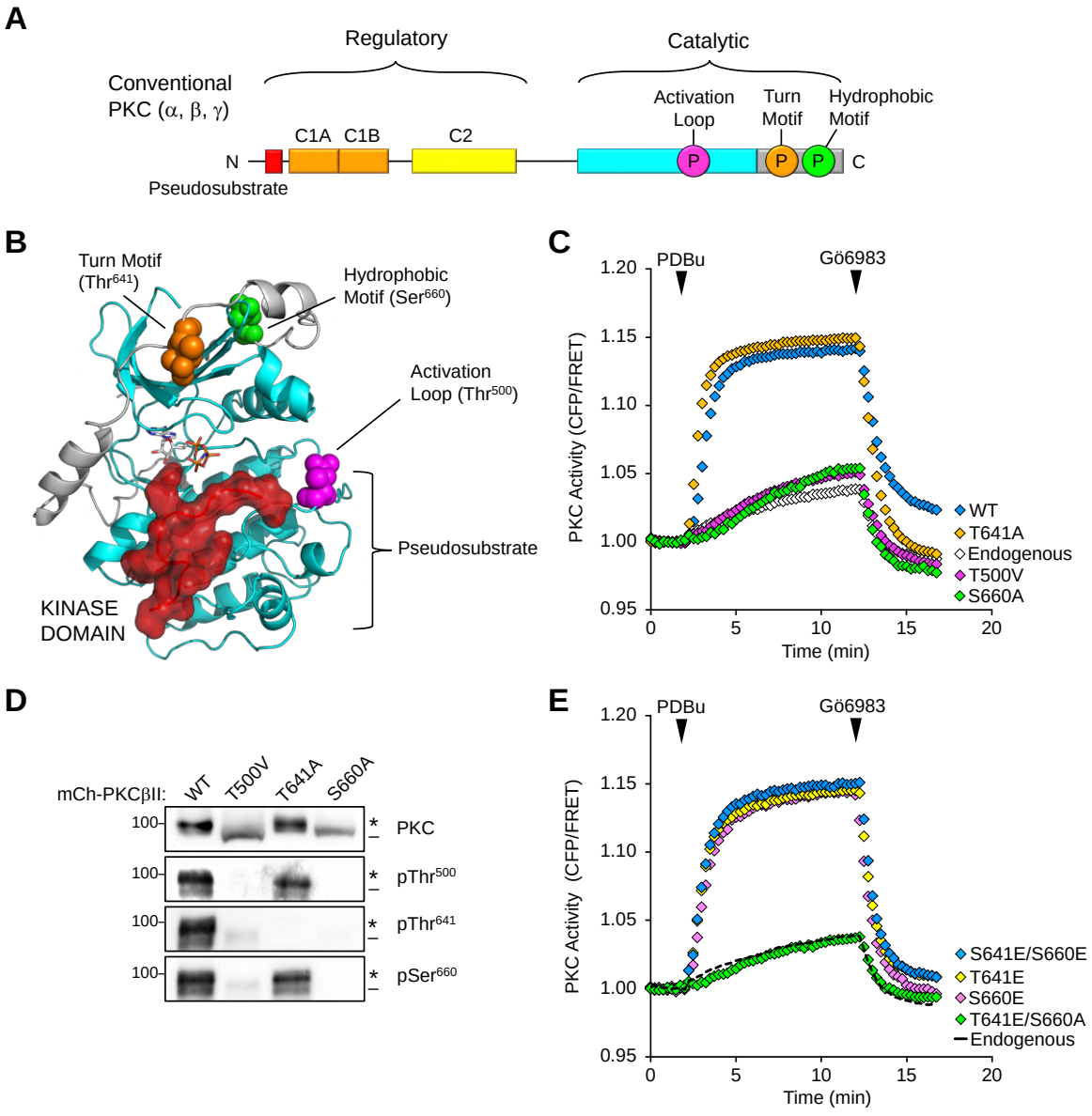
A
Regulatory
Catalytic
Conventional
PKC (α, β, γ)
Activation
Loop
Turn
Motif
Hydrophobic
Motif
C1A C1B
C2
N
P
P
P
C
Pseudosubstrate
B
Turn Motif
(Thr641)
Hydrophobic
Motif (Ser660)
Activation
Loop (Thr500)
Pseudosubstrate
KINASE
DOMAIN
C
PDBu
Gö6983
PKC Activity (CFP/FRET)
1.20
1.15
1.10
1.05
1.00
0.95
0
5
10
15
20
Time (min)
WT
T641A
Endogenous
T500V
S660A
D
mCh-PKCβII:
WT
T500V
T641A
S660A
100
PKC
pThr500
pThr641
pSer660
E
PDBu
Gö6983
PKC Activity (CFP/FRET)
Time (min)
S641E/S660E
T641E
S660E
T641E/S660A
Endogenous

The Autoinhibitory Pseudosubstrate Is Required for Cellular PKC Phosphorylation

Extensive *in vitro* biochemical studies have established that the pseudosubstrate is necessary to restrain PKC activity in the absence of second messengers (House and Kemp, 1987; Orr et al., 1992; Pears etal., 1990). To probe the role of the pseudosubstrate in a cellular context, we deleted the 18-amino-acid-pseudosubstrate segment of two cPKC isozymes, PKCα and PKCβII (Figure 3.2A; PKCα ΔPS and PKCβII ΔPS) and examined the phosphorylation state and cellular activity of the expressed proteins. Deletion of the pseudosubstrate abolished phosphorylation at all three priming sites (Figure 3.2B), which could not be rescued by treatment with the phosphatase inhibitor Calyculin A (Figure 3.8). Surprisingly, however, analysis of PKC basal activity, assessed by the drop in CKAR phosphorylation upon addition of PKC inhibitor, revealed that PKCβII ΔPS had high basal activity despite the absence of priming phosphorylations (Figure 3.2C). Whereas both WT PKCα and PKCβII were activated by treatment of cells with uridine triphosphate (UTP) and PDBu, neither PKCα ΔPS nor PKCβII ΔPS responded to either agonist, but constitutive, maximal activity was revealed upon inhibitor addition (Figures 2D and 2E). Thus, deletion of the pseudosubstrate results in constitutively active PKC that, unexpectedly, has maximal activity in the absence of priming phosphorylations.

Given that replacement of the hydrophobic motif Ser with Ala abolished cellular PKC activity (Figure 3.1C), we used phosphorylation mutants of PKCβII ΔPS (which is not phosphorylated and constitutively active) to assess whether negative charge at the hydrophobic motif is required in the maturation of PKC but becomes dispensable thereafter. Turn motif mutants PKCβII ΔPS T641A and PKCβII ΔPS T641E had enhanced basal activity with little preference for Ala versus Glu (Figure 3.2F). In contrast, only the phosphomimetic Glu, but not Ala or Asn, at the hydrophobic motif site conferred activity (Figure 3.2G). Mutation of the hydrophobic

motif did not simply alter substrate specificity to abolish recognition of CKAR; western blot analysis using a phospho-Ser PKC substrate antibody revealed no significant phosphorylation above basal levels in cells expressing PKCβII ΔPS S660A but robust phosphorylation in cells expressing PKCβII ΔPS (Figure 3.9). These data reveal that deletion of the pseudosubstrate (1) results in a constitutively active PKC that retains no phosphorylation at the priming sites and (2) does not bypass the requirement for negative charge at the hydrophobic motif to gain catalytic competence.

Figure 3.2: **The Autoinhibitory Pseudosubstrate Is Required for Cellular PKC Phosphorylation.**
(A) Schematic of pseudosubstrate-deleted PKC (PS) lacking amino acids 19-36 of PKC or PKCβII.
(B) IB analysis of lysates from COS7 cells transfected with indicated PKC constructs and probed with phospho-specific or total PKC antibodies.
(C-G) PKC activity analysis in COS7 cells expressing CKAR alone or co-expressing the indicated mCherry-PKC constructs treated with Gö6976 (1 μM) **(C)**, agonists UTP (100 μM), PDBu (200 nM), and inhibitors BisIV (2μ M) **(D)** and Gö6983 (1 μM) **(E)**, or Gö6976 (1 μM). (F and G). PKCβII PS trace in **(F)** is reproduced in **(G)** for comparison (dashed line).
CKAR data represent the normalized FRET ratio changes (mean $\pm$ SEM) from three independent experiments of >100 cells for each condition.

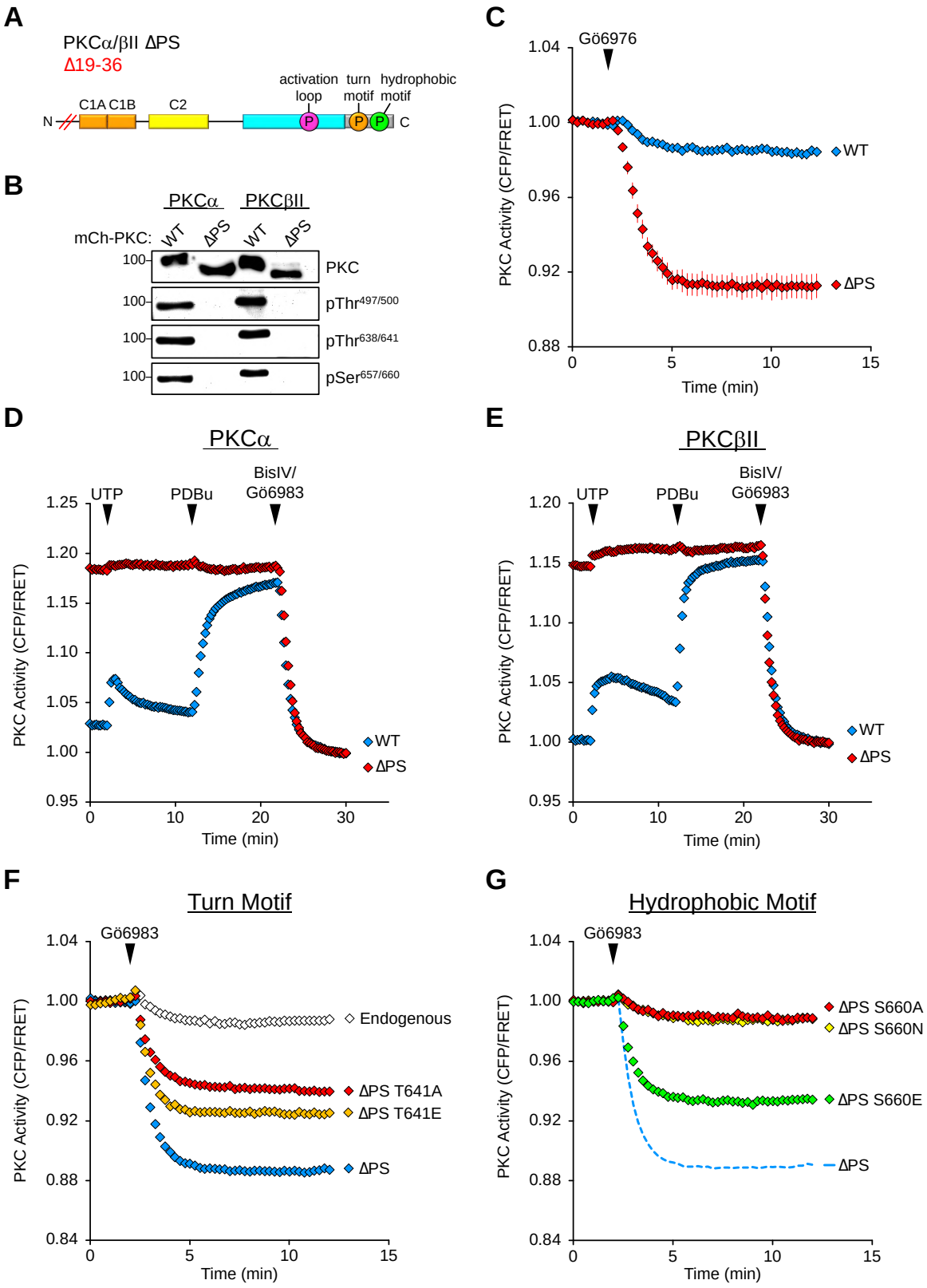
A
PKCα/βII ΔPS
Δ19-36
activation loop
turn motif
hydrophobic motif
C1A C1B
C2
N
C
P
B
PKCα
PKCβII
mCh-PKC:
WT
ΔPS
WT
ΔPS
100
PKC
pThr497/500
pThr638/641
pSer657/660
C
Gö6976
PKC Activity (CFP/FRET)
Time (min)
WT
ΔPS
D
PKCα
UTP
PDBu
BisIV/ Gö6983
PKC Activity (CFP/FRET)
Time (min)
WT
ΔPS
E
PKCβII
UTP
PDBu
BisIV/ Gö6983
PKC Activity (CFP/FRET)
Time (min)
WT
ΔPS
F
Turn Motif
Gö6983
PKC Activity (CFP/FRET)
Time (min)
Endogenous
ΔPS T641A
ΔPS T641E
ΔPS
G
Hydrophobic Motif
Gö6983
PKC Activity (CFP/FRET)
Time (min)
ΔPS S660A
ΔPS S660N
ΔPS S660E
ΔPS

The Autoinhibited Conformation of PKC Retains Priming Phosphorylations

To explore the relationship between PKC phosphorylation and activity, we used a PKC conformation reporter, Kinameleon, wherein intramolecular rearrangements within PKC alter Förster resonance energy transfer (FRET) between flanking cyan fluorescent protein (CFP) and yellow fluorescent protein (YFP) molecules (Figure 3.3A). Using this reporter, we showed previously that PKC adopts at least three distinct conformations: (1) a low-FRET unprimed state, in which the regulatory domains are exposed; (2) an intermediate-FRET primed state, in which PKC is fully phosphorylated at the C-terminal sites and autoinhibited, with the regulatory domains masked; and (3) a high-FRET active state, in which the regulatory domains are engaged on the plasma membrane (Figure 3.3A; Antal et al., 2014). To examine how autoinhibition affects PKC conformation, we altered the affinity of the pseudosubstrate for the kinase domain by either scrambling the position of positively charged amino acids in the pseudosubstrate (Figure 3.3B; scrambled mutant) or replacing them with neutral residues (Figure 3.3B; neutral mutant) in the Kinameleon reporter. Analysis of basal FRET, indicative of the average conformation of the PKC embedded in the reporter, revealed that the scrambled (PKCβII Scram PS) and neutral (PKCβII Neu PS) pseudosubstrate mutants had significantly lower basal FRET ratios than WT PKCβII, consistent with an unprimed, open conformation (Figure 3.3C). However, the scrambled mutant displayed modest propensity to autoinhibit; introduction of a kinase-dead mutation in PKCβII Scram PS (Scram PS K371R) which abolishes hydrophobic motif autophosphorylation and induces the unprimed conformation) (Antal et al., 2014; Behn-Krappa and Newton, 1999), further reduced the FRET ratio (Figure 3.3C). The FRET ratio of PKCβII Neu PS was indistinguishable from that of kinase-dead PKC (K371R).

Next, we examined the ability of these mutants to adopt the active conformation upon

agonist stimulation. PDBu treatment caused an increase in FRET ratio for WT PKCβII, reflecting the conformational rearrangement of the N and C termini (Figure 3.3D). PKCβII Scram PS underwent a more rapid conformational transition, and the FRET change plateaued at a lower amplitude (Figure 3.3D). No conformational change was observed for kinase-inactive PKCβII Scram PS K371R, PKCβII Neu PS, or PKCβII K371R (Figure 3.3D). These data suggest that while PKCβII Scram PS is loosely autoinhibited and rapidly adopts the open/active conformation in the presence of agonist, PKCβII Neu PS resembles unprimed PKC and is incapable of transitioning to the active state. Upon agonist stimulation, cPKC isozymes translocate to the plasma membrane where their C2 domain recognizes PIP_2 and C1B domain binds DAG. However, PKC that has not been properly processed by phosphorylation exists in an open conformation with unmasked C1 domains, resulting in localization to DAG-rich Golgi membranes (Antal et al., 2014; Scott et al., 2013). PKCβII Kinameleon reporter proteins that were incapable of acquiring or retaining priming phosphorylations (Neu PS, K371R, Scram PS K371R) translocated primarily to intracellular compartments resembling Golgi membranes following PDBu stimulation (Figure 3.3E). In contrast, PKCβII that was fully (WT) or partially (Scram PS) phosphorylated/autoinhibited primarily distributed to the plasma membrane (Figure 3.3E). Co-localization analysis between PKC and membrane-targeted CFP confirmed that PKCβII Neu PS co-distributed with the Golgi marker and WT PKCβII co-distributed with the plasma membrane marker upon PDBu stimulation (Figure 3.3F). Thus, disruption of the pseudosubstrate unmasks the C1 domains to promote interaction with Golgi membranes. To assess exposure of the C1 domains in the pseudosubstrate mutants, we used FRET to monitor real-time translocation of YFP-tagged PKC to plasma membrane-targeted CFP in live cells (Figure 3.3G). In response to PDBu, PKCβII Scram PS and PKCβII Neu PS translocated to the plasma membrane with

significantly faster kinetics than WT PKCβII (Figure 3.3H; $t_{1/2}$ = 2.3 ± 0.1 min and 3.1 ± 0.2 min, respectively, versus 5.0 ± 0.2 min), but with slower kinetics than kinase-dead PKCβII K371R (Figure 3.3H; $t_{1/2}$ = 1.0 ± 0.1 min), which has fully exposed C1 domains. The accelerated membrane translocation and enhanced affinity for Golgi membranes of the pseudosubstrate mutants support an unprimed, open conformation.

Next, we assessed the relationship between pseudosubstrate-dependent conformational changes and PKC activity using CKAR (Figure 3.3I). Addition of PKC inhibitor caused a minimal decrease in CKAR phosphorylation in cells expressing WT PKCβII, indicating low basal activity and effective autoinhibition, but a large decrease in cells expressing PKCβII Neu PS or PKCβII ΔPS, reflecting high basal activity and no autoinhibition. PKCβII Scram PS had slightly lower basal activity than that of the constitutively active PKCβII Neu PS, consistent with weak autoinhibition. Lastly, whereas WT PKCβII was phosphorylated at all three priming sites, the pseudosubstrate mutants had impaired phosphorylation; the weakly autoinhibited PKCβII Scram PS was minimally phosphorylated, while the unprimed PKCβII Neu PS and PKCβII ΔPS had no detectable phosphorylation (Figure 3.3J). Thus, the degree of PKC phosphorylation correlates with the extent of autoinhibition.

Figure 3.3: **The Autoinhibited Conformation of PKC Retains Priming Phosphorylations**
(A) Schematic showing PKC conformations assessed using the Kinameleon C FRET reporter.
(B) PKCβII pseudosubstrate mutants with basic (red) and neutral (green) residues highlighted. Crystal structure of PKCβII showing the pseudosubstrate modeled into the active site of the kinase domain with basic residues shown as sticks is shown. The pseudo-P-site is indicated by an asterisk (*).
(C) Absolute FRET ratio (mean ± SEM) of the indicated PKCβII Kinameleon C constructs expressed in COS7 cells. Each data point represents the average absolute FRET ratio from an individual cell.
(D) FRET ratio changes (mean ± SEM) of the indicated PKCβII Kinameleon C constructs expressed in COS7 cells following PDBu (200 nM) treatment.
(E) Representative YFP images of indicated PKCβII Kinameleon C constructs in COS7 cells before (basal) or after (post-PDBu) 25 min stimulation with PDBu (200 nM).
(F) Representative pseudo-colored images of plasma membrane-targeted (PM) or Golgi-targeted (Golgi) mCFP and the indicated mCherry-PKCβII in COS7 cells. Co-localization is shown as yellow in an overlay of mCFP and mCherry images (Merge).
(G) Schematic for PKC Translocation Assay: agonist-stimulated movement of mYFP-tagged PKC to plasma membrane-localized myristoylated-palmitoylated mCFP is monitored by FRET increase upon PKC membrane association.
(H) Translocation analysis of the indicated mYFP-PKCβII was monitored by FRET ratio change in COS7 cells co-expressing myristoylated-palmitoylated mCFP and treated with PDBu (100 nM).
(I) Basal PKC activity in COS7 cells expressing CKAR and the indicated mCherry-PKCβII constructs treated with Gö6983 (1 μM). Quantification (right) shows the normalized magnitude of FRET ratio change.
(J) IB analysis of lysates of COS7 cells expressing indicated PKCβII constructs and probed with indicated phospho-specific or total PKC antibodies.
****$p < 0.0001$, by repeated-measures one-way ANOVA and Brown-Forsythe Test; n.s., not significant. Kinameleon and CKAR represent the normalized FRET ratio changes (mean ± SEM) from three independent experiments with >100 cells for each condition.

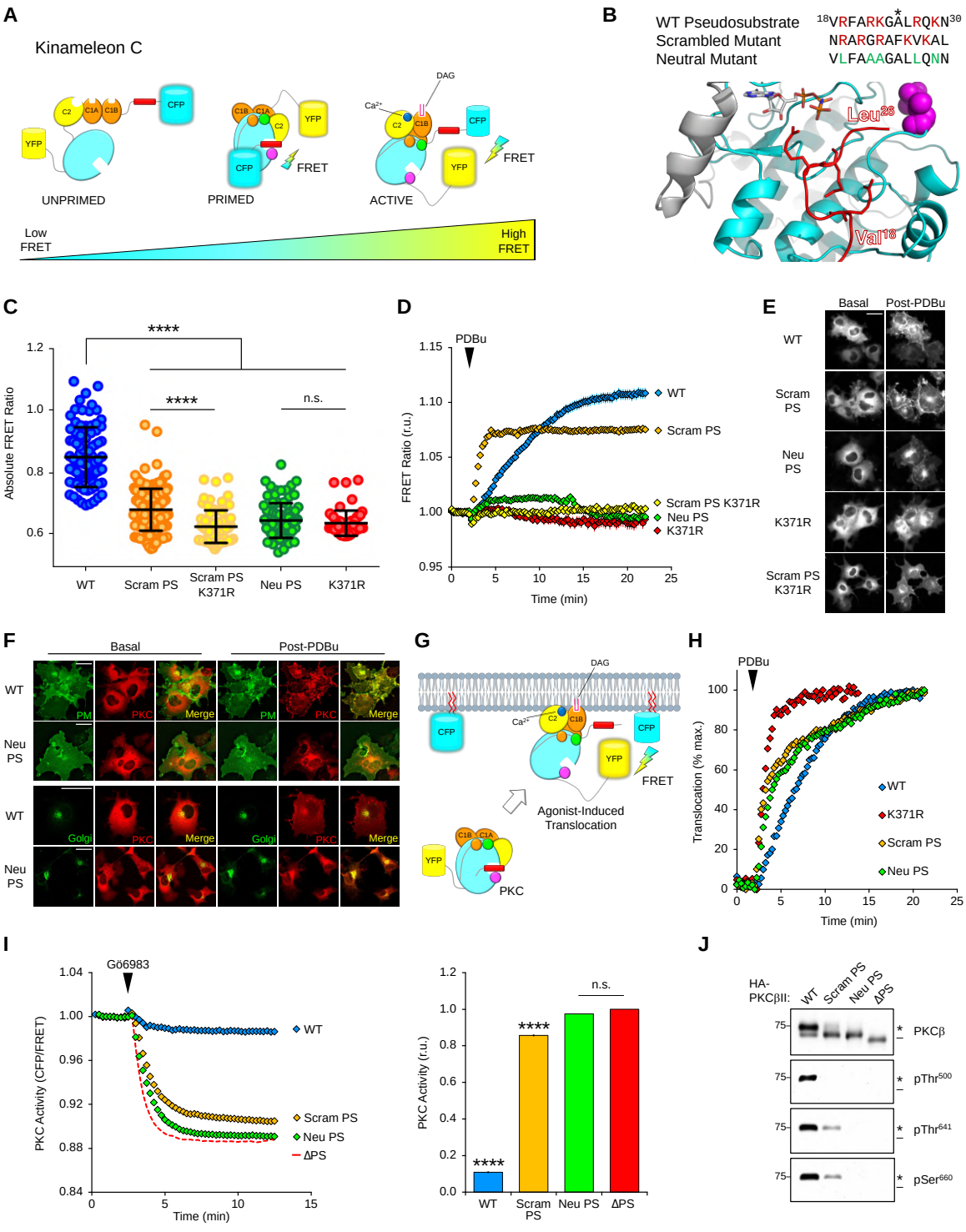
A
Kinameleon C
C2
C1A
C1B
CFP
YFP
UNPRIMED
PRIMED
FRET
DAG
Ca2+
ACTIVE
Low FRET
High FRET
B
WT Pseudosubstrate 18VRFARKGALRQKN30
Scrambled Mutant NRARGRAFKVKAL
Neutral Mutant VLFAAGALLQNN
Leu28
Val18
C
Absolute FRET Ratio
****
n.s.
WT
Scram PS
Scram PS K371R
Neu PS
K371R
D
PDBu
FRET Ratio (r.u.)
Time (min)
WT
Scram PS
Scram PS K371R
Neu PS
K371R
E
Basal
Post-PDBu
WT
Scram PS
Neu PS
K371R
Scram PS K371R
F
Basal
Post-PDBu
WT
Neu PS
PM
PKC
Merge
Golgi
G
DAG
Ca2+
CFP
YFP
FRET
Agonist-Induced Translocation
PKC
H
PDBu
Translocation (% max.)
Time (min)
WT
K371R
Scram PS
Neu PS
I
Gö6983
PKC Activity (CFP/FRET)
Time (min)
WT
Scram PS
Neu PS
ΔPS
PKC Activity (r.u.)
n.s.
****
WT
Scram PS
Neu PS
ΔPS
J
HA-PKCβII:
WT
Scram PS
Neu PS
ΔPS
PKCβ
pThr500
pThr641
pSer660
75

Autoinhibition Protects PKC from PHLPP1-Mediated Dephosphorylation and Degradation

Next, we investigated whether autoinhibition-deficient PKC was subject to dephosphorylation of the exposed hydrophobic motif site. We showed previously that activation of pure PKC via membrane binding increases its sensitivity to phosphatases by two orders of magnitude (Dutil et al., 1994). Furthermore, this phosphatase sensitivity is prevented by occupancy of the active site with protein or peptide substrates or with small-molecule inhibitors (Cameron et al., 2009; Dutil and Newton, 2000; Gould et al., 2011). To assess whether the pseudosubstrate of PKC can similarly protect the kinase domain from dephosphorylation in trans, we examined the phosphorylation state of the isolated catalytic domain (Cat) expressed alone or co-expressed with the isolated regulatory domain containing (Reg) or lacking (Reg ΔPS) the pseudosubstrate (Figure 3.4A). The catalytic domain alone was not phosphorylated at either of the C-terminal priming sites in COS7 cells; however, co-expression with the PKC regulatory domain (Cat + Reg) was sufficient to rescue phosphorylation at the hydrophobic motif, but not the turn motif (Figure 3.4B). Co-expression with the regulatory domain lacking the pseudosubstrate (Cat + Reg ΔPS), in contrast, did not promote catalytic domain hydrophobic motif phosphorylation (Figure 3.4B). These data reveal that autoinhibition by the pseudosubstrate is responsible for retaining phosphate specifically at the hydrophobic motif.

Next, we addressed whether the known hydrophobic motif phosphatase PHLPP was responsible for the dephosphorylation of newly synthesized autoinhibition-deficient PKC. We employed pulse-chase analysis to ^{35}S radiolabel a pool of newly synthesized PKC and monitored the maturation of the nascent protein via the electrophoretic mobility shift that accompanies phosphorylation (Borner et al., 1989; Sonnenburg et al., 2001). The kinetics of PKC phospho-

rylation were unaffected by ectopic PHLPP1 expression (Figure 3.4C), indicating that PHLPP1 may be saturating in any regulation of PKC. Immunoprecipitation revealed that PHLPP1 exclusively bound the faster-mobility, unphosphorylated species of ^{35}S-labeled (newly synthesized) PKC and did not bind the slower-mobility band that had become phosphorylated by 60 min (Figure 3.4C; asterisk). Further co-immunoprecipitation studies revealed that PHLPP1 effectively bound unphosphorylated ΔPS or kinase-dead (K371R) PKCβII mutants. This interaction was independent of the C1A, C1B, or C2 domains, as mutants lacking these regulatory domains still associated with PHLPP1 (Figure 3.4D). Deletion of the C2 domain with the pseudosubstrate intact (ΔC2) also resulted in enhanced PHLPP1 association (Figure 3.4D), consistent with our previous report that the C2 domain clamps the pseudosubstrate in the substrate-binding cavity (Antal et al., 2015a). Analysis of phosphorylation state and CKAR-reported activity revealed that the PKCβII ΔC2 mutant had decreased phosphorylation and enhanced basal activity, consistent with a loosening of autoinhibition as observed upon disruption of pseudosubstrate binding (Figures 3.4E and 3.4F). Deletion of the C1 and C2 domains concurrently (ΔC1A/C1B/C2) resulted in greater dephosphorylation than that observed upon deletion of the C2 domain alone (ΔC2). However, PKCβII ΔC1A/C1B/C2, which retains only the pseudosubstrate segment of the regulatory domain, was effectively autoinhibited: despite its enhanced sensitivity to dephosphorylation, its basal activity was indistinguishable from that of PKCβII ΔC1A, PKCβII ΔC2, and PKCβII ΔC1A/C1B (Figure 3.4F). These data reveal that the pseudosubstrate functions not only as an inhibitor of the kinase domain but also as a tether to position the regulatory domains that protect PKC from dephosphorylation.

Next, we used pulse-chase analysis to examine if phosphorylation could be detected on newlysynthesized autoinhibition-deficient PKC. PKCβII ΔPS, like kinase-dead PKC (K371R),

did not undergo the characteristic mobility shift observed for WT PKC (Figure 3.4G). This finding suggests that PHLPP1 dephosphorylates newly synthesized PKC that cannot be autoinhibited, thus preventing accumulation of the phosphorylated species on any open PKC. Previous studies have shown that the isolated catalytic domain of PKC is phosphorylated at the priming sites when expressed in insect cells (Behn-Krappa and Newton, 1999), suggesting a different phosphatase environment in insect versus mammalian cells. To determine whether PKCβII ΔPS also evades dephosphorylation in this system, we analyzed the phosphorylation state of WT PKCβII or PKCβII ΔPS expressed in Sf9 cells. In marked contrast to its unphosphorylated state in mammalian cells, PKCβII ΔPS was phosphorylated at all three priming sites in Sf9 cells, revealing that PKC lacking the pseudosubstrate does incorporate phosphate but is dephosphorylated in the absence of autoinhibition in certain contexts, such as in COS7 cells (Figure 3.4H). Co-expression of the PP2C phosphatase domain of PHLPP1 caused a 4-fold decrease in both PKCβII WT and ΔPS steady-state levels, along with a commensurate decrease in phosphorylation, relative to cells that did not express the PHLPP1 PP2C domain (Figure 3.4H). The PHLPP1-induced decrease in steady-state levels and loss of the dephosphorylated species is consistent with the dephosphorylated protein displaying enhanced sensitivity to downregulation (Figure 3.4H). Upon dephosphorylation, PKC is subject to ubiquitination and proteasome-dependent degradation (Parker et al., 1995). Analysis of PKC's half-life via cycloheximide treatment of cells confirmed that autoinhibition-deficient PKC was significantly less stable than WT PKC (Figure 3.4I; WT PKCβII $t_{1/2} > 48$ h, Scram PS $t_{1/2} = 16 \pm 2$ h, Neu PS $t_{1/2} = 10.1 \pm 0.5$ h). Furthermore, endogenous PKCα was more resistant to PDBu-induced downregulation in the absence of PHLPP1 (Figure 3.4J; *Phlpp1*$^{-/-}$ $t_{1/2} = 14 \pm 2$ h, *Phlpp1*$^{+/+}$ $t_{1/2} = 6.6 \pm 0.9$ h). Moreover, the steady-state levels of endogenous PKCα were 2-fold higher in *Phlpp1*$^{-/-}$ MEFs compared to *Phlpp1*$^{+/+}$ MEFs

(Figure 3.4K). These results demonstrate that unphosphorylated PKC is unstable and support a role for PHLPP1 in regulating PKC stability by opposing hydrophobic motif phosphorylation and consequently promoting PKC degradation.

Figure 3.4: **Autoinhibition Protects PKC from PHLPP1-Mediated Dephosphorylation and Degradation**
(A) Schematic of indicated PKCβII truncation mutants.
(B) IB analysis of COS7 cells expressing indicated PKCβII constructs probed with indicated phospho-specific or total PKC antibodies.
(C) Autoradiogram (^{35}S) and IB analysis of newly synthesized PKC pulse-chase immunoprecipitates from COS7 cells expressing HA-PKCβII and FLAG-PHLPP1 (see STAR Methods).
(D) IB analysis of FLAG immunoprecipitates from COS7 cells transfected with indicated HA-PKCβII and FLAG-PHLPP1 constructs and probed with indicated antibodies. Vinculin was used as a loading control.
(E) IB analysis of lysates from COS7 cells transfected with indicated HA-PKCβII constructs probed with phospho-specific or total PKC antibodies. PKCβII Δ37-86 (ΔC1A), PKCβII Δ159-291 (ΔC2), PKCβII Δ101-291 (ΔC1B/C2), PKCβII Δ37-291 (ΔC1A/C1B/C2), or PKCβII 296-673 (Cat). Quantification (bottom) of pSer660 band intensity relative to WT (mean $\pm$ range, n = 2) is shown.
(F) COS7 cells co-expressing CKAR and indicated mCherry-PKCβII regulatory domain deletion constructs were treated with BisIV (2 μM). Insert shows trace for Cat activity, with cluster of traces in main Figure 3.reproduced for comparison. Quantification (bottom) shows magnitude of the FRET ratio change from 3 independent experiments.
(G) Autoradiogram (^{35}S) of HA immunoprecipitates from pulse chase of COS7 cells expressing the indicated PKC constructs.
(H) IB analysis of lysates from Sf9 insect cells infected with the indicated GST-PKC constructs and His-PHLPP1 PP2C (PHLPP1; 1154-1422) baculovirus, probed with the indicated phospho-specific or total PKC antibodies. Quantification (right) of total PKC protein normalized to Tubulin or PKC phosphorylation normalized to total PKC is shown.
(I) IB analysis of lysates from COS7 cells expressing the indicated HA-PKC constructs treated with cycloheximide (CHX, 250 μM) for the indicated times prior to lysis and probed with the indicated antibodies. Quantification (bottom) of PKC band intensity normalized to Tubulin loading control and plotted as percentage of protein at time zero is shown.
(J) IB analysis of lysates from WT MEFs treated with PDBu (200 nM) for the indicated time points prior to lysis and probed with the indicated antibodies. Quantification (bottom) of PKC band intensity normalized to Hsp90 loading control and plotted as percentage of protein at time zero is shown.
(K) IB analysis of lysates from untreated WT MEFs probed with the indicated antibodies. Quantification (bottom) of PKC band intensity normalized to Tubulin loading control is shown. *p $<$ 0.05, **p $<$ 0.01, ***p $<$ 0.001, ****p $<$ 0.0001 by repeated-measures one-way ANOVA and Tukey HSD test. IB quantification (excluding E) represent the mean $\pm$ SEM from at least three independent experiments. Dashed line (B and E) indicates splicing of irrelevant lanes from a single blot.

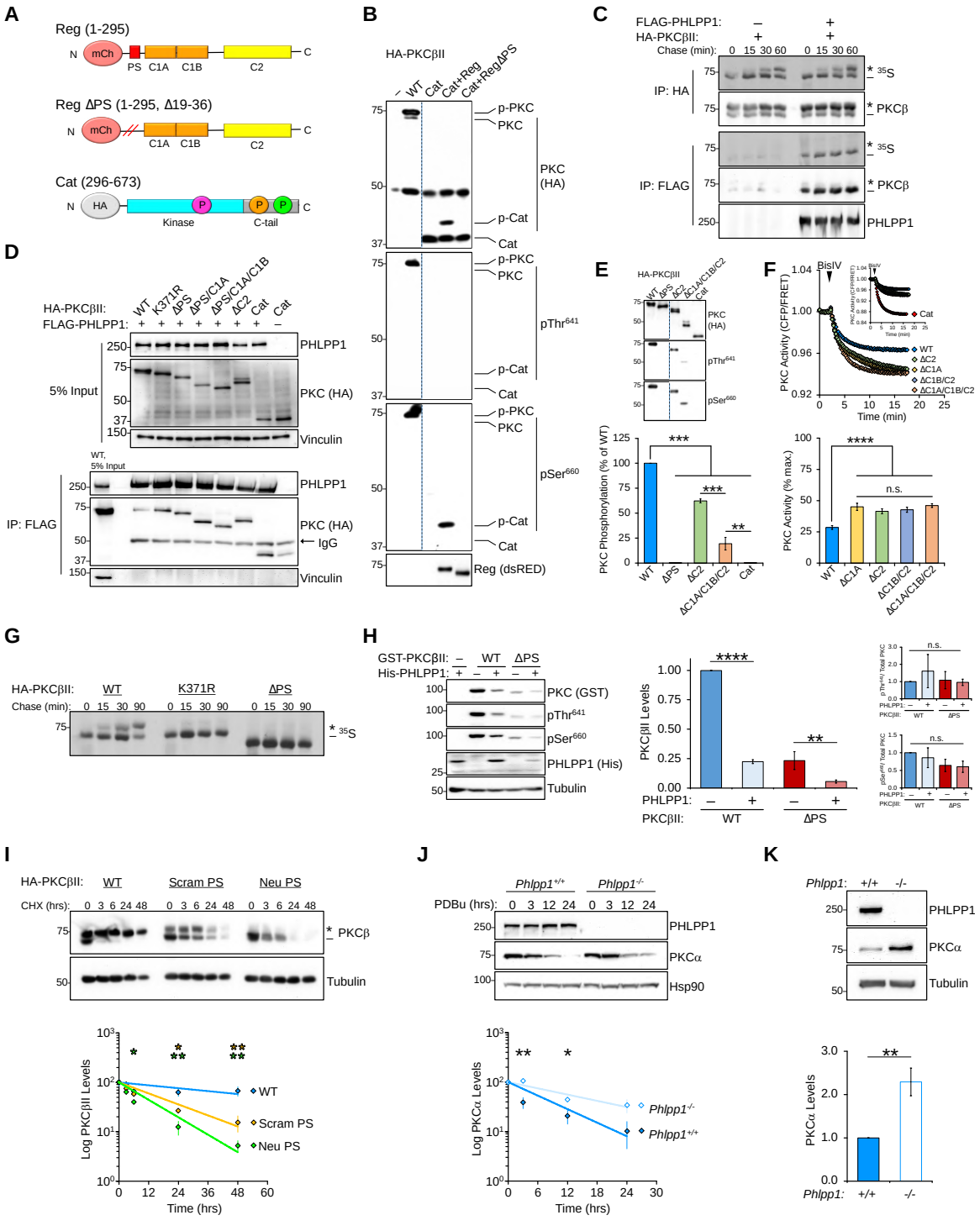
A
Reg (1-295)
N
mCh
PS C1A C1B
C2
C
Reg ΔPS (1-295, Δ19-36)
C1A C1B
Cat (296-673)
HA
P
Kinase
C-tail
B
HA-PKCβII
– WT Cat Cat+Reg Cat+RegΔPS
p-PKC
PKC
PKC (HA)
p-Cat
Cat
pThr641
pSer660
Reg (dsRED)
C
FLAG-PHLPP1:
HA-PKCβII:
Chase (min): 0 15 30 60 0 15 30 60
IP: HA
IP: FLAG
35S
PKCβ
PHLPP1
D
HA-PKCβII:
FLAG-PHLPP1:
WT K371R ΔPS ΔPS/C1A ΔPS/C1A/C1B ΔC2 Cat Cat
5% Input
PHLPP1
PKC (HA)
Vinculin
WT, 5% Input
IP: FLAG
IgG
E
HA-PKCβII
PKC (HA)
pThr641
pSer660
PKC Phosphorylation (% of WT)
WT ΔPS ΔC2 ΔC1A/C1B/C2 Cat
F
BisIV
PKC Activity (CFP/FRET)
Time (min)
WT
ΔC2
ΔC1A
ΔC1B/C2
ΔC1A/C1B/C2
Cat
PKC Activity (% max.)
n.s.
G
HA-PKCβII: WT K371R ΔPS
Chase (min): 0 15 30 90 0 15 30 90 0 15 30 90
H
GST-PKCβII: – WT ΔPS
His-PHLPP1: + – + – + –
PKC (GST)
pThr641
pSer660
PHLPP1 (His)
Tubulin
PKCβII Levels
PHLPP1:
PKCβII:
WT
ΔPS
I
HA-PKCβII: WT Scram PS Neu PS
CHX (hrs): 0 3 6 24 48 0 3 6 24 48 0 3 6 24 48
PKCβ
Tubulin
Log PKCβII Levels
Time (hrs)
WT
Scram PS
Neu PS
J
Phlpp1+/+ Phlpp1-/-
PDBu (hrs): 0 3 12 24 0 3 12 24
PHLPP1
PKCα
Hsp90
Log PKCα Levels
Phlpp1-/-
Phlpp1+/+
K
Phlpp1: +/+ -/-
PHLPP1
PKCα
Tubulin
PKCα Levels

Cancer-Associated Pseudosubstrate Hotspot Mutations Reveal a Distinct PKC LOF Mechanism

Given the tumor-suppressive role of PKCβ, we asked whether PKC mutations that perturb autoinhibition, and are thus subject to PHLPP1 quality control, could present a LOF mechanism in cancer. In support of this, the pseudosubstrate of PKCβ is a 3D-clustered functional hotspot of cancer-associated mutations (Gao et al., 2017). 10 distinct mutations, identified in 16 tumor samples, occur in the region preceding the P0 position (Ala^{25}) of the pseudosubstrate (P-7 through P-1) (Figure 3.10, Figure 3.5A). These include Arg^{22} at the P-3 position in the pseudosubstrate, a critical residue for effective autoinhibition that makes multiple contacts with both the bound nucleotide and Asp^{470} in the active site (Figure 3.5B) (House and Kemp, 1990; Pears et al., 1990). Analysis of sequence conservation among PKC isozymes using the protein alignment tool KinView (McSkimming et al., 2016) reveals that this interaction partner, which resides between the HRD and DFG motifs of the kinase activation segment, is highly conserved in PKC isozymes compared to other kinases (Figure 3.5B; asterisk). Given the conservation of this interaction pair, we reasoned that the Arg^{22} mutations would have the largest effect on PKC autoinhibition. Introducing each of the 10 mutations into PKCβII, we measured basal activity via CKAR upon inhibitor addition in COS7 cells. The activity of every pseudosubstrate mutant differed significantly from that of WT and segregated into two distinct groups: 56% of mutations were less active than WT and 44% of mutations were more active (Figures 5C and 5D). Mutations displaying enhanced autoinhibition (Figure 3.5E; blue) had a higher fraction of phosphorylated PKC to unphosphorylated PKC compared to WT PKC, as assessed by the intensity of the slower-migrating phosphorylated species (asterisk) to the faster-migrating unphosphorylated species (dash) and staining with antibodies to the three processing phosphorylations (Figure

3.5E). Conversely, mutations displaying reduced autoinhibition (Figure 3.5E; red) had a lower fraction of phosphorylated PKC to unphosphorylated PKC compared to WT PKC (Figure 3.5E). Thus, mutants with reduced basal activity had increased phosphorylation relative to WT and mutants with increased basal activity had reduced phosphorylation (Figure 3.5F). These data show that aberrant autoinhibition of cancer-associated PKC pseudosubstrate mutations causes LOF in either of two ways: (1) enhancing pseudosubstrate affinity to reduce PKC output or (2) weakening pseudosubstrate affinity to reduce PKC phosphorylation and stability.

Figure 3.5: **Cancer-Associated Pseudosubstrate Hotspot Mutations Reveal a Distinct PKC LOF Mechanism**
(A) Mutations in the N terminus (1-40) of PKCβ identified in human cancers showing 3D-clustered functional hotspots (red).
(B) Crystal structure of PKCβII with the pseudosubstrate modeled into the active site. Interactions between the pseudosubstrate (Arg^{22}), bound nucleotide (AMP-PNP), and kinase domain (Asp^{470}) are highlighted. KinView analysis showing evolutionary protein sequence conservation of the activation segment from all PKC isozymes (top) or all protein kinases (bottom) is shown. Height of the letter indicates the residue frequency at that position.
(C) COS7 cells co-expressing CKAR and indicated mCherry-PKCβII cancer-associated pseudosubstrate mutants were treated with Gö6983 (1 mM) to determine basal activity.
(D) Quantification of **(C)** showing the magnitude of FRET ratio change upon inhibitor addition. Data represent three independent experiments of >100 cells for each construct; dotted line indicates WT activity; ****$p < 0.0001$, by repeated-measures one-way ANOVA and Tukey-Kramer HSD test.
(E) IB analysis of lysates from COS7 cells expressing indicated PKC constructs probed with phospho-specific or total PKC antibodies.
(F) Schematic of cancer-associated pseudosubstrate mutants. Pseudosubstrate mutations manifest as LOF, either by enhancing (reduced activity) or disrupting (reduced stability) PKC autoinhibition.

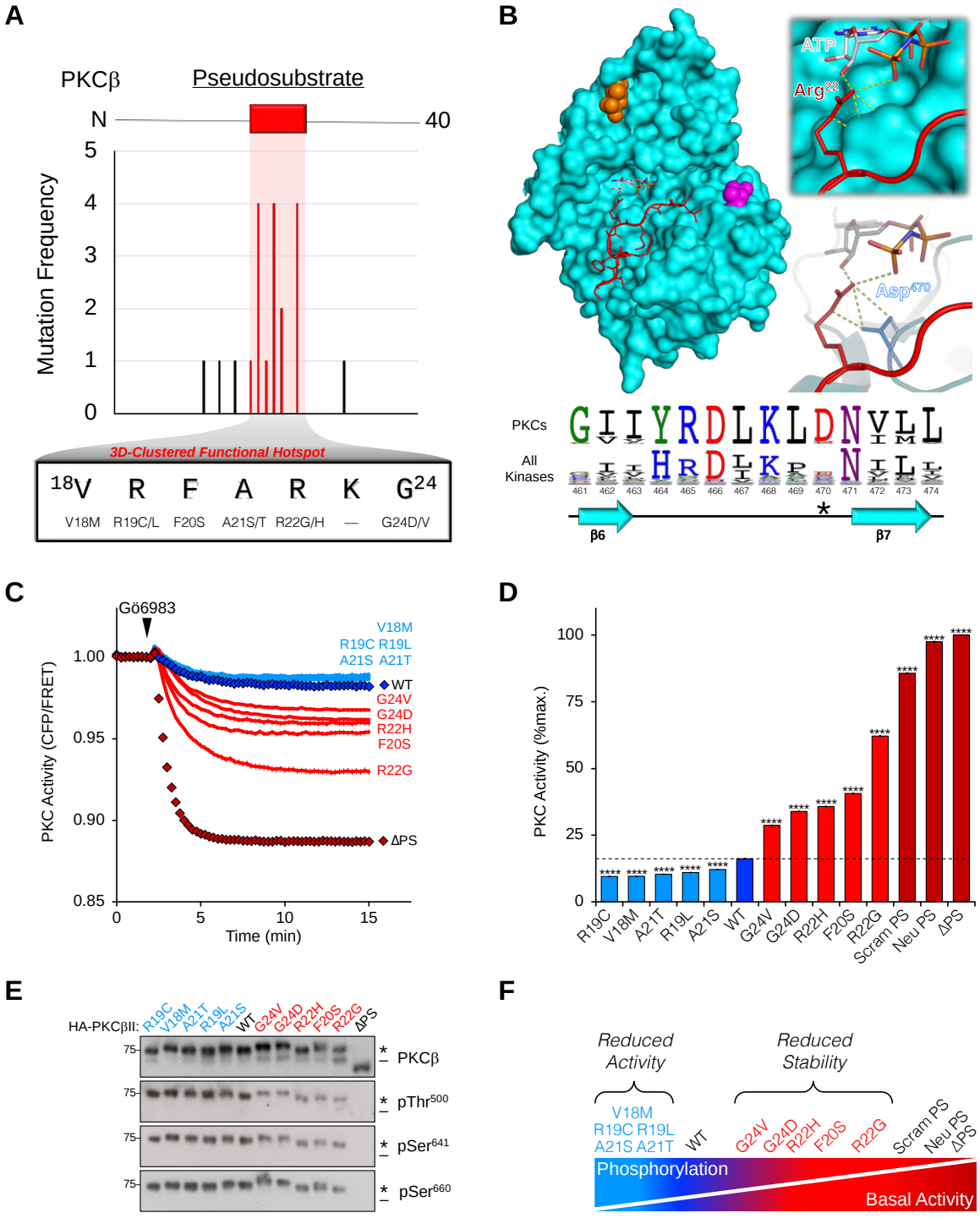
A
PKCβ
Pseudosubstrate
N
40
Mutation Frequency
3D-Clustered Functional Hotspot
18V R F A R K G24
V18M R19C/L F20S A21S/T R22G/H — G24D/V
B
ATP
Arg22
Asp470
PKCs
All Kinases
β6
β7
C
Gö6983
V18M
R19C R19L
A21S A21T
WT
G24V
G24D
R22H
F20S
R22G
ΔPS
PKC Activity (CFP/FRET)
Time (min)
D
PKC Activity (%max.)
R19C
V18M
A21T
R19L
A21S
WT
G24V
G24D
R22H
F20S
R22G
Scram PS
Neu PS
ΔPS
E
HA-PKCβII:
PKCβ
pThr500
pSer641
pSer660
F
Reduced Activity
Reduced Stability
V18M
R19C R19L
A21S A21T
WT
G24V
G24D
R22H
F20S
R22G
Scram PS
Neu PS
ΔPS
Phosphorylation
Basal Activity

PKC Quality Control Is Conserved in Human Cancer

More broadly, we explored whether PHLPP1-mediated quality control may be a ubiquitous mechanism employed by tumors to suppress PKC output. To assess whether PKC quality control by PHLPP1 is a conserved process in human cancer, we analyzed the phosphorylation state and total protein levels of PKC in patient tumor samples by reverse-phase protein array (RPPA), a high-throughput antibody-based method for quantitative detection of protein markers from cell lysates (Tibes et al., 2006). Analysis of 5,157 patient samples from 19 cancers comprising The Cancer Genome Atlas (TCGA) Pan-Can 19 revealed a striking 1:1 correlation between PKCα hydrophobic motif phosphorylation (pSer^{657}) and total PKCα protein (Figures 6A and 6B; R = 0.923). We also analyzed hydrophobic motif phosphorylation of Akt and S6K, two other AGC kinases regulated by PHLPP1. In contrast to PKC, hydrophobic motif phosphorylation of Akt (pSer^{473}) and S6K (pThr^{389}) did not correlate with total protein (Figures 3.6A and 3.6B; R = 0.214 and -0.081, respectively). Consistent with the tumor data, analysis of cancer cell lines from the Cancer Cell Line Encyclopedia (CCLE) and MD Anderson Cell Lines Project (MCLP) also displayed a strong correlation between PKCα hydrophobic motif phosphorylation (pSer^{657}) and total PKCα protein, which was not observed with the Akt activation loop (pThr^{308}) or hydrophobic motif (pSer^{473}) phosphorylation sites and total Akt protein (Figure 3.11). These data demonstrate that the hydrophobic motif site is generally phosphorylated in essentially 100% of the PKC species present in the cell, regardless of cell or tissue type. The one exception may be head and neck squamous carcinomas (HNSC), where a small number of samples had hypophosphorylated PKC; whether defects in the PKC degradation pathway allow accumulation of unphosphorylated PKC in this cancer remains to be determined. In summary, RPPA analyses validate cellular studies showing that unphosphorylated PKC is unstable and rapidly degraded,

indicating that only phosphorylated PKC accumulates in cells in an endogenous context.

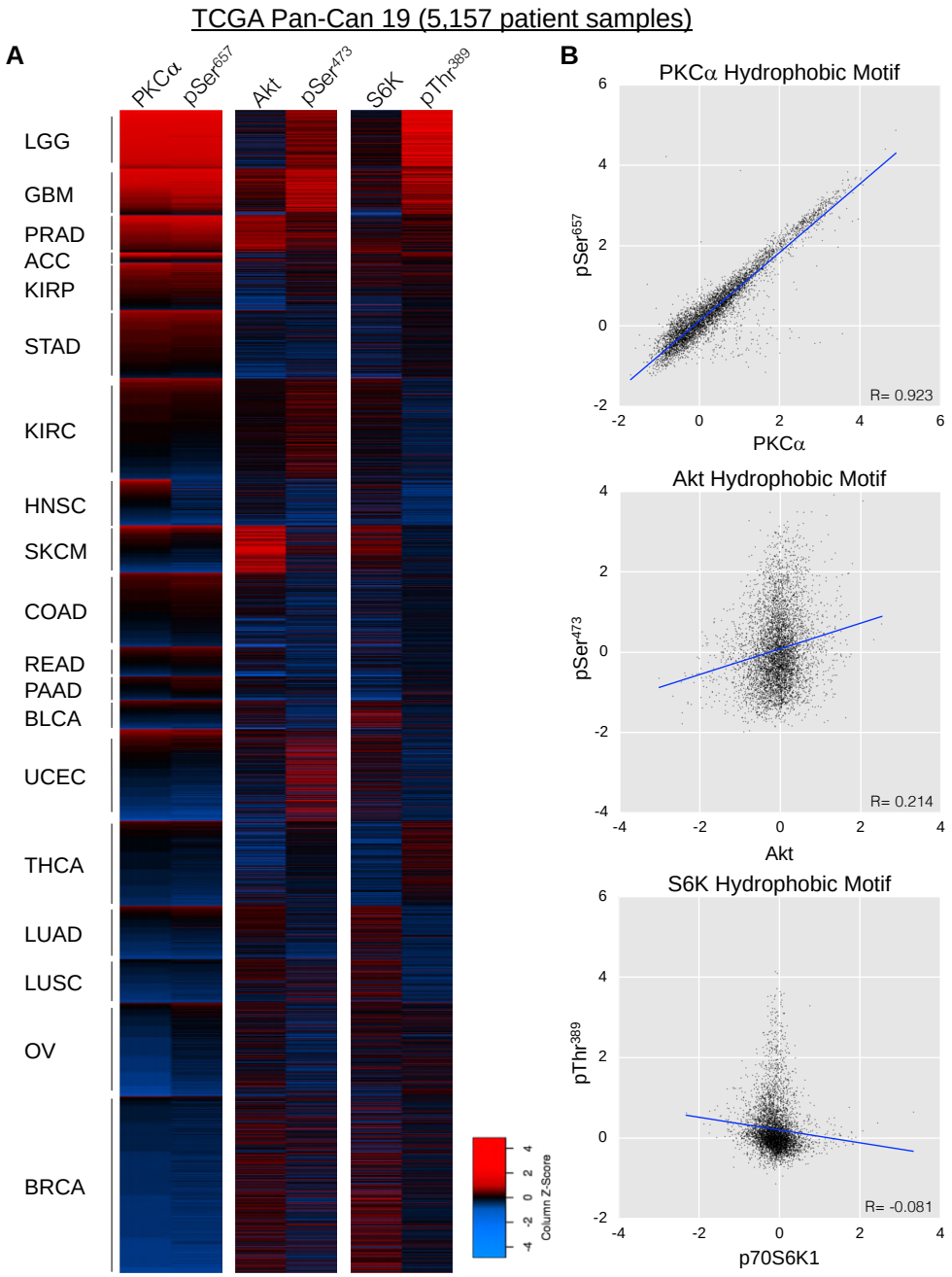

Figure 3.6: **PKC Quality Control Is Conserved in Human Cancer**
(A) RPPA analysis of TCGA Pan Cancer Atlas tumor samples showing hydrophobic motif phosphorylation and total protein levels for PKC, Akt, or S6K. Cancer types are indicated by TCGA study abbreviations.
(B) Quantification of **(A)**: scatterplot of the expression of the indicated phosphorylation correlated with the associated total protein.

High PKC and Low PHLPP1 Levels Are Protective in Pancreatic Adenocarcinoma

Next, we sought to identify which cancer subtype exhibits the most robust PKC quality control by PHLPP1, a finding that could be therapeutically relevant. We reasoned that cancers in which PKC phosphorylation was strongly dependent on PHLPP1 would have (1) a strong correlation between PKCα and PKCβ hydrophobic motif phosphorylation due to common regulation of their levels and (2) relatively low PKC steady-state levels because of dominant regulation by PHLPP1. Thus, we examined the correlation of total PKCα and PKCβ hydrophobic motif phosphorylation as a function of cancer type (Figure 3.7A; column 2). We also examined the association of known positive regulators of PKC processing, such as PDK-1 and mTORC2 components, with the PKCα:PKCβ hydrophobic motif correlation (Figure 3.7A; columns 3-7). In general, cancers with relatively high levels of PKC expression (e.g., low-grade glioma [LGG], glioblastoma multiforme [GBM], and kidney renal papillary cell carcinoma [KIRP]) had relatively high correlation with these positive regulators, and those with low levels of PKC expression had low correlation with these positive regulators. One notable outlier was pancreatic adenocarcinoma (PAAD), which showed correlation signatures with positive regulators similar to those observed in high-PKC-expressing cancers despite much lower PKCα expression levels (Figure 3.7A). Thus, we hypothesized that PKC expression in PAAD, which is suppressed by a common mechanism due to the strong correlation of PKCα:PKCβ hydrophobic motif phosphorylation (Figure 3.7A; column 2), may be dominantly regulated by PHLPP1 quality control. Indeed, RPPA analysis of the 105 PAAD samples revealed an inverse correlation between PHLPP1 levels and PKCα levels (Figures 3.7B and 3.7C). In contrast, this inverse correlation between PHLPP1 levels and PKCα was not observed in the glioma tumor samples (Figure 3.7B), two cancers in which positive regulators dominate in controlling PKC levels. This suggests that in gliomas,

which generally have very low levels of PHLPP1 (Warfel et al., 2011), positive regulators dominate in controlling PKC levels. However, in pancreatic cancer, PKC levels are determined by the negative regulator PHLPP1 via PKC quality control, as evidenced by the inverse correlation between PHLPP1 and PKCα protein levels. Together, these findings reveal a consistent 1:1 stoichiometry of phosphorylated PKC and total PKC protein levels regardless of cell or tumor type; in some malignancies, such as pancreatic cancer, the amount of PHLPP1 is the dominant mechanism controlling PKC levels.

Next, we measured the impact of PKC expression on patient outcome by stratifying survival rates by levels of PKC hydrophobic motif phosphorylation. We focused on pancreatic cancer as PKC levels are subject to PHLPP1-mediated quality control in this cancer. Analysis of the cohort of 105 PAAD patients revealed that high levels of hydrophobic motif phosphorylation in PKCα (pSer^{657}) or PKCβ (pSer^{660}) co-segregated with significantly improved survival (Figure 3.7D). Thus, as PKC hydrophobic motif phosphorylation demarcates stable PKC and improved patient survival, it serves as a potential prognostic marker and avenue for intervention in pancreatic cancer, for which there are limited effective therapeutic options.

Figure 3.7: **High PKC and Low PHLPP1 Levels Are Protective in Pancreatic Adenocarcinoma**
(A) Heatmap of PKCα expression by cancer type (Expression; column 1). Heatmap showing coefficient of determination between PKCα hydrophobic motif phosphorylation and the indicated protein or phosphorylation (correlation; columns 2-8) is shown. Cancer types are indicated by TCGA study abbreviations. **(B)** RPPA analysis of PHLPP1 and PKCα levels in patient samples from the indicated cancers with Least-Squares Regression Line.
(C) Heatmap of individual PAAD patients showing relative abundance of the indicated protein or modification.
(D) Kaplan-Meier survival plots from PAAD patients stratified by PKC hydrophobic motif phosphorylation levels. p = log-rank p value.
(E) Model of PKC Quality Control by PHLPP1: newly synthesized PKC (i) binds PHLPP1 where it surveys the conformation of this unprimed PKC to regulate phosphorylation of the hydrophobic motif. This species is in an open conformation, with the pseudosubstrate (PS; red rectangle) and all membrane-targeting modules unmasked. PKC that becomes phosphorylated (ii) is immediately autoinhibited, releasing PHLPP1 and entering the pool of stable, catalytically competent but inactive enzyme (iii). This primed species is transiently and reversibly activated by binding second messengers (iv). PKC that does not properly autoinhibit following priming phosphorylations (v), for example due to mutations that impair autoinhibition, is rapidly dephosphorylated by PHLPP1 at the hydrophobic motif, leading to further dephosphorylation and degradation (vi).

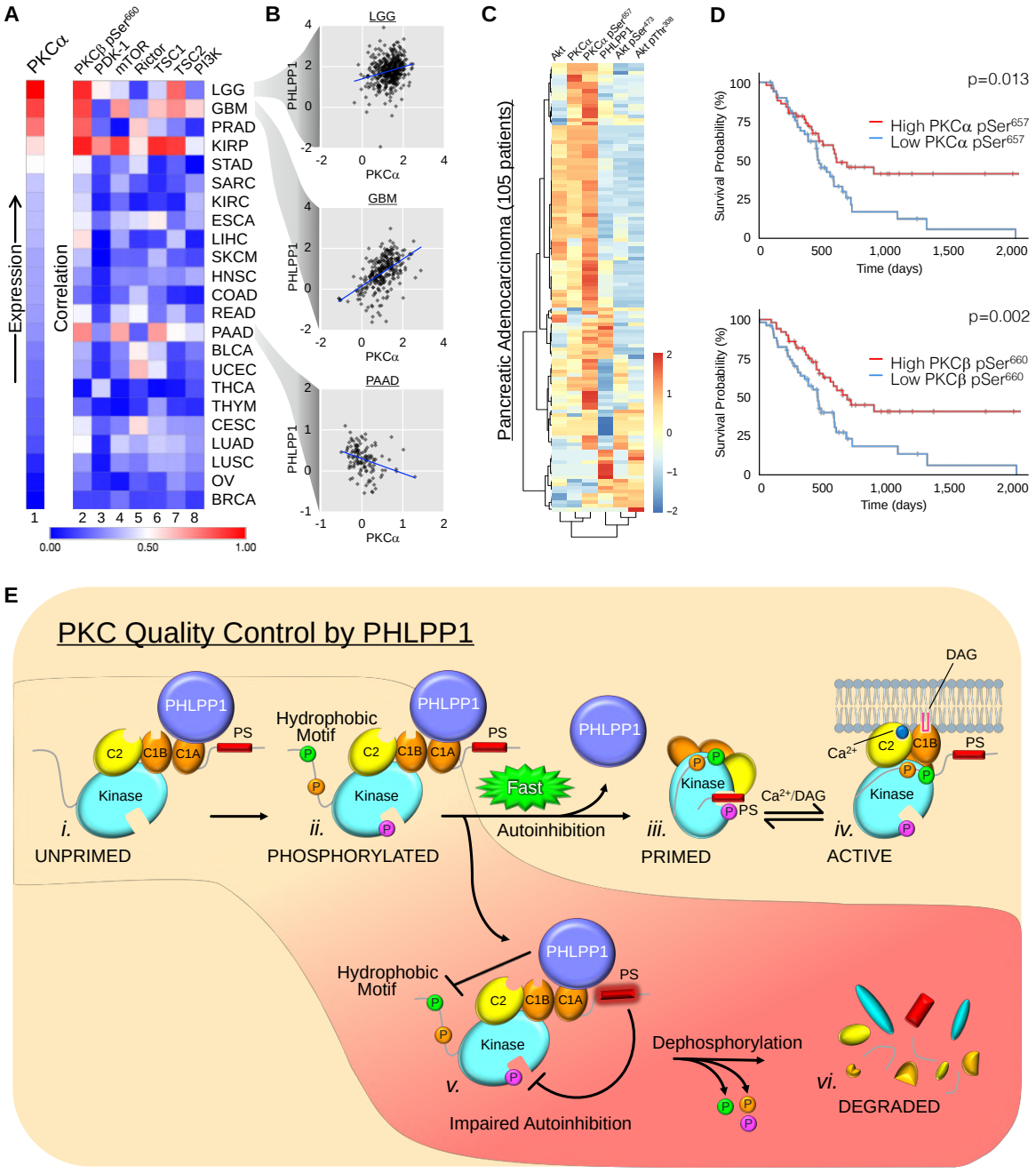
A
PKCα
PKCβ pSer660
PDK-1
mTOR
Rictor
TSC1
TSC2
PI3K
Expression
Correlation
LGG
GBM
PRAD
KIRP
STAD
SARC
KIRC
ESCA
LIHC
SKCM
HNSC
COAD
READ
PAAD
BLCA
UCEC
THCA
THYM
CESC
LUAD
LUSC
OV
BRCA
B
LGG
GBM
PAAD
PHLPP1
PKCα
C
Pancreatic Adenocarcinoma (105 patients)
D
p=0.013
High PKCα pSer657
Low PKCα pSer657
p=0.002
High PKCβ pSer660
Low PKCβ pSer660
Survival Probability (%)
Time (days)
E
PKC Quality Control by PHLPP1
PHLPP1
PS
C2
C1B
C1A
Kinase
Hydrophobic Motif
Fast
Autoinhibition
DAG
Ca2+
Ca2+/DAG
i. UNPRIMED
ii. PHOSPHORYLATED
iii. PRIMED
iv. ACTIVE
v.
Impaired Autoinhibition
Dephosphorylation
vi. DEGRADED

3.4 Discussion

Pseudosubstrate and phosphorylation play an interdependent and essential function in PKC homeostasis that is exploited in cancer to effectively lose PKC. First, phosphorylation of the hydrophobic motif is necessary for the pseudosubstrate-dependent transition of newly synthesized PKC to the mature, autoinhibited conformation that prevents basal signaling in the absence of second messengers. In this manner, phosphorylation serves as an off switch, ensuring that the deregulated activity of newly synthesized enzyme is immediately quenched (Figure 3.7E; iii). This pseudosubstrate-engaged conformation, in turn, is necessary to protect newly synthesized PKC from dephosphorylation by bound PHLPP1 (Figure 3.7E; ii). Because lack of phosphate at the hydrophobic motif results in proteasomal degradation of PKC, PHLPP1 provides a quality control step that prevents aberrant PKC from accumulating in the cell (Figure 3.7E; v). The vulnerability of aberrant PKC to dephosphorylation/degradation is exploited in cancer. Notably, the pseudosubstrate is a hotspot for cancer-associated mutations. Those that loosen autoinhibition are LOF because phosphorylation cannot be retained at the hydrophobic motif, resulting in an unstable protein that is degraded (Figure 3.7E; vi). Those that enhance autoinhibition are also LOF by decreasing signaling output, pushing the equilibrium to the closed conformation (Figure 3.7; iii). Validating the requirement for phosphorylation at the hydrophobic motif for PKC stability, analysis of over 5,000 tumor samples and 1,500 cell lines reveals an almost 1:1 correlation between total PKC levels and hydrophobic motif phosphorylation. Additionally, we identify PAAD as a malignancy in which PHLPP1 quality control dominates in controlling PKC levels. Consistent with a tumor-suppressive role of PKC, low levels of PKC are associated with poor survival outcome in this cancer. Thus, in PAAD, there is a dependence upon PHLPP1 to suppress PKC expression, providing a potential therapeutic target to stabilize PKC and increase

patient survival.

Our findings delineate a mechanism that results in the loss of a tumor suppressor at the post-translational level, rather than the prevalent mechanism involving genetic deletion of regions encoding tumor-suppressor genes (Weinberg, 1991). Indeed, the tumor-suppressive role of PKC isozymes remained uncharacterized for several decades in part due to relatively infrequent deletion of PKC genes compared to other notable tumor suppressors. However, impairing protein stability is an equally effective method for LOF, as epitomized by the tumor suppressor p53, which is also stabilized by phosphorylation to prevent its degradation in the context of the DNA damage response (Chehab et al., 1999). Attesting to its key regulatory role, the hydrophobic motif was recently identified as a hotspot for cancer mutations across most AGC kinases, including PKCβ (Huang et al., 2018). However, phosphate at this PHLPP-regulated position plays distinct roles among these kinases. For Akt and S6K, dephosphorylation at the hydrophobic motif attenuates catalytic activity (Gao et al., 2005; Liu et al., 2011) without affecting stability. This latter point is evident from our own analysis showing no significant correlation between the total levels of these two AGC kinases and phosphorylation of their respective hydrophobic motifs. But in PKC, phosphorylation serves a very different function in stabilizing the enzyme. Thus, PKC is unique among PHLPP1 hydrophobic motif substrates in that phosphate protects the kinase from degradation. An unexpected finding from this study is that deletion of the autoinhibitory pseudosubstrate abolished any detectable phosphorylation at the three processing sites yet resulted in constitutively and maximally active PKC. Thus, surprisingly, PKC with no priming phosphates can have full, unrestrained catalytic activity. Furthermore, as is the case for the activation loop phosphate (Sonnenburg et al., 2001), transient phosphorylation at the hydrophobic motif is necessary for PKC to progress to a catalytically competent conformation but then

becomes dispensable for activity. We were unable to observe even transient phosphorylation of the autoinhibition-deficient PKC during processing in mammalian cells, underscoring the strict homeostatic control of the hydrophobic motif site. Phosphorylation of autoinhibition-deficient PKC, however, was readily observed in Sf9 insect cells. PKC may evade PHLPP quality control in insect cells because of the evolutionary functional divergence of the PHLPP PH domain (Park et al., 2008), a key determinant in its dephosphorylation of PKC in cells (Gao et al., 2008). One possible explanation for the requirement of negative charge at the hydrophobic motif early in the life cycle of PKC is that autophosphorylation of this site triggers association of the C-tail with the kinase domain, an important step in aligning the regulatory spine (Taylor and Kornev, 2011). Although protein kinases share a common active conformation, numerous mechanisms of autoinhibition have evolved to maintain kinases in inactive states (Bayliss et al., 2015). For nearly all protein kinases, phosphorylation serves to relieve autoinhibition, usually elicited by binding to regulatory molecules following agonist stimulation. For example, Akt autoinhibition by the PH domain is relieved via binding phosphatidylinositol-3,4,5-trisphosphate (PIP_3) to promote activating phosphorylations at the activation loop and hydrophobic motif (Alessi et al., 1996). Indeed, oncogenic mutations that dislodge the PH domain from the kinase domain activate Akt independently of PIP_3 generation (Parikh et al., 2012). In a similar manner, we found that cancer-associated PKC mutations in the pseudosubstrate also elicit constitutive activity. However, by impairing autoinhibition, these mutations induce PHLPP1-dependent dephosphorylation and are effectively LOF by promoting PKC degradation. Thus, cancer-associated activating mutations that disrupt autoinhibition present as gain-of-function mutations in Akt but manifest as LOF mutations in PKC. The role of PHLPP1 quality control in setting the level of PKC in cells has important ramifications for cancer therapies, as higher expression levels of PKC isozymes

have been reported to predict improved patient survival in diverse malignancies (Newton, 2018). For example, higher levels of PKCα and PKCβII protein predict improved outcome in T cell acute lymphoblastic leukemia (T-ALL) and colorectal cancer, respectively (Dowling et al., 2016; Milani et al., 2014). Here, we show that high PKC hydrophobic motif phosphorylation correlated with dramatically increased survival in PAAD. Because greater than 90% of pancreatic cancers harbor an activating K-Ras mutation (Almoguera et al., 1988), one possibility is that high PKC levels suppress K-Ras signaling. Consistent with this, PKC phosphorylation of K-Ras on Ser^{181} in the farnesyl-electrostatic switch was reported to disengage K-Ras from the plasma membrane (Bivona et al., 2006). Although the role of this specific PKC phosphorylation in tumors is unclear (Barcel et al., 2014), Wang et al. (2015) have shown that oral administration of a phorbol ester with very weak potency promoted K-Ras phosphorylation and repressed growth in orthotopic mouse models of human pancreatic cancer. Furthermore, PKC suppresses growth of oncogenic K-Ras-driven tumors in a xenograft mouse model of colorectal adenocarcinoma, and deletion or mutation of only one PKC allele is sufficient to enhance tumor growth (Antal et al., 2015b). Additionally, K-Ras is among the most frequently co-mutated genes in tumors with LOF PKC mutations (Antal et al., 2015b). Together, these data support a role for functional PKC in suppressing oncogenic K-Ras signaling. Another mechanism by which PKC suppresses oncogenic signaling was recently unveiled by Black and coworkers, who showed that PKCα deficiency in endometrial tumors enhances oncogenic Akt signaling via a mechanism involving its modulation of the activity of a PP2A family phosphatase (Hsu et al., 2018). Thus, targeting the PHLPP1-dependent quality control step of PKC processing may be a promising approach to stabilize PKC in cancers involving oncogenes controlled by PKC. Our work underscores the importance of careful consideration of PKC phosphorylation mechanisms in cancer therapies.

Notably, mTOR kinase inhibitors and Hsp90 inhibitors currently in clinical trials will have the unwanted result of preventing PKC processing, thus depleting levels of this tumor suppressor. Coupling such therapies with disruption of PHLPP1-dependent quality control may have significant therapeutic benefit. Thus, the post-translational inactivation of PKC by PHLPP1, distinct from loss of other tumor suppressors via genetic mechanisms, presents a druggable interaction and potential vulnerability in cancers that respond to PKC restoration.

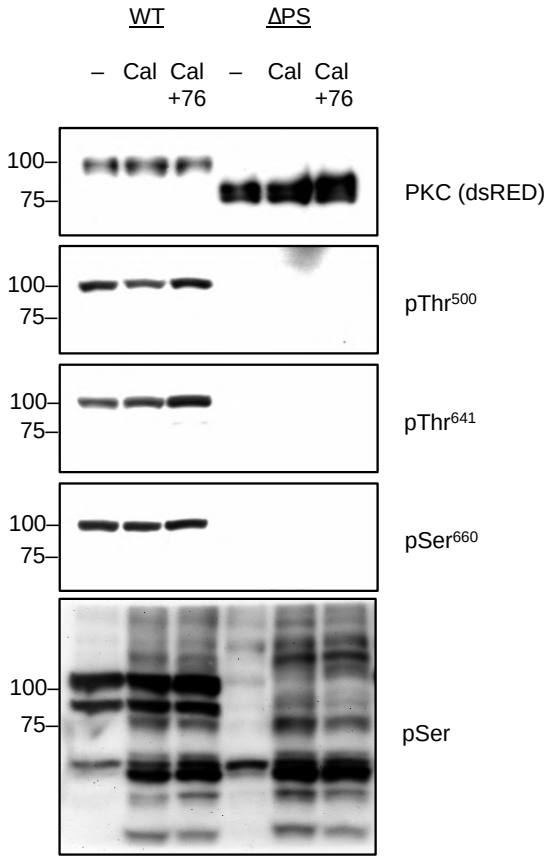

Figure 3.8: **Supplemental Data Related to Figure 3.2. PKC ΔPS Phosphorylation Is Not Regulated by a Calyculin-Sensitive Phosphatase.** Western blot of lysates from COS-7 cells expressing RFP-tagged PKCβII wild-type (WT) or deleted pseudosubstrate (ΔPS) and treated with DMSO (-) or Calyculin A (Cal, 100μM) and Gö6976 (6μM) for 20 minutes prior to lysis. Immunoblots were probed with PKC phospho-specific antibodies against the activation loop (pThr^{500}), turn motif (pThr^{641}), or hydrophobic motif (pSer^{660}), total overexpressed PKC (HA), or phospho-serine substrate (pSer) as a positive control for Calyculin A.

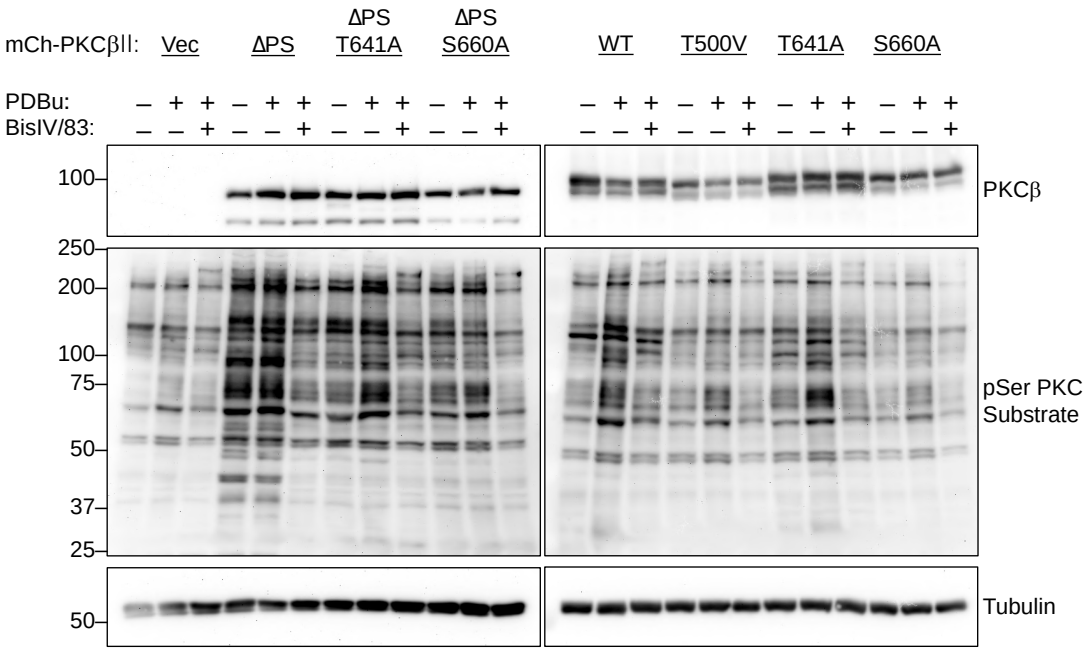

Figure 3.9: **Supplemental Data Related to Figure 3.2. Substrate Specificity of PKC Phosphorylation Site Mutants.** Western blot of lysates from COS-7 cells expressing mCherry-tagged PKCβII wild-type (WT), or PKCβII mutants PKCβII T500V, PKCβII T641A, PKCβII S660A, PKCβII ΔPS, PKCβII ΔPS T641A, PKCβII ΔPS S660A, or mCherry vector control (Vec) stimulated (PDBu) with DMSO (-) or 200nM PDBu (+) for 3 min prior to lysis and pretreated (BisIV/83) with either DMSO (-) or 1μM BisIV/1μM Gö6983 (+) 10 min prior to PDBu addition. Immunoblots were probed for total PKCβ, phospho-Ser PKC substrate antibodies, and Tubulin loading control.

Table 3.1: **Supplemental Data Related to Figure 3.5. Table of Cancer-Associated PKCβII Pseudosubstrate Mutations.** Mutations identified from patient-derived tumor samples showing the resultant missense mutation in PKCβ, cancer type, sample identifier, and database source.

Mutation	Cancer Type	Sample Identifier	Source
V18M	Skin Cutaneous Melanoma	TCGA-EE-A2GL	cBioPortal
R19C	Pancreatic Adenocarcinoma Large Intestine Adenocarcinoma	TCGA-IB-7651-01 T3118	cBioPortal COSMIC
R19L	Lung Adenocarcinoma Liver Cancer	TCGA-05-4389-01 CHG-13-09220T	cBioPortal ICGC
F20S	Head and Neck Squamous Cell Carcinoma	TCGA-F7-A624-01	cBioPortal
A21S	Adrenocortical Carcinoma	TCGA-OR-A5K9-01	cBioPortal
A21T	Ampullary Carcinoma Uterine Endometrioid Carcinoma Stomach Adenocarcinoma	AMPAC_95 TCGA-AX-A05Z-01 TCGA-BR-4184-01	cBioPortal cBioPortal cBioPortal
R22H	Pancreatic Ductal Adenocarcinoma	N/A	mutation3D
R22G	Adult T Cell Lymphoma-Leukaemia	ATL399	COSMIC
G24D	Adult T Cell Lymphoma-Leukaemia Adult T Cell Lymphoma-Leukaemia	ATL351 ATL126	COSMIC COSMIC
G24V	Adult T Cell Lymphoma-Leukaemia Diffuse large B cell lymphoma	ATL318 QC2-25-T2	COSMIC COSMIC

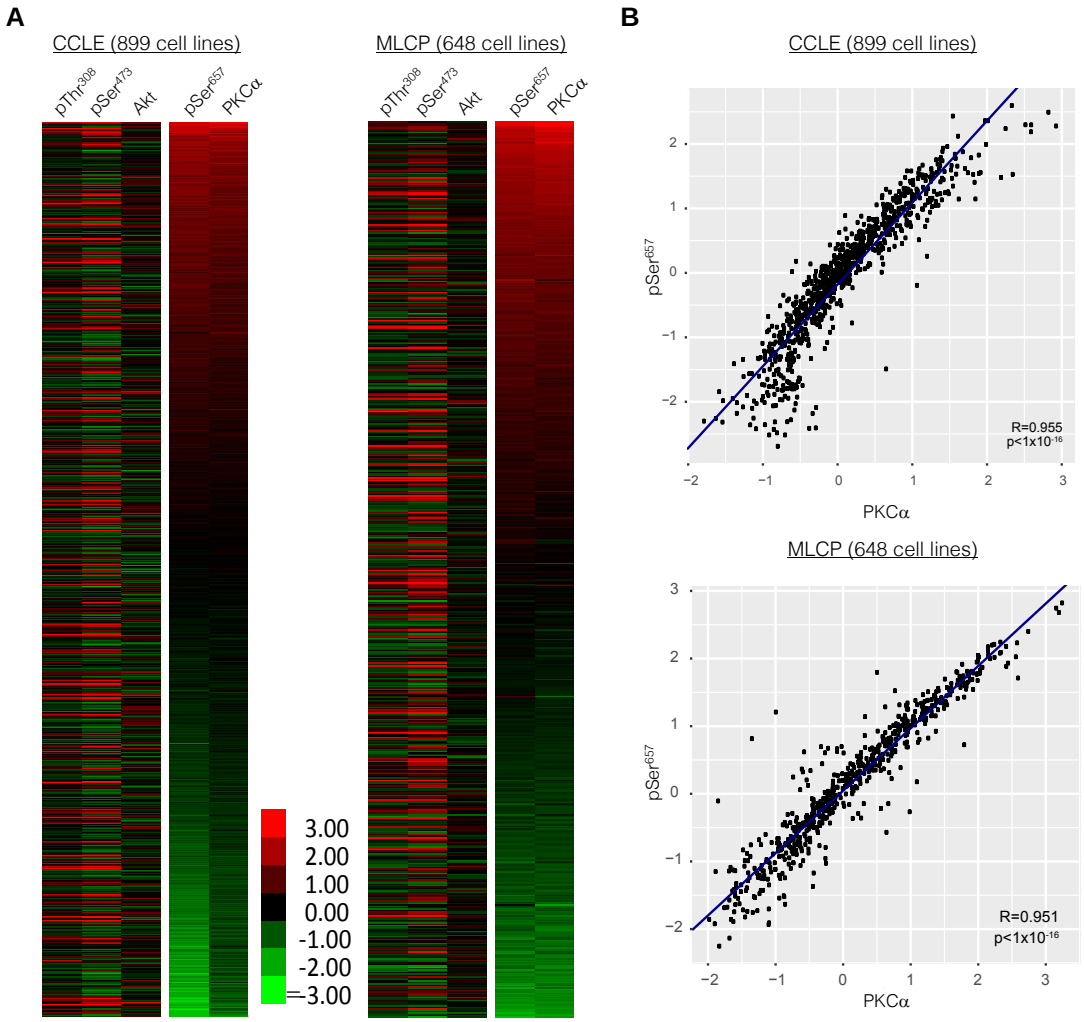

Figure 3.10: **Supplemental Data Related to Figure 3.6. PKC is Fully Phosphorylated at the Hydrophobic Motif in Human Cancer Cell Lines.**
(A) Heatmap of kinase levels versus their hydrophobic motif phosphorylation for PKC or Akt1 obtained from 5,157 patient samples from TCGA Pan Cancer Atlas measured by Reverse Phase Protein Array (RPPA). Shown are total PKCα versus pSer^{657} and total Akt1 versus pSer^{473} and pThr^{308}.
(B) Quantification of data in **(A)**: Scatterplot of the expression of the indicated phosphorylations correlated with PKCα or Akt1 protein levels; R= Spearman's rank correlation coefficient.

3.5 Methods

EXPERIMENTAL MODEL AND SUBJECT DETAILS

Cell Culture and Transfection

COS7 cells, *Phlpp1*$^{+/+}$ MEFs, and *Phlpp1*$^{-/-}$ MEFs were cultured in DMEM (Corning) containing 10% fetal bovine serum (Atlanta Biologicals) and 1% penicillin/streptomycin (Gibco) at 37°C in 5% CO_2. Generation of the PHLPP1 MEFs was described previously (Masubuchi et al., 2010). Transient transfection was carried out using the Lipofectamine 3000 Transfection Reagent (Thermo Fisher Scientific). Sf9 cells were grown in Sf-900 II SFM media (Gibco) in shaking cultures at 27°C.

METHOD DETAILS

Plasmids and Constructs

The C Kinase Activity Reporter (CKAR) was previously described (Violin et al., 2003). PKC pseudosubstrate-deleted constructs were generated by looping out the 54 bases comprising residues 19-36 of PKCα or PKCβII by QuikChange Mutagenesis (Agilent). Scrambled and Neutral Pseudosubstrate constructs were generated by QuikChange Mutagenesis (Agilent). The catalytic domain was generated by cloning residues 296-673 of human PKCβII into pcDNA3 containing an N-terminal HA tag at the NotI and XbaI sites. Regulatory domain constructs were generated by cloning residues 1-295 of human PKCβ into pcDNA3 with mCherry at the N-terminus at the BamHI and XbaI sites. mCherry-tagged constructs were cloned into pcDNA3 with mCherry at the N-terminus at the BamHI and XbaI sites. mYFP-tagged constructs were cloned into pcDNA3 with mYFP at the N-terminus at the XhoI and XbaI sites. HA-tagged rat

PKCβII constructs were cloned into pcDNA3 with HA at the N-terminus at the NotI and XbaI sites. HA-tagged human PKCβII constructs were cloned into pcDNA3 with HA at the N-terminus at the XhoI and XbaI sites. Kinameleon was cloned into pcDNA3 as mYFP-PKCβII-mCFP. All mutants were generated by QuikChange Mutagenesis (Agilent). Rat PKC constructs were used with the exception of human PKCα in Figure 3.2D and human PKCβII in Figures 3.5C, 3.5D, and 3.5E.

FRET Imaging and Analysis

Cells were imaged as described previously (Gallegos et al., 2006). For activity experiments COS7 cells were co-transfected with the indicated mCherry-tagged PKC construct and CKAR. For Kinameleon experiments, the indicated Kinameleon construct containing mYFP and mCFP was transfected alone. For translocation experiments, COS7 cells were co-transfected with the indicated mYFP-tagged construct and plasma-membrane targeted mCFP at a ratio of 10:1. Baseline images were acquired every 15 s for 2 min prior to ligand addition. Förster resonance energy transfer (FRET) ratios represent mean ± SEM from at least three independent experiments. All data were normalized to the baseline FRET ratio of each individual cell unless noted that absolute FRET ratio was plotted or traces were normalized to levels post-inhibitor addition. When comparing translocation kinetics, data were also normalized to the maximal amplitude of translocation for each, as previously described, in order to compare translocation rates (Antal et al., 2014). Every experiment contained an mCherry-transfected control to measure endogenous activity, and an mCherry-tagged WT (or deleted pseudosubstrate) PKC. Control traces are depicted as dotted lines: specifically, the endogenous trace in Figure 3.1E and the deleted pseudosubstrate trace in Figure 3.2G and 3.3I, were redrawn to serve as a point of reference in

those Figures (data were acquired and derived in the same experiments which generated all the data in Figure 3.1 and Figure 3.2, respectively).

Immunoblotting and Antibodies

Cells were lysed in PPHB: 50 mM $NaPO_4$ (pH 7.5), 1% Triton X-100, 20 mM NaF, 1 mM $Na_4P_2O_7$, 100 mM NaCl, 2 mM EDTA, 2 mM EGTA, 1 mM Na_3VO_4, 1 mM PMSF, 40 mg/ml leupeptin, 1mM DTT, and 1 mM microcystin. *Phlpp1*$^{+/+}$ and *Phlpp1*$^{-/-}$ MEFs were lysed in 50 mM Tris (pH 7.4), 1% Triton X-100, 50 mM NaF, 10 mM $Na_4P_2O_7$, 100 mM NaCl, 5 mM EDTA, 1 mM Na_3VO_4, 1 mM PMSF, 40 mg/ml leupeptin, and 1 mM microcystin. Triton-soluble fractions were analyzed by SDS-PAGE on 7% big gels to observe phosphorylation shift, transfer to PVDF membrane (Biorad), and western blotting via chemiluminescence SuperSignal West reagent (Thermo Fisher) on a FluorChem Q imaging system (ProteinSimple). In Western blots, the asterisk (*) denotes the position of mature, phosphorylated PKC; whereas, the dash (-) indicates the position of unphosphorylated PKC. The turn motif and hydrophobic motif phosphorylations, but not the activation loop phosphorylation, induces an electrophoretic mobility shift that retards the migration of the phosphorylated species. The pan anti-phospho-PKC activation loop antibody (PKC pThr^{500}) was described previously (Dutil et al., 1998). The anti-phospho-PKCα/βII turn motif (pT$^{638/641}$; 9375S) and pan anti-phospho-PKC hydrophobic motif (βII pS^{660}; 9371S) antibodies and Calyculin A were purchased from Cell Signaling. Anti-PKCβ (610128) and PKCα (610128) antibodies were purchased from BD Transduction Laboratories. The DsRed antibody was purchased from Clontech. The anti-PHLPP1 antibody was purchased from Proteintech (22789-1-AP). The anti-HA antibody for immunoblot was purchased from Roche. The anti-HA (clone 16B12; 901515) and anti-FLAG (Clone L5; 637301)

antibodies used for immunoprecipitation were purchased from BioLegend. The anti-α-tubulin (T6074) and anti-His (H1029) antibodies were from Sigma.

Baculovirus Expression of PKC and PHLPP1 PP2C

Human PKCβII, PKCβII PS, and PHLPP1 PP2C (residues 1154-1422) were cloned into the pFastBac vector (Invitrogen) containing an N-terminal GST or His tag. Using the Bac-to-Bac Baculovirus Expression System (Invitrogen), the pFastBac plasmids were transformed into DH10Bac cells, and the resulting bacmid DNA was transfected into Sf9 insect cells via Cell-FECTIN (ThermoFisher Scientific). Sf9 cells were grown in Sf-900 II SFM media (Gibco) in shaking cultures at 27°C. The recombinant baculoviruses were harvested and amplified. Sf9 cells were seeded in 35 mm dishes (1 x 106 cells/dish) and infected with baculovirus. Following 2 days of incubation, Sf9 cells were lysed directly in 1x Laemmli sample buffer, sonicated, and boiled at 95°C for 5 min.

Pulse-Chase Experiments

For pulse-chase experiments, COS7 cells were incubated with Met/Cys-deficient DMEM for 30 min at 37 °C. The cells were then pulse-labeled with 0.5 mCi/ml [^{35}S]Met/Cys in Met/Cys-deficient DMEM for 7 min at 37°C, media were removed, washed with dPBS (Corning), and chased with DMEM culture media (Corning) containing 200 mM unlabeled methionine and 200 mM unlabeled cysteine. At the indicated times, cells were lysed in PPHB and centrifuged at 13,000 x g for 3 min at 22 °C, supernatants were pre-cleared for 30 min at 4 °C with Protein A/G Beads (Santa Cruz), and protein complexes were immunoprecipitated from the supernatant with either an anti-HA or anti-FLAG monoclonal antibody (BioLegend, 16B12; BioLegend L5)

overnight at 4 °C. The immune complexes were collected with Protein A/G Beads (Santa Cruz) for 2 hrs, washed 3x with PPHB, separated by SDS-PAGE, transferred to PVDF membrane (Bio-rad), and analyzed by autoradiography and western blot. Co-immunoprecipitation experiments were performed similarly, omitting the labeling and autoradiography steps.

Reverse Phase Protein Array

For RPPA experiments, patient samples and cell line samples were prepared and antibodies were validated as described previously (Li et al., 2017; Tibes et al., 2006).

Cancer Mutation Identification

Cancer-associated pseudosubstrate mutations were identified by querying the cBioPortal (cbioportal.org), COSMIC (https://cancer.sanger.ac.uk/cosmic), mutation3D (mutation3d.org), and ICGC (https://dcc.icgc.org) databases.

QUANTIFICATION AND STATISTICAL ANALYSIS

Statistical significance was determined via Repeated Measures One-Way ANOVA and Brown-Forsythe Test or Student's t-test performed in GraphPad Prism 6.0a (GraphPad Software). The half-time of translocation or degradation was calculated by fitting the data to a non-linear regression using a one-phase exponential association equation with GraphPad Prism 6.0a (GraphPad Software). Western blots were quantified by densitometry using the AlphaView software (Protein Simple).

Acknowledgements

The following individuals contributed to this work: T.R.B. and A.C.N. conceived the project and designed the experiments. T.R.B. and A.-A.N.V. performed the experiments. W.Z. performed the tumor profiling under the mentorship of G.B.M. T.R.B. and A.C.N. wrote the manuscript.

Chapter 3 is a reprint in full of material published in:

Baffi TR, Van AN, Zhao W, Mills GB, Newton AC. "Protein kinase C quality control by phosphatase PHLPP1 unveils loss-of-function mechanism in cancer." *Molecular Cell.* 2019 Apr 18;74(2):378-392.

DOI: 10.1016/j.molcel.2019.02.018

The dissertation author is the primary author of this work.

Chapter 4

Recurrent PKCα Driver Mutation is Dominant-Negative in Chordoid Glioma

4.1 Abstract

A recurrent mutation in the tumor-suppressor kinase PKCα was recently identified as the probable driver of chordoid glioma. This mutation, PKCα D463H, is found in the catalytic Asp, which functions as the catalytic base of the phosphotransfer reaction to abstract a protein from the substrate hydroxyl group to facilitate nucleophilic attack. How this mutation affects protein function and whether the oncogenic D463H mutant protein is gain-of-function (GOF) or loss-of-function (LOF) in the context of the disease is not known. Here we utilize biochemical and live-cell imaging techniques to demonstrate that PKCα D463H exhibits cellular mislocalization,

impaired phosphorylation, and is catalytically inactive. Investigating the reason for the recurrence of the identical function, we identify a neomorphic function of the overexpressed D463H mutant protein as a dominant-negative, capable of reducing the activity of endogenous PKCs. The dominant-negative function of PKCα D463H, as well as a cancer-associated LOF PKCβII mutation, required the ability of these mutant proteins to bind the activating second messenger diacyclglycerol. Taken together, our data is consistent with a model by which LOF PKC mutations act as dominant-negatives by sequestering diacylglycerol to globally suppress PKC output in cancer. Thus, approaches to target PKCα D463H in chordoid glioma should focus not on developing PKC inhibitors, but rather on restoring PKC function and combating the dominant-negative effects.

4.2 Introduction

Genomic analysis of cancer subsets has aided the identification of activating mutations in putative oncogenic kinases, which are often disease hallmarks and can be targeted therapeutically. This principle is well illustrated by the characterization core oncogenic pathways sustained by oncogenic kinases such as PI3K, EGFR, BRAF, and Akt among others that harbor constitutively activating mutations present in a variety of malignancies (Blume-Jensen and Hunter, 2001; Tsatsanis and Spandidos, 2000). Molecular characterization of how cancer-associated mutations alter kinase catalysis, substrate specificity, stability, localization, binding to adaptors and ligands, and autoinhibitory constraints is critical to determining whether they are likely to be gain-of-function (GOF) mutations in oncoproteins or loss-of-function (LOF) mutations in tumor suppressors. Although enhanced kinase activity is generally regarded as oncogenic driver event, perhaps due to discovery that the first-characterized viral oncogenes encoded protein kinases

(Hunter et al., 1984). Several kinases appear to have tumor-suppressing functions, however, displaying reduced protein levels and LOF mutations in proliferative disorders (An and Brognard, 2019; Hudson et al., 2018). Perhaps the most iconic example of tumor-suppressor kinases, which were misattributed with oncogenic function, are the protein kinase c (PKC) family kinases (Newton and Brognard, 2017).

Determining the role of PKC in cancer has long been obfuscated by the lag in mechanistic understanding of PKC biochemistry following its implication as an important cancer effector. PKC was first proposed as an oncogene when it was discovered that the C1 domain was the receptor of the tumor-promoting phorbol esters, which are potent PKC activators (Kikkawa et al., 1983; Ono et al., 1989). Recent work has demonstrated PKC's role as a tumor-suppressor, rather than an oncogene, however, as the primary effect of chronic phorbol-ester treatment is PKC dephosphorylation and downregulation, effectively depleting PKC from cells. Prevalent LOF cancer-associated mutations and low expression levels in tumors generally supports a tumor-suppressive role for PKC. Therefore, efforts to target PKC in cancer have shifted to promote PKC stability, rather than inhibit its activity.

PKCα was recently implicated as a driver in chordoid glioma due to a recurrent D463H mutation as the only genetic aberration found in nearly 100% of patients (Goode et al., 2018; Rosenberg et al., 2018). Chordoid glioma is a histologically low-grade tumor of the third ventricle with ependymal origin, which is difficult to resect, molecularly uncharacterized due to its rarity, and is associated with high degrees of morbidity and mortality (Pomper et al., 2001). The initial studies of the PKCα D463H mutation reported upregulated transcript levels, decreased protein stability, and robust transforming potential of immortalized astrocytes and 3T3 fibroblasts. Whether the observed effects are due to enhanced or reduced PKCα activity, however,

is unclear. Therefore, we performed biochemical and cellular characterization of PKCα D463H activity and phosphorylation to determine whether the mutant protein alters PKC catalysis or confers neomorphic functions that underlie its oncogenic potential.

Here we show that the PKCα D463H mutation severely impairs PKC cellular activity, likely by abrogating the ability of the highly conserved HRD motif Asp to function as the catalytic base in the phosphotransfer reaction. In addition to reduced catalytic activity, the PKCα D463H mutant displays defective phosphorylation, explaining the finding that the protein is less stable. PKCα D463H retains the ability to autophosphorylates when PKC dephosphorylation is blocked. Additionally, we observed basal localization of PKCα D463H protein to the plasma membrane and cells expressing PKCα D463H exhibited dramatically suppressed endogenous PKC activity. This effect was dependent upon the ability of PKCα D463H mutant to bind the membrane, as C1 domain mutations that abrogate ligand binding abolished the dominant-negative effect. Finally, we show that the dominant negative function is likely inherent to unprocessed PKC, as mutation the hydrophoic motif phospho-acceptor Ser was sufficient to produce PKCβ with dominant-negative capabilities, dependent upon its ligand-binding ability. Thus, we find that the PKCα D463H mutation is a LOF, inactive mutant that additionally suppresses the global cellular activity of WT PKC by a novel dominant-negative mechanism.

4.3 Results

PKCα D463H Mutation is a Hallmark of Chordoid Glioma

In order to understand the pathophysiology of the PKCα D463H mutant in chordoid glioma, we sought to characterize the effects of the mutation on the kinase domain. KinView analysis of the sequence surrounding the mutation revealed absolute conservation of the mutated

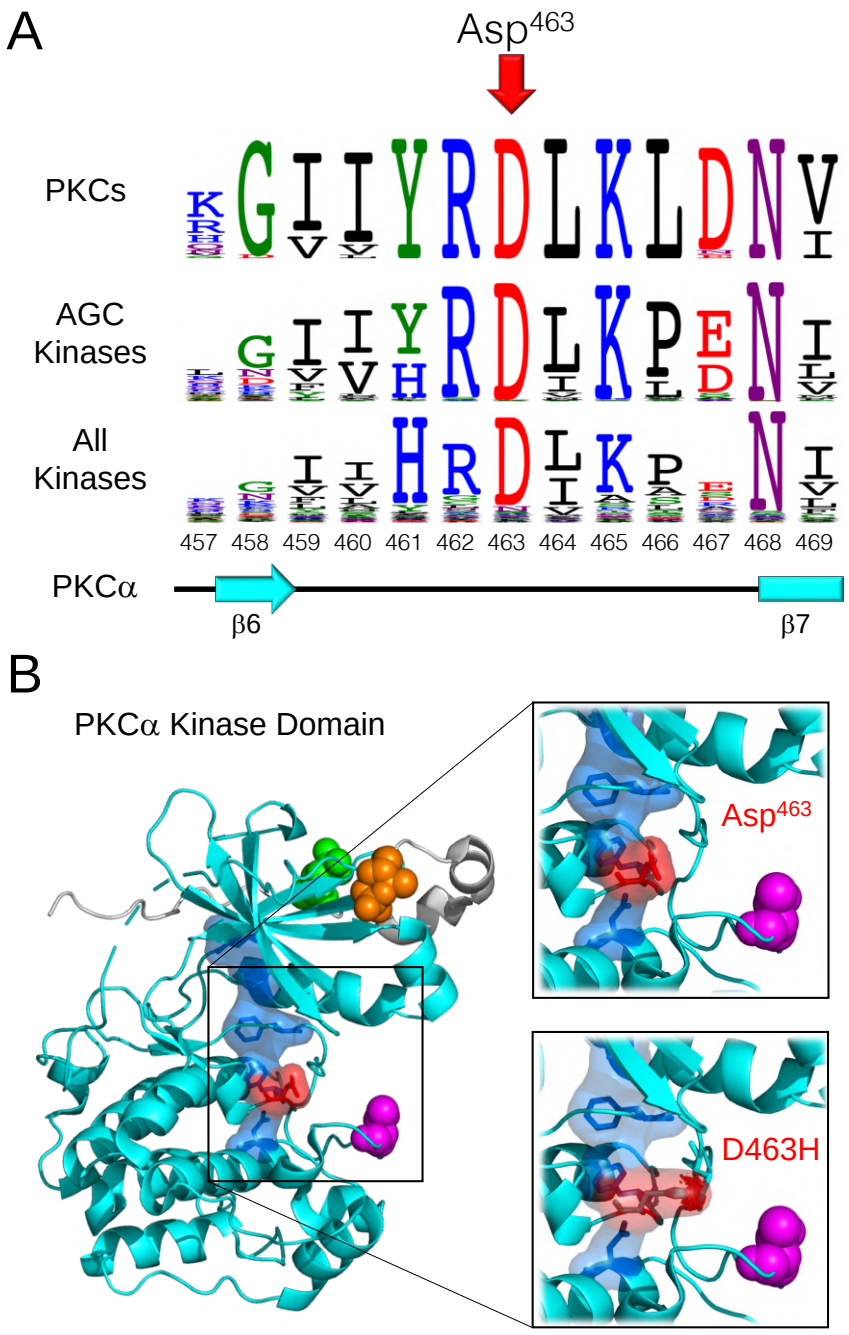

Figure 4.1: **PKCα D463H Mutation is a Hallmark of Chordoid Glioma.**
(A) Kinview analysis of the kinase region containing the catalytic Asp in the HRD motif of PKCs, AGC kinases, or all kinases. The position of the PKCα D463H mutation is indicated. **(B)** Crystal Structure of the PKCα kinase domain with the position of Asp^{463} adjacent to the RS2 hydrophobic spine residue Tyr^{461}. Molecular modeling of D463H substitution shows a steric clash of the His side chain with the activation segment.

Asp^{463} in all PKCs (McSkimming et al., 2016) (Figure 4.1A). As the catalytic Asp forming the HRD motif, this Asp is highly conserved in AGC kinases and more broadly in all eukaryotic protein kinases (Adams, 2001; Valiev et al., 2007). Accordingly, we hypothesized that mutation of this residue would have detrimental effects on catalysis, owing to the key role of this residue as the catalytic base in the phosphotransfer reaction. Molecular modeling and mutagenesis revealed that Asp463 resides in the region forming the RS2 hydrophobic spine and that mutation to His produced clashes with the activation segment (Kornev et al., 2006; Meharena et al., 2013) (Figure 4.1B). Thus, the PKCα D463H mutation not only potential impairs the biochemical properties of this residue to act as a catalytic base in the catalysis reaction, but also sterically clashes with the activation loop, perhaps altering phosphorylation and affecting the ability of the kinase to adopt the active conformation.

D463H Mutation Impairs PKCα Cellular Activity

To experimentally assess how the D463H mutation affects PKCα activity, we utilized the C Kinase Activity Reporter (CKAR2) (Ross et al., 2018; Violin et al., 2003) to measure agonist-induced cellular PKC activity upon addition of physiological agonist UTP, which stimulates DAG and Ca^{2+} production, or PDBu, a maximally activating phorbol ester. Compared to the WT PKCα that was robustly activated upon agonist stimulation, D463H and D463N displayed no activity above the endogenous cellular response (Figure 4.2A). In fact, both mutations suppressed endogenous activity, particularly the D463H mutation, suggesting that substitution at the Asp^{463} residue is not only detrimental to catalytic activity, but also confers a dominant-negative function (Figure 4.2B). This effect was not due to differential expression of the PKCα proteins, as PKC levels as measured by mCherry intensity were indistinguishable (Figure 4.2C). Thus, PKCα

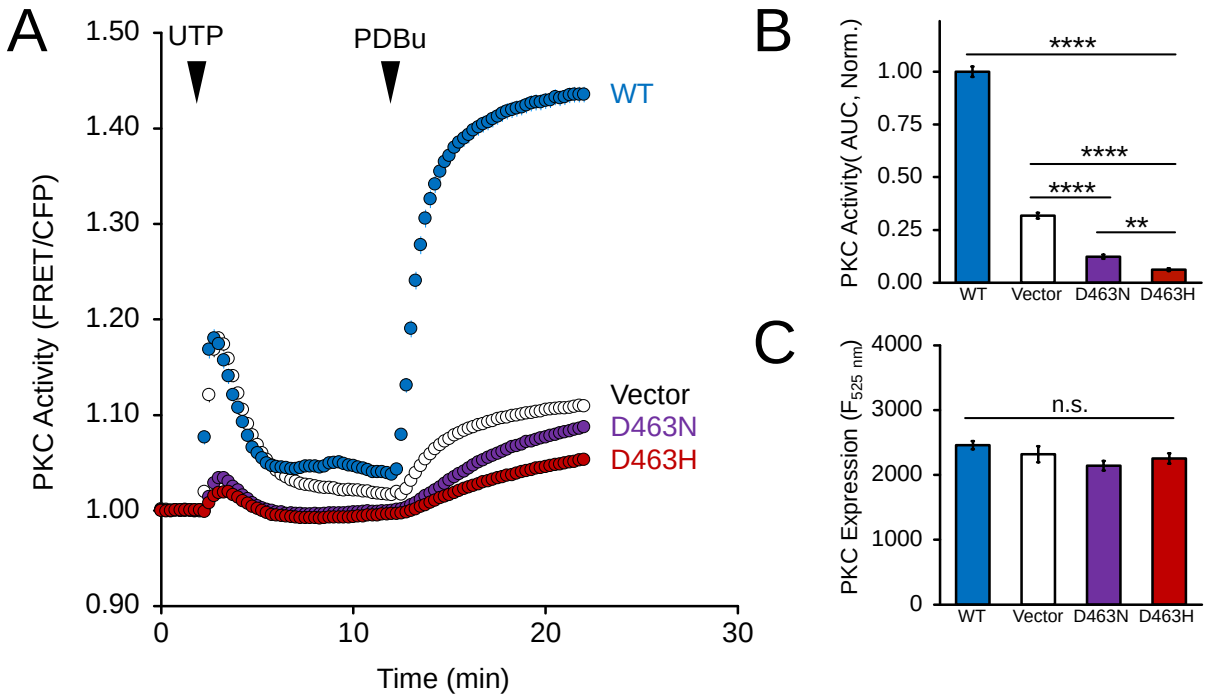

Figure 4.2: **D463H Mutation Impairs PKCα Cellular Activity.**
(A) PKC activity in COS7 cells expressing CKAR2 and the indicated mCherry-PKCα constructs and treated with UTP (100μM) and PDBu (200nM). Data represent the normalized FRET ratio changes (mean ± SEM) from three independent experiments.
(B) Quantification of PKC activity represents the normalized area under the curve (AUC; mean ± SEM) normalized to that of WT.
(C) PKC expression levels measured by mCherry intensity (mean ± SEM) from 3 independent experiments. **p $<$ 0.01; ****p $<$ 0.0001; n.s., not significant by One-way ANOVA and Tukey HSD Test.

D463H is not only inactive in a cellular context, but also suppresses the activity of endogenous WT PKC.

PKCα D463H is Capable of Autophosphorylation and Displays Enhanced Phosphatase Sensitivity

In addition to catalytic activity, PKC phosphorylation is a critical measure of its function, as phosphorylations are required for autoinhibition and protein stability. We next assessed the phosphorylation state of PKCα D463H. In agreement with impaired catalytic activity, PKCα D463H exhibited impaired phosphorylation at the activation loop, turn motif, and hydrophobic motif sites, suggesting a defect in PKC processing (Figure 4.3A). The loss of PKCα phosphorylation was greatest for the D463H mutant compared to Ala or Asn substitutions at Asp^{463}, emphasizing an especially detrimental effect of mutation this site (Figure 4.3B). Importantly, the minimal amount of phosphorylation present in the D463H mutant was abolished by additional mutation of the catalytic Lys (K368M/D463H) (Iyer et al., 2005), implying that the defect observed is likely due to comprised autophosphorylation or autoinhibition (Figure 4.3A, 3B). Therefore, we hypothesized that impaired PKCα D463H processing that prevents the incorporation or stabilization of the hydrophobic motif autophosphorylation may account for its phosphorylation deficiency. To address this, we treated cells expressing PKCα with PDBu, which promotes PKC dephosphorylation (Hansra et al., 1999), or PKC inhibitor Gö6983, which protects PKC from dephephosphorylation (Cameron et al., 2009; Gould et al., 2011). Treatment of cells expressing PKCα D463H with PDBu alone resulted in the rapid desphosphorylation of PKCα within three hours. Addition of Gö6983, however, not only blocked PDBu-induced dephosphorylation, but also promoted the complete phosphorylation of PKCα D463H, comparable to levels of WT

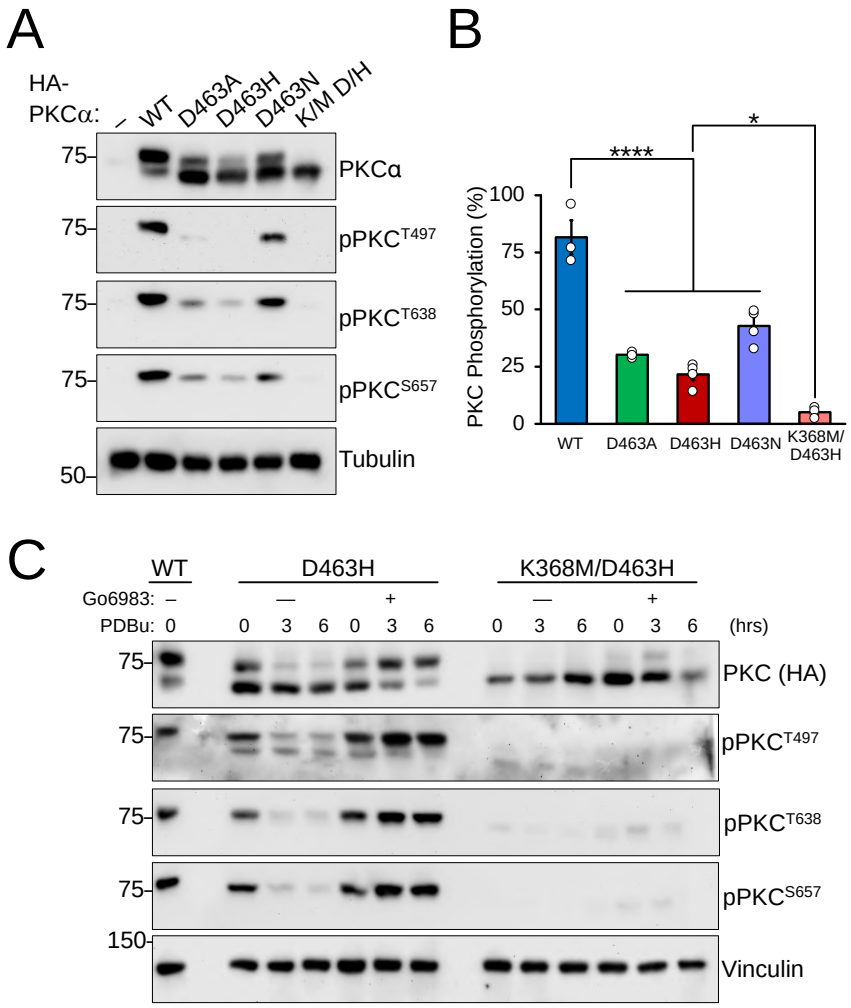

Figure 4.3: **PKCα D463H is Capable of Autophosphorylation and Displays Enhanced Phosphatase Sensitivity.**
(A) Immunoblot of whole-cell lysates from COS7 cells expressing HA-PKCα WT, D463A, D463H, D463N, or K368M/D463H (K/M D/H) constructs and probed with phospho-antibodies antibodies against the activation loop (Thr^{497}), turn motif (Thr^{638}), hydrophobic motif (Ser^{657}), and antibodies against total PKCα and loading control (Tubulin).
(B) Quantification of **(A)**, measuring PKC phosphorylation as a percent of the faster mobility total PKCα band.
(C) Immunoblot of whole-cell lysates from COS7 cells expressing HA-PKCα WT, D463A, D463H, D463N, or K368M/D463H (K/M D/H) constructs, treated with PKC inhibitor Gö6983 (6μM) 20min prior to lysis and PDBu (200nM) for the indicated timepoints, probed with the indicated phospho-antibodies antibodies against the activation loop (Thr^{497}), turn motif (Thr^{638}), hydrophobic motif (Ser^{657}), and antibodies against total PKCα and loading control (Vinculin). The double asterisk (**) denotes the position of mature, fully phosphorylated PKC and the dash (-) indicates the position of unphosphorylated PKC.

PKCα (Figure 4.3C). This effect was dependent upon the catalytic activity of PKCα, as double kinase-dead mutant K368M/D463H was completely unphosphorylated and unable to incorporate phosphate even upon Gö6983 treatment. Thus, protecting PKCα D463H from dephosphorylation permits processing, suggesting that either impaired autophosphorylation and autoinhibition or increased susceptibility to dephosphorylation accounts for the observed decrease in phosphorylation of this mutant. Importantly, although PKCα D463H lacks detectable cellular activity against substrates in a cellular context, it retains the ability to autophosphorylate.

C1 Domains of PKCα D463H Are Necessary for Dominant-Negative Function

We have previously shown that PKCβ is haploinsufficient for tumor suppression, in that loss of just one copy of PKC is sufficient to promote tumorigenesis (Antal et al., 2015a). We also found that PKC loss-of-function mutations are dominant-negative, such that a heterozygous inactivating PKC mutation is more detrimental than deletion of a single PKC allele. Since PKCα D463H not only abolished PKC activity, but also appeared to be dominant-negative, we sought to understand the mechanism by which this mutant suppressed endogenous PKC activity. Upon phosphorylation, PKC autoinhibits to mask its ligand-binding C1 domains (Antal et al., 2014). Failure to properly autoinhibit results in dephosphorylation and exposure of the C1 domains, which confers 10-fold increased cellular sensitivity to ligand. Likewise, membrane-bound PKC exhibits two orders of magnitude increased susceptibility to dephosphorylation (Dutil et al., 1994). To assess PKCα D463H membrane affinity we examined the subcellular localization of the mutant protein. Under basal conditions, WT PKCα was cytosolically localized and nuclear excluded, only localizing to membranes upon agonist-stimulation. PKCα D463H, in contrast, was constitutively associated with the plasma membrane (Figure 4.4A). Accordingly, we

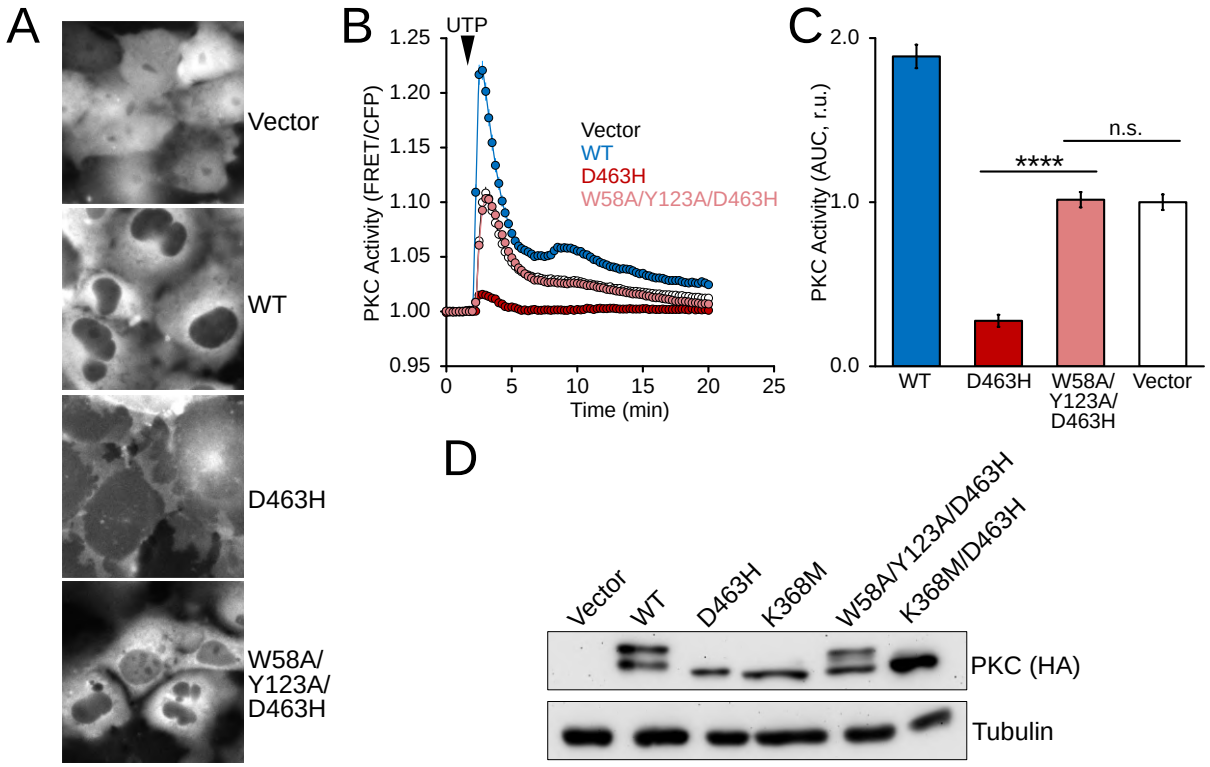

Figure 4.4: **C1 Domains of PKCα D463H Are Necessary for Dominant-Negative Function.**

(A) mCherry images of PKC localization in untreated COS7 cells.

(B) PKC activity in COS7 cells expressing CKAR2 and the indicated mCherry-PKCα constructs and treated with UTP (100μM). Data represent the normalized FRET ratio changes (mean $\pm$ SEM) from three independent experiments.

(C) Quantification of **(A)**. PKC activity represents the normalized area under the curve (AUC; mean $\pm$ SEM) normalized to that of Vector.

(D) Immunoblot of whole-cell lysates from COS7 cells expressing the indicated HA-PKCα constructs and probed with antibodies against total PKCα (HA) and loading control (Tubulin).

The double asterisk (**) denotes the position of mature, fully phosphorylated PKC and the dash (-) indicates the position of unphosphorylated PKC. ****p < 0.0001; n.s., not significant by One-way ANOVA and Tukey HSD Test or Student's t-test. IB quantifications represent the mean $\pm$ SEM from at least 3 independent experiments.

hypothesized that PKCα D463H mutants may outcompete WT PKC for ligand upon agonist-stimulation, effectively suppressing their ability to be recruited to membrane and become active. To test this, we generated ligand-insensitive mutations in the C1 domains, which abolish the ability to bind DAG (W58A/Y123A). Whereas PKCα D463H abolished nearly all endogenous UTP-induced activity, cells expressing ligand-insensitive PKCα D463H (W58A/Y123A/D463H) abrogated the dominant-negative effect, displaying a UTP response indistinguishable from that of Vector control (Figure 4.4B, 4.4C). Additionally, the ligand-insensitive PKCα D463H mutant recovered phosphorylation, suggesting that the constitutive membrane association is responsible for promoting dephosphorylation. Thus, PKCα D463H exerts its dominant-negative effect through its C1 domains, likely suppressing endogenous PKC translocation and activation by sequestering DAG.

Unprocessed PKC Suppresses WT Activity via Exposed C1 Domains.

Given that PKCα D463H is unprocessed and dominant-negative, we next addressed whether the suppression of endogenous PKC activity by unprocessed PKCs was a general dominant-negative mechanism. To assess this, we generated PKCβII mutants lacking the C-tail (ΔCT; Δ629-673), which is required for PKC processing. We then assessed the requirement for the regulatory domain in the dominant-negative function of unprocessed PKCβII. Compared to Vector control, cells expressing full-length PKCβII ΔCT displayed strongly impaired PDBu-induced activity (Figure 4.5A, 4.5B). Cells expressing PKCβII Cat ΔCT (296-628), which also lacks the regulatory domains, did not alter endogenous PKC activity (Figure 4.5A, 4.5B). This suppression of cellular PKC activity by the regulatory domain of unprocessed PKC was confirmed to be generally applicable to PKC substrates by reduced staining using the pSer PKC

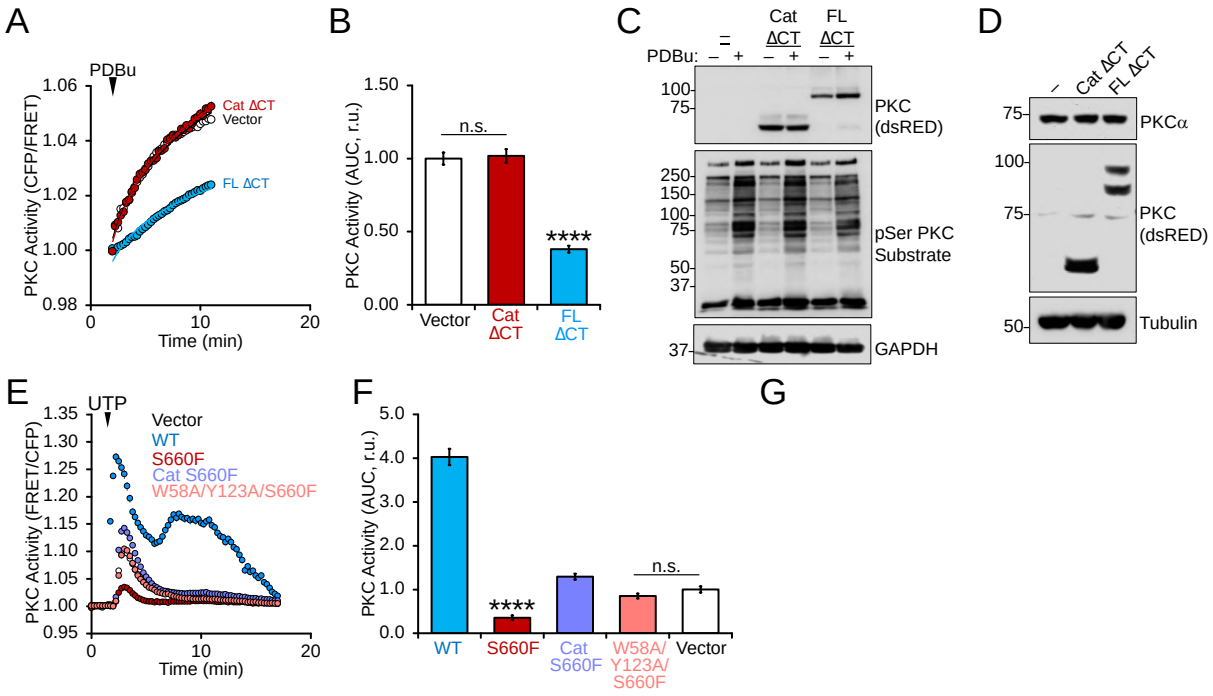

Figure 4.5: **Unprocessed PKC Suppresses WT Activity via Exposed C1 Domains.**
(A) PKC activity in COS7 cells expressing CKAR2 and mCherry-PKCβII Cat ΔCT (296-629) or FL ΔCT (1-629) constructs and treated with PDBu (200nM). Data represent the normalized FRET ratio changes (mean $\pm$ SEM) from three independent experiments.
(B) Quantification of **(A)**. PKC activity represents the normalized area under the curve (AUC; mean $\pm$ SEM) normalized to that of Vector.
(C) Immunoblot of whole-cell lysates from COS7 cells expressing mCherry-PKCβII Cat ΔCT (296-629) or FL ΔCT (1-629) constructs treated with PDBu (200nM) for 15min prior to lysis and probed with antibodies against total PKC (dsRED), pSer PKC Substrate, and loading control (GAPDH).
(D) Immunoblot of whole-cell lysates from COS7 cells expressing mCherry-PKCβII Cat ΔCT (296-629) or FL ΔCT (1-629) constructs treated with PDBu (200nM) for 15min prior to lysis and probed with antibodies against total PKC (dsRED), endogenous PKCα, and loading control (Tubulin).
(E) PKC activity in COS7 cells expressing CKAR2 and the indicated mCherry-PKCβII constructs treated with UTP (100μM). Data represent the normalized FRET ratio changes (mean $\pm$ SEM) from three independent experiments.
(F) Quantification of **(E)**. PKC activity represents the normalized area under the curve (AUC; mean $\pm$ SEM) normalized to that of Vector.
****$p < 0.0001$; n.s., not significant by One-way ANOVA and Tukey HSD Test or Student's t-test.

substrate antibody from cells expressing PKCβII FL ΔCT (Figure 4.5C). We also confirmed that this effect was independent of PKC expression levels, as neither PKCβII FL ΔCT or Cat ΔCT altered the levels of endogenous PKCα (Figure 4.5D). As a further characterization of the dominant-negative mechanism, we performed the similar experiments with cancer-associated hydrophobic motif mutant, PKCβII S660F, which blocks phosphorylation at the site, abolishes PKC activity, and prevents PKC from adopting the processed, autoinhibited conformation. (Huang et al., 2018). Consistent with loss of hydrophobic motif phosphorylation being sufficient for PKC dominant-negative function, PKCβII S660F effectively suppressed UTP-induced cellular PKC activity, which was relieved by mutation of the C1 domain ligand binding sites or deletion of the regulatory domains (Figure 4.5E, 4.5F). Thus, unprocessed PKC, which is characterized by impaired hydrophobic motif phosphorylation, possesses dominant-negative activity against WT PKC via exposure of its C1 domains and sequestration of ligand.

Generation of Stable Expressing YFP-PKCα NIH 3T3 Cell Lines

Having established the mechanism by which PKCα D463H exerts its dominant-negative function through impaired autophosphorylation that enhances its ligand sensitivity, we next tested whether this dominant-negative function was necessary or sufficient for its oncogenic effects. To this end, we generated cell lines stably expressing various YFP-tagged PKCα mutants in NIH 3T3 cells, which transform in the presence of an oncogene. The parental cells are contact-inhibited and lack the ability to grow in anchorage-independent conditions; however, cells expressing an oncogene may acquire these characteristics, enabling measurement of the transformation potential of the introduced gene. Following transfection of the PKCα mutants and Geneticin selection, we confirmed expression of the introduced YFP-PKCα proteins by Western

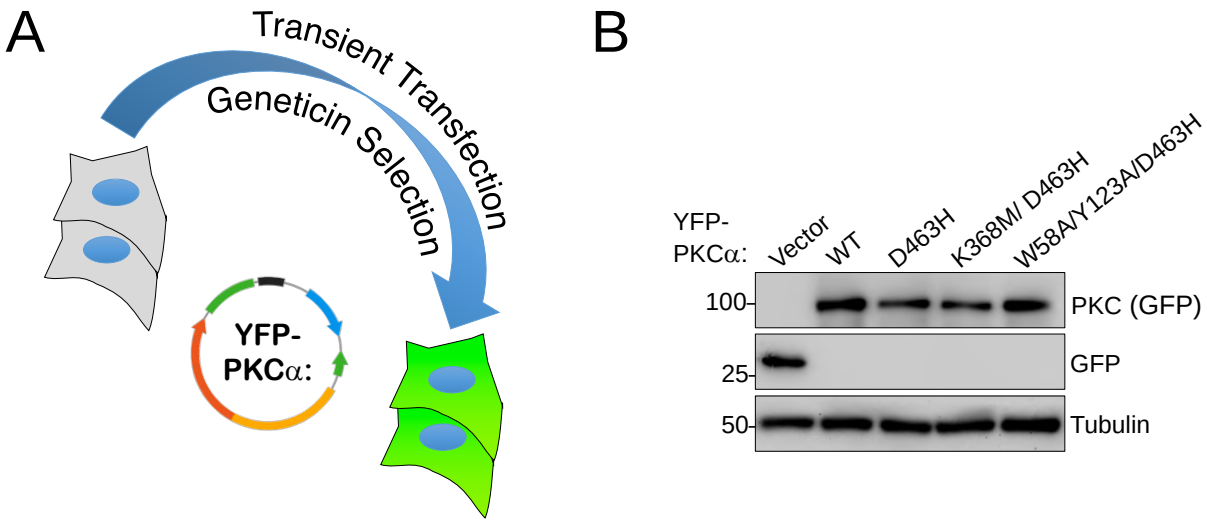

Figure 4.6: **Generation of Stable Expressing YFP-PKCα NIH 3T3 Cell Lines.** **(A)** Schematic for pooled stable cell line generation. NIH 3T3 cells were transfected with pcDNA3 YFP-PKCα DNA and treated with Geneticin for 6 weeks to select for stably-expressing cells. **(B)** Immunoblot of whole-cell lysates from NIH 3T3 stable cell lines probed with antibodies against GFP and Tubulin.

blot (Figure 4.6B). Using these cell lines, experiments assessing cell proliferation, focus-formation, anchorage-independent colony growth, and tumor formation in mouse models may be conducted to determine the role of PKCα D463H dominant-negative function in cellular transformation.

4.4 Discussion

In this study, we provide evidence that the PKCα D463H mutant is a LOF rather than a GOF mutation in chordoid glioma. Biochemical and cellular analysis of the mutant lead us to the intriguing hypothesis that PKCα D463H in the context of chordoid glioma is a LOF mutation with neomorphic dominant-negative capabilities.

It is curious that this tumor would harbor an identical and recurrent LOF point mutation. More commonly, recurrent mutations are found to be activating, as evidenced by KRas G12 mutations or BRAF V600E, presumably due to the limited ways in which a single amino acid

substitution can activate a protein (Davies et al., 2002; Smit et al., 1988). LOF mutations tend to be more arbitrarily distributed in critical protein domains, as is the case for PKC, since there exist relatively many ways in which enzymes can be inactivated. Substantial truncations can confer both activating effects as seen with EGFR and ASXL1 truncations and inactivating effects as observed for APC truncation, depending on whether the portion of the truncated domain conferred a tumor-suppressive function or autoinhibitory constraint (Balasubramani et al., 2015; Nishikawa et al., 1994; Tighe et al., 2004). And of course, genetic deletions are frequently observed for tumor-suppressor genes like PTEN, p53, and APC.

Our analysis of PKCα D463H cellular activity suggests that this mutation abolishes catalytic activity. This is not surprising at the outset, as the catalytic aspartate is one of the most highly conserved residues among all protein kinases. And due to the precision of the chemistry involved in phosphotransfer, kinases cannot even tolerate less drastic substitutions such as D463N. We have previously shown that PKC LOF mutations target conserved kinase motifs (McSkimming et al., 2016). If this were another example of an indiscriminate LOF mutation that can inactivate PKC by mutation at any number of sites to any number of residues, we would not expect to see an invariant mutation in every patient that presents with chordoid glioma. Thus, in our characterization of PKCα D463H function, we uncovered a neomorphic function that explains the specificity of the mutation. Unprocessed PKC that adopts an open conformation can be achieved either by disrupting autoinhibition or, as in the case of PKCα D463H, by impairing catalytic efficiency sufficiently enough that it cannot overcome PHLPP1-mediated PKC quality control. The result of this open conformation is that the ligand binding C1 domains are exposed, including the C1A, which possess 100-fold higher affinity for DAG and is usually masked in the autoinhibited, closed conformation (Antal et al., 2014; Dries et al.,

2007). Accordingly, we observed constitutive membrane association of PKCα D463H and blunted cellular activity in response to Ca^{2+}/DAG and phorbol ester. This function was also observed for cancer-associated PKCβII hydrophobic motif mutant S660F, suggesting that any mutation resulting in unprocessed PKC can be dominant-negative if it is stably expressed. We have previously shown that PKC hydrophobic motif phosphorylation that accompanies autoinhibition is required for PKC stability across a variety of cancers (Baffi et al., 2019). Therefore, PKC mutants that were completely incapable of becoming phosphorylated would not be expressed at sufficient levels to outcompete PKC for ligand. Our assays demonstrated, however, that PKCα D463H is capable of autophosphorylation when it is protected from dephosphorylation, in this case, by active site inhibitors that counter-intuitively promote PKC autophosphorylation by locking the enzyme in a phosphatase-resistant state. Furthermore, our analysis of PKC levels in a pan-cancer analysis revealed that the highest expressing cancer was low-grade glioma, suggesting reduced PHLPP1 levels or inefficient PKC quality control that allows higher levels of PKC to accumulate. In support of this, we have also found that brain cancers represented in the NCI60 cell line panel have low PHLPP levels (Warfel et al., 2011). Despite its ability to become phosphorylated, PKCα D463H exhibits dramatically enhanced ligand affinity and effectively outcompetes WT PKC to globally suppress Ca^{2+}-dependent PKC activity. Thus, an explanation for the specificity of the PKCα D463H mutation may be explained by this mutant's ability to evade PKC quality control mechanisms.

The studies described herein would be further supported by cellular and cellular assays attesting that the dominant-negative function is necessary for cellular transformation. From our analyses, we would expect that the PKCα W58A/Y123A/D463H mutant would be incapable of transforming cells due to its inability to outcompete endogenous PKC to suppress global

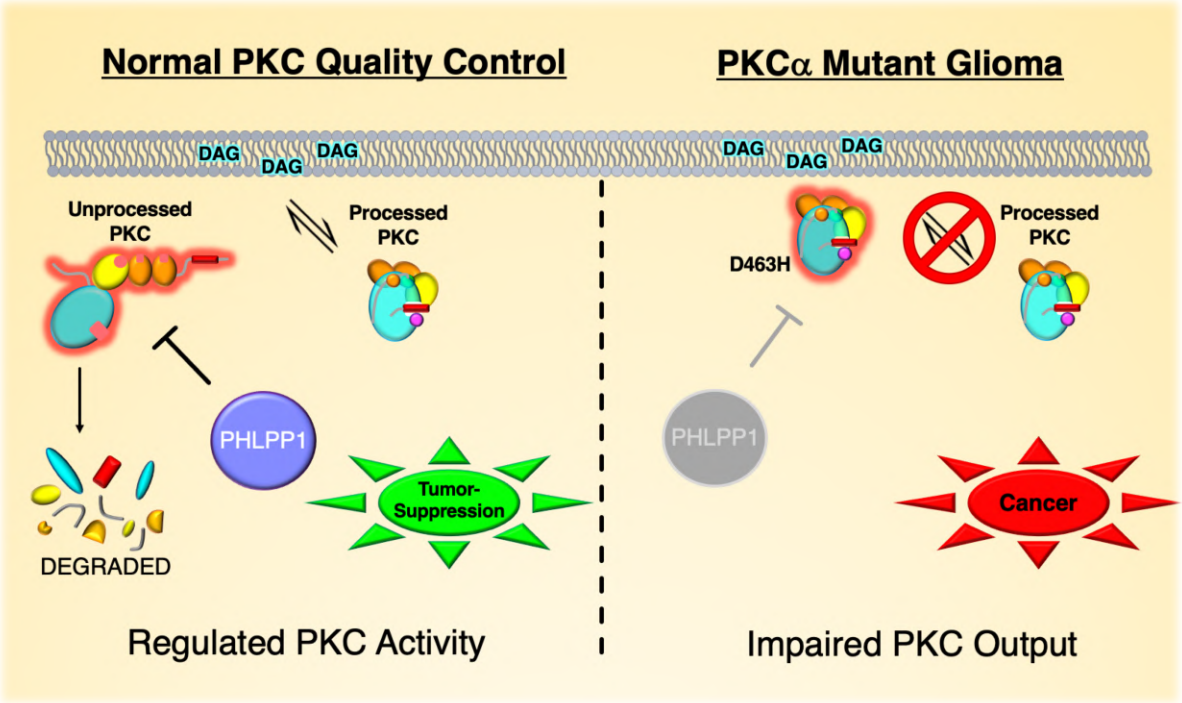

Figure 4.7: **Model of PKCα D463H Mutant Function in Chordoid Glioma.** Under normal conditions, PHLPP1 surveys the conformation of newly-synthesized PKC to dephosphorylate aberrantly active PKCs, promoting their degradation (left). In glioma, not only are PHLPP1 levels relatively low, the PKCα D463H mutant is capable of autophosphorylation despite its impaired activity (right). It's exposed C1 domains however, increase membrane localization and allow the mutant to outcompete endogenous, functional PKC for DAG upon activating stimuli, suppressing overall PKC cellular activity.

signaling. Additionally, to unequivocally demonstrate that residual PKCα D463H activity against substrates is not responsible for its oncogenic effects, we would predict the K368M/D463H kinase-dead mutant that was unable to incorporate phosphate under any conditions would still transform cells. Furthermore, clinical analysis of the PKCα D463H mutant in patient tumors or mouse models to determine the levels of the endogenously expressed protein would indicate the stability of the mutant and whether sufficient levels are present to sequester DAG.

The findings from this study suggest that the use of PKC inhibitors in chordoid glioma would be ineffective at best and detrimental at worst. Identification of the PKCα D463H

dominant-negative function that may be driving this disease, however, raises new avenues for therapeutic intervention. For example, use of a mutant-specific PROTAC (Schneekloth, et al., 2004) or dTAG (Nabet et al., 2018) chemical degrader to remove the dominant-negative PKC would restore the function of the remaining WT PKC . This approach is theoretically feasible because the D463H mutant at the catalytic Asp resides in the active site, potentiating the exploitation of the differential chemical properties of Asp and His at that position for mutant-specific inhibitor design. Taken together, we have identified a potential neomorphic function of the PKCα D463H driver mutation in chordoid glioma that is therapeutically actionable and merits further cellular investigation into the molecular requirements for its oncogenic potential.

EXPERIMENTAL MODEL AND SUBJECT DETAILS

Cell Culture and Transfection

COS7 cells were cultured in DMEM (Corning) containing 10% fetal bovine serum (Atlanta Biologicals) and 1% penicillin/streptomycin (Gibco) at 37°C in 5% CO_2. NIH-3T3 cells were cultured in identical conditions as listed above, replacing FBS for newborn calf serum. Cells were cultured at 5% NCS, and selected with Geneticin for 3-4 weeks using 1 mg/mL geneticin with 10% NCS. Transient transfection was carried out using the Lipofectamine 3000 Transfection Reagent (Thermo Fisher Scientific).

METHOD DETAILS

Plasmids and Constructs

The C Kinase Activity Reporter (CKAR) was (Violin et al., 2003). All constructs were generated by QuikChange Mutagenesis (Agilent) or subcloning into pcDNA3 or pCMV vectors with N-

terminal affinity tags. Human PKCα and rat PKCβ were used throughout.

FRET Imaging and Analysis

Cells were imaged as described previously (Gallegos et al., 2006). For activity experiments COS7 cells were co-transfected with the indicated mCherry-tagged PKC construct and CKAR. Baseline images were acquired every 15 s for 2 min prior to ligand addition. Förster resonance energy transfer (FRET) ratios represent mean ± SEM from at least three independent experiments. All data were normalized to the baseline FRET ratio of each individual cell unless noted that absolute FRET ratio was plotted or traces were normalized to levels post-inhibitor addition. Every CKAR experiment contained an mCherry-transfected control to measure endogenous activity, and an mCherry-tagged WT control. UTP, PDBu, and Gö6983 were purchased from Calbiochem.

Immunoblotting and Antibodies

Cells were lysed in PPHB: 50 mM $NaPO_4$ (pH 7.5), 1% Triton X-100, 20 mM NaF, 1 mM $Na_4P_2O_7$, 100 mM NaCl, 2 mM EDTA, 2 mM EGTA, 1 mM Na_3VO_4, 1 mM PMSF, 40 mg/ml leupeptin, 1mM DTT, and 1 mM microcystin. Triton-soluble fractions were analyzed by SDS-PAGE on 7% big gels to observe phosphorylation shift, transfer to PVDF membrane (Biorad), and western blotting via chemiluminescence SuperSignal West reagent (Thermo Fisher) on a FluorChem Q imaging system (ProteinSimple). In Western blots, the double asterisk (**) denotes the position of mature, and the single asterisk (*) denotes the position of partially phosphorylated PKC at the turn or hydrophobic motif; whereas, the dash (-) indicates the position of unphosphorylated PKC. The turn motif and hydrophobic motif phosphorylations, but not the activation loop phosphorylation, induces an electrophoretic mobility shift that retards the migra-

tion of the phosphorylated species. The pan anti-phospho-PKC activation loop antibody (PKC pThr^{500}) was described previously (Dutil et al., 1998). The anti-phospho-PKCα/βII turn motif (pT$^{638/641}$; 9375S), anti-phospho-PKCδ/θ, pan anti-phospho-PKC hydrophobic motif (βII pS^{660}; 9371S), and anti-pSer PKC substrate antibodies antibodies and Calyculin A were purchased from Cell Signaling. Anti-PKCβ (610128) and PKCα (610128) antibodies were purchased from BD Transduction Laboratories. The DsRed antibody was purchased from Clontech. The anti-HA antibody for immunoblot was purchased from Roche. The anti-HA (clone 16B12; 901515) and anti-FLAG (Clone L5; 637301) antibodies used for immunoprecipitation were purchased from BioLegend. The anti-α-tubulin (T6074) and anti-FLAG immunoblot antibodies were from Sigma.

Molecular Modeling

Molecular modeling experiments were performed using PyMOL.

QUANTIFICATION AND STATISTICAL ANALYSIS

Statistical significance was determined via Repeated Measures One-Way ANOVA and Brown-Forsythe Test or Student's t-test performed in GraphPad Prism 6.0a (GraphPad Software). The half-time of translocation was calculated by fitting the data by non-linear regression using a one-phase exponential association equation with GraphPad Prism 6.0a (GraphPad Software). Western blots were quantified by densitometry using the AlphaView software (Protein Simple).

Acknowledgements

The following individuals contributed to this work: Timothy R. Baffi and Alexandra C. Newton conceived the study and disigned the experiments. Timothy R. Baffi performed the experiments

with assistance from Monica Gonzalez-Ramirez. Timothy R. Baffi wrote the manuscript.

Chapter 5

Activating Protein Kinase Cγ Mutations that Cause Spinocerebellar Ataxia Uncouple PKC Quality Control to Alter the Cerebellar Phosphoproteome

5.1 Abstract

Germline mutations in PKCγ are the hallmark of Spinocerebellar Ataxia Type 14 (SCA14), an autosomal dominant neurodegenerative disorder characterized by progressive motor function loss and senescence of cerebellar Purkinje neurons. The molecular underpinnings of

SCA14 are not well defined and the role of PKCγ mutations in the pathophysiology is unknown. In this study, we use biochemical and proteomic approaches to determine the effects of these mutations on PKCγ function and identify affected signaling pathways. We show that PKCγ mutations target the diacylglycerol-binding C1B domain in residues that are critical for ligand binding. Furthermore, we show that mutation or deletion of the C1B domain confers resistance to phorbol ester-mediated PKC down-regulation; however, only PKCγ SCA14 mutants and not C1B deleted PKC is processed by phosphorylation. Phosphopreoteomic analysis from the cerebellum of SCA14 model transgenic PKCγ mutant mice revealed alterations in core neurodegenerative signaling pathways. Specifically, we observed a significant reduction in phosphorylation at multiple KSP repeat phosphorylations of the Neurofilament Heavy Polypeptide (NF-H). We also identified a significant increase in an inhibitory phosphorylation of GSK3β (pSer^{389}), a reported kinase of the NF-H KSP repeats. Accordingly, phorbol-ester stimulation induced phosphorylation at GSK3β^{S389} in a PKC-dependent, and MAPK-independent, manner, suggesting that PKC may be the direct kinase of this site. Thus, we propose that the molecular basis of SCA14, which may be relevant to other ataxias that exhibit dysregulated Ca^{2+} signaling, may involve PKC inhibition of GSK3β to prevent NF-H homeostatic hyperphosphorylation.

5.2 Introduction

Cellular and genetic analysis have elucidated much of the pathology of neurogenerative disease; however, the signal transduction mechanisms underlying dysregulation of key pathways that drive disease remain largely unexplored, hindering the development of effective therapeutics. Dysregulation of Ca^{2+} homeostasis is a hallmark of neurodegeneration (Marambaud et al., 2009), and the conventional protein kinase C isozymes, as master regulators of Ca^{2+} signaling, pose

attractive targets to curb aberrant signaling through these pathways.

Contrary to its role as a tumor-suppressor in cancer, protein kinase C (PKC) activity is thought to be enhanced in neurodegenerative disease (Callender and Newton, 2017). Upregulated PKC signaling is among the earliest events in Alzheimer's Disease (Tagawa et al., 2015). Furthermore, Alzheimer's-associated PKCα rare variants co-segregate with affected family members and enhance PKC output by increasing the catalytic rate of the enzyme (Alfonso et al., 2016; Callender et al., 2018). Additionally, germline PKCγ mutations are the cause of spinocerebellar ataxia type 14 (SCA14), characterized by progressive loss of motor control and degeneration of the cerebellum where PKCγ is predominantly expressed (Chen et al., 2003; Hashimoto et al., 1988). These mutations cluster in the C1B domain of the enzyme and have been reported to enhance PKC activity, although the mechanisms by which this occurs are unknown (Adachi et al., 2008).

The Ca^{2+}-regulated conventional PKCs have long been known to be important effectors of various neurological processes including Purkinje cell maturation and long-term depression (LTD) (Ichise et al., 2000; Kano et al., 1998; Kleppisch et al., 2001). It was recently shown that PICK1-scaffolded PKCα is the PKC isozyme responsible for LTD, which was required for the depressive effects of amyloid beta (Alfonso et al., 2014; Citri et al., 2010). PKCγ, in contrast, was implicated in regulating climbing fiber elimination though the mGluR1/Gα_q/PLCβ4 pathway during the maturation of Purkinje cells in the cerebellum (Chen et al., 1995; Hashimoto et al., 2000; Kano et al., 1997). PKCγ knockout mice display improper pruning of climbing fibers, establishing that the role of PKCγ is to fine tune motor control by priming Purkinje neurons to receive the appropriate excitatory inputs (Kano et al., 1995). Accordingly, PKC activation in *ex-vivo* cultured Purkinje cells results in dendrite retraction, while PKC inhibition results

in dendrite outgrowth (Schrenk et al., 2002). Thus, it is the excessive and pervasive activity of PKCγ in the cerebellum that is thought to drive the neurodegeneration observed in SCA14 patients (Ji et al., 2014).

Indeed, many genetically-defined forms of SCA are characterized by mutations in regulators of Ca^{2+} homeostasis (Becker, 2017). Specifically, SCA harbors causative mutations in regulators of Ca^{2+} modulation including GluR1 (SCA44) (Watson et al., 2017), Ca^{2+}-channel subunits $Ca_V2.1$ (SCA6) (Zhuchenko et al., 1997) and $Ca_V3.1$ (SCA42) (Kimura et al., 2017), the voltage-gated K+ channel $K_V3.3$ (SCA13) (Herman-Bert et al., 2000) and KV3.3 (SCA19/22) (Chung et al., 2003; Verbeek et al., 2002), the DAG-sensitive ion channel TRPC3 (SCA41) (Becker et al., 2011), and the primary neuronal IP_3 receptor IP3R1 (SCA15, 16, 29) (van de Leemput et al., 2007; Novak et al., 2010; Zambonin et al., 2017) and its regulators the ataxin 2 and 3 (SCA2, 3)(Gispert et al., 1993; Takiyama et al., 1993). Additionally, mutations occur in PKC substrates such as the ionotropic glutamate delta-2 subunit (GRID2; SCAR18) (Hills et al., 2013) and negative regulators of PKC signaling such as a regulatory subunit of the phosphatase PP2A, PPP2R2B (SCA12) (Holmes et al., 1999). Thus, SCA mutations converge upon Ca^{2+} homeostasis and PKC signaling, indicating that PKCγ mutations in SCA14 may be the central node of the pathological signaling pathway underlying ataxia.

The specific role of mutant PKCγ in SCA14 and its pathological effects are controversial. Biochemical analyses have shown a general increase in mutant PKCγ basal activity; however, PKCγ activity has also been shown to be dispensable for the ataxia pathology in mouse models (Adachi et al., 2008; Shimobayashi and Kapfhammer, 2017). Another hypothesis involves the aggregation of mutant PKCγ (Seki et al., 2005; Takahashi et al., 2015), as has been described for other SCA types harboring triplet nucleotide repeat expansion, as well as aggregation of amyloid

beta, Tau, and α-synuclein characteristic of Alzheimer's and Parkinson's (Ross and Poirier, 2004). Whether PKCγ aggregates and how these aggregates affect signaling is crucial to understanding SCA14 pathology.

In order to address the knowledge gaps in spinocerebellar ataxia that pose barriers to identifying affected signaling pathways and therapeutic targets, we endeavored to perform cerebellar phosphoproteomics from transgenic mouse models of SCA14. We identify several hallmarks of neurodegeneration that were represented in two independent PKCγ models, as well as potential direct PKC substrates and downstream dysregulation of these pathways. In particular, we implicate dysregulation in a PKCγ/GSK3β/NF-H signaling axis through validation of a PKC-mediated inhibitory phosphorylation on GSK3β Ser^{389}. These studies merit further investigation into the substrates and affected pathways of mutant PKCγ and whether their contribution to SCA14 pathology is a common feature of cerebellar ataxias.

5.3 Results

PKCγ Mutations that Cause Spinocerebellar Ataxia Type 14 Cluster in the C1B Domain

PKCγ mutations that cause SCA14 are reported to be activating; however, since the majority of these mutations lie outside the catalytic domain, the mechanism by which this occurs is unknown. Listing all identified mutations on the PKCγ secondary structure revealed that mutations cluster in the C1B domain (Figure 5.1A). Additionally, several mutation pairs at homologus positions in the C1A and C1B domains were observed including ΔF48/ΔF113, C66Y/C131Y, and C77S/C142S, suggesting that similar effects are exerted on each of the C1 domains (Figure 5.1A). To determine how these mutations might be impacting the function of the C1B domain,

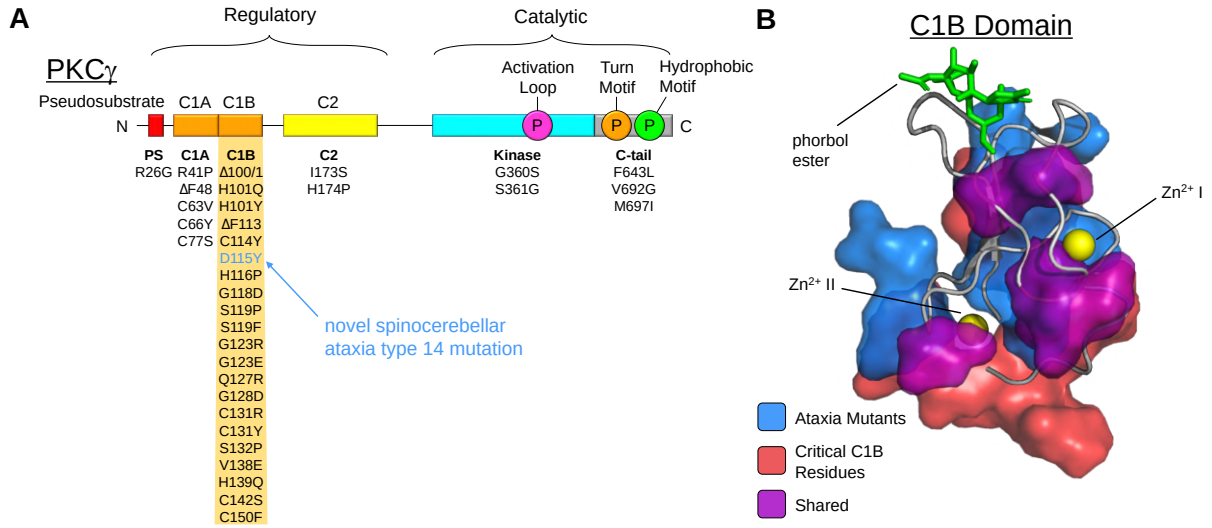

Figure 5.1: **PKCγ Mutations that Cause Spinocerebellar Ataxia Type 14 Cluster in the C1B Domain.**
(A) Diagram of PKCγ mutations in Spinocerebellar Ataxia Type 14 (SCA14). Secondary structure of PKCγ showing kinase domain (cyan), C-terminal tail (grey), Ca^{2+}-binding C2 domain (yellow), DAG-binding C1 domains (orange), and autoinhibitory pseudosubstrate (red). Unreported PKCγ ataxia-associated mutation in the C1B domain D115Y is indicated.
(B) SCA14 PKCγ mutations (blue) mapped onto the crystal structure of the PKCγ C1B domain bound to phorbol ester. Residues critical for ligand binding are shown in red, and SCA14-associated mutations that are also required for ligand binding are shown in purple.

we mapped all identified SCA14 mutations on the crystal structure of the PKCγ C1B domain (Figure 5.1B). SCA14 mutations appear to cluster in regions critical for C1B function, including in the ligand binding pocket and in residues required for coordinating the two Zn^{2+} ions that maintain its fold (Figure 5.1B). Many of the SCA14 mutations occur in residues that have been experimentally shown to be necessary for ligand binding by mutagenesis studies with the isolated C1B domain (Kazanietz et al., 1995) (Figure 5.2B). Thus, SCA14 mutations that cluster in the C1 domains may exert their function by inactivating the C1 domain.

SCA14-Associated PKCγ D115Y Mutant is Refractory to PHLPP1-mediated Quality Control

Biochemical analysis of several SCA14 PKCγ mutants suggests that they likely increase basal activity (Adachi et al., 2008) (Figure 5.2A). We have previously shown that PKCα and PKCβ exhibiting elevated basal activity due to impaired autoinhibition are targeted by PHLPP1 for dephosphorylation and degradation to provide PKC quality control (Baffi et al., 2019). To determine whether PKCγ is also subject to PHLPP1-mediated quality control, we assessed the phosphorylation and cellular activity of PKCγ lacking the pseudosubstrate (ΔPS; Δ18-35). Similar to the effect observed with other conventional PKCs upon deletion of the pseudosubstrate, PKCγ ΔPS was devoid of phosphorylation at the activation loop, turn motif, and hydrophobic motif, and displayed agonist-independent constitutive activity (Figure 5.2B, 5.2C). Interestingly, PKCγ ΔPS displayed elevated basal activity even greater than that of agonist-induced WT PKCγ, suggesting a relief of autoinhibitory constraints that is not recapitulated upon canonical activation (Figure 5.2C).

Given that PKCγ is also subject, to PHLPP1-mediated quality control, we would predict that PKCγ mutants that enhance activity would display greater sensitivity to dephosphorylation. Accordingly, we treated cells expressing PKCγ WT or D115Y mutant with increasing concentrations of PDBu to induce PKC dephosphorylation and degradation and measured the concentration of phorbol ester required for half-maximal PKCγ down-regulation. Surprisingly, PKCγ D115Y exhibited reduced sensitivity to phorbol ester-induced down-regulation, requiring over an order of magnitude more PDBu to achieve comparable degradation (Figure 5.2D, 5.2E). PKCγ ΔC1B (Δ100-150) showed low basal levels of phosphorylation and was completely refractory to down-regulation (Figure 5.2D, 5.2E). These results suggest that a mutant C1B do-

main protects PKC from dephosphorylation in untreated conditions and reduces sensitivity to down-regulation in stimulated conditions.

Figure 5.2: **SCA14-Associated PKCγ D115Y Mutant is Refractory to PHLPP1-mediated Quality Control.**
(A) Hypothesis for PKCγ pathology in SCA14. PKCγ mutants have been reported to be activating. PHLPP1-mediated PKC Quality Control ensures that aberrantly active PKC is degraded. Thus, we hypothesize that PKCγ mutants concomitantly disrupt autoinhibition and confer resistance to dephosphorylation by PHLPP1, leading to enhanced stability despite their increased activity.
(B) Immunoblot of triton-solubilized lysates from COS7 cells expressing mCherry-PKCγ WT or ΔPS (Δ18-35) and probed with phospho-antibodies antibodies against the activation loop (Thr^{514}), turn motif (Thr^{655}), hydrophobic motif (Thr^{674}), and antibodies against total PKCγ (dsRED).
(C) PKC activity in COS7 cells expressing CKAR and the indicated mCherry-PKCγ constructs and treated with PKC agonists UTP (100μM) and PDBu (200nM) and PKC inhibitors BisIV (1μM)/Gö6983 (1μM). Data represent the normalized FRET ratio changes (mean $\pm$ SEM) from three independent experiments.
(D) PKC down-regulation immunoblots of whole-cell lysates from COS7 cells expressing HA-tagged PKCγ WT, D115Y, or ΔC1B (Δ100-150), treated with the indicated concentrations of PDBu for 24hrs after 24hrs of transfection, and probed with the indicated phospho-antibodies, total PKCγ antibody (HA), or loading control antibody (Tubulin). Null-treated cells ($\emptyset$) were treated with equivalent volume of DMSO.
(E) Quantification of **(D)**. PKC levels represent the total PKCγ normalized to Tubulin (mean $\pm$ SEM) from at least two independent experiments. Data were fit to an exponential decay curve assuming eventual complete protein degradation and the concentration of PDBu producing half-maximal degradation of each protein is indicated by the dotted line.
(F) Autoradiograph and immunoblots from PKC pulse-chase HA immunoprecipitates of triton-solubilized COS7 cells expressing HA-tagged PKCβII WT, ΔC1B (101-151), or ΔPS (Δ19-36) and exposed to X-ray film (^{35}S) and probed with a PKCβ antibody.
(G) Autoradiograph and immunoblots from PKC pulse-chase HA and FLAG immunoprecipitates of triton-solubilized COS7 cells expressing FLAG-PHLPP1 and HA-tagged PKCγ WT, ΔC1B (100-150), exposed to X-ray film (^{35}S), and probed with antibodies against PHLPP (FLAG) and PKCγ (HA).
(H) Model for PKCγ evasion of PHLPP1-mediated quality control. PKCγ SCA14 mutants are constitutively active and are bound by PHLPP1, but are insensitive to PHLPP1 dephosphorylation, permitting agonist-independent activity and autoinhibition-independent phosphorylation and stability.
In immunoblots, the double asterisk (**) denotes the position of mature, phosphorylated PKC; the single asterisk (*) denotes the position of PKC phosphorylated at the hydrophobic motif, and the dash (-) indicates the position of unphosphorylated PKC. Immunoblots represent the average of at least three independent experiments.

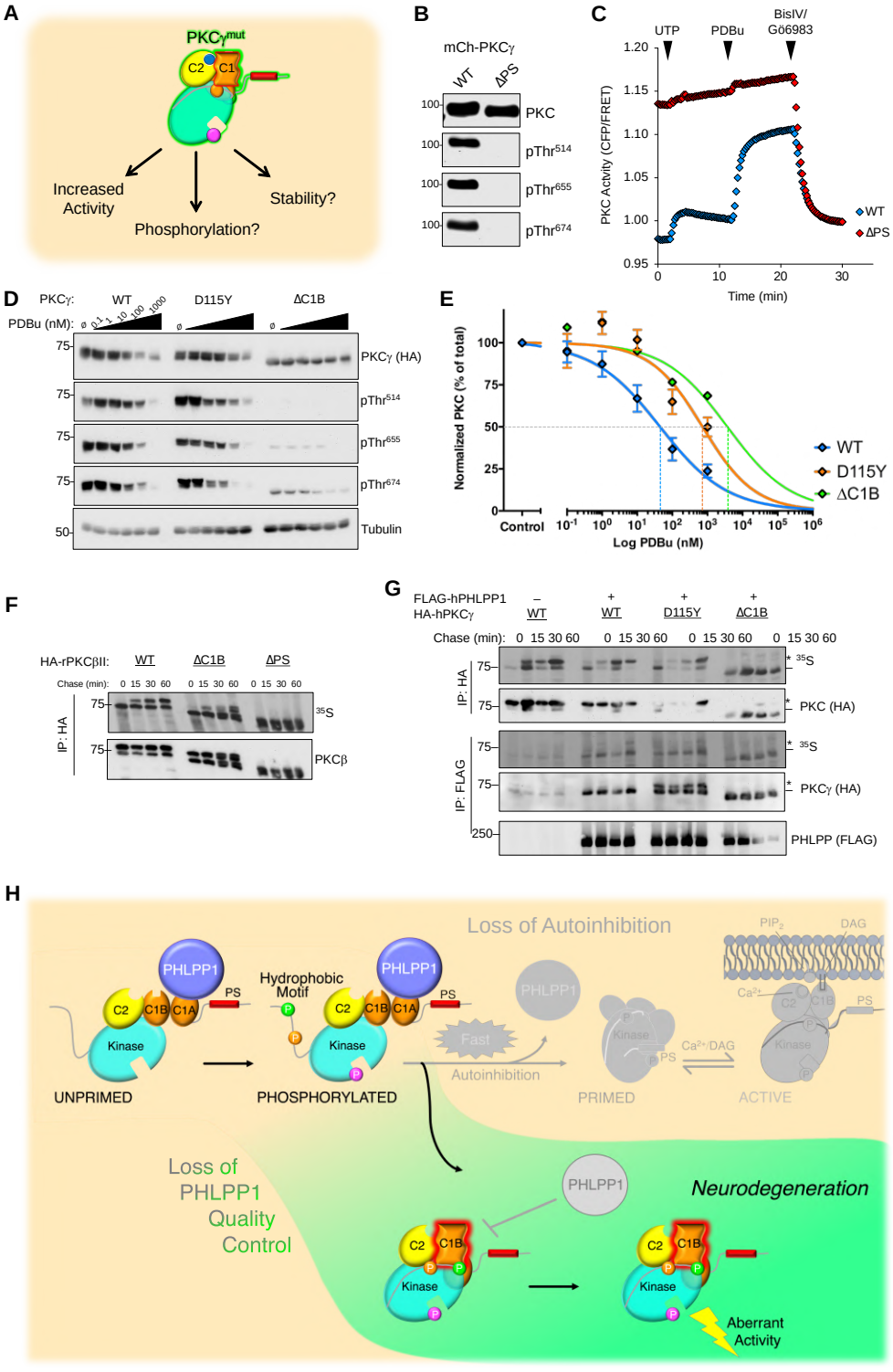
A
PKCγmut
C2
C1
Increased Activity
Phosphorylation?
Stability?
B
mCh-PKCγ
WT
ΔPS
PKC
pThr514
pThr655
pThr674
C
UTP
PDBu
BisIV/ Gö6983
PKC Activity (CFP/FRET)
Time (min)
WT
ΔPS
D
PKCγ:
WT
D115Y
ΔC1B
PDBu (nM):
PKCγ (HA)
pThr514
pThr655
pThr674
Tubulin
E
Normalized PKC (% of total)
Control
Log PDBu (nM)
WT
D115Y
ΔC1B
F
HA-rPKCβII:
WT
ΔC1B
ΔPS
Chase (min):
IP: HA
35S
PKCβ
G
FLAG-hPHLPP1
HA-hPKCγ
WT
WT
D115Y
ΔC1B
Chase (min):
IP: HA
35S
PKC (HA)
IP: FLAG
35S
PKCγ (HA)
PHLPP (FLAG)
H
Loss of Autoinhibition
PHLPP1
Hydrophobic Motif
PS
Kinase
UNPRIMED
PHOSPHORYLATED
Fast
Autoinhibition
PRIMED
ACTIVE
PIP2
DAG
Ca2+
Ca2+/DAG
Loss of PHLPP1 Quality Control
Neurodegeneration
Aberrant Activity

Since PKC quality control by PHLPP1 occurs during processing, shortly after synthesis, we assessed PKC phosphorylation kinetics by pulse-chase analysis. Interestingly, PKCβII ΔC1B (Δ101-151), which we have shown displays enhanced basal activity, exhibits a much subtler phosphorylation defect (Figure 5.2F). Compared to WT PKCβII that became majority phosphorylated during the 60 min chase and in the bulk protein, PKCβII ΔC1B phosphorylation kinetics were slowed; however, contrary to PKCγ ΔC1B, achieved 50% phosphorylation in the bulk protein (Figure 5.2F). We then assessed PKCγ processing by pulse-chase and ability to bind to PHLPP1. While PKCγ ΔC1B was not phosphorylated and did not undergo a mobility shift during processing as observed previously, PKCγ D115Y exhibited similar phosphorylation kinetics to that of WT PKCγ (Figure 5.2G). PHLPP1 has been shown to bind the unphosphorylated, faster mobility species of PKC, owing to its ability to recognize and dephosphorylate the open conformation. Surprisingly, PHLPP1 bound both the phosphorylated and unphosphorylated forms of PKCγ D115Y (Figure 5.2G). Taken together, these results suggest that PKCγ D115Y mutant, which harbors an impaired C1B domain, is refractory to PHLPP1 quality control and exhibits enhanced stability, due to reduced dephosphorylation by PHLPP1 (Figure 5.2H).

SCA14 Model PKCγ Mutant Transgenic Mice Display Dramatic Cerebellar Phosphoproteome Changes

In order to determine the molecular pathology of enhanced activity conferred by SCA14 PKCγ mutations, we obtained cerebellum tissue from H101Y, F643L, and WT human PKCγ transgenic mice (Figure 5.3A). The two PKCγ mutant mice, harboring PKCγ mutations in the C1B (H101Y) and C-tail (F643) display Ataxia-like phenotypes, with the H101Y pathology being more severe. Cerebellum from these mice were homogenized and subjected to tandem mass-

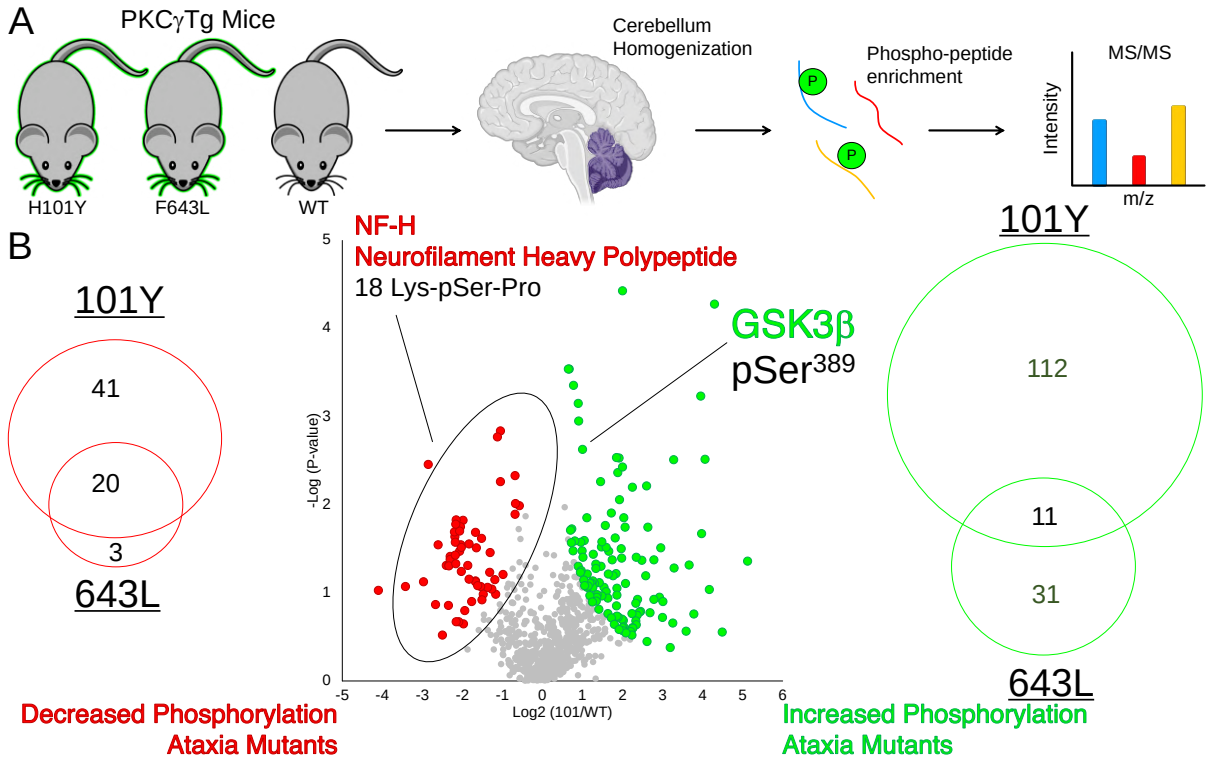

Figure 5.3: **SCA14 Model PKCγ Mutant Transgenic Mice Display Dramatic Cerebellar Phosphoproteome Changes.**
(A) Schematic for cerebellar phosphoproteomic analysis from SCA14 model mice. PKCγ transgenic mice expressing human PKCγ H101Y, F643L, or WT PKCγ were cerebellum homogenization and phosphoproteomic analysis by tandem mass-spectrometry.
(B) Analysis of upregulated (green) and downregulated (red) phosphoproteins in H101Y or F643L PKCγ mouse cerebellum. The degree of overlap between altered phosphoproteins in H101Y and F643L is shown by Venn diagram.

spectrometry to profile the phosphoproteome in PKCγ mutant versus PKCγ WT samples (Figure 5.3A). There were numerous phosphoproteins whose phosphorylation was increased (green) or decreased (red) in the PKCγ mutant mice (Figure 5.3B). There was a considerable degree of overlap between the H101Y and F643L mice, suggesting that similar pathways were affected (Figure 5.3B). Interestingly, the majority of down-regulated phosphorylations were contained in a single protein, Neurofilament-Heavy Polypeptide, in which the phosphorylation on 18 Lys-Ser-Pro repeat sites was significantly reduced in H101Y and F643L mutant mice (Figure 5.3B). Among

the increased phosphorylation sites was phosphorylation at Ser^{389} of GSK3β. PKCs have been reported to phosphorylate and suppress the activity of GSK3β although the site of phosphorylation is unknown (Goode et al., 1992). Additionally, phosphorylation at Ser^{389} has been shown to decrease its activity, from a mechanism distinct from the well-characterized inhibitory sites at Ser9/21 phosphorylated by Akt (Thornton et al., 2008). Furthermore, GSK3β is among the kinases proposed to maintain hyperphosphorylation of Neurofilament-Heavy Polypeptide at the Lys-Ser-Pro repeats (Sasaki et al., 2002). Thus, phosphoproteomic analysis of the cerebellum from PKCγ mutant SCA14 model mice implicates potential altered signaling pathways that may underlie the degenerative pathology.

PKC Promotes GSK3β Ser^{389} Phosphorylation in an Akt and MAPK Independent Manner

Due to the identification of GSK3β as a potential PKC substrate that may drive SCA14, we sought to validate this finding in a cellular context. Performing a time-course of PDBu treatment, we observed an increase in phosphorylation on GSK3β Ser^{389} that was blocked by pretreatment with PKC inhibitors (Figure 5.4A). The kinetics of this phosphorylation differed from the induction of ERK1/2 phosphorylation, a known downstream target of PKC-induced MAPK pathway activation (Figure 5.4B). As a further measure that PKC-dependent GSK3β Ser^{389} phosphorylation was MAPK-independent, we treated cells with MEK or JNK inhibitors prior to PDBu stimulation and observed no inhibition of PDBu-induced phosphorylation at this site (Figure 5.4C). Neither were Akt inhibitors sufficient to block PDBu-mediated phosphorylation at GSK3β Ser^{389}, despite at reduction at the known direct Akt phosphorylation site, Ser9/21 (Figure 5.4C). Thus, GSK3β Ser^{389} is phosphorylated in a PKC-dependent, Akt and MAPK-

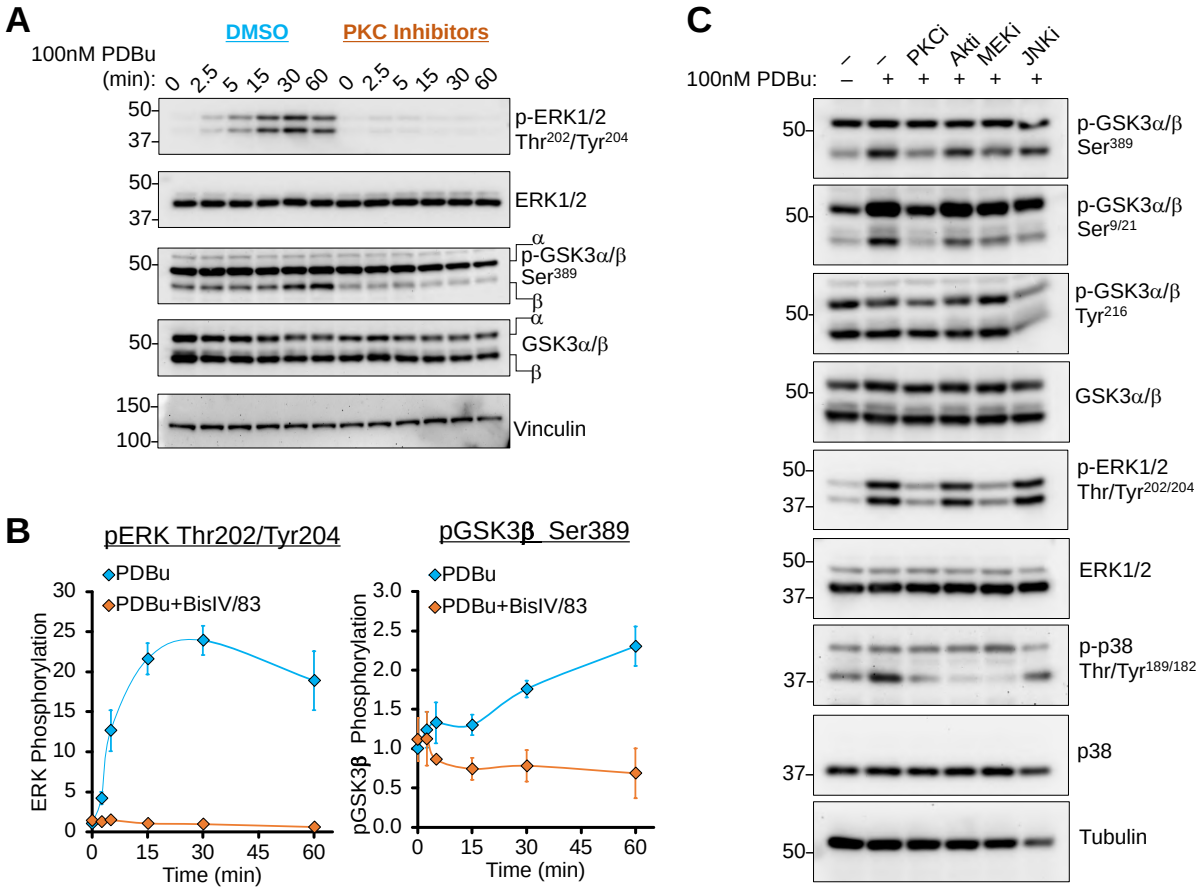

Figure 5.4: **PKC Promotes GSK3β Ser^{389} Phosphorylation in an Akt and MAPK Independent Manner.**
(A) Immunoblots of WT MEFs starved for 24hrs, treated with DMSO or PKC inhibitors (BisIV (1μM)/Gö6983 (1μM)) 15min prior to PDBu (100nM) treatment for the indicated timepoints, and probed with the indicated antibodies.
(B) Quantification of **(A)**. ERK and pGSK3β phosphorylation (mean $\pm$ SEM) reflects phospho-signal over total protein from three independent experiments.
(C) Immunoblots of WT MEFs starved for 24hrs, treated with DMSO (-), PKC inhibitors (BisIV (1μM)/Gö6983 (1μM)), Akt inhibitor (GDC-0068 (1μM)), MEK inhibitor (GSK1120212,20μM.), or JNK inhibitor (SP600125, 10μM) 15min prior to PDBu (100nM) treatment for 60 min, and probed with the indicated antibodies.

independent manner, suggesting that GSK3β Ser^{389} is a potential direct PKC phosphorylation site that is enhanced in SCA14.

5.4 Discussion

The prevailing finding of this study is the identification of a potential dysregulated signaling mediated by mutant PKCγ that may underlie the pathology of SCA14 and other cerebellar ataxias. Consistent with enhanced PKCγ activity in SCA14, PKCγ mutants display enhanced basal activity and evade PHLPP1-mediated PKC quality control. Thus, uncoupling the quality control regulatory mechanisms that maintain proper levels of autoinhibited and second-messenger-responsive PKC is fundamental to the pathology of SCA14.

A critical advance in the understanding of SCA14 PKCγ function is that mutations confer increased catalytic activity without promoting PKC down-regulation, effectively uncoupling dephosphorylation by PHLPP1 from PKC degradation. Impairing the function of the C1B domain, in particular, has the dual function of loosening autoinhibition, and conferring resistance to phorbol ester-induced dephosphorylation and down-regulation. Curiously, PKCγ mutants appear to adopt an open conformation and translocate rapidly to the plasma membrane, presumably mediated through the C1A domain (Verbeek et al., 2008). Simply deleting the C1B domain, however, resulted in robust dephosphorylation, suggesting that a neomorphic function of ligand-insensitive or misfolded C1B domain is responsible for this effect. The localization of mutant PKCγ in an insoluble fraction and the ability of PDK1 to bring it in the cytosol may be responsible for its protection from dephosphorylation (Jezierska et al., 2014). How the mutant C1B mutation specifically promotes a PKC open conformation that is protected from dephosphorylation remains to be determined. An intriguing hypothesis related to the idea of

PKCγ aggregation is that disruption of the C1B:C-tail interface, such as the C1B mutations that misfold the domain or the F643L mutation in the active-site tether, could promote the PKC oligomerization through the TOR-interaction motif helix. Of note, PKCγ harbors substantial insertions in key regulatory elements such as the αC-β4 loop and extreme C-tail. These regions are among the most disordered regions of the catalytic domain, are predicted to be spatially close in the tertiary structure, and present novel binding interfaces and steric constraints for the C1 domains. Structural insights into the autoinhibited, active, and mutant forms of PKCγ through crystallographic and cryo-EM studies will better inform the intermolecular interactions between regulatory and kinase domains necessary to maintain the spatiotemporal control of PKC output.

Identification of GSK3β as a potential direct PKCγ phosphorylation that is upregulated in PKCγ mutant cerebellum is a promising lead in revealing the dysregulated signaling in SCA14. GSK3β has long been known to be negatively regulated by PKC; however, the site of phosphorylation was unknown. Mapping this phosphorylation to a known inhibitory site in GSK3β, Ser^{389}, strongly suggests that this the long-sought-after direct PKC phosphorylation site. GSK3β is implicated in various neurogenerative diseases, including Alzheimer's and Parkinson's, through its phosphorylation of tau, amyloid beta, and α-synuclein to prevent their aggregation (Lei et al., 2011). Additionally, the neuronal effects of lithium are thought to be mediated in part through GSK3β inhibition (Cade, 1949). PKC phosphorylation at GSK3β Ser^{389}, however, suggests that inhibition of GSK3β, rather than its activity, is driving ataxia pathology. Characterization of additional PKCγ substrates and how GSK3β Ser^{389} phosphorylation effects its activity and substrate specificity in the context of Purkinje cells merits further investigation.

Another important group of neuronal proteins whose integrity mediated by phosphorylation is critical for preventing aggregation and cellular dysfunction are the neurofilament proteins.

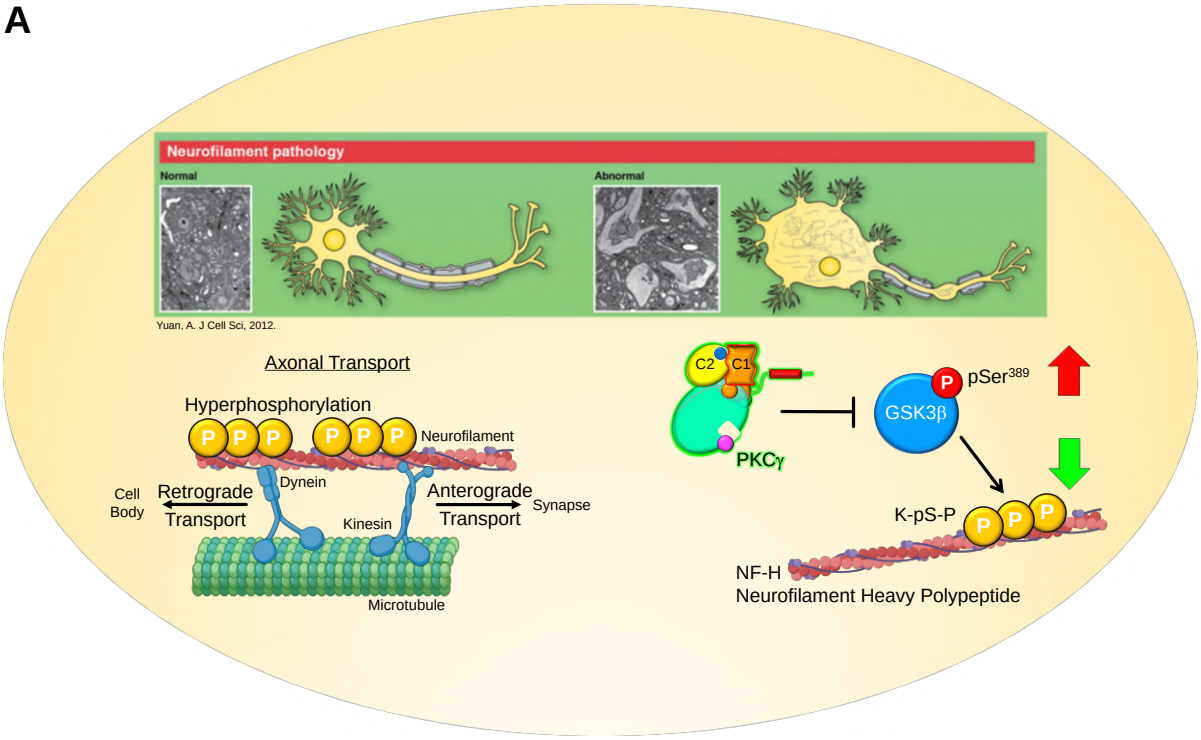

Figure 5.5: **Hypothesis for PKCγ Pathology in Spinocerebellar Ataxia.**
(A) Neuronal dysfunction often presents with neurofilament pathology, and PKCγ hyperactivity in the cerebellum is known to cause the cerebellar degeneration characteristic of SCA14. Maintenance of neurofilament phosphorylation is thought to promote axonal transport and prevent filament aggregation. This phosphorylation, particularly at Lys-Ser-Pro repeats, is facilitated in part by GSK3β. SCA-14 PKCγ mutant mice displayed both decreased neurofilament heavy polypeptide phosphorylation and increased phosphorylation of an inhibitory site on GSK3β (Ser^{389}). Thus, aberrantly active PKCγ may block phosphorylation of neurofilaments through inhibition of GSK3β leading to neuronal death and cerebellar degeneration. Neurofilament and Purkinje cell images courtesy of (Yuan et al., 2012) and (Schrenk et al., 2002).

A dramatic result of our phosphoproteomic analysis was the marked down-regulation of NF-H KSP repeats in SCA14 PKCγ mutant mouse cerebellum. Neurofilament proteins, which play support structural and axonal transport functions and are abundant in neurons, are heavily phosphorylated at the KSP repeats, with 40-51 KSP phosphorylation sites per molecule that are constitutively phosphorylated by GSK3β/Cdk5/ERK1/2 and p38/JNK (Holmgren et al., 2012; Yuan et al., 2012). These findings present the attractive hypothesis that PKCγ inhibition of GSK3β through Ser^{389} phosphorylation impairs GSK3β phosphorylation of NF-H KSP repeats,

promoting aggregation, impaired axonal transport, and Purkinje cell degeneration. Validation of this signaling pathway in primary PKCγ mutant neurons is necessary to implicate neurofilament pathology as a driver of ataxia and establish the PKCγ/GSK3β axis as a therapeutic target.

Taken together, our data advance the molecular understanding of the signaling pathways that become dysregulated in SCA14. Elucidating the molecular drivers of SCA14 may have applications in other SCAs that converge on similar pathways and will provide insight into the maintenance of neuronal homeostasis. Should further studies reveal that general Ca^{2+} dysregulation converges on PKCγ in most cerebellar ataxias, development of PKCγ inhibitors would be potentially efficacious therapeutic endeavor. As most patients present with ataxia later in life but may be identified by genomic sequencing, preventative measures to delay the onset of disease by modulation of PKCγ activity may be a viable approach. Although developing PKCγ inhibitors that cross the blood-brain barrier poses a significant challenge, since PKCγ activity is largely restricted to Purkinje neurons and inhibitors may selectively target the hyperactive mutants, low levels of toxicity and side-effects would be anticipated. Moreover, efforts to understand the molecular basis of mutant PKCγ hyperactivation and identify the differentially regulated pathological substrates will potentiate therapeutic interventions in cerebellar ataxias.

EXPERIMENTAL MODEL AND SUBJECT DETAILS

Cell Culture and Transfection

COS7 cells, HEK-293t cells, and +/+ MEFs were cultured in DMEM (Corning) containing 10% fetal bovine serum (Atlanta Biologicals) and 1% penicillin/streptomycin (Gibco) at 37°C in 5% CO_2. Transient transfection was carried out using the Lipofectamine 3000 Transfection Reagent (Thermo Fisher Scientific). The mutant PKCγ SCA14 model mouse tissue was obtained

from the lab of Wendy Raskind at University of Washington.

METHOD DETAILS

Plasmids and Constructs

The C Kinase Activity Reporter (CKAR) was previously described (Violin et al., 2003). All constructs were generated by QuikChange Mutagenesis (Agilent) or subcloning into pcDNA3 or pCMV vectors with N-terminal affinity tags. Rat PKCβ and human PKCγ were used throughout.

FRET Imaging and Analysis

Cells were imaged as described previously (Gallegos et al., 2006). For activity experiments COS7 cells were co-transfected with the indicated mCherry-tagged PKC construct and CKAR. Baseline images were acquired every 15 s for 2 min prior to ligand addition. Förster resonance energy transfer (FRET) ratios represent mean ± SEM from at least three independent experiments. All data were normalized to the baseline FRET ratio of each individual cell unless noted that absolute FRET ratio was plotted or traces were normalized to levels post-inhibitor addition. Every CKAR experiment contained an mCherry-transfected control to measure endogenous activity, and an mCherry-tagged WT control.

Immunoblotting and Antibodies

Cells were lysed in PPHB: 50 mM $NaPO_4$ (pH 7.5), 1% Triton X-100, 20 mM NaF, 1 mM $Na_4P_2O_7$, 100 mM NaCl, 2 mM EDTA, 2 mM EGTA, 1 mM Na_3VO_4, 1 mM PMSF, 40 mg/ml leupeptin, 1mM DTT, and 1 mM microcystin. Triton-soluble fractions were analyzed by SDS-PAGE on 7% big gels to observe phosphorylation shift, transfer to PVDF membrane (Biorad),

and western blotting via chemiluminescence SuperSignal West reagent (Thermo Fisher) on a FluorChem Q imaging system (ProteinSimple). In Western blots, the double asterisk (**) denotes the position of mature, and the single asterisk (*) denotes the position of partially phosphorylated PKC at the turn or hydrophobic motif; whereas, the dash (-) indicates the position of unphosphorylated PKC. The turn motif and hydrophobic motif phosphorylations, but not the activation loop phosphorylation, induces an electrophoretic mobility shift that retards the migration of the phosphorylated species. The pan anti-phospho-PKC activation loop antibody (PKC pThr^{500}) was described previously (Dutil et al., 1998). The anti-phospho-PKCγ activation loop (pT^{514}), anti-phospho-PKCγ turn motif (pT^{655}; 9375S), pan anti-phospho-PKC hydrophobic motif (γ pS^{674}; 9371S), antibodies and Calyculin A were purchased from Cell Signaling. Anti-PKCβ (610128) and PKCα (610128) antibodies were purchased from BD Transduction Laboratories. The DsRed antibody was purchased from Clontech. The anti-HA antibody for immunoblot was purchased from Roche. The anti-HA (clone 16B12; 901515) and anti-FLAG (Clone L5; 637301) antibodies used for immunoprecipitation were purchased from BioLegend. The anti-α-tubulin (T6074) and anti-FLAG immunoblot antibodies were from Sigma. UTP, PDBu, Gö6983, Gö6976, and BisIV were purchased from Calbiochem.

Pulse-Chase Experiments

For pulse-chase experiments, COS7 cells were incubated with Met/Cys-deficient DMEM for 30 min at 37 °C. The cells were then pulse-labeled with 0.5 mCi/ml [^{35}S]Met/Cys in Met/Cys-deficient DMEM for 7 min at 37°C, media were removed, washed with dPBS (Corning), and chased with DMEM culture media (Corning) containing 200 mM unlabeled methionine and 200 mM unlabeled cysteine. At the indicated times, cells were lysed in PPHB and centrifuged at

13,000 x g for 3 min at 22 °C, supernatants were pre-cleared for 30 min at 4 °C with Protein A/G Beads (Santa Cruz), and protein complexes were immunoprecipitated from the supernatant with either an anti-HA, anti-Myc, or anti-FLAG monoclonal antibody overnight at 4 °C. The immune complexes were collected with Protein A/G Beads (Santa Cruz) for 2 hrs, washed 3x with PPHB, separated by SDS-PAGE, transferred to PVDF membrane (Biorad), and analyzed by autoradiography and western blot. Co-immunoprecipitation experiments were performed similarly, omitting the labeling and autoradiography steps.

Mass Spectrometry

Multiplex Substrate Profiling by Mass Spectrometry (qMSP-MS) on resected cerebellar tissues were performed as described in (Lapek, et al., 2019).

Molecular Modeling

Molecular modeling experiments were performed using PyMOL.

QUANTIFICATION AND STATISTICAL ANALYSIS

Statistical significance was determined via Repeated Measures One-Way ANOVA and Brown-Forsythe Test or Student's t-test performed in GraphPad Prism 6.0a (GraphPad Software). The half-time of translocation was calculated by fitting the data by non-linear regression using a one-phase exponential association equation with GraphPad Prism 6.0a (GraphPad Software). Western blots were quantified by densitometry using the AlphaView software (Protein Simple).

Acknowledgements

The following individuals contributed to this work: Timothy R. Baffi and Alexandra C. Newton designed the experiments. Timothy R. Baffi performed the experiments. Mario Malfavon performed the mass spectrometry and analysis under the mentorship of Daivd Gonzalez. Dawn Chen and Wendy Raskind from University of Washington supplied the cerebellum from the SCA14 model mice.

Chapter 6

Targeting PKC Regulatory Mechanisms in Disease

Addressing the dogma that mTORC2 is the hydrophobic motif kinase, Chapter 2 of this dissertation re-evaluates the identity of the bona fide hydrophobic motif kinase by systematically dissecting the biochemical relationships between mTORC2, AGC kinase phosphorylation, and catalytic activity (Figure 6.1). Consistent with early studies that implicated the hydrophobic motif as an autophosphorylation site, the studies contained herein propose a unifying model that explains the requirements for mTOR activity through the identification of a novel and conserved TOR-Interaction Motif (TIM) phosphorylation site. Demonstrating that mTORC2-dependent phosphorylation of this site in PKC is the first and rate-limiting step in recruiting PDK1 to activate the kinase and permit intramolecular hydrophobic motif phosphorylation, this work redefines mTORC2 as an AGC kinase chaperone that may serve similar roles in other mTOR-regulated AGC kinases.

Expanding the role of hydrophobic motif function in PKC, Chapters 2 and 3 also find that this phosphorylation is the final step and driving force that promotes the conformational rearrangements necessary for autoinhibition and stabilization of PKC in the primed state. This finding may explain the variable requirement of hydrophobic motif phosphorylation for kinase activity among AGC kinases, dependent upon both the phosphorylation of the activation loop and also the ability of the C-tail to associate with the N-lobe in the phosphorylated or unphosphorylated hydrophobic motif states. Indeed, hydrophobic motif phosphorylation that precedes activation loop phosphorylation in some kinases recruits PDK1 by providing a direct phospho-docking site; whereas, hydrophobic motif phosphorylation that follows activation loop phosphorylation must recruit PDK1, instead, through conformational transitions. This model perhaps explains why truncation of N-terminal AGC kinase regulatory segments promotes agonist and mTOR-independent phosphorylation in the C-tail, as is observed for Akt and PKN yeast homologue Ypk1, and may underlie the intramolecular basis for autoinhibition. Importantly, the complexity of PKC processing, which involves several regulatory proteins including PDK1, mTORC2, Hsp90, and PHLPP1, are targets of many drugs that are clinically approved or undergoing therapeutic development (Figure 6.1). In particular, mTOR and Hsp90 inhibitors are extensively utilized as anti-cancer therapies and would have the unwanted effect of impairing PKC maturation. Thus, the effect of any therapeutics on PKC function should be considered, and efforts to mitigate these effects merit investigation. In summary, the PKC phosphorylation arc that culminates with hydrophobic motif phosphorylation achieves complete activation of the kinase, initiating the process of PKC quality control that selectively stabilizes autoinhibited enzymes during PKC maturation.

6.1 Updating the Model of PKC Maturation

PKC maturation by phosphorylation is not only a critical process to specify PKC function and stability, but also serves as a paradigm for kinase regulation by phosphorylation. Activation loop phosphorylation, for example, is the nearly ubiquitous mechanism by which eukaryotic protein kinases become activated through structuring of the activation segment to adopt an active conformation (Adams, 2002). This activation is regulated by a variety of mechanisms including transphosphorylation by an upstream activation loop kinase as is the case for LKB1 phosphorylation of AMPK family members (Lizcano et al., 2004) and PDK1 phosphorylation of AGC kinase family members (Mora et al., 2004), as well as cis or trans autophosphorylation (Lochhead, 2009). Alternatively, hydrophobic motif phosphorylation has proven more enigmatic, as the stimuli and associated kinases that result in phosphorylation at this site in AGC kinases vary between kinases and suffer from lack of mechanistic studies. Indeed, even the function of the Akt hydrophobic motif, a well-studied and widely regarded marker of activation, is still debated. The uncertainty regarding the hydrophobic motif may be explained in part by the decade-long search for the hydrophobic motif kinase PDK2, following the identification of PDK1 as the activation loop kinase (Alessi et al., 1997; Chan and Tsichlis, 2001; Stokoe et al., 1997). Although there existed evidence that the hydrophobic motif site was regulated by autophosphorylation for PKC, Akt, and S6K (Behn-Krappa and Newton, 1999; Romanelli et al., 2002; Toker and Newton, 2000), this finding could not be reconciled by the unequivocal requirement of mTOR kinase activity for hydrophobic motif phosphorylation in these kinase among others, upon the discovery of mTORC2.

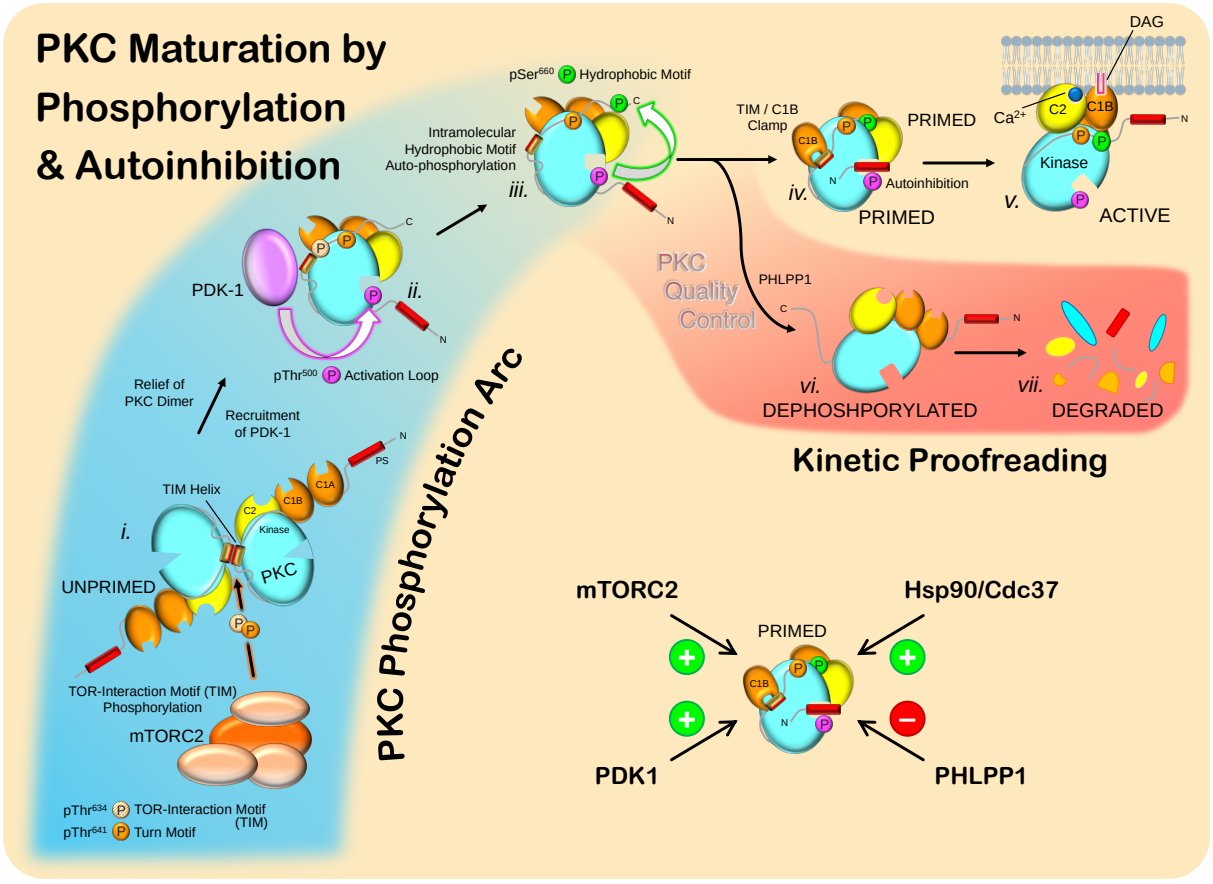

Figure 6.1: **Updating the Model of PKC Maturation.** In order to become both active and stable, PKC must undergo a series of ordered phosphorylations and confomational transitions, followed by kinetic proofreading quality control. Newly-synthesized PKC (i) exists in an unphosphorylated and inactive dimer, mediated by the TIM Helix. TIM and turn motif phosphorylation by mTORC2 dissociates the PKC dimer to recruit PDK1 (ii). PDK1 phosphorylation of the activation loop then triggers intramolecular hydrophobic motif autophosphorylation (iii). At this phase, the apex of PKC maturation and critical decision branch point, PKC is catalytically active and has overcome the energy barrier to achieve the autoinhibited conformation. PKC is then subject to quality control by PHLPP1 as a kinetic proofreading checkpoint, in which PHLPP1 surveys the conformation of PKC to dephosphorylate aberrantly active enzyme (vi),leading to its degradation (vii) and ensuring the fidelity of PKC autoinhibition. This proofreading step maintains the integrity of the PKC maturation process by selectively stabilizing only those PKCs that have become both phosphorylated and autoinhibited (iv). It is this primed PKC species that comprises the major cellular fraction and is appropriately tuned to respond to fluctuations in second messengers to provide tightly regulated control of spatiotemporal activation (v). PKC processing relies upon the activity of several enzymes, including positive regulation by the kinases mTORC2 and PDK1 and chaperone Hsp90, as well as negative regulation by phosphatase PHLPP1. These enzymes are frequently therapeutic targets in disease; thus, the outcome on PKC due to their inhibition must be considered in the context of the disease.

6.2 PHLPP1 as the Master Regulator of PKC Quality Control

A major finding from this dissertation is the characterization of PKC quality control, described in Chapter 3, mediated by PHLPP1 (Figure 6.2) (Baffi et al., 2019). To ensure the fidelity of PKC maturation, the process of PKC quality control relies upon the ability of PHLPP1 to recognize the unprimed and open PKC conformation that has not become autoinhibited to promote selective dephosphorylation and degradation. The conformational transitions that result in autoinhibition, set in motion by hydrophobic motif phosphorylation and dependent upon the affinity of the pseudosubstrate, act as a molecular clock that renders PKC subject to degradation if they do not occur sufficiently rapidly to protect PKC from PHLPP1 dephosphorylation. Thus, PKC quality control represents a novel example of kinetic proofreading, or a specificity mechanism for error correction that allows enzymes to discriminate between two possible pathways to achieve higher accuracy than one would predict based solely on the free energy difference between the two possibilities (Hopfield, 1974; Lemmon et al., 2016). In the case of PKC quality control, this kinetic proofreading confers a high degree of autoinhibition fidelity following phosphorylation by utilizing a PHLPP1 conformational surveying mechanism to take advantage of PKC's dependence upon phosphorylation for stability.

Given the essential role this process plays in regulating enzyme integrity and protein levels, PKC quality control dysregulation is readily apparent in multiple pathological states. For example, the foregoing data demonstrated that PKC quality control maintains near stoichiometric phosphorylation at the hydrophobic motif across 19 different cancers, and is exploited in pancreatic cancer to suppress PKC expression, resulting in worsened patient survival (Baffi et al., 2019). Furthermore, PKC quality control may explain why dozens of LOF PKC mutations in cancer display defects in phosphorylation, as slight perturbations to their catalytic efficiency or confor-

mational integrity allow kinetic proofreading by PHLPP1 to dominate. In addition to excess PKC quality control, PKC mutations that evade this process also cause disease. In chordoid glioma described in Chapter 4, low quality control pressure that results in higher levels of PKC potentiates the dominant-negative effects of a recurrent LOF PKCα D463H mutation, which acts to globally suppress PKC output. Conversely, activating mutations in spinocerebellar ataxia described in Chapter 5 bypass PKC quality control to avoid degradation and become aberrantly stabilized, which promotes neurodegeneration through enhanced, agonist-independent activity. Thus, PKC quality control underlies GOF, LOF, and neomorphic effects of PKC disease-associated mutations and presents a critical node for regulating PKC output through the coordinated control of PKC expression levels, autoinhibition, and sensitivity to activation.

While PHLPP phosphatases are known to remove the hydrophobic motif phosphate to regulate PKC levels, this effect was shown in the context of chronic phorbol ester treatment at the plasma membrane (Gao et al., 2008). The studies in Chapter 3 supplement previous work by establishing the role of PHLPP1 in regulating PKC in an agonist-independent manner by conformationally surveying the newly-synthesized protein to the ensure the fidelity of PKC maturation. Thus, the physiological and perhaps predominant role of PHLPP1 in controlling PKC levels may be through quality control of the nascent protein. While PHLPP is also necessary for PKC down-regulation by phorbol esters, which likely accounts for their well-described oncogenic effects, this process may reflect the affinity of PHLPP1 for the open and active PKC conformation, resigning this particular capability of PHLPP regulation to cases of PKC hyperactivation during persistent and elevated levels of second messengers, rather than a constitutive surveying process. Thus, the interrelated PHLPP1 functions of conformationally surveying the newly-synthesized protein to ensure autoinhibition following maturation and, in a related man-

ner, dephosphorylating activated PKC to terminate signaling at the membrane both serve to quench aberrantly active enzyme and suppress protein levels under resting conditions and in the presence of agonist, respectively. Taken together, the identification of differential PHLPP1 regulation of the nascent and activated PKC protein relies upon precise intramolecular conformational rearrangements, which occur upon PKC phosphorylation and upon activation. These homeostatic processes highlight the importance of restricted spatial and temporal PKC activation orchestrated by intramolecular constraints and second messengers, as enzymes aberrantly activated in an agonist-dependent or independent manner are rapidly removed from the cell.

Figure 6.2: **PHLPP1 as the Master Regulator of PKC Quality Control.**
(A) The process of PHLPP1-mediated PKC quality control, as the critical step of PKC maturation controlling protein levels and activity, is frequently dysregulated in disease. This dissertation has illustrated how excessive PKC quality control functions as a pervasive loss-of-function mechanism in cancer to suppress expression, particularly relevant in pancreatic cancer where low PKC levels correlated with worsened survival. Loss of PHLPP1 quality control, conversely potentiates the pathological effects of both loss-of-function and gain-of-function mutations in cancer and ataxia, respectively. Failure to degrade unprimed PKCα mutants in chordoid glioma unleashes their dominant-negative function to globally suppress PKC out by sequestering diacylglycerol. In spinocerebellar ataxia, aberrently active PKCγ mutats evade dephosphorylation by PHLPP1 to drive neurodegeneration. Thus, the integrity of PHLPP1-mediated PKC quality control is essential to maintain signaling homeostasis through PKC and avoid pathophysiologies.

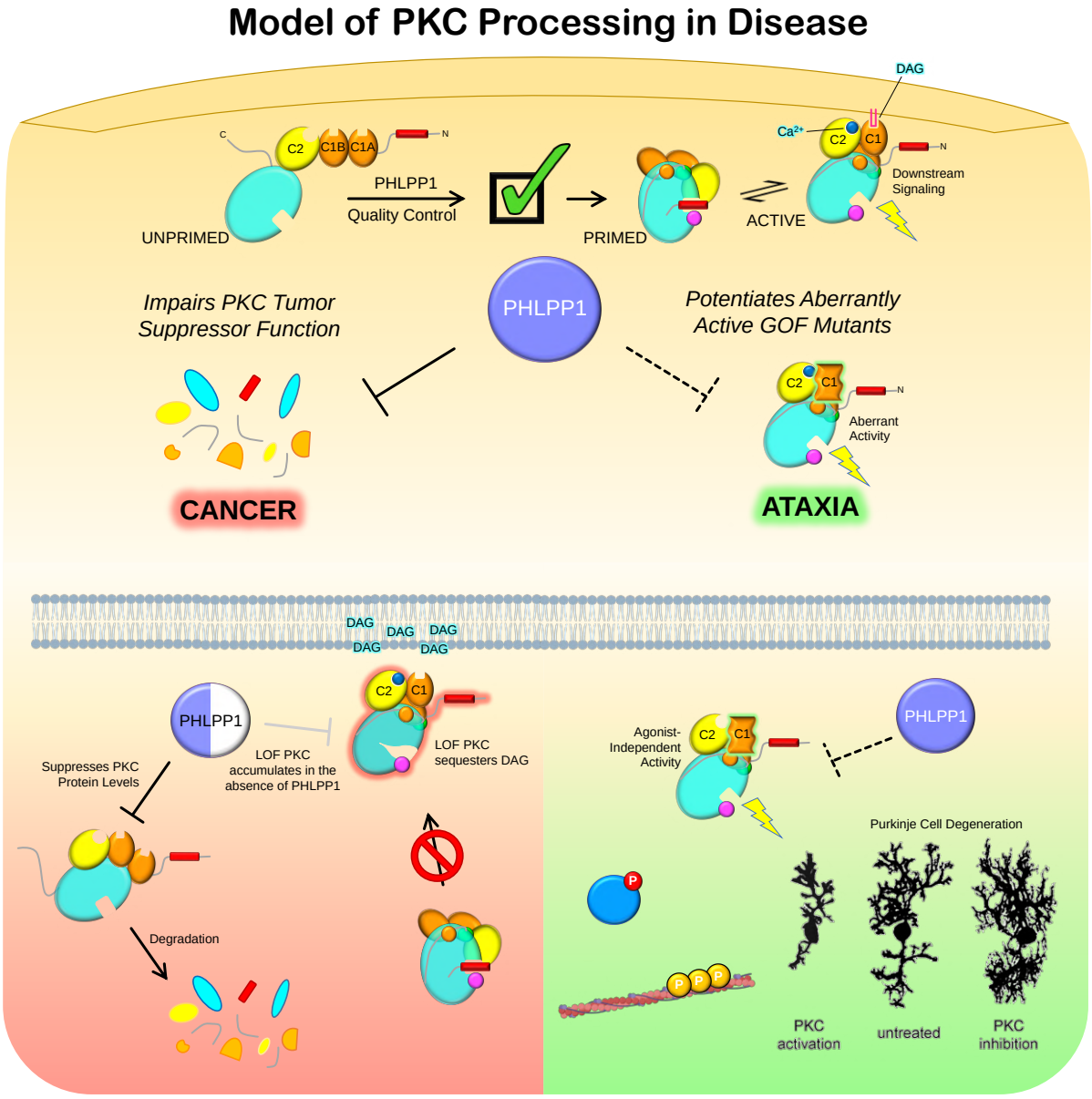
Model of PKC Processing in Disease
DAG
C
C2
C1B
C1A
N
PHLPP1
Quality Control
UNPRIMED
PRIMED
Ca2+
C2
C1
ACTIVE
Downstream
Signaling
PHLPP1
Impairs PKC Tumor
Suppressor Function
Potentiates Aberrantly
Active GOF Mutants
C2
C1
N
Aberrant
Activity
CANCER
ATAXIA
DAG
DAG
DAG
DAG
DAG
PHLPP1
C2
C1
LOF PKC
sequesters DAG
Suppresses PKC
Protein Levels
LOF PKC
accumulates in the
absence of PHLPP1
Degradation
Agonist-
Independent
Activity
C2
C1
PHLPP1
Purkinje Cell Degeneration
P
P
P
P
PKC
activation
untreated
PKC
inhibition

6.3 A High-Throughput Approach for Identifying Therapeutic PKC Modulators

The clinical PKC field has suffered from the misguided attempts to inhibit PKC in cancer; however, PKC remains an attractive therapeutic target, given its involvement in several disease pathologies and the wealth of knowledge on its function and regulation. Evidence from this dissertation supports the notion that approaches should generally aim to enhance PKC output in cancer and inhibit its output in neurodegeneration. Caution should of course be exercised in targeting PKC by rigorous mechanistic validation of its role in the specific disease context. Fortunately, there exist a multitude of potent and specific orthosteric and allosteric PKC inhibitors that may be re-purposed in neurodegenerative disease and incorporated in emerging technologies such as proteolysis targeting chimera (PROTAC) (Sakamoto et al., 2001; Schneekloth, et al., 2004) and degradation tag (dTAG) (Nabet et al., 2018) chemical degraders. Developing therapies for cancer treatment poses a more difficult challenge, as PKC activators generally have the opposite effect of causing PKC down-regulation when administered chronically. Studies utilizing intermittent dosing schedules of bryostatins, a relatively weak phorbol ester, suggest that use of some PKC activators may have the desired effects in some contexts (Wang et al., 2015). Additionally, recruitment of PKC to differential membrane compartments upon activation has distinct effects on selective agonist-induced degradation, which may identify classes of agonists to strategically activate PKC in a manner that prevents its down-regulation (Lum et al., 2016). Nonetheless, novel approaches outside of diacylglycerol analogs are required both to appropriately study PKC and to develop effective therapeutics.

The work of this dissertation reveals a novel approach to modulate PKC output via con-

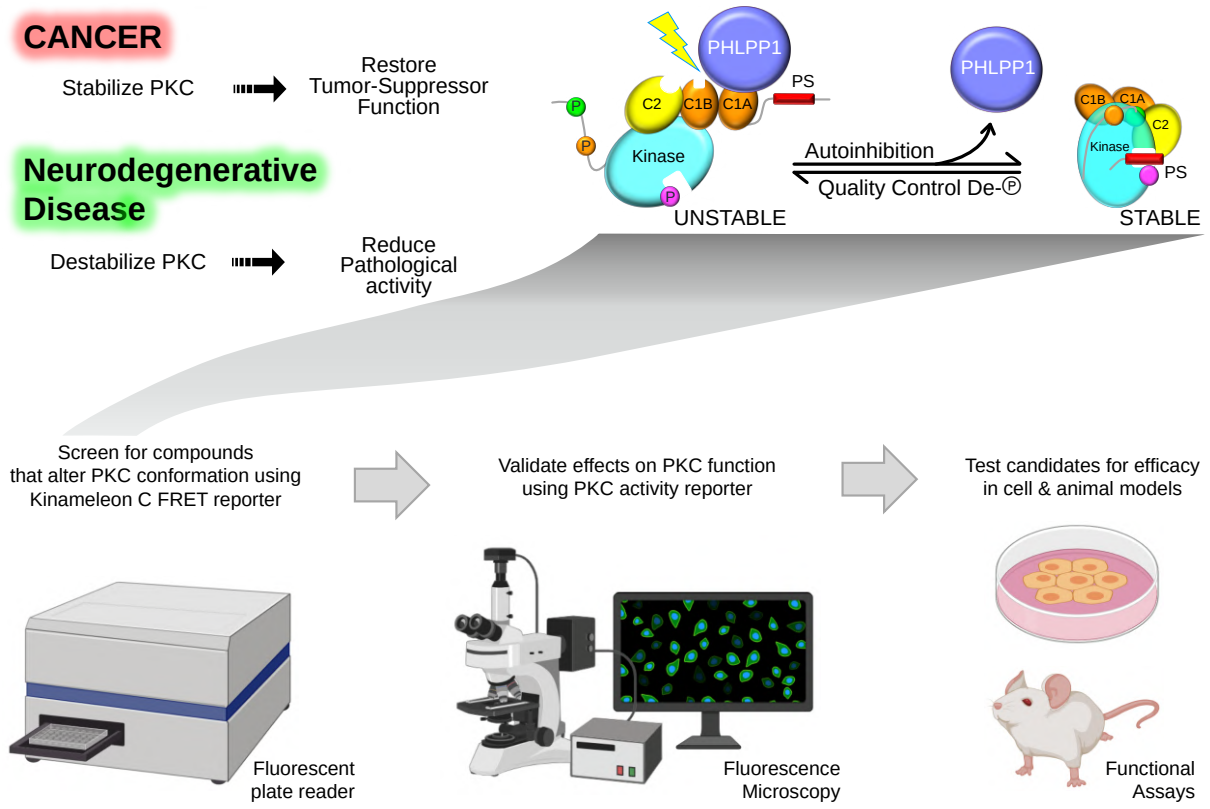

Figure 6.3: **A High-Throughput Approach for Identifying Therapeutic PKC Modulators.** Therapeutic approaches should generally attempt to restore PKC tumor-suppressive function in cancer and reduce its pathological activity in neurodegenerative disease. Targeting the process of PKC maturation to influence the balance of PHLPP1 kinetic proofreading is a viable method to screen for novel allosteric regulators to modulate PKC output. Using the Kinameleon C FRET reporter to measure PKC conformation in live cells, compounds may be screened in a high-throughput format to identify modulators of PKC conformation, which can be validated for effects on PKC activity and cellular processes using fluorescence microscopy studies and functional assays.

formation that affords both positive and negative regulation. The ability of PHLPP1 to survey the unprimed PKC conformation to orchestrate PKC quality control suggests that there are interfaces on the kinase domain that mediate binding to PHLPP1 and become masked upon autoinhibition to preclude binding. Thus, allosteric regulators may have the potential of targeting these interfaces to either facilitate or disrupt the interaction of the regulatory domains with the kinase domain, enabling the modulation of PKC sensitivity to PHLPP1 kinetic proofreading. In

this way, PKC levels can be increased or decreased by using the cell's endogenous machinery involved in PKC quality control. In cases where PKC quality control is lost or impaired, therapeutics that target this interface would instead alter PKC sensitivity to agonist to modulate its activity. This conformational targeting approach has the additional benefit of primarily targeting PKC processing, sparing the canonical PKC activation mechanisms through Ca^{2+} and DAG, which regulate a host of other effectors, intact.

Importantly, targeting PKC conformation enables high-throughput screening of small-molecular libraries utilizing the FRET-based Kinameleon C reporter, which reads out cellular PKC conformational changes (Figure 6.3). Thus, using a single screening platform, compounds could be assessed for their ability to promote or disrupt the autoinhibited state, which would lead to increased or decreased PKC stability, respectively. Compounds that modulate PKC conformation could then be validated for their effects on PKC activity by fluorescence microscopy using CKAR and on stability using biochemical assays. In this manner, identification of PKC modulators would expedite the development of potential therapeutics and isozyme-specific research tools that selectively increase or decrease PKC output. In summary, the contributions of this dissertation to understanding the mechanisms by which PKC becomes phosphorylated and the quality control process that arbitrates its maturation will facilitate the development of next-generation PKC therapeutics that harness the cell's intrinsic regulatory machinery to modulate PKC expression at the post-translational level.

Bibliography

Abrahamsen, H., O'Neill, A.K., Kannan, N., Kruse, N., Taylor, S.S., Jennings, P.A., and Newton, A.C. (2012). Peptidyl-prolyl isomerase Pin1 controls down-regulation of conventional protein kinase C isozymes. J Biol Chem 287, 13262–13278.

Adachi, N., Kobayashi, T., Takahashi, H., Kawasaki, T., Shirai, Y., Ueyama, T., Matsuda, T., Seki, T., Sakai, N., and Saito, N. (2008). Enzymological analysis of mutant protein kinase Cgamma causing spinocerebellar ataxia type 14 and dysfunction in Ca2+ homeostasis. J Biol Chem 283, 19854–19863.
Adams, J.A. (2001). Kinetic and catalytic mechanisms of protein kinases. Chem. Rev. 101, 2271–2290.

Adams*, J.A. (2002). Activation Loop Phosphorylation and Catalysis in Protein Kinases: Is There Functional Evidence for the Autoinhibitor Model?†.

Alessi D.R., Andjelkovic M., Caudwell B., Cron P., Morrice N., Cohen P. and Hemmings B.A., Mechanism of activation of protein kinase B by insulin and IGF-1, Embo J. 15, 1996, 6541–6551.

Alessi, D.R., James, S.R., Downes, C.P., Holmes, A.B., Gaffney, P.R.J., Reese, C.B., and Cohen, P. (1997). Characterization of a 3-phosphoinositide-dependent protein kinase which phosphorylates and activates protein kinase Bα. Curr. Biol. 7, 261–269.

Alfonso, S., Kessels, H.W., Banos, C.C., Chan, T.R., Lin, E.T., Kumaravel, G., Scannevin, R.H., Rhodes, K.J., Huganir, R., Guckian, K.M., et al. (2014). Synapto-depressive effects of amyloid beta require PICK1. Eur. J. Neurosci. 39, 1225.

Alfonso, S.I., Callender, J.A., Hooli, B., Antal, C.E., Mullin, K., Sherman, M.A., Lesné, S.E., Leitges, M., Newton, A.C., Tanzi, R.E., et al. (2016). Gain-of-function mutations in protein kinase Cα (PKCα) may promote synaptic defects in Alzheimer's disease. Sci. Signal. 9, ra47.

Almoguera C., Shibata D., Forrester K., Martin J., Arnheim N. and Perucho M., Most human carcinomas of the exocrine pancreas contain mutant c-K-ras genes, Cell 53, 1988, 549–554.

An, E., and Brognard, J. (2019). Orange is the new black: Kinases are the new master regulators of tumor suppression. IUBMB Life 71, 738–748.

Andjelković, M., Maira, S.-M., Cron, P., Parker, P.J., and Hemmings, B.A. (1999). Domain Swapping Used To Investigate the Mechanism of Protein Kinase B Regulation by 3-Phosphoinositide-Dependent Protein Kinase 1 and Ser473 Kinase. Mol. Cell. Biol. 19, 5061–5072.

Antal C.E., Callender J.A., Kornev A.P., Taylor S.S. and Newton A.C., Intramolecular C2 Domain-Mediated Autoinhibition of Protein Kinase C βII, Cell Rep. 12, 2015a, 1252–1260.

Antal C.E., Hudson A.M., Kang E., Zanca C., Wirth C., Stephenson N.L., Trotter E.W., Gallegos L.L., Miller C.J., Furnari F.B., et al., Cancer-associated protein kinase C mutations reveal kinase's role as tumor suppressor, Cell 160, 2015b, 489–502.

Antal C.E., Violin J.D., Kunkel M.T., Skovsø S. and Newton A.C., Intramolecular conformational changes optimize protein kinase C signaling, Chem. Biol. 21, 2014, 459–469.

Antal, C.E., and Newton, A.C. (2013). Spatiotemporal Dynamics of Phosphorylation in Lipid Second Messenger Signaling. Mol. Cell. Proteomics 12, 3498–3508.

Antal, C.E., and Newton, A.C. (2014). Tuning the signalling output of protein kinase C. Biochem Soc Trans 42, 1477–1483.

Baffi, M.O., Slattery, E., Sohn, P., Moses, H.L., Chytil, A., and Serra, R. (2004). Conditional deletion of the TGF-β type II receptor in Col2a expressing cells results in defects in the axial skeleton without alterations in chondrocyte differentiation or embryonic development of long bones. Dev. Biol. 276, 124–142.

Baffi, T.R., Van, A.-A.N., Zhao, W., Mills, G.B., and Newton, A.C. (2019). Protein Kinase C Quality Control by Phosphatase PHLPP1 Unveils Loss-of-Function Mechanism in Cancer. Mol. Cell 74, 378-392.e5.

Balasubramani, A., Larjo, A., Bassein, J.A., Chang, X., Hastie, R.B., Togher, S.M., Lähdesmäki, H., and Rao, A. (2015). Cancer-associated ASXL1 mutations may act as gain-of-function mutations of the ASXL1–BAP1 complex. Nat. Commun. 6, 7307.

Balasuriya, N., Kunkel, M.T., Liu, X., Biggar, K.K., Li, S.S.-C., Newton, A.C., and O'Donoghue, P. (2018). Genetic code expansion and live cell imaging reveal that Thr308 phosphorylation is irreplaceable and sufficient for Akt1 activity. J. Biol. Chem. jbc.RA118.002357.

Balendran A., Hare G.R., Kieloch A., Williams M.R. and Alessi D.R., Further evidence that 3-phosphoinositide-dependent protein kinase-1 (PDK1) is required for the stability and phosphorylation of protein kinase C (PKC) isoforms, FEBS Lett. 484, 2000, 217–223.

Balendran, A., Casamayor, A., Deak, M., Paterson, A., Gaffney, P., Currie, R., Downes, C.P., and Alessi, D.R. (1999). PDK1 acquires PDK2 activity in the presence of a synthetic peptide derived from the carboxyl terminus of PRK2. Curr. Biol. 9, 393–404.

Barceló C., Paco N., Morell M., Alvarez-Moya B., Bota-Rabassedas N., Jaumot M., Vilardell F., Capella G. and Agell N., Phosphorylation at Ser-181 of oncogenic KRAS is required for tumor growth, Cancer Res. 74, 2014, 1190–1199.

Bayliss R., Haq T. and Yeoh S., The Ys and wherefores of protein kinase autoinhibition, Biochim, Biophys, Acta-Proteins and Proteomics 1854, 2015, 1586–1594.

Becker, E.B.E. (2017). From Mice to Men: TRPC3 in Cerebellar Ataxia. Cerebellum 16, 877–879.
Becker, E.B.E., Fogel, B.L., Rajakulendran, S., Dulneva, A., Hanna, M.G., Perlman, S.L., Geschwind, D.H., and Davies, K.E. (2011). Candidate Screening of the TRPC3 Gene in Cerebellar Ataxia. The Cerebellum 10, 296–299.

Behn-Krappa, A., and Newton, A.C. (1999). The hydrophobic phosphorylation motif of conventional protein kinase C is regulated by autophosphorylation. Curr. Biol. 9, 728–737.

Bellacosa, A., Chan, T.O., Ahmed, N.N., Datta, K., Malstrom, S., Stokoe, D., McCormick, F., Feng, J., and Tsichlis, P. (1998). Akt activation by growth factors is a multiple-step process: the role of the PH domain. Oncogene 17, 313–325.

Benjamin, D., Colombi, M., Moroni, C., and Hall, M.N. (2011). Rapamycin passes the torch: a new generation of mTOR inhibitors. Nat. Rev. Drug Discov. 10, 868–880.

Biondi, R.M., Cheung, P.C., Casamayor, A., Deak, M., Currie, R.A., and Alessi, D.R. (2000). Identification of a pocket in the PDK1 kinase domain that interacts with PIF and the C-terminal residues of PKA. EMBO J. 19, 979–988.

Biondi, R.M., Kieloch, A., Currie, R.A., Deak, M., and Alessi, D.R. (2001). The PIF-binding pocket in PDK1 is essential for activation of S6K and SGK, but not PKB. EMBO J. 20, 4380–4390.

Bivona T.G., Quatela S.E., Bodemann B.O., Ahearn I.M., Soskis M.J., Mor A., Miura J., Wiener H.H., Wright L., Saba S.G., et al., PKC regulates a farnesyl-electrostatic switch on K-Ras that promotes its association with Bcl-XL on mitochondria and induces apoptosis, Mol. Cell 21, 2006, 481–493.

Black, A.R., and Black, J.D. (2013). Protein kinase C signaling and cell cycle regulation. Front. Immunol. 3, 423.

Blume-Jensen, P., and Hunter, T. (2001). Oncogenic kinase signalling. Nature 411, 355–365.

Bornancin F. and Parker P.J., Phosphorylation of protein kinase C-alpha on serine 657 controls the accumulation of active enzyme and contributes to its phosphatase-resistant state, J. Biol. Chem. 272, 1997, 3544–3549.

Bornancin, F., and Parker, P.J. (1996). Phosphorylation of threonine 638 critically controls the dephosphorylation and inactivation of protein kinase Cα. Curr. Biol. 6, 1114–1123.

Borner C., Filipuzzi I., Wartmann M., Eppenberger U. and Fabbro D., Biosynthesis and posttranslational modifications of protein kinase C in human breast cancer cells, J. Biol. Chem. 264, 1989, 13902–13909.

Brognard J. and Hunter T., Protein kinase signaling networks in cancer, Curr. Opin. Genet. Dev. 21, 2011, 4–11.

Burnett, P.E., Barrow, R.K., Cohen, N.A., Snyder, S.H., and Sabatini, D.M. (1998). RAFT1 phosphorylation of the translational regulators p70 S6 kinase and 4E-BP1. Proc. Natl. Acad. Sci. 95, 1432–1437.

Burns, D.J., and Bell, R.M. (1991). Protein kinase C contains two phorbol ester binding domains. J. Biol. Chem. 266, 18330–18338.

Cade, J.F.J. (1949). Lithium salts in the treatment of psychotic excitement. Med. J. Aust. 2, 349–352.

Callender J.A., Yang Y., Lordén G., Stephenson N.L., Jones A.C., Brognard J. and Newton A.C., Protein kinase Cα gain-of-function variant in Alzheimer's disease displays enhanced catalysis by a mechanism that evades down-regulation, Proc. Natl. Acad. Sci. USA 115, 2018, E5497–E5505.

Callender, J.A., and Newton, A.C. (2017). Conventional protein kinase C in the brain: 40 years later. Neuronal Signal. 1, NS20160005.

Cameron A.J., Escribano C., Saurin A.T., Kostelecky B. and Parker P.J., PKC maturation is promoted by nucleotide pocket occupation independently of intrinsic kinase activity, Nat. Struct. Mol. Biol. 16, 2009, 624–630.

Cameron, A.J.M., Linch, M.D., Saurin, A.T., Escribano, C., and Parker, P.J. (2011). mTORC2 targets AGC kinases through Sin1-dependent recruitment. Biochem. J. 439, 287–297.

Cazaubon S., Bornancin F. and Parker P.J., Threonine-497 is a critical site for permissive activation of protein kinase C alpha, Biochem. J. 301, 1994, 443–448.

Chan, T.O., and Tsichlis, P.N. (2001). PDK2: A Complex Tail in One Akt. Sci. Signal. 2001, pe1–pe1.

Chan, T.O., Rittenhouse, S.E., and Tsichlis, P.N. (1999). AKT/PKB and Other D3 Phosphoinositide-Regulated Kinases: Kinase Activation by Phosphoinositide-Dependent Phosphorylation. Annu. Rev. Biochem. 68, 965–1014.

Chan, T.O., Zhang, J., Tiegs, B.C., Blumhof, B., Yan, L., Keny, N., Penny, M., Li, X., Pascal, J.M., Armen, R.S., et al. (2015). Akt kinase C-terminal modifications control activation loop dephosphorylation and enhance insulin response. Biochem. J. 471, 37–51.

Chehab N.H., Malikzay A., Stavridi E.S. and Halazonetis T.D., Phosphorylation of Ser-20 mediates stabilization of human p53 in response to DNA damage, Proc. Natl. Acad. Sci. USA 96, 1999, 13777–13782.

Chen M., Pratt C.P., Zeeman M.E., Schultz N., Taylor B.S., O'Neill A., Castillo-Martin M., Nowak D.G., Naguib A., Grace D.M., et al., Identification of PHLPP1 as a tumor suppressor reveals the role of feedback activation in PTEN-mutant prostate cancer progression, Cancer Cell 20, 2011, 173–186.

Chen, C., Kano, M., Abeliovich, A., Chen, L., Bao, S., Kim, J.J., Hashimoto, K., Thompson, R.F., and Tonegawa, S. (1995). Impaired motor coordination correlates with persistent multiple climbing fiber innervation in PKC gamma mutant mice. Cell 83, 1233–1242.

Chen, D.-H., Brkanac, Z., Christophe Verlinde, L.M.J., Tan, X.-J., Bylenok, L., Nochlin, D., Matsushita, M., Lipe, H., Wolff, J., Fernandez, M., et al. (2003). Missense Mutations in the Regulatory Domain of PKCγ: A New Mechanism for Dominant Nonepisodic Cerebellar Ataxia. Am. J. Hum. Genet. 72, 839–849.

Chen, D., Gould, C., Garza, R., Gao, T., Hampton, R.Y., and Newton, A.C. (2007). Amplitude control of protein kinase C by RINCK, a novel E3 ubiquitin ligase. J Biol Chem 282, 33776–33787.

Chu, N., Salguero, A.L., Liu, A.Z., Chen, Z., Dempsey, D.R., Ficarro, S.B., Alexander, W.M., Marto, J.A., Li, Y., Amzel, L.M., et al. (2018). Akt Kinase Activation Mechanisms Revealed Using Protein Semisynthesis. Cell 174, 897-907.e14.

Chung, M., Lu, Y., Cheng, N., and Soong, B. (2003). A novel autosomal dominant spinocerebellar ataxia (SCA22) linked to chromosome 1p21-q23. Brain 126, 1293–1299.

Citri, A., Bhattacharyya, S., Ma, C., Morishita, W., Fang, S., Rizo, J., and Malenka, R.C. (2010). Calcium binding to PICK1 is essential for the intracellular retention of AMPA receptors underlying long-term depression. J. Neurosci. 30, 16437–16452.

Clark, J.A., Black, A.R., Leontieva, O. V., Frey, M.R., Pysz, M.A., Kunneva, L., Woloszynska-Read, A., Roy, D., and Black, J.D. (2004). Involvement of the ERK Signaling Cascade in Protein Kinase C-mediated Cell Cycle Arrest in Intestinal Epithelial Cells. J. Biol. Chem. 279, 9233–9247.

Cochet, C., Gill, G.N., Meisenhelder, J., Cooper, J.A., and Hunter, T. (1984). C-kinase phosphorylates the epidermal growth factor receptor and reduces its epidermal growth factor-stimulated tyrosine protein kinase activity. J. Biol. Chem. 259, 2553–2558.

Collins, B.J., Deak, M., Murray-Tait, V., Storey, K.G., and Alessi, D.R. (2005). In vivo role of the phosphate groove of PDK1 defined by knockin mutation. J Cell Sci 118, 5023–5034.

Correas, I., Díaz-Nido, J., and Avila, J. (1992). Microtubule-associated protein tau is phosphorylated by protein kinase C on its tubulin binding domain. J. Biol. Chem. 267, 15721–15728.

Coussens, L., Parker, P., Rhee, L., Yang-Feng, T., Chen, E., Waterfield, M., Francke, U., and Ullrich, A. (1986). Multiple, distinct forms of bovine and human protein kinase C suggest diversity in cellular signaling pathways. Science (80-.). 233, 859–866.

Crooks, G.E., Hon, G., Chandonia, J.-M., and Brenner, S.E. (2004). WebLogo: A Sequence Logo Generator. Genome Res. 14, 1188–1190.

Datta, K., Franke, T.F., Chan, T.O., Makris, A., Yang, S.I., Kaplan, D.R., Morrison, D.K., Golemis, E.A., and Tsichlis, P.N. (1995). AH/PH domain-mediated interaction between Akt molecules and its potential role in Akt regulation. Mol. Cell. Biol. 15, 2304–2310.

Davies, H., Bignell, G.R., Cox, C., Stephens, P., Edkins, S., Clegg, S., Teague, J., Woffendin, H., Garnett, M.J., Bottomley, W., et al. (2002). Mutations of the BRAF gene in human cancer. Nature 417, 949–954.

Dowling C.M., Phelan J., Callender J.A., Cathcart M.C., Mehigan B., McCormick P., Dalton T., Coffey J.C., Newton A.C., O'Sullivan J. and Kiely P.A., Protein kinase C beta II suppresses colorectal cancer by regulating IGF-1 mediated cell survival, Oncotarget 7, 2016, 20919–20933.

Dries, D.R., Gallegos, L.L., and Newton, A.C. (2007). A single residue in the C1 domain sensitizes novel protein kinase C isoforms to cellular diacylglycerol production. J Biol Chem 282, 826–830.

Dudek, H., Datta, S.R., Franke, T.F., Birnbaum, M.J., Yao, R., Cooper, G.M., Segal, R.A., Kaplan, D.R., and Greenberg, M.E. (1997). Regulation of neuronal survival by the serine-threonine protein kinase Akt. Science 275, 661–665.

Dutil E.M. and Newton A.C., Dual role of pseudosubstrate in the coordinated regulation of protein kinase C by phosphorylation and diacylglycerol, J. Biol. Chem. 275, 2000, 10697–10701.

Dutil E.M., Keranen L.M., DePaoli-Roach A.A. and Newton A.C., In vivo regulation of protein kinase C by trans-phosphorylation followed by autophosphorylation, J. Biol. Chem. 269, 1994, 29359–29362.

Dutil, E.M., Keranen, L.M., DePaoli-Roach, A.A., and Newton, A.C. (1994). In vivo regulation of protein kinase C by trans-phosphorylation followed by autophosphorylation. J. Biol. Chem. 269, 29359–29362.

Dutil, E.M., Toker, A., and Newton, A.C. (1998). Regulation of conventional protein kinase C isozymes by phosphoinositide-dependent kinase 1 (PDK-1). Curr Biol 8, 1366–1375.

Ebner, M., Lučić, I., Leonard, T.A., and Yudushkin, I. (2017). PI(3,4,5)P 3 Engagement Restricts Akt Activity to Cellular Membranes. Mol. Cell 65, 416-431.e6.

Edwards, A.S., and Newton, A.C. (1997). Phosphorylation at conserved carboxyl-terminal hydrophobic motif regulates the catalytic and regulatory domains of protein kinase C. J. Biol. Chem. 272, 18382–18390.

Facchinetti, V., Ouyang, W., Wei, H., Soto, N., Lazorchak, A., Gould, C., Lowry, C., Newton, A.C., Mao, Y., Miao, R.Q., et al. (2008). The mammalian target of rapamycin complex 2 controls folding and stability of Akt and protein kinase C. EMBO J. 27, 1932–1943.

Flint, A.J., Paladini, R.D., and Koshland, D.E. (1990). Autophosphorylation of protein kinase C at three separated regions of its primary sequence. Science 249, 408–411.

Franke, T.F., Yang, S.-I., Chan, T.O., Datta, K., Kazlauskas, A., Morrison, D.K., Kaplan, D.R., and Tsichlis, P.N. (1995). The protein kinase encoded by the Akt proto-oncogene is a target of the PDGF-activated phosphatidylinositol 3-kinase. Cell 81, 727–736.

Gallegos, L.L., Kunkel, M.T., and Newton, A.C. (2006). Targeting protein kinase C activity reporter to discrete intracellular regions reveals spatiotemporal differences in agonist-dependent signaling. J Biol Chem 281, 30947–30956.

Gao J., Chang M.T., Johnsen H.C., Gao S.P., Sylvester B.E., Sumer S.O., Zhang H., Solit D.B., Taylor B.S., Schultz N. and Sander C., 3D clusters of somatic mutations in cancer reveal numerous rare mutations as functional targets, Genome Med. 9, 2017, 4.

Gao T., Brognard J. and Newton A.C., The phosphatase PHLPP controls the cellular levels of protein kinase C, J. Biol. Chem. 283, 2008, 6300–6311.

Gao T., Furnari F. and Newton A.C., PHLPP: a phosphatase that directly dephosphorylates Akt, promotes apoptosis, and suppresses tumor growth, Mol. Cell 18, 2005, 13–24.

Gao, T., and Newton, A.C. (2002). The turn motif is a phosphorylation switch that regulates the binding of Hsp70 to protein kinase C. J Biol Chem 277, 31585–31592.

Gao, T., Toker, A., and Newton, A.C. (2001). The Carboxyl Terminus of Protein Kinase C Provides a Switch to Regulate Its Interaction with the Phosphoinositide-dependent Kinase, PDK-1. J. Biol. Chem. 276, 19588–19596.

Garcia-Martinez, J.M., and Alessi, D.R. (2008). mTOR complex 2 (mTORC2) controls hydrophobic motif phosphorylation and activation of serum- and glucocorticoid-induced protein kinase 1 (SGK1). Biochem J 416, 375–385.

Gereau, R.W., and Heinemann, S.F. (1998). Role of Protein Kinase C Phosphorylation in Rapid Desensitization of Metabotropic Glutamate Receptor 5. Neuron 20, 143–151.

Gibbs, C.S., and Zoller, M.J. (1991). Rational scanning mutagenesis of a protein kinase identifies functional regions involved in catalysis and substrate interactions. J. Biol. Chem. 266, 8923–8931.

Gispert, S., Twells, R., Orozco, G., Brice, A., Weber, J., Heredero, L., Scheufler, K., Riley, B., Allotey, R., Nothers, C., et al. (1993). Chromosomal assignment of the second locus for autosomal dominant cerebellar ataxia (SCA2) to chromosome 12q23–24.1. Nat. Genet. 4, 295–299.

Goode, B., Mondal, G., Hyun, M., Ruiz, D.G., Lin, Y.-H., Van Ziffle, J., Joseph, N.M., Onodera, C., Talevich, E., Grenert, J.P., et al. (2018). A recurrent kinase domain mutation in PRKCA defines chordoid glioma of the third ventricle. Nat. Commun. 9, 810.

Goode, N., Hughes, K., Woodgett, J.R., and Parker, P.J. (1992). Differential regulation of glycogen synthase kinase-3 beta by protein kinase C isotypes. J. Biol. Chem. 267, 16878–16882.

Gould C.M., Antal C.E., Reyes G., Kunkel M.T., Adams R.A., Ziyar A., Riveros T. and Newton A.C., Active site inhibitors protect protein kinase C from dephosphorylation and stabilize its mature form, J. Biol. Chem. 286, 2011, 28922–28930.

Gould, C.M., Kannan, N., Taylor, S.S., and Newton, A.C. (2009). The chaperones Hsp90 and Cdc37 mediate the maturation and stabilization of protein kinase C through a conserved PXXP motif in the C-terminal tail. J Biol Chem 284, 4921–4935.

Griner E.M. and Kazanietz M.G., Protein kinase C and other diacylglycerol effectors in cancer, Nat. Rev. Cancer 7, 2007, 281–294.

Griner, E.M., and Kazanietz, M.G. (2007). Protein kinase C and other diacylglycerol effectors in cancer. Nat Rev Cancer 7, 281–294.

Grodsky, N., Li, Y., Bouzida, D., Love, R., Jensen, J., Nodes, B., Nonomiya, J., and Grant, S. (2006). Structure of the catalytic domain of human protein kinase C beta II complexed with a bisindolylmaleimide inhibitor. Biochemistry 45, 13970–13981.

Guertin D.A., Stevens D.M., Thoreen C.C., Burds A.A., Kalaany N.Y., Moffat J., Brown M., Fitzgerald K.J. and Sabatini D.M., Ablation in mice of the mTORC components raptor, rictor, or mLST8 reveals that mTORC2 is required for signaling to Akt-FOXO and PKCalpha, but not S6K1, Dev. Cell 11, 2006, 859–871.
Hansra G., Garcia-Paramio P., Prevostel C., Whelan R.D., Bornancin F. and Parker P.J., Multisite dephosphorylation and desensitization of conventional protein kinase C isotypes, Biochem. J. 342, 1999, 337–344.

Gunaratne, A., Benchabane, H., and Di Guglielmo, G.M. (2012). Regulation of TGFβ receptor trafficking and signaling by atypical protein kinase C. Cell. Signal. 24, 119–130.

Hashimoto, K., Watanabe, M., Kurihara, H., Offermanns, S., Jiang, H., Wu, Y., Jun, K., Shin, H.S., Inoue, Y., Wu, D., et al. (2000). Climbing fiber synapse elimination during postnatal cerebellar development requires signal transduction involving G alpha q and phospholipase C beta 4. Prog Brain Res 124, 31–48.

Hashimoto, T., Ase, K., Sawamura, S., Kikkawa, U., Saito, N., Tanaka, C., and Nishizuka, Y. (1988). Postnatal development of a brain-specific subspecies of protein kinase C in rat. J. Neurosci. 8, 1678–1683.

Hauge, C., Antal, T.L., Hirschberg, D., Doehn, U., Thorup, K., Idrissova, L., Hansen, K., Jensen, O.N., Jorgensen, T.J., Biondi, R.M., et al. (2007). Mechanism for activation of the growth factor-activated AGC kinases by turn motif phosphorylation. Embo J 26, 2251–2261.

He, Q., Dent, E.W., and Meiri, K.F. (1997). Modulation of actin filament behavior by GAP-43 (neuromodulin) is dependent on the phosphorylation status of serine 41, the protein kinase C site. J. Neurosci. 17, 3515–3524.

Hein, M.Y., Hubner, N.C., Poser, I., Cox, J., Nagaraj, N., Toyoda, Y., Gak, I.A., Weisswange, I., Mansfeld, J., Buchholz, F., et al. (2015). A Human Interactome in Three Quantitative Dimensions Organized by Stoichiometries and Abundances. Cell 163, 712–723.

Herman-Bert, A., Stevanin, G., Netter, J.-C., Rascol, O., Brassat, D., Calvas, P., Camuzat, A., Yuan, Q., Schalling, M., Dürr, A., et al. (2000). Mapping of Spinocerebellar Ataxia 13 to Chromosome 19q13.3-q13.4 in a Family with Autosomal Dominant Cerebellar Ataxia and Mental Retardation. Am. J. Hum. Genet. 67, 229–235.

Hills, L.B., Masri, A., Konno, K., Kakegawa, W., Lam, A.-T.N., Lim-Melia, E., Chandy, N., Hill, R.S., Partlow, J.N., Al-Saffar, M., et al. (2013). Deletions in GRID2 lead to a recessive syndrome of cerebellar ataxia and tonic upgaze in humans. Neurology 81, 1378–1386.

Holmes, S.E., O'Hearn, E.E., McInnis, M.G., Gorelick-Feldman, D.A., Kleiderlein, J.J., Callahan, C., Kwak, N.G., Ingersoll-Ashworth, R.G., Sherr, M., Sumner, A.J., et al. (1999). Expansion of a novel

CAG trinucleotide repeat in the 5′ region of PPP2R2B is associated with SCA12. Nat. Genet. 23, 391–392.

Holmgren, A., Bouhy, D., and Timmerman, V. (2012). Neurofilament phosphorylation and their proline-directed kinases in health and disease. J. Peripher. Nerv. Syst. 17, 365–376.

Hopfield, J.J. (1974). Kinetic proofreading: a new mechanism for reducing errors in biosynthetic processes requiring high specificity. Proc. Natl. Acad. Sci. U. S. A. 71, 4135–4139.

Hornbeck, P. V., Zhang, B., Murray, B., Kornhauser, J.M., Latham, V., and Skrzypek, E. (2015). PhosphoSitePlus, 2014: mutations, PTMs and recalibrations. Nucleic Acids Res. 43, D512–D520.

House C. and Kemp B.E., Protein kinase C contains a pseudosubstrate prototope in its regulatory domain, Science 238, 1987, 1726–1728.

House C. and Kemp B.E., Protein kinase C pseudosubstrate prototope: structure-function relationships, Cell. Signal. 2, 1990, 187–190.

Hsu A.H., Lum M.A., Shim K.-S., Frederick P.J., Morrison C.D., Chen B., Lele S.M., Sheinin Y.M., Daikoku T., Dey S.K., et al., Crosstalk between PKCα and PI3K/AKT Signaling Is Tumor Suppressive in the Endometrium, Cell Rep. 24, 2018, 655–669.

Huang L.C., Ross K.E., Baffi T.R., Drabkin H., Kochut K.J., Ruan Z., D'Eustachio P., McSkimming D., Arighi C., Chen C., et al., Integrative annotation and knowledge discovery of kinase post-translational modifications and cancer-associated mutations through federated protein ontologies and resources, Sci. Rep. 8, 2018, 6518.

Huang, S.-M., Leventhal, P.S., Wiepz, G.J., and Bertics, P.J. (1999). Calcium and Phosphatidylserine Stimulate the Self-Association of Conventional Protein Kinase C Isoforms †. Biochemistry 38, 12020–12027.

Hudson, A.M., Stephenson, N.L., Li, C., Trotter, E., Fletcher, A.J., Katona, G., Bieniasz-Krzywiec, P., Howell, M., Wirth, C., Furney, S., et al. (2018). Truncation- and motif-based pan-cancer analysis reveals tumor-suppressing kinases. Sci. Signal. 11, eaan6776.

Hui, X., Sauer, B., Kaestner, L., Kruse, K., and Lipp, P. (2017). PKCα diffusion and translocation are independent of an intact cytoskeleton. Sci. Rep. 7.

Hunter, T. (1995). Protein kinases and phosphatases: The Yin and Yang of protein phosphorylation and signaling. Cell 80, 225–236.

Hunter, T., Gould, K.L., and Cooper, J.A. (1984). Tyrosine protein kinases, viral transformation and the control of cell proliferation. Biochem. Soc. Trans. 12, 757–759.

Hurley, J.H., Newton, A.C., Parker, P.J., Blumberg, P.M., and Nishizuka, Y. (2008). Taxonomy and function of C1 protein kinase C homology domains. Protein Sci. 6, 477–480.

Ichise, T., Kano, M., Hashimoto, K., Yanagihara, D., Nakao, K., Shigemoto, R., Katsuki, M., and Aiba, A. (2000). mGluR1 in cerebellar Purkinje cells essential for long-term depression, synapse elimination, and motor coordination. Science (80-.). 288, 1832–1835.

Ikenoue, T., Inoki, K., Yang, Q., Zhou, X., and Guan, K.-L. (2008). Essential function of TORC2 in PKC and Akt turn motif phosphorylation, maturation and signalling. EMBO J. 27, 1919–1931.

Iyer, G.H., Moore, M.J., and Taylor, S.S. (2005). Consequences of lysine 72 mutation on the phosphorylation and activation state of cAMP-dependent kinase. J. Biol. Chem. 280, 8800–8807.
Jacinto, E., Facchinetti, V., Liu, D., Soto, N., Wei, S., Jung, S.Y., Huang, Q., Qin, J., and Su, B. (2006). SIN1/MIP1 maintains rictor-mTOR complex integrity and regulates Akt phosphorylation and substrate specificity. Cell 127, 125–137.

Jacinto, E., Loewith, R., Schmidt, A., Lin, S., Rüegg, M.A., Hall, A., and Hall, M.N. (2004). Mammalian TOR complex 2 controls the actin cytoskeleton and is rapamycin insensitive. Nat. Cell Biol. 6, 1122–1128.

Jaken S., Tashjian A.H., Jr. and Blumberg P.M., Characterization of phorbol ester receptors and their down-modulation in GH4C1 rat pituitary cells, Cancer Res. 41, 1981, 2175–2181.

Jezierska, J., Goedhart, J., Kampinga, H.H., Reits, E.A., and Verbeek, D.S. (2014). SCA14 mutation V138E leads to partly unfolded PKCγ associated with an exposed C-terminus, altered kinetics, phosphorylation and enhanced insolubilization. J. Neurochem. 128, 741–751.

Ji, J., Hassler, M.L., Shimobayashi, E., Paka, N., Streit, R., and Kapfhammer, J.P. (2014). Increased protein kinase C gamma activity induces Purkinje cell pathology in a mouse model of spinocerebellar ataxia 14. Neurobiol Dis 70, 1–11.

Kajimoto, T., Caliman, A.D., Tobias, I.S., Okada, T., Pilo, C.A., Van, A.-A.N., McCammon, J.A., Nakamura, S., and Newton, A.C. (2019). Activation of atypical protein kinase C by sphingosine 1-phosphate revealed by an aPKC-specific activity reporter. Sci. Signal. 12, eaat6662.

Kannan, N., Haste, N., Taylor, S.S., and Neuwald, A.F. (2007). The hallmark of AGC kinase functional divergence is its C-terminal tail, a cis-acting regulatory module. Proc. Natl. Acad. Sci. U. S. A. 104, 1272–1277.

Kano, M., Hashimoto, K., Chen, C., Abeliovich, A., Aiba, A., Kurihara, H., Watanabe, M., Inoue, Y., and Tonegawa, S. (1995). Impaired synapse elimination during cerebellar development in PKC gamma mutant mice. Cell 83, 1223–1231.

Kano, M., Hashimoto, K., Kurihara, H., Watanabe, M., Inoue, Y., Aiba, A., and Tonegawa, S. (1997). Persistent multiple climbing fiber innervation of cerebellar Purkinje cells in mice lacking mGluR1. Neuron 18, 71–79.

Kano, M., Hashimoto, K., Watanabe, M., Kurihara, H., Offermanns, S., Jiang, H., Wu, Y., Jun, K., Shin, H.S., Inoue, Y., et al. (1998). Phospholipase cbeta4 is specifically involved in climbing fiber synapse elimination in the developing cerebellum. Proc Natl Acad Sci U S A 95, 15724–15729.

Kazanietz, M.G., Bustelo, X.R., Barbacid, M., Kolch, W., Mischak, H., Wong, G., Pettit, G.R., Bruns, J.D., and Blumberg, P.M. (1994). Zinc finger domains and phorbol ester pharmacophore. Analysis of binding to mutated form of protein kinase C zeta and the vav and c-raf proto-oncogene products. J Biol Chem 269, 11590–11594.

Kazanietz, M.G., Wang, S., Milne, G.W., Lewin, N.E., Liu, H.L., and Blumberg, P.M. (1995). Residues in the second cysteine-rich region of protein kinase C delta relevant to phorbol ester binding as revealed by site-directed mutagenesis. J Biol Chem 270, 21852–21859.

Keranen, L.M., Dutil, E.M., and Newton, A.C. (1995). Protein kinase C is regulated in vivo by three functionally distinct phosphorylations. Curr. Biol. 5, 1394–1403.

Keshwani, M.M., Klammt, C., von Daake, S., Ma, Y., Kornev, A.P., Choe, S., Insel, P.A., and Taylor, S.S. (2012). Cotranslational cis-phosphorylation of the COOH-terminal tail is a key priming step in the maturation of cAMP-dependent protein kinase. Proc Natl Acad Sci U S A 109, E1221-9.

Kikkawa, U., Takai, Y., Tanaka, Y., Miyake, R., and Nishizuka, Y. (1983). Protein kinase C as a possible receptor protein of tumor-promoting phorbol esters. J Biol Chem 258, 11442–11445.

Kimura, M., Yabe, I., Hama, Y., Eguchi, K., Ura, S., Tsuzaka, K., Tsuji, S., and Sasaki, H. (2017). SCA42 mutation analysis in a case series of Japanese patients with spinocerebellar ataxia. J. Hum. Genet. 62, 857–859.

Kishimoto, A., Kajikawa, N., Shiota, M., and Nishizuka, Y. (1983). Proteolytic activation of calcium-activated, phospholipid-dependent protein kinase by calcium-dependent neutral protease. J. Biol. Chem. 258, 1156–1164.

Kleppisch, T., Voigt, V., Allmann, R., and Offermanns, S. (2001). G(alpha)q-deficient mice lack metabotropic glutamate receptor-dependent long-term depression but show normal long-term potentiation in the hippocampal CA1 region. J. Neurosci. 21, 4943–4948.

Knighton, D., Zheng, J., Ten Eyck, L., Ashford, V., Xuong, N., Taylor, S., and Sowadski, J. (1991). Crystal structure of the catalytic subunit of cyclic adenosine monophosphate-dependent protein kinase. Science (80-.). 253, 407–414.

Knudson, A.G. (1971). Mutation and cancer: statistical study of retinoblastoma. Proc. Natl. Acad. Sci. U. S. A. 68, 820–823.

Kornev, A.P., Haste, N.M., Taylor, S.S., and Eyck, L.F. Ten (2006). Surface comparison of active and inactive protein kinases identifies a conserved activation mechanism. 103, 17783–17788.

Lamark, T., Perander, M., Outzen, H., Kristiansen, K., Øvervatn, A., Michaelsen, E., Bjørkøy, G., and Johansen, T. (2003). Interaction Codes within the Family of Mammalian Phox and Bem1p Domain-containing Proteins. J. Biol. Chem. 278, 34568–34581.

Langzam, L., Koren, R., Gal, R., Kugel, V., Paz, A., Farkas, A., and Sampson, S.R. (2001). Patterns of Protein Kinase C Isoenzyme Expression in Transitional Cell Carcinoma of Bladder. Am. J. Clin. Pathol. 116, 377–385.

Lapek, J.D., Jiang, Z., Wozniak, J.M., Arutyunova, E., Wang, S.C., Lemieux, M.J., Gonzalez, D.J., and O'Donoghue, A.J. (2019). Quantitative Multiplex Substrate Profiling of Peptidases by Mass Spectrometry. Mol. Cell. Proteomics 18, 968–981.ow to

Le Good J.A., Ziegler W.H., Parekh D.B., Alessi D.R., Cohen P. and Parker P.J., Protein kinase C isotypes controlled by phosphoinositide 3-kinase through the protein kinase PDK1, Science 281, 1998, 2042–2045.
Le Good, J.A., Ziegler, W.H., Parekh, D.B., Alessi, D.R., Cohen, P., and Parker, P.J. (1998). Protein kinase C isotypes controlled by phosphoinositide 3-kinase through the protein kinase PDK1. Science (80-.). 281, 2042–2045.

Lee, J.Y., Chiu, Y.-H., Asara, J., and Cantley, L.C. (2011). Inhibition of PI3K binding to activators by serine phosphorylation of PI3K regulatory subunit p85α Src homology-2 domains. Proc. Natl. Acad. Sci. 108, 14157–14162.

Lei, P., Ayton, S., Bush, A.I., and Adlard, P.A. (2011). GSK-3 in Neurodegenerative Diseases. Int. J. Alzheimers. Dis. 2011, 189246.

Lemmon, M.A., Freed, D.M., Schlessinger, J., and Kiyatkin, A. (2016). The Dark Side of Cell Signaling: Positive Roles for Negative Regulators. Cell 164, 1172–1184.

Leonard, T.A., Różycki, B., Saidi, L.F., Hummer, G., and Hurley, J.H. (2011). Crystal Structure and Allosteric Activation of Protein Kinase C βII. Cell 144, 55–66.

Leroux, A.E., Schulze, J.O., and Biondi, R.M. (2018). AGC kinases, mechanisms of regulation and innovative drug development. Semin. Cancer Biol. 48, 1–17.

Li J., Zhao W., Akbani R., Liu W., Ju Z., Ling S., Vellano C.P., Roebuck P., Yu Q., Eterovic A.K., et al., Characterization of human cancer cell lines by reverse-phase protein arrays, Cancer Cell 31, 2017, 225–239.

Lin, K., Lin, J., Wu, W.-I., Ballard, J., Lee, B.B., Gloor, S.L., Vigers, G.P.A., Morales, T.H., Friedman, L.S., Skelton, N., et al. (2012). An ATP-site on-off switch that restricts phosphatase accessibility of Akt. Sci. Signal. 5, ra37.

Lin, Y., Jover-Mengual, T., Wong, J., Bennett, M.V.L., and Zukin, R.S. (2006). PSD-95 and PKC converge in regulating NMDA receptor trafficking and gating. Proc. Natl. Acad. Sci. 103, 19902–19907.
Linden, D.J., and Connor, J.A. (1991). Participation of postsynaptic PKC in cerebellar long-term depression in culture. Science (80-.). 254, 1656–1659.

Liu J., Stevens P.D., Li X., Schmidt M.D. and Gao T., PHLPP-mediated dephosphorylation of S6K1 inhibits protein translation and cell growth, Mol. Cell. Biol. 31, 2011, 4917–4927.

Lizcano, J.M., Göransson, O., Toth, R., Deak, M., Morrice, N.A., Boudeau, J., Hawley, S.A., Udd, L., Mäkelä, T.P., Hardie, D.G., et al. (2004). LKB1 is a master kinase that activates 13 kinases of the AMPK subfamily, including MARK/PAR-1. EMBO J. 23, 833–843.

Lochhead, P.A. (2009). Protein kinase activation loop autophosphorylation in cis: overcoming a Catch-22 situation. Sci. Signal. 2, pe4.

Lu Z., Liu D., Hornia A., Devonish W., Pagano M. and Foster D.A., Activation of protein kinase C triggers its ubiquitination and degradation, Mol. Cell. Biol. 18, 1998, 839–845.

Lučić, I., Truebestein, L., and Leonard, T.A. (2016). Novel Features of DAG-Activated PKC Isozymes Reveal a Conserved 3-D Architecture. J. Mol. Biol. 428, 121–141.

Lum, M.A., Barger, C.J., Hsu, A.H., Leontieva, O. V, Black, A.R., and Black, J.D. (2016). PKCα is Resistant to Long-Term Desensitization/Downregulation by Prolonged Diacylglycerol Stimulation. J. Biol. Chem.

Manning, B.D., and Toker, A. (2017). AKT/PKB Signaling: Navigating the Network. Cell 169, 381–405.

Marambaud, P., Dreses-Werringloer, U., and Vingtdeux, V. (2009). Calcium signaling in neurodegeneration. Mol. Neurodegener. 4, 20.

Masubuchi S., Gao T., O'Neill A., Eckel-Mahan K., Newton A.C. and Sassone-Corsi P., Protein phosphatase PHLPP1 controls the light-induced resetting of the circadian clock, Proc. Natl. Acad. Sci. USA 107, 2010, 1642–1647.

McSkimming D.I., Dastgheib S., Baffi T.R., Byrne D.P., Ferries S., Scott S.T., Newton A.C., Eyers C.E., Kochut K.J., Eyers P.A. and Kannan N., KinView: a visual comparative sequence analysis tool for integrated kinome research, Mol. Biosyst. 12, 2016, 3651–3665.

Mebratu, Y., and Tesfaigzi, Y. (2009). How ERK1/2 activation controls cell proliferation and cell death: Is subcellular localization the answer? Cell Cycle 8, 1168–1175.

Meharena, H.S., Chang, P., Keshwani, M.M., Oruganty, K., Nene, A.K., Kannan, N., Taylor, S.S., and Kornev, A.P. (2013). Deciphering the structural basis of eukaryotic protein kinase regulation. PLoS Biol 11, e1001680.

Metz, K.S., Deoudes, E.M., Berginski, M.E., Jimenez-Ruiz, I., Aksoy, B.A., Hammerbacher, J., Gomez, S.M., and Phanstiel, D.H. (2018). Coral: Clear and Customizable Visualization of Human Kinome Data. Cell Syst. 7, 347-350.e1.

Milani G., Rebora P., Accordi B., Galla L., Bresolin S., Cazzaniga G., Buldini B., Mura R., Ladogana S., Giraldi E., et al., Low PKCα expression within the MRD-HR stratum defines a new subgroup of childhood T-ALL with very poor outcome, Oncotarget 5, 2014, 5234–5245.

Mora, A., Komander, D., van Aalten, D.M.F., and Alessi, D.R. (2004). PDK1, the master regulator of AGC kinase signal transduction. Semin. Cell Dev. Biol. 15, 161–170.

Mundt, F., Rajput, S., Li, S., Ruggles, K. V, Mooradian, A.D., Mertins, P., Gillette, M.A., Krug, K., Guo, Z., Hoog, J., et al. (2018). Mass Spectrometry-Based Proteomics Reveals Potential Roles of NEK9 and MAP2K4 in Resistance to PI3K Inhibition in Triple-Negative Breast Cancers. Cancer Res. 78, 2732–2746.

Nabet, B., Roberts, J.M., Buckley, D.L., Paulk, J., Dastjerdi, S., Yang, A., Leggett, A.L., Erb, M.A., Lawlor, M.A., Souza, A., et al. (2018). The dTAG system for immediate and target-specific protein degradation. Nat. Chem. Biol. 14, 431–441.

Namkung, Y., and Sibley, D.R. (2004). Protein Kinase C Mediates Phosphorylation, Desensitization, and Trafficking of the D 2 Dopamine Receptor. J. Biol. Chem. 279, 49533–49541.

Newton, A.C. (1995). Protein kinase C: structure, function, and regulation. J. Biol. Chem. 270, 28495–28498.
Newton, A.C. (2003). Regulation of the ABC kinases by phosphorylation: protein kinase C as a paradigm. Biochem J 370, 361–371.

Newton, A.C. (2010). Protein kinase C: poised to signal. Am. J. Physiol. Endocrinol. Metab. 298, E395-402.

Newton, A.C. (2018). Protein kinase C: perfectly balanced. Crit. Rev. Biochem. Mol. Biol. 53, 208–230.

Newton, A.C. (2018b). Protein kinase C as a tumor suppressor. Semin. Cancer Biol. 48, 18–26.

Newton, A.C., and Brognard, J. (2017). Reversing the Paradigm: Protein Kinase C as a Tumor Suppressor. Trends Pharmacol Sci 38, 438–447.

Newton, A.C., and Koshland, D.E. (1987). Protein kinase C autophosphorylates by an intrapeptide reaction. J. Biol. Chem. 262, 10185–10188.

Newton, A.C., and Koshland, D.E. (1989). High cooperativity, specificity, and multiplicity in the protein kinase C-lipid interaction. J. Biol. Chem. 264, 14909–14915.

Newton, A.C., Bootman, M.D., and Scott, J.D. (2016). Second Messengers. Cold Spring Harb. Perspect. Biol. 8, a005926.

Nishikawa, R., Ji, X.D., Harmon, R.C., Lazar, C.S., Gill, G.N., Cavenee, W.K., and Huang, H.J. (1994). A mutant epidermal growth factor receptor common in human glioma confers enhanced tumorigenicity. Proc. Natl. Acad. Sci. U. S. A. 91, 7727–7731.

Nishizuka, Y. (1984). The role of protein kinase C in cell surface signal transduction and tumour promotion. Nature 308, 693–698.

Novak, M.J.U., Sweeney, M.G., Li, A., Treacy, C., Chandrashekar, H.S., Giunti, P., Goold, R.G., Davis, M.B., Houlden, H., and Tabrizi, S.J. (2010). An ITPR1 gene deletion causes spinocerebellar ataxia 15/16: A genetic, clinical and radiological description. Mov. Disord. 25, 2176–2182.

O'Neill, A.K., Gallegos, L.L., Justilien, V., Garcia, E.L., Leitges, M., Fields, A.P., Hall, R.A., and Newton, A.C. (2011). Protein kinase Cα promotes cell migration through a PDZ-dependent interaction with its novel substrate discs large homolog 1 (DLG1). J. Biol. Chem. 286, 43559–43568.

Oh, W.J., Wu, C., Kim, S.J., Facchinetti, V., Julien, L.-A., Finlan, M., Roux, P.P., Su, B., and Jacinto, E. (2010). mTORC2 can associate with ribosomes to promote cotranslational phosphorylation and stability of nascent Akt polypeptide. EMBO J. 29, 3939–3951.

Ono, Y., Fujii, T., Igarashi, K., Kuno, T., Tanaka, C., Kikkawa, U., and Nishizuka, Y. (1989). Phorbol ester binding to protein kinase C requires a cysteine-rich zinc-finger-like sequence. Proc. Natl. Acad. Sci. U. S. A. 86, 4868–4871.

Orr, J.W., and Newton, A.C. (1994). Requirement for negative charge on "activation loop" of protein kinase C. J Biol Chem 269, 27715–27718.

Orr, J.W., Keranen, L.M., and Newton, A.C. (1992). Reversible exposure of the pseudosubstrate domain of protein kinase C by phosphatidylserine and diacylglycerol. J. Biol. Chem. 267, 15263–15266.
Oster, H., and Leitges, M. (2006). Protein Kinase C α but not PKCζ Suppresses Intestinal Tumor Formation in Apc Min/+ Mice. Cancer Res. 66, 6955–6963.

Ouyang, X., Gulliford, T., and Epstein, R.J. (1998). The duration of phorbol-inducible ErbB2 tyrosine dephosphorylation parallels that of receptor endocytosis rather than threonine-686 phosphorylation: implications for the physiological role of protein kinase C in growth factor receptor signalling. Carcinogenesis 19, 2013–2019.

Pappa, H., Murray-Rust, J., Dekker, L. V, Parker, P.J., and McDonald, N.Q. (1998). Crystal structure of the C2 domain from protein kinase C-delta. Structure 6, 885–894.

Parikh C., Janakiraman V., Wu W.I., Foo C.K., Kljavin N.M., Chaudhuri S., Stawiski E., Lee B., Lin J., Li H., et al., Disruption of PH-kinase domain interactions leads to oncogenic activation of AKT in human cancers, Proc. Natl. Acad. Sci. USA 109, 2012, 19368–19373.

Park W.S., Heo W.D., Whalen J.H., O'Rourke N.A., Bryan H.M., Meyer T. and Teruel M.N., Comprehensive identification of PIP3-regulated PH domains from C. elegans to H. sapiens by model prediction and live imaging, Mol. Cell 30, 2008, 381–392.

Parker P.J., Bosca L., Dekker L., Goode N.T., Hajibagheri N. and Hansra G., Protein kinase C (PKC)-induced PKC degradation: a model for down-regulation, Biochem. Soc. Trans. 23, 1995, 153–155.

Parker, P., Coussens, L., Totty, N., Rhee, L., Young, S., Chen, E., Stabel, S., Waterfield, M., and Ullrich, A. (1986). The complete primary structure of protein kinase C--the major phorbol ester receptor. Science (80-.). 233, 853–859.

Pearce, L.R., Komander, D., and Alessi, D.R. (2010). The nuts and bolts of AGC protein kinases. Nat. Rev. Mol. Cell Biol. 11.

Pearlman, S.M., Serber, Z., and Ferrell, J.E. (2011). A Mechanism for the Evolution of Phosphorylation Sites. Cell 147, 934–946.

Pears C.J., Kour G., House C., Kemp B.E. and Parker P.J., Mutagenesis of the pseudosubstrate site of protein kinase C leads to activation, Eur. J. Biochem. 194, 1990, 89–94.

Pomper, M.G., Passe, T.J., Burger, P.C., Scheithauer, B.W., and Brat, D.J. (2001). Chordoid glioma: a neoplasm unique to the hypothalamus and anterior third ventricle. AJNR. Am. J. Neuroradiol. 22, 464–469.

Prince, W.S., Pungor, E., Sluzky, V., and Baffi, R.A. (2011). Therapeutic Enzymes and Biomimetic Substrates: A Case Study of Recombinant Human Arylsulfatase B (Naglazyme®) Substrate Selection and Application. Compr. Biotechnol. 377–389.

Pu, Y., Peach, M.L., Garfield, S.H., Wincovitch, S., Marquez, V.E., and Blumberg, P.M. (2006). Effects on Ligand Interaction and Membrane Translocation of the Positively Charged Arginine Residues Situated along the C1 Domain Binding Cleft in the Atypical Protein Kinase C Isoforms. J. Biol. Chem. 281, 33773–33788.

Reddig, P.J., Dreckschmidt, N.E., Ahrens, H., Simsiman, R., Tseng, C.P., Zou, J., Oberley, T.D., and Verma, A.K. (1999). Transgenic mice overexpressing protein kinase Cdelta in the epidermis are resistant to skin tumor promotion by 12-O-tetradecanoylphorbol-13-acetate. Cancer Res. 59, 5710–5718.

Reddig, P.J., Dreckschmidt, N.E., Zou, J., Bourguignon, S.E., Oberley, T.D., and Verma, A.K. (2000). Transgenic mice overexpressing protein kinase C epsilon in their epidermis exhibit reduced papilloma burden but enhanced carcinoma formation after tumor promotion. Cancer Res. 60, 595–602.

Regala, R.P., Weems, C., Jamieson, L., Khoor, A., Edell, E.S., Lohse, C.M., and Fields, A.P. (2005). Atypical Protein Kinase Cι Is an Oncogene in Human Non–Small Cell Lung Cancer. Cancer Res. 65, 8905–8911.

Roelants, F.M., Leskoske, K.L., Martinez Marshall, M.N., Locke, M.N., and Thorner, J. (2017). The TORC2-Dependent Signaling Network in the Yeast Saccharomyces cerevisiae. Biomolecules 7.

Romanelli, A., Dreisbach, V.C., and Blenis, J. (2002). Characterization of phosphatidylinositol 3-kinase-dependent phosphorylation of the hydrophobic motif site Thr(389) in p70 S6 kinase 1. J. Biol. Chem. 277, 40281–40289.

Romano, R.A., Kannan, N., Kornev, A.P., Allison, C.J., and Taylor, S.S. (2009). A chimeric mechanism for polyvalent trans-phosphorylation of PKA by PDK1. Protein Sci. 18, 1486–1497.

Rosenberg, S., Simeonova, I., Bielle, F., Verreault, M., Bance, B., Le Roux, I., Daniau, M., Nadaradjane, A., Gleize, V., Paris, S., et al. (2018). A recurrent point mutation in PRKCA is a hallmark of chordoid gliomas. Nat. Commun. 9, 2371.

Ross, B.L., Tenner, B., Markwardt, M.L., Zviman, A., Shi, G., Kerr, J.P., Snell, N.E., McFarland, J.J., Mauban, J.R., Ward, C.W., et al. (2018). Single-color, ratiometric biosensors for detecting signaling activities in live cells. Elife 7.

Ross, C.A., and Poirier, M.A. (2004). Protein aggregation and neurodegenerative disease. Nat. Med. 10, S10–S17.

K. M. Sakamoto, K. B. Kim, A. Kumagai, F. Mercurio, C. M. Crews, R. J. Deshaies, Proc. Natl. Acad. Sci. USA 2001, 98, 8554.

Sarbassov, D.D., Ali, S.M., Kim, D.H., Guertin, D.A., Latek, R.R., Erdjument-Bromage, H., Tempst, P., and Sabatini, D.M. (2004). Rictor, a novel binding partner of mTOR, defines a rapamycin-insensitive and raptor-independent pathway that regulates the cytoskeleton. Curr Biol 14, 1296–1302.

Sarbassov, D.D., Guertin, D.A., Ali, S.M., and Sabatini, D.M. (2005). Phosphorylation and regulation of Akt/PKB by the rictor-mTOR complex. Science 307, 1098–1101.

Sasaki, T., Taoka, M., Ishiguro, K., Uchida, A., Saito, T., Isobe, T., and Hisanaga, S. (2002). In Vivo and in Vitro Phosphorylation at Ser-493 in the Glutamate (E)-segment of Neurofilament-H Subunit by Glycogen Synthase Kinase 3β. J. Biol. Chem. 277, 36032–36039.

Schalm, S.S., and Blenis, J. (2002). Identification of a conserved motif required for mTOR signaling. Curr. Biol. 12, 632–639.

Schneekloth, J.S., Fonseca, F.N., Koldobskiy, M., Mandal, A., Deshaies, R., Sakamoto, K., and Crews, C.M. (2004). Chemical Genetic Control of Protein Levels: Selective in Vivo Targeted Degradation. J. Am. Chem. Soc. 126, 3748–3754.

Schrenk, K., Kapfhammer, J.P., and Metzger, F. (2002). Altered dendritic development of cerebellar Purkinje cells in slice cultures from protein kinase Cgamma-deficient mice. Neuroscience 110, 675–689.

Sciarretta, S., Zhai, P., Maejima, Y., Del Re, D.P., Nagarajan, N., Yee, D., Liu, T., Magnuson, M.A., Volpe, M., Frati, G., et al. (2015). mTORC2 Regulates Cardiac Response to Stress by Inhibiting MST1. Cell Rep. 11, 125–136.

Scott, A.M., Antal, C.E., and Newton, A.C. (2013). Electrostatic and hydrophobic interactions differentially tune membrane binding kinetics of the C2 domain of protein kinase Calpha. J Biol Chem 288, 16905–16915.

Seki, T., Adachi, N., Ono, Y., Mochizuki, H., Hiramoto, K., Amano, T., Matsubayashi, H., Matsumoto, M., Kawakami, H., Saito, N., et al. (2005). Mutant protein kinase Cgamma found in spinocerebellar ataxia type 14 is susceptible to aggregation and causes cell death. J Biol Chem 280, 29096–29106.

Shimobayashi, E., and Kapfhammer, J.P. (2017). Increased biological activity of protein Kinase C gamma is not required in Spinocerebellar ataxia 14. Mol Brain 10, 34.

Smit, V.T., Boot, A.J., Smits, A.M., Fleuren, G.J., Cornelisse, C.J., and Bos, J.L. (1988). KRAS codon 12 mutations occur very frequently in pancreatic adenocarcinomas. Nucleic Acids Res 16, 7773–7782.

Sonnenburg, E.D., Gao, T., and Newton, A.C. (2001). The phosphoinositide-dependent kinase, PDK-1, phosphorylates conventional protein kinase C isozymes by a mechanism that is independent of phosphoinositide 3-kinase. J Biol Chem 276, 45289–45297.

Sossin, W.S., and Schwartz, J.H. (1993). Ca(2+)-independent protein kinase Cs contain an amino-terminal domain similar to the C2 consensus sequence. Trends Biochem. Sci. 18, 207–208.

Staudinger, J., Lu, J., and Olson, E.N. (1997). Specific interaction of the PDZ domain protein PICK1 with the COOH terminus of protein kinase C-alpha. J. Biol. Chem. 272, 32019–32024.

Stokoe, D., Stephens, L.R., Copeland, T., Gaffney, P.R.J., Reese, C.B., Painter, G.F., Holmes, A.B., McCormick, F., and Hawkins, P.T. (1997). Dual Role of Phosphatidylinositol-3,4,5-trisphosphate in the Activation of Protein Kinase B. Science (80-.). 277, 567–570.

Stumpo, D.J., Graff, J.M., Albert, K.A., Greengard, P., and Blackshear, P.J. (1989). Molecular cloning, characterization, and expression of a cDNA encoding the "80- to 87-kDa" myristoylated alanine-rich C kinase substrate: a major cellular substrate for protein kinase C. Proc. Natl. Acad. Sci. 86, 4012–4016.

Swanson, C.J., Ritt, M., Wang, W., Lang, M.J., Narayan, A., Tesmer, J.J., Westfall, M., and Sivaramakrishnan, S. (2014). Conserved Modular Domains Team up to Latch-open Active Protein Kinase Cα. J. Biol. Chem. 289, 17812–17829.

Sweatt, J.D., Atkins, C.M., Johnson, J., English, J.D., Roberson, E.D., Chen, S.-J., Newton, A., and Klann, E. (2002). Protected-Site Phosphorylation of Protein Kinase C in Hippocampal Long-Term Potentiation. J. Neurochem. 71, 1075–1085.

Tagawa, K., Homma, H., Saito, A., Fujita, K., Chen, X., Imoto, S., Oka, T., Ito, H., Motoki, K., Yoshida, C., et al. (2015). Comprehensive phosphoproteome analysis unravels the core signaling network that initiates the earliest synapse pathology in preclinical Alzheimer's disease brain. Hum. Mol. Genet. 24, 540–558.

Takahashi, H., Adachi, N., Shirafuji, T., Danno, S., Ueyama, T., Vendruscolo, M., Shuvaev, A.N., Sugimoto, T., Seki, T., Hamada, D., et al. (2015). Identification and characterization of PKCgamma, a kinase associated with SCA14, as an amyloidogenic protein. Hum Mol Genet 24, 525–539.

Takiyama, Y., Nishizawa, M., Tanaka, H., Kawashima, S., Sakamoto, H., Karube, Y., Shimazaki, H., Soutome, M., Endo, K., Ohta, S., et al. (1993). The gene for Machado–Joseph disease maps to human chromosome 14q. Nat. Genet. 4, 300–304.

Tanaka, C., and Nishizuka, Y. (1994). The Protein Kinase C Family for Neuronal Signaling. Annu. Rev. Neurosci. 17, 551–567.

Tatebe, H., Murayama, S., Yonekura, T., Hatano, T., Richter, D., Furuya, T., Kataoka, S., Furuita, K., Kojima, C., and Shiozaki, K. (2017). Substrate specificity of TOR complex 2 is determined by a ubiquitin-fold domain of the Sin1 subunit. Elife 6.

Taylor, S.S., and Kornev, a. P. (2011). Protein kinases: evolution of dynamic regulatory proteins. Trends Biochem. Sci. 36, 65–77.

Taylor, S.S., Keshwani, M.M., Steichen, J.M., and Kornev, A.P. (2012). Evolution of the eukaryotic protein kinases as dynamic molecular switches. Philos. Trans. R. Soc. B Biol. Sci. 367, 2517–2528.

Thornton, T.M., Pedraza-Alva, G., Deng, B., Wood, C.D., Aronshtam, A., Clements, J.L., Sabio, G., Davis, R.J., Matthews, D.E., Doble, B., et al. (2008). Phosphorylation by p38 MAPK as an Alternative Pathway for GSK3 Inactivation. Science (80-.). 320, 667–670.

Tibes R., Qiu Y., Lu Y., Hennessy B., Andreeff M., Mills G.B. and Kornblau S.M., Reverse phase protein array: validation of a novel proteomic technology and utility for analysis of primary leukemia specimens and hematopoietic stem cells, Mol. Cancer Ther. 5, 2006, 2512–2521.

Tighe, A., Johnson, V.L., Taylor, S.S., Elderkin, S., and Morrow, C.J. (2004). Truncating APC mutations have dominant effects on proliferation, spindle checkpoint control, survival and chromosome stability. J. Cell Sci. 117, 6339–6353.

Tobias, I.S., and Newton, A.C. (2016). Protein Scaffolds Control Localized Protein Kinase Cζ Activity. J. Biol. Chem. 291, 13809–13822.

Tobias, I.S., Kaulich, M., Kim, P.K., Simon, N., Jacinto, E., Dowdy, S.F., King, C.C., and Newton, A.C. (2015). Protein kinase Cζ exhibits constitutive phosphorylation and phosphatidylinositol-3,4,5-triphosphate-independent regulation. Biochem. J. BJ20151013.

Toker, A., and Newton, A.C. (2000). Akt/protein kinase B is regulated by autophosphorylation at the hypothetical PDK-2 site. J. Biol. Chem. 275, 8271–8274.

Tsatsanis, C., and Spandidos, D.A. (2000). The role of oncogenic kinases in human cancer (Review). Int. J. Mol. Med. 5, 583–673.

Valge, V.E., Wong, J.G.P., Datlof, B.M., Sinskey, A.J., and Rao, A. (1988). Protein kinase C is required for responses to T cell receptor ligands but not to interleukin-2 in T cells. Cell 55, 101–112.

Valiev, M., Yang, J., Adams, J.A., Taylor, S.S., and Weare, J.H. (2007). Phosphorylation Reaction in cAPK Protein Kinase-Free Energy Quantum Mechanical/Molecular Mechanics Simulations. J. Phys. Chem. B 111, 13455–13464.

van de Leemput, J., Chandran, J., Knight, M.A., Holtzclaw, L.A., Scholz, S., Cookson, M.R., Houlden, H., Gwinn-Hardy, K., Fung, H.-C., Lin, X., et al. (2007). Deletion at ITPR1 Underlies Ataxia in Mice and Spinocerebellar Ataxia 15 in Humans. PLoS Genet. 3, e108.

van Eis, M.J., Evenou, J.-P., Floersheim, P., Gaul, C., Cowan-Jacob, S.W., Monovich, L., Rummel, G., Schuler, W., Stark, W., Strauss, A., et al. (2011). 2,6-Naphthyridines as potent and selective inhibitors of the novel protein kinase C isozymes. Bioorg. Med. Chem. Lett. 21, 7367–7372.

Verbeek, D., Schelhaas, J., Ippel, E., Beemer, F., Pearson, P., and Sinke, R. (2002). Identification of a novel SCA locus (SCA19) in a Dutch autosomal dominant cerebellar ataxia family on chromosome region 1p21-q21. Hum. Genet. 111, 388–393.

Verbeek, D.S., Goedhart, J., Bruinsma, L., Sinke, R.J., and Reits, E.A. (2008). PKC gamma mutations in spinocerebellar ataxia type 14 affect C1 domain accessibility and kinase activity leading to aberrant MAPK signaling. J Cell Sci 121, 2339–2349.

Violin J.D., Zhang J., Tsien R.Y. and Newton A.C., A genetically encoded fluorescent reporter reveals oscillatory phosphorylation by protein kinase C, J. Cell Biol. 161, 2003, 899–909.

Wang M.T., Holderfield M., Galeas J., Delrosario R., To M.D., Balmain A. and McCormick F., K-Ras Promotes Tumorigenicity through Suppression of Non-canonical Wnt Signaling, Cell 163, 2015, 1237–1251.

Wang, M.T., Holderfield, M., Galeas, J., Delrosario, R., To, M.D., Balmain, A., and McCormick, F. (2015). K-Ras Promotes Tumorigenicity through Suppression of Non-canonical Wnt Signaling. Cell 163, 1237–1251.

Warfel, N.A., Niederst, M., and Newton, A.C. (2011). Disruption of the interface between the pleckstrin homology (PH) and kinase domains of Akt protein is sufficient for hydrophobic motif site phosphorylation in the absence of mTORC2. J Biol Chem 286, 39122–39129.

Warfel, N.A., Niederst, M., Stevens, M.W., Brennan, P.M., Frame, M.C., and Newton, A.C. (2011). Mislocalization of the E3 ligase, beta-transducin repeat-containing protein 1 (beta-TrCP1), in glioblastoma uncouples negative feedback between the pleckstrin homology domain leucine-rich repeat protein phosphatase 1 (PHLPP1) and Akt. J Biol Chem 286, 19777–19788.

Watson, L.M., Bamber, E., Schnekenberg, R.P., Williams, J., Bettencourt, C., Lickiss, J., Jayawant, S., Fawcett, K., Clokie, S., Wallis, Y., et al. (2017). Dominant Mutations in GRM1 Cause Spinocerebellar Ataxia Type 44. Am. J. Hum. Genet. 101, 451–458.

Weinberg, R.A. (1991). Tumor suppressor genes. Science (80-.). 254, 1138–1146.

Wheeler, D.L., Ness, K.J., Oberley, T.D., and Verma, A.K. (2003). Protein kinase Cepsilon is linked to 12-O-tetradecanoylphorbol-13-acetate-induced tumor necrosis factor-alpha ectodomain shedding and the development of metastatic squamous cell carcinoma in protein kinase Cepsilon transgenic mice. Cancer Res. 63, 6547–6555.

Wu, W.-I., Voegtli, W.C., Sturgis, H.L., Dizon, F.P., Vigers, G.P.A., and Brandhuber, B.J. (2010). Crystal Structure of Human AKT1 with an Allosteric Inhibitor Reveals a New Mode of Kinase Inhibition. PLoS One 5, e12913.

Xu, Z.-B., Chaudhary, D., Olland, S., Wolfrom, S., Czerwinski, R., Malakian, K., Lin, L., Stahl, M.L., Joseph-McCarthy, D., Benander, C., et al. (2004). Catalytic Domain Crystal Structure of Protein Kinase C-θ (PKCθ). J. Biol. Chem. 279, 50401–50409.

Yabe, I., Sasaki, H., Chen, D.-H., Raskind, W.H., Bird, T.D., Yamashita, I., Tsuji, S., Kikuchi, S., and Tashiro, K. (2003). Spinocerebellar Ataxia Type 14 Caused by a Mutation in Protein Kinase C γ. Arch. Neurol. 60, 1749.

Yang, C.-S., Melhuish, T.A., Spencer, A., Ni, L., Hao, Y., Jividen, K., Harris, T.E., Snow, C., Frierson, H.F., Wotton, D., et al. (2017). The protein kinase C super-family member PKN is regulated by mTOR and influences differentiation during prostate cancer progression. Prostate 77, 1452–1467.

Yang, J., Cron, P., Thompson, V., Good, V.M., Hess, D., Hemmings, B.A., and Barford, D. (2002). Molecular Mechanism for the Regulation of Protein Kinase B/Akt by Hydrophobic Motif Phosphorylation. Mol. Cell 9, 1227–1240.

Yang, J., Kennedy, E.J., Wu, J., Deal, M.S., Pennypacker, J., Ghosh, G., and Taylor, S.S. (2009). Contribution of non-catalytic core residues to activity and regulation in protein kinase A. J. Biol. Chem. 284, 6241–6248.

Yoshida, K., Liu, H., and Miki, Y. (2006). Protein Kinase C δ Regulates Ser 46 Phosphorylation of p53 Tumor Suppressor in the Apoptotic Response to DNA Damage. J. Biol. Chem. 281, 5734–5740.

Youmell, M., Park, S.J., Basu, S., and Price, B.D. (1998). Regulation of the p53 Protein by Protein Kinase Cα and Protein Kinase Cζ. Biochem. Biophys. Res. Commun. 245, 514–518.

Yuan, A., Rao, M. V, Veeranna, Nixon, R.A., and Goldman, R.D. (2012). Neurofilaments at a glance. J. Cell Sci. 125, 3257–3263.

Yuan, T.L., and Cantley, L.C. (2008). PI3K pathway alterations in cancer: variations on a theme. Oncogene 27, 5497–5510.

Zambonin, J.L., Bellomo, A., Ben-Pazi, H., Everman, D.B., Frazer, L.M., Geraghty, M.T., Harper, A.D., Jones, J.R., Kamien, B., Kernohan, K., et al. (2017). Spinocerebellar ataxia type 29 due to mutations in ITPR1: a case series and review of this emerging congenital ataxia. Orphanet J. Rare Dis. 12, 121.

Zhang, L.L., Cao, F.F., Wang, Y., Meng, F.L., Zhang, Y., Zhong, D.S., and Zhou, Q.H. (2015). The protein kinase C (PKC) inhibitors combined with chemotherapy in the treatment of advanced non-small cell lung cancer: meta-analysis of randomized controlled trials. Clin. Transl. Oncol. 17, 371–377.

Zhuchenko, O., Bailey, J., Bonnen, P., Ashizawa, T., Stockton, D.W., Amos, C., Dobyns, W.B., Subramony, S.H., Zoghbi, H.Y., and Lee, C.C. (1997). Autosomal dominant cerebellar ataxia (SCA6) associated with small polyglutamine expansions in the α1A-voltage-dependent calcium channel. Nat. Genet. 15, 62–69.